Spatiotemporal regulation of organelle transport in *Saccharomyces cerevisiae*

Abdulaziz Mohammed Alqahtani

This thesis is submitted to the University of Sheffield for the degree of Doctor of Philosophy

Faculty of Science
School of Biosciences

June 2023

Abstract

Eukaryotic cells possess diverse membrane-bound compartments called organelles, which play crucial roles in facilitating specialised biochemical processes necessary for maintaining cellular metabolism under different growth conditions. Consequently, cells have evolved specific molecular mechanisms to control organelle inheritance and maintenance during the process of cell growth and division. Proper transport of organelles to their designated locations in dividing cells is crucial for maintaining a full complement of organelles across multiple cell generations. Dysfunctional organelle inheritance or maintenance has been linked to numerous human diseases. *Saccharomyces cerevisiae*, has been extensively used to study organelle-related processes, leading to a deeper understanding of fundamental concepts underlying organelle inheritance and functions. Furthermore, it is recognised that many core principles regarding organelle inheritance and maintenance are conserved throughout eukaryotic evolution.

The first part of this research focuses on the transport of vacuoles and peroxisomes by studying the interactions between Class V myosin, Myo2, and its vacuolar and peroxisomal adaptors, Vac17 and Inp2, which are essential for organelle transport. Experimental validations confirm the significance of specific regions in Vac17 and Inp2, known as Myo2 interaction sites (MIS), for vacuole and peroxisome transport. This helped us to generate MIS tools that could be used to study the regulation of vacuole and peroxisome transport from the mother cell during the early stages of organelle transport.

Additionally, by utilising the generated MIS tools, the thesis examines the influence of the protein kinase Kin4 and its paralog Frk1 on vacuole and peroxisome inheritance. The study demonstrates that Kin4 and Frk1 play a crucial role in stabilizing Vac17 and Inp2 in the mother cell by preventing their early degradation during organelle transport. These findings provide insights into the function of Kin4 in antagonizing the role of Cla4 during vacuole and peroxisome inheritance.

Furthermore, the research aims to identify novel factors involved in vacuole and peroxisome transport. To accomplish this, an overexpression screen was conducted, which led to the identification of new genes associated with peroxisome and vacuole inheritance. This comprehensive analysis sheds light on the forward transport and retention of organelles. Notably, the study also identifies Yck1 and its paralog Yck2 as novel factors potentially involved in regulating peroxisome retention by influencing the function of Inp1, a peroxisomal membrane protein essential for peroxisome retention.

Acknowledgements

"In the name of Allah, the Most Gracious, the Most Merciful."

Allah says in the Noble Qur'an, in Surah Al-Isra, verse 85, the following statement: 'And you have not been given of knowledge except a little' (وَمَا أُوتِيتُم مِّنَ الْعِلْمِ إِلَّا قَلِيلًا).

This verse reminds me of the importance of humility and acknowledging that our knowledge is limited and insignificant compared to the comprehensive knowledge that Allah possesses. Thanks be to Allah.

Firstly, I would like to dedicate this achievement to the soul of my dear mother, who spared no effort in raising and educating me until I grew up. She eagerly awaited this beautiful moment when I would conclude my academic journey and return to her embrace. May Allah have mercy on you, my mother. I also dedicate this achievement to my beloved father, whom I hope to see soon. I dedicate this success to him because he was behind every step I took in my life and has been my foremost supporter throughout my academic journey. I dedicate this accomplishment to my beloved wife, who has been my constant companion throughout my studies. She has been a source of endless love, inspiration, happiness, and unwavering support at all times. I dedicate this achievement to my beautiful little daughters, Jomanah and Durrah, who have been a source of strength and perseverance for me during this journey. Many thanks to all my family members for their support and encouragement.

I also express immense gratitude to my supervisor Dr Ewald Hettema for his commitment and enthusiasm in guiding me throughout my PhD. His instructions have been the main motivation during my PhD. He was not just a supervisor, but a great colleague and friend. He dedicated his time for me and my colleagues and continued his guidance and supervision until the last moment of my PhD. I would also like to express my deepest gratitude to Professor Kathryn Ayscough, who was my great supervisor with Dr Ewald Hettema. She dedicated her time and support for guiding me through my PhD.

I am also very thankful to Dr Lakhan Ekal and Dr Donald watts for their support and teaching me many things of what I know today.

I would also like to pay my special regards to Dr Patrick Baker and Dr Dan Bose for their advisory guidance and support.

Finally, many thanks to all former and current fantastic members of Dr Hettema lab. Thanks to Dr Georgia, Dr Sondos, Dr Selva, Tarad Abalkhail, Yousef Alhamad, Ibrahim Sumaily, Quentin, Nourah, and Afroza.

Table of Contents

The list of figures

Chapter 1

Chapter 2

Chapter 3

Chapter 4

Chapter 5

Chapter 6

The list of tables

Chapter 1

Chapter 2

Chapter 5

Abbreviations

DNA	Deoxyribonucleic acid
dATP	Deoxyadenosine triphosphate
dCTP	Deoxycytidine triphosphate
dGTP	Deoxyguanosine triphosphate
dH2O	Deionised water
C-terminal	Carboxyl-terminal
dNTPs	Equimolar mixture of dATP, dTTP, dCTP, dGTP
DTT	Dithiothreitol
dTTP	Deoxythymidine triphosphate
DRP	Dynamin related protein
EDTA	Ethylenediaminetetraacetic acid
ER	Endoplasmic reticulum
GFP	Green fluorescent protein
°C	Degrees Celsius
E. coli	*Escherichia coli*
ECL	Enhanced chemiluminescence
aa	Amino acids
ADP	Adenosine diphosphate
APS	Ammonium persulphate
H. polymorpha	*Hansenula polymorpha*
H	Hour(s)

HRP	Horseradish peroxidase
IgG	Immunoglobulin G
IRD	Infantile Refsum disease
M	Molar
Min	Minute(s)
mKate2	monomeric far-red fluorescent protein
mM	Millimolar
mNG	monomeric Neon Green
mPTS	Peroxisomal membrane protein targeting signal.
mRNA	Messenger RNA
mRuby2	monomeric bright red fluorescent protein
NaCl	Sodium chloride
NALD	Neonatal adrenoleukodystrophy
N-terminal	Amino-terminal
Nt	Nucleotide(s)
OD600	Optical density at 600nm
ORF	Open reading frame
PEG	Polyethylene glycol
PBD	Peroxisome biogenesis disorder
PCR	Polymerase chain reaction
PED	Peroxisomal enzyme deficiency
PMP	Peroxisomal membrane protein
PTS	Peroxisome targeting signal

S. cerevisiae	*Saccharomyces cerevisiae*
SDS	Sodium dodecyl sulphate
SDS-PAGE	Sodium dodecyl sulphate-polyacrylamide gel electrophoresis
Sec	Second(s)
TEMED	N, N, N-Tetramethylethlenediamine
WT	Wild type
ZS	Zellweger syndrome
ZSD	Zellweger spectrum of disorders
α	Alpha
β	Beta
β-ME	β-mercaptoethanol
γ	Gamma
µ	Micro
µM	Micromolar
Δ	Delta
geneΔ	*GENE* deletion mutant
MIS	Myo2 interaction site
CBD	Cargo binding domain

Amino acids

Leu	L	Leucine
Met	M	Methionine
Asn	N	Asparagine
Pro	P	Proline
Gln	Q	Glutamine
Arg	R	Arginine
Ile	I	Isoleucine
Lys	K	Lysine
Tyr	Y	Tyrosine
Ala	A	Alanine
Ser	S	Serine
Thr	T	Threonine
Val	V	Valine
Trp	W	Tryptophan
Cys	C	Cysteine
Glu	E	Glutamic acid
Phe	F	Phenylalanine
Gly	G	Glycine
Asp	D	Aspartic acid
His	H	Histidine
	X	Any amino acid

Chapter 1 Introduction

1.1 The Life inside eukaryotic cells

In eukaryotic cells, there are specialised compartments enclosed by membranes, referred to as organelles. The presence of organelles in eukaryotic cells is an important characteristic of cellular function. Although they house various chemical environments, they have also evolved different specific roles and functions. Therefore, the role of organelles is essential for the proper functioning of cells, encompassing a wide range of functions. Certain organelles play vital roles in cell survival and must be inherited during cell division, as they cannot be formed *de novo*. Examples of such organelles include the nucleus, mitochondria, and chloroplasts. Alternatively, other organelles, peroxisomes and vacuoles can be formed *de novo*, but this is less favourable for the cell rather than going through the process of replicating pre-existing organelles and partitioning them, as this is the preferred process for the cell to sustain its compartmentalization benefits (Warren and Wickner, 1996; Knoblach and Rachubinski, 2015a; Nunnari and Walter, 1996). Inheriting mature organelles can offer a competitive edge, even for organelles like vacuoles, which can be created *de novo* (Jin and Weisman, 2015). Asymmetric inheritance provides additional advantages, such as rejuvenating the bud while leaving potentially harmful materials such as old organelles in the mother cell, thereby extending its lifespan (Hill *et al.*, 2014). This may also serve as a protective mechanism; for example, acute stress may inhibit ER inheritance, rendering daughter cells non-viable (Babour *et al.*, 2010).

1.2 Vacuoles

Yeast cells contain a large membrane-bound organelle known as the vacuole (the yeast equivalent to the mammalian lysosome) that is essential for its degradative and storage abilities. Several studies have shown that vacuoles in *Saccharomyces cerevisiae* provide perspectives related to protein degradation, autophagy, and ion homeostasis, and these functions are broadly overlapping with those of mammalian cell lysosomes (Li and Kane, 2009). The functions performed by vacuoles are essential for cell growth and survival (Li and Kane, 2009). Vacuoles can degrade and sequestrate cellular waste products and unwanted materials (Delorme-Axford *et al.*, 2015).

In addition, yeast vacuole can engulf and break down damaged organelles, misfolded proteins, and other macromolecules in a process known as autophagy. This is important for maintaining a healthy internal environment in the cell (Nakatogawa *et al.*, 2009). They also play an important role in protecting the cell from damage by detoxifying harmful products and substances such as heavy metals (Klionsky, Herman and Emr, 1990), as well as regulating the intracellular pH and ion homeostasis (Kane, 2006). Vacuoles have the ability to store the essential nutrients that the cell needs such as amino acids and polyphosphate. These stored compounds can be released from the vacuole according to cellular needs (Bonangelino, Catlett and Weisman, 1997). The ability of vacuoles to store and release resources required for the cell can also prevent the potential toxicity due to any accumulation of materials in the cytoplasm (Ogawa, DeRisi and Brown, 2000). Studies have demonstrated the involvement of vacuoles in the regulation of cellular aging and lifespan (Hughes and Gottschling, 2012).

1.2.1 Vacuole biogenesis in *Saccharomyces cerevisiae*

Vacuole biogenesis is a highly regulated mechanism that involves complexes of molecular players and cellular pathways to ensure the precise formation and function of this vital organelle. Vacuole biogenesis is mediated by genes known as *VPS* genes. They encode for proteins involved in vacuolar protein sorting (VPS) which are required for regulating vacuole function and morphology as well as protein sorting, packaging, and delivery to vacuole. Stevens, Emr and colleagues were the first to identify VPS mutants (Rothman and Stevens, 1986) (Johnson, Bankaitis and Emr, 1987).This was then followed by additional investigations resulted in categorising *VPS* genes into six distinct groups based on their mutant phenotype shown in **Table 1.1** (Raymond *et al.*, 1992) (Banta *et al.*, 1988).

Table 1.1 The known vacuolar proteins in *S. cerevisiae* divided into six classes.

Class	Gene	Phenotype
Class A	*VPS8, 10, 13, 29, 30, 35,38, 55, 63, 70, 74*	Mutants exhibited wild type vacuole morphology
Class B	*VPS5, 17, 39, 41, 43, 51, 52, 53, 54, 61, 64, 66, 69, 71, 72, 73, 75*	Mutants exhibited altered vacuole morphology

Class C	*VPS11, 16, 18, 33*	Mutants are defective in vacuole assembly and functions
Class D	*VPS3, 6, 8, 9, 15, 19, 21, 43, 45*	Mutants are defective in vacuole acidification and inheritance
Class E	*VPS2, 4, 20, 22, 23, 24, 25, 27, 28, 31, 32, 36, 37, 44, 46, 60*	Mutants exhibited accumulation of exaggerated pre-vacuolar endosome-like compartments
Class F	*VPS1, 26, 62, 65, 68,71*	Mutants showed vacuole encircled by small vacuolar compartments.

Some of these genes beside different other genes are involved in many different complexes and pathways required for vacuole biogenesis, for instance, the class C core vacuole and endosome tethering complex (CORVET); the homotypic fusion and vacuole protein sorting complex (HOPS) (Balderhaar and Ungermann, 2013); the soluble *N*-ethylmaleimide-sensitive factor attachment receptors complex (SNARE) (Wickner, 2010); and the endosomal sorting complexes required for transport (ESCRT0, ESCRT I, ESCRT II, ESCRT III) complexes (Hurley and Emr, 2006). Each complex contains several genes involved in vacuole biogenesis in different pathways **Table 1.2.**

Table 1.2 Complexes involved in vacuole biogenesis and function.

Complex	Genes included
CORVET	*VPS8, 3, 16, 33, PEP3, PEP5*
HOPS	*VPS39, 41, 11, 18, 16, 33*
SNARE	*VAM3, 7, NYV1, VTI1, YKT6, PEP12*
ESCRT 0	*STP32, VPS27, HSE1*
ESCRT I	*VPS23, 28, 37*
ESCRT II	*VPS22, 25, 36*
ESCRT III	*VPS20, 2, 24, 32, 60, SNF7, DID2*

In addition, the membrane trafficking pathways such as the Endocytic pathway, carboxypeptidase Y (CPY) pathway, alkaline phosphatase (ALP) pathway and the cytosol to vacuole transport (CVT) pathway reviewed in (Li and Kane, 2009) play an essential role in vacuole biogenesis by delivering proteins to the vacuole membrane and lumen **Figure 1.1**.

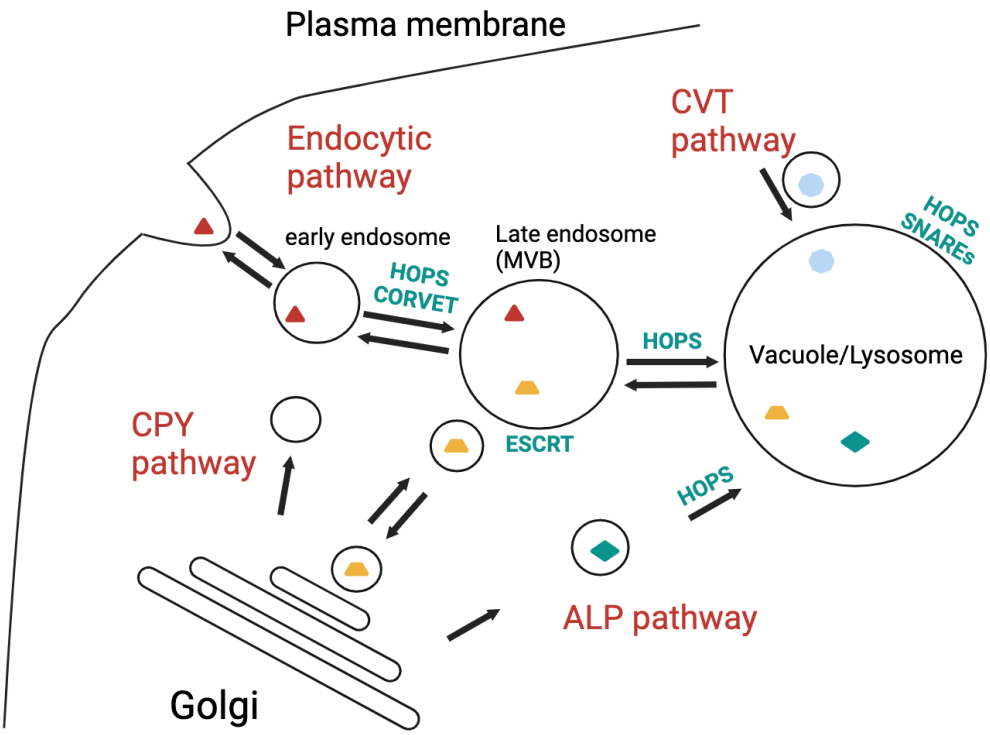

Figure 1.1 Schematic representation of the current proteins complexes and membrane trafficking pathways involved in vacuole biogenesis. The model involves four pathways, i) Endocytic pathway, ii) ALP pathway, iii) CPY pathway and iv) CVT pathway. Endocytosis is responsible for conveying both soluble and membrane-bound cargo from the plasma membrane and the extracellular space to the vacuole. This cargo undergoes a progression from early endosomes to late endosomes, which are also known as multivesicular bodies, before eventually reaching the vacuole. The ALP pathway facilitates the transport of cargo from the late Golgi apparatus to the vacuole. The CPY pathway also originates in the late Golgi but takes a route through multivesicular bodies (MVBs) before reaching the vacuole. The CVT pathway serves to transport newly synthesized cargo from the cytosol to the vacuole and shares common components with autophagy. There are four complexes involved in vacuole biogenesis i) HOPS complex, ii) SNAREs complex, iii). CORVET complex and iv) ESCRT complex.

The VPS proteins can be divided into four functional groups, with each group playing a specific role in the trafficking process. These groups include cargo recognition, vacuole formation, vacuole targeting, and vacuole fusion (Bonangelino, Chavez and Bonifacino, 2002). The Vps10

protein for instance, is a transmembrane receptor, that plays a crucial role in cargo recognition. It binds to vacuolar hydrolases such as carboxypeptidase Y (CPY) in the Golgi apparatus and directs their transport to the vacuole via CPY pathway (Marcusson *et al.*, 1994). The Vps10 protein interacts with the retromer complex, consisting of Vps29, Vps26, and Vps35 proteins (Seaman, 2004)The retromer complex facilitates the recycling of Vps10 from the endosome back to the Golgi. The ALP pathway is distinguished by the direct transportation of vesicles from the Golgi apparatus straight to the vacuole (Cowles *et al.*, 1997).

Vacuole formation involves the recruitment of proteins to the trans-Golgi network (TGN) and endosomes, where they facilitate the budding of vesicles containing cargo destined for the vacuole. The CORVET and HOPS tethering complexes are crucial for the proper functioning of vacuole formation. The proteins involved in these two complexes are indicated in **Table 1.2** which tether transport vesicles to their target membranes (Balderhaar and Ungermann, 2013). Vacuole targeting involves the recognition of target membranes by vacuoles through the interaction of specific proteins. The small GTPase Ypt7p is essential for the proper localization of vesicles to the vacuole. It associates with the vacuolar membrane and interacts with VPS proteins, such as Vps39 and Vps41, which are part of the HOPS complex, to facilitate vacuole targeting (Rieder and Emr, 1997). Vacuole fusion is one of the steps required for the merging of the vesicular and vacuolar membranes. SNAREs are a class of proteins found in cell membranes that play a crucial role in membrane fusion events within cells. They function by facilitating the fusion of vesicles, which transport cellular cargo, with their target membranes, allowing the efficient release of contents and maintaining essential cellular processes like neurotransmission and intracellular trafficking. SNAREs proteins such as Sec18 and Sec17 have been shown to be involved in vesicle fusion (Mayer and Wickner, 1997). The ESCRT machinery is another critical component of vacuole biogenesis. The ESCRT complexes (ESCRT-0, -I, -II, and -III) work in concert with the Vps4p ATPase to sort ubiquitinated cargo proteins into intraluminal vesicles of the multivesicular body (MVB), which then fuses with the vacuole (Babst *et al.*, 2002). This process ensures that the vacuole is supplied with the necessary cargo for its proper function and maintenance (Hurley and Emr, 2006).

Autophagy is a vital process in which cellular components are engulfed within a double-membrane structure known as the autophagosome and subsequently transported to the vacuole for degradation. This process plays a crucial role in the biogenesis of vacuoles. The Atg (autophagy-related) genes and their corresponding proteins are required for the formation and function of autophagosomes, which ultimately fuse with the vacuole (Yorimitsu and Klionsky, 2005). Examples of key Atg proteins include Atg8p and Atg12p, which are involved in autophagosome expansion, and Atg1p, which is required for the initiation of autophagy (Ohsumi, 2001). In addition, the cytoplasm-to-vacuole targeting (CVT) pathway is a form of selective autophagy process in the yeast *Saccharomyces cerevisiae*. It facilitates the transport of specific cytoplasmic proteins to the vacuole for degradation (Klionsky, Cueva and Yaver, 1992). This CVT pathway plays a critical role in ensuring the proper functioning and maintenance of the vacuole in yeast.

In addition, vacuoles can also be formed *de novo* which is an alternative pathway of forming vacuoles when vacuoles are not inherited during cell division. Basically, when cells exhibit defects in vacuole inheritance, they undergo arrest in the G1 phase until a new vacuole is formed *de novo* in the bud. The proteins Pep12 and Vps45 are essential for the *de novo* formation of vacuoles. Once the newly formed vacuole matures, the TORC1-Sch9 pathway is activated, leading to the resumption of the cell cycle (Jin and Weisman, 2015).

1.2.2 Maintenance of vacuoles

Vacuoles abundance and proliferation is important for proper vacuole function and for the ensurance of cellular homeostasis. Cells growing under normal conditions contain approximately (2-3) medium sized vacuoles. This number may change from one single large vacuole in hypo-osmotic media to, multiple small lobes in hyper-osmotic media reviewed in (Li and Kane, 2009). Vacuoles undergo continuous cycles of inheritance, fusion, and fission, which contribute to their proper proliferation and distribution within the cell. During cell division, vacuoles are distributed between the mother cell and the daughter cell to ensure that both cells have functional vacuoles. This process is regulated by a set of proteins called the vacuole inheritance machinery, which includes the Myo2 motor protein, the Vac17 adaptor protein, and the Vac8 tethering protein (Tang et al., 2003; Hill et al., 1996; Wang et al., 1998). The fusion of vacuoles is an essential process for vacuole proliferation and

maintenance. This process is mediated by SNARE and HOPS complexes and the Rab GTPase Ypt7 protein (Wada and Anraku, 1992; Nichols *et al.*, 1997; Price *et al.*, 2000; Wurmser, Sato and Emr, 2000). The CORVET subunits are also involved in facilitating the tethering of endosomes to vacuoles and promote membrane fusion (Balderhaar and Ungermann, 2013).This process is then followed by the process of vacuole fission which is necessary for generating new vacuoles and maintaining their proper size and distribution within the cell. Vacuole fission is regulated by a set of proteins called dynamin-like proteins, such as Vps1 which is involved in membrane remodelling and scission (Peters *et al.*, 2004).

1.2.3 Disorders related to lysosomes/vacuoles.

Human lysosomes play various essential roles in the cell similar to those of the yeast vacuoles such as degrading the damaged organelles, macromolecules, and cellular waste. Not surprisingly, many inherited diseases have been identified that are the result of dysfunctional lysosomes. Among these diseases are the lysosomal storage diseases (LSDs). These (LSDs) include more than fifty different diseases due either to lysosomal enzyme dysfunction, or proteins responsible for lysosomal biogenesis (M. and A., 2011) and are characterised through the accumulation of the non-degraded products within the lysosome (Platt *et al.*, 2018). One of the most well-characterised LSDs is Gaucher disease, which is caused by an autosomal recessive disease in which the glucocerebrosidase enzyme is not efficiently functional due to a mutation in the GBA1 (acid-beta-glucosidase) gene. This mutation results in an accumulation of abnormal lipids in lysosomes which leads to a spectrum of phenotypical variations (Grabowski, 2008; Nagral, 2014). This disease is classified into three types based on the severity and presence of neurological symptoms. It can appear as hepatosplenomegaly, anaemia, thrombocytopenia, and skeletal abnormalities, among other symptoms (Cox, 2010).

Another LSD is the Niemann-Pick disease, which is characterised by an accumulation of cholesterol and other lipids inside lysosome. It is a disease that is divided into different categories due to a mutation in the genes *NPC1* or *NPC2* (Vanier, 2010, 2015). In addition, Btn1 is a protein that has been shown to be required for maintaining cellular arginine levels in yeast. When the human homolog of Btn1p (CLN3) loses functionality, it leads to juvenile Batten disease. Gaining insight into Btn1p's role may help uncover not only the foundation of this illness but also the processes that control amino acid storage in vacuoles and lysosomes

(Vitiello, Wolfe and Pearce, 2007). Lastly, Fabry disease, which is another LSD disease that can occur due to mutations in the GLA gene which is responsible for producing the lysosomal enzyme alpha-galactosidase A. Deficiency of this gene results in the accumulation of the globotriaosylceramide (Gb3) and related glycosphingolipids in different cells such as endothelial cells and the smooth muscle cells of blood vessels (Mehta *et al.*, 2010). Fabry disease can cause many deficiencies, including neuropathic pain, angiokeratomas, renal dysfunction, and cardiovascular complications (Mehta *et al.*, 2010), suggesting that an early diagnosis and management of Fabry disease is important for improving the long-term prognosis and quality of life.

1.3 Peroxisomes

Peroxisomes are conserved single membrane-bound organelles present in eukaryotic cells. They house different metabolic reactions that are important to cell metabolism including ß-oxidation of fatty acid, detoxification, and some biosynthetic processes such as plasmalogen biosynthesis in animals (Smith and Aitchison, 2009; Sibirny, 2016). Peroxisomal functions are different between cell types, organisms, or environmental conditions. They mainly possess the β-oxidation in yeast and plant cells. In mammalian cells, peroxisomes can degrade very long and branched fatty acid chains whereas long, medium, and short fatty acid chains are oxidised in mitochondria. Substrate specificity is the only regulatory mechanism that distinguishes peroxisomes from mitochondria in β-oxidation (Fidaleo, 2010). They are also partially responsible for the synthesis of cholesterol, docosahexaenoic acid as well as plasmalogens. Plasmalogens are ether lipids that are structurally essential in myelin sheath in nerve cells in mammals. In addition, peroxisomes have many enzymes responsible for degradation of cholesterol to bile acids (Pedersen, 1993). Peroxides and superoxides are toxic oxides that damage biomolecules, but this process can be prevented by peroxisomal enzymes like catalase, manganese superoxides dismutase and copper-zinc dismutase (Pedersen, 1993). Besides the core functions in fatty acid oxidation and other hydrogen peroxide forming oxidation reactions many other processes rely on peroxisomes including for instance methanol and amino acid degradation and biosynthesis of lysine in yeasts and glycolysis in Kinetoplastida (Brown and Baker, 2003; Al-Saryi *et al.*, 2017).

1.3.1 Peroxisome biogenesis

Peroxisomes biogenesis is mediated by genes called *PEX* genes. They encode for various proteins called peroxins or Pex proteins. In *S. cerevisiae* there are about 30 *PEX* genes **(listed in**

Table 1.3) discovered with roles in different phases of peroxisomes biogenesis including i) peroxisomal membrane biosynthesis, ii) matrix protein import and iii) peroxisomes proliferation.

Table 1.3 List of genes associated with peroxisomes biogenesis.

S. cerevisiae PEX Genes	Phases
PEX3, 19.	Membrane biosynthesis & ER to peroxisome transport
PEX,1, 2, 4, 5, 6, 7, 8, 9, 10, 12, 13, 14, 15, 17, 18, 20, 21, 22.	Matrix protein import
PEX11, 32, 34, 35, 25, 27, 28, 29, 30, 31, DNM1, VPS1.	Number, morphology, and fission.

The peroxisomal membrane contains a high level of lipids which their biosynthesis is dependent on the (ER) endoplasmic reticulum (Lazarow and Fujiki, 1985). It has been shown that Pex3 is involved in transporting these lipids from ER to the peroxisomes (Hoepfner *et al.*, 2005). In *S. cerevisiae*, deletion of *PEX3* and or *PEX19* have shown a peroxisomal structural deficiency (Hettema *et al.*, 2000). However, it was stated that *pex3Δ* cells contained pre-peroxisomal structures with Pex13 and Pex14 proteins (Wróblewska *et al.*, 2017), and the same pre-peroxisomal structures have been shown also in both *pex3Δ* and *pex19Δ* cells in *Hansenula polymorpha* (Knoops *et al.*, 2014). The peroxisomal membrane proteins (PMPs) are divided into different classes according to their sorting to the peroxisomal membrane in various pathways based on the involvement of Pex19 (Hettema *et al.*, 2014). Newly synthesised Class I of PMPs can be recognised and bound by Pex19. This complex subsequently docks on the peroxisomal membrane by binding to Pex3 (Jones, Morrell and Gould, 2004), before the PMPs are inserted into the membrane. Class II PMPs are translocated to peroxisomes without binding to Pex19 and docking onto Pex3 and are thought to travel

from ER to peroxisomes. Class III of PMPs are the Pex13 and Pex14 based on their presence in the pre-peroxisomal structure in *pex3Δ* and *pex19Δ* cells in *H. polymorpha* and *pex3Δ* cells in *S. cerevisiae.* However, the origin of the peroxisomal membranes and how these proteins are inserted into it is not yet clear.

The import of peroxisomal matrix proteins relies on a group of peroxins, with Pex5 and Pex7 playing major roles (Stanley *et al.*, 2006; Pan, Nakatsu and Kato, 2013). These peroxins are responsible for recognizing specific signals known as PTS1 and PTS2 on the peroxisomal matrix proteins. The PTS1 signal peptide is typically located at the C-terminus of most peroxisomal matrix proteins, while the PTS2 signal peptide is found near the N-terminus of a limited number of enzymes(Subramani, 1993; Titorenko and Rachubinski, 2001). The import process initiates with the recognition of cargo containing the PTS signals within the cytosol, which can be recognised by either the PTS1 receptor, Pex5, or the PTS2 receptor, Pex7 (Pan, Nakatsu and Kato, 2013). Receptor-cargo complexes on the peroxisomal membrane associate with a specific docking complex (Pex13/Pex14/Pex17). After that, Pex14 assembles with the import complex in order to form a transient pore then the cargo proteins transported into the peroxisomal matrix by an unknown mechanism (Platta, Girzalsky and Erdmann, 2004). Pex8 or Pex14 are suggested to be involved in cargo release in the peroxisome lumen. The import receptor undergoes monoubiquitination at a conserved cysteine residue through a collaborative action involving an E2-enzyme complex composed of Pex4 and Pex22. This process occurs in tandem with E3-ligases called RING-peroxins (Pex2, Pex10, Pex12) (Ma and Subramani, 2009). Subsequently, the ubiquitinated import receptor is released through an ATP dependent pathway by Pex1 and Pex6. During the last stage, the ubiquitin moiety is removed, and the receptor goes into a new cycle of targeting and importing **Figure 1.2** (Hettema *et al.*, 2014).

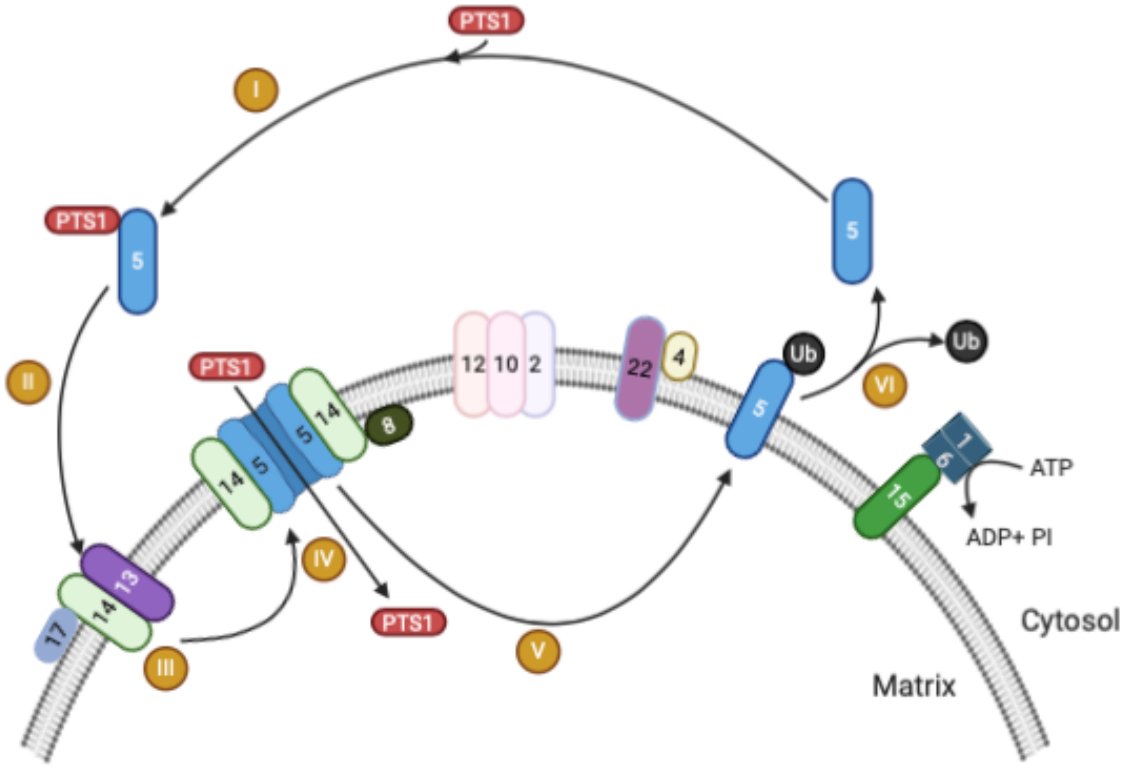

Figure 1.2 A diagram illustrating the sequential events in the import of peroxisomal matrix proteins is presented (adapted from Hettema et al., 2014). The import process consists of six main steps: cargo recognition by the receptor (I), docking of the cargo at the peroxisome membrane (II), formation of a pore (III), release of the cargo (IV), followed by receptor ubiquitination (V) and subsequent removal from the peroxisomal membrane for recycling (VI).

Peroxisomes proliferation involves three subsequent phases i) elongation ii) constriction iii) fission and the role of the Pex11 family in this process has been extensively studied and thoroughly understood. In most fungal species, the Pex11 family contains Pex11, Pex25 and Pex27. In yeast, Pex11 has been shown to be required for the tubulation of the peroxisomes (Opaliński *et al.*, 2011). Pex25 has also been shown to induce the elongation of peroxisomes but only under conditions when it is over-expressed (Huber *et al.*, 2012). Peroxisome constriction is the following phase after elongation and the molecular mechanism and essential proteins for this are currently unknown. Finally, peroxisome fission in yeast is controlled by the dynamin-related proteins (Drps) GTPases Vps1 (Vacuolar Sorting Protein 1) and Dnm1. Peroxisomes in cells lacking Dnm1 and Vps1 will eventually be enlarged and elongated and pulled to the bud via well characterised transport and tethering mechanisms. The recruitment of Dnm1 to the peroxisomal membrane is facilitated by the anchored protein Fis1 (Fission 1). This process also relies on the involvement of helper proteins Caf4 and Mdv1.(Motley, Ward and Hettema, 2008; Kaur and Hu, 2009). However, the Vps1 acts

independent of Fis1, and new data has indicated that Pex27 is playing a role in Vps1-dependent peroxisomes fission (Ekal, Alqahtani and Hettema, 2023). The Vps1 dependent peroxisome fission in *S. cerevisiae* is more dominant than Dnm1 whereas in *H. polymorpha* Dnm1 is more prominent in peroxisomes fission (Nagotu et al., 2008; Motley et al., 2008).

In mammalian cells, Pex11 has three different isoforms Pex11 α, β, and γ, reviewed in (Kiel, Veenhuis and van der Klei, 2006). Drp1 (The dynamin related protein) is also involved in peroxisome fission in mammalian cells, (Li and Gould, 2003). Analogous to Dnm1, Drp1 is targeted to the peroxisomal membrane via Fis1. In addition, the Mitochondria Fission Factor (Mff) is also another protein involved in peroxisome and mitochondria fission (Gandre-Babbe and Van Der Bliek, 2008). It has been demonstrated that Mff recruit Drp1 because siRNA mediated knockdown of Mff resulted in tubulated peroxisomes in mammalian cell (Otera *et al.*, 2010). The human Pex11ß has also been shown to interact with Fis1 through its C-terminus as well as it was found in a complex with Drp1, Fis1, and Mff (Kobayashi, Tanaka and Fujiki, 2007). Moreover, a recent study demonstrated that Pex11ß is capable of initiating peroxisome division without Mff, relying instead on a process dependent on both Drp1 and Fis1 (Schrader *et al.*, 2022). This shows that Pex11 is the initiator of the peroxisome fission process by i) modulating the peroxisome membrane followed by ii) recruiting Fis1 in which it recruits Drps to their active fission sites **Figure 1.3**.

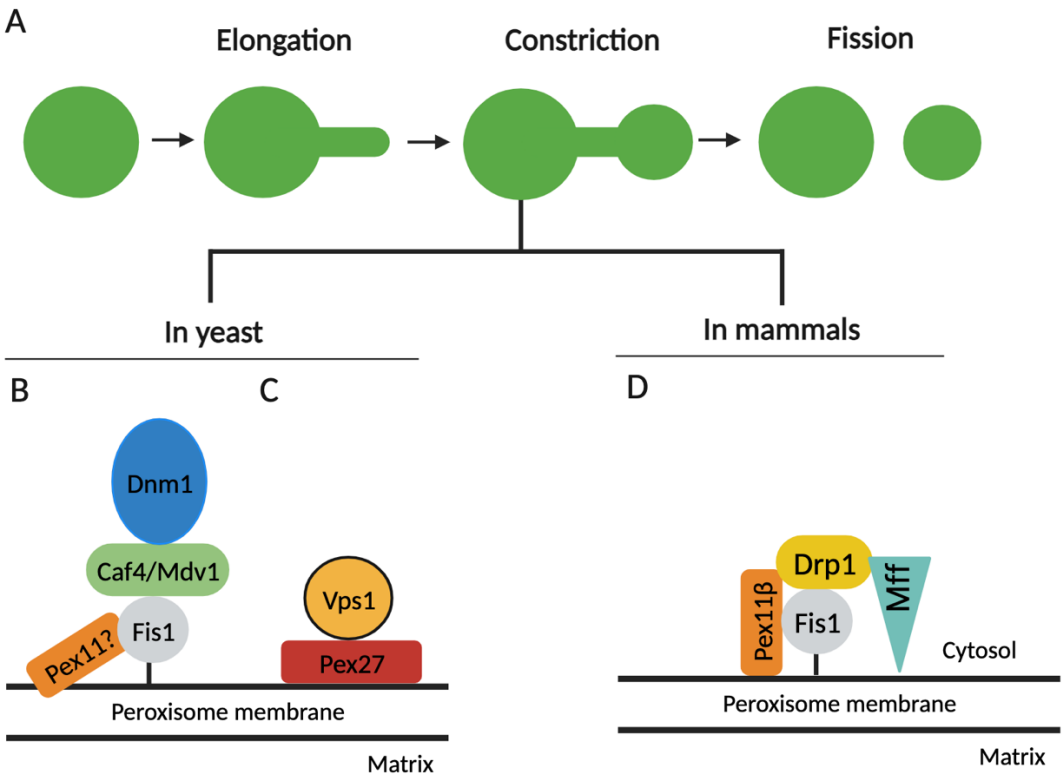

Figure 1.3 Several models have been proposed for the recruitment of fission machinery in both *S. cerevisiae* and mammalian cells. A) Peroxisome undergoes 3 different stages of elongation; constriction; and fission in the growth and division model B) The recruitment and function of peroxisomal Dnm1 rely on various elements, including Pex11, Fis1, and Mdv1/Caf4. C) Despite Vps1 being the primary dynamin-related protein (DRP) required for peroxisome fission, Pex27 has been shown to be necessary for Vps1-dependent fission. D) Drp1 is recruited to the peroxisomal membrane through its interaction with Fis1 and Mff. This complex also interacts with Pex11β.

1.3.2 Maintenance of peroxisomes

Peroxisome number and morphology can be maintained by four different processes i) *de novo* formation ii) peroxisome fission iii) pexophagy and iv) inheritance. Peroxisome number varies in cells based on growth conditions. Cells that grow in glucose medium have approximately (8-9) peroxisomes while cells growing in oleic-acid contain around (10-13) peroxisomes (Tower et al., 2011; Ekal et al., 2023). Some research implies that *de novo* formation takes place in all cells (Sugiura et al., 2017; Kim et al., 2006; Van Der Zand et al., 2012). The predominant evidence from yeast studies demonstrates that fission is the favoured method of multiplication (Knoops et al., 2015; Menendez-Benito et al., 2013; Motley and Hettema, 2007; Knoblach et al., 2013; Motley et al., 2015). Several detailed studies found that *pex3Δ* and *pex19Δ* cells devoid of peroxisomal membrane and upon the reintroduction of the wild

type copies of *PEX3* and *PEX19* the peroxisome structure start to appear again (Hohfeld et al., 1991; Hettema et al., 2000). In addition, it has been observed that *de novo* formation of peroxisomes can occur in cells that experience a temporary absence of these organelles (Motley et al., 2015; Motley and Hettema, 2007). Many studies have indicated that *de novo* formation originates from the endoplasmic reticulum (ER) (Hoepfner *et al.*, 2005). Different concepts regarding peroxisome biogenesis have been proposed in models revolve around the idea of vesicular transport from the ER to (pre)peroxisomes reviewed in (Hettema *et al.*, 2014). There are several reports have shown that fission is a key mechanism to control peroxisomes number (Motley and Hettema, 2007; Knoblach et al., 2013; Lazarow and Fujiki, 1985; Menendez-Benito et al., 2013; Motley et al., 2015). Under starvation conditions peroxisomes are degraded via a form of selective autophagy called, pexophagy (Klionsky, 1997; Hutchins et al., 1999;). Pexophagy is dependent on the ability of Pex3 to recruit the pexophagy receptor, Atg36 (Motley, Nuttall and Hettema, 2012a, 2012b). The protein kinase such as Hrr25 has been shown to be activated during starvation to induce pexophagy which eventually leads to the phosphorylation of Atg36 *in vivo* (Tanaka *et al.*, 2014). Furthermore, peroxisome inheritance is a highly efficient process in segregating peroxisomes and ensures maintenance of peroxisomes in both daughter cell and mother and this is described more fully below in **Section 1.9**

1.3.3 Disorders related to peroxisomes

Peroxisomes are essential in maintaining metabolism, and consequently the survival of an organism. Peroxisome dysfunction, due to mutations in over 30 genes responsible for peroxisome biogenesis and function, has been shown to result in various disorders (Wanders, 2018). Disorders associated with peroxisomes can be categorised into two main groups: i) peroxisome biogenesis disorders (PBDs), and ii) peroxisomal enzyme deficiencies (PEDs). The PBD group comprises four distinct disorders, with Zellweger syndrome being the most severe form, followed by neonatal adrenoleukodystrophy (NALD), Infantile Refsum disease, and Heimler syndrome. Collectively, these disorders are referred to as Zellweger spectrum disorders (ZSDs). These disorders are autosomal recessive disorders involved in brain development abnormalities, hypotonia, craniofacial dysmorphia, and kidney and liver dysfunction. In addition, many enzymes are involved in a set of biochemical reactions in the peroxisomal matrix. In the case of PEDs, any enzyme deficiency will result in a disorder that

has symptoms shared with ZSDs. They are considered as consequences of enzyme deficiencies responsible for β-oxidation, ether phospholipid synthesis, alpha-oxidation and peroxide detoxification (Steinberg et al., 2019; Fidaleo, 2010; Klouwer et al., 2015; Wanders, 2018).

Proteins required for peroxisome maintenance such as Drp1, Mff, and Pex11β have been shown to be linked to some diseases. The blinding disease optic atrophy is linked to Drp1 missense mutations (Gerber *et al.*, 2017). The loss Mff protein function has been shown to be linked to Leigh-Like encephalopathy, peripheral neuropathy and optic atrophy (Koch *et al.*, 2016). Patients with Pex11β deficiency experience neurological defects, eye problems, and loss of hearing (Taylor et al., 2017; Ebberink et al., 2012).

1.4 Lysosome and peroxisome motility in human cells

Lysosomes are dynamic organelles within human cells that display intricate movement, influenced by various factors. The microtubules, principal components of the cytoskeleton, provide the scaffolding for lysosome motility. Lysosomes traverse along these microtubules in a bidirectional manner, their positioning regulated by the equilibrium between plus-end (outward) and minus-end (inward) directed movements. This complex movement is coordinated by motor proteins, particularly dynein and kinesin, which facilitate the minus-end and plus-end directed transport, respectively **Figure 1.4 A** (Pu *et al.*, 2016).

The positioning and motility of lysosomes are crucially regulated to align with cellular requirements. In response to nutrient availability, lysosomes reposition themselves; they migrate towards the cell periphery under nutrient-rich conditions and relocate towards the centre during nutrient scarcity, thereby optimizing macromolecule degradation. Lysosome positioning is also sensitive to cell adhesion and migration dynamics; during cell migration, lysosomes progress towards the cell periphery, supplying necessary constituents for membrane expansion. However, defects in lysosome positioning and motility, such as those caused by mutations in dynein and kinesin genes, can result in pathological conditions, including neurodegenerative diseases (Wijdeven *et al.*, 2016; De Pace *et al.*, 2018).

The BLOC-One-Related Complex (BORC) is a key player in the regulation of lysosome positioning. This multi-subunit complex, composed of eight distinct subunits, coordinates the positioning and movement of lysosomes along microtubules. BORC, acting as a critical switch,

recruits the small GTPase Arl8 and motor protein kinesin, initiating the outward movement of lysosomes, a process essential for cell migration, plasma membrane repair, and the distribution of specific signalling receptors **Figure 1.4 A**. Disruption of BORC function, however, culminates in lysosome accumulation near the cell nucleus, impeding their outward movement (Pu *et al.*, 2015). SKIP, also referred to as PLEKHM2 (Pleckstrin homology domain-containing family M member 2), plays a vital role in the regulation of lysosome positioning. SKIP is an effector protein of the small GTPase Arl8, which, as mentioned earlier, plays a vital role in directing the movement of lysosomes along microtubules.

SKIP binds to Arl8 and helps recruit the kinesin motor protein to the lysosomal surface, which in turn facilitates the lysosomes movement toward the cell periphery (Rosa-Ferreira and Munro, 2011). Rab Interacting Lysosomal Protein (RILP) is a key player in the regulation of lysosome positioning within the cell. RILP is a downstream effector of the small GTPase Rab7, which is predominantly associated with late endosomes and lysosomes. RILP plays a critical role in the minus-end-directed movement of lysosomes towards the microtubule-organizing centre (MTOC) near the cell nucleus. This is achieved through its interaction with the dynein-dynactin motor complex, which drives the inward movement of lysosomes along microtubules. Therefore, through the Rab7-RILP-dynein/dynactin pathway, lysosomes are positioned towards the centre of the cell (Cantalupo *et al.*, 2001; Jordens *et al.*, 2001).

The movement and positioning of peroxisomes is primarily mediated by the cell's cytoskeletal network and motor proteins. Microtubules and actin filaments are the primary components of the cytoskeleton that play essential roles in facilitating peroxisome transport. Microtubules often provide long-distance transport for peroxisomes, while actin filaments are involved in short-distance transport and precise positioning (Wiemer *et al.*, 1997). The motor proteins dynein and kinesin mediate the movement along these tracks, with dynein responsible for the retrograde transport (toward the cell centre) and kinesin for the anterograde transport (toward the cell periphery) (Schrader *et al.*, 2000).

Miro (Mitochondrial Rho GTPase) is a well-studied protein primarily known for its role in the dynamics and motility of mitochondria. It is anchored in the outer mitochondrial membrane and acts as a receptor for the motor/adaptor protein complex, thus linking mitochondria to

the cytoskeleton and enabling their movement along microtubules (Schrader and Fahimi, 2006). Recent studies have discovered that Miro also plays a crucial role in peroxisome motility. In mammalian cells, Miro proteins have been shown to be localised at the peroxisomal membrane, where they facilitate peroxisome transport along microtubules **Figure 1.4 B** (Nemani *et al.*, 2018). The TRAK family of proteins, including TRAK1 and TRAK2, are well-known for their role in mitochondrial trafficking. They function as adaptor proteins linking mitochondria to motor proteins on microtubules, thereby mediating mitochondrial movement along these cytoskeletal tracks (Smith *et al.*, 2006).

This is achieved through their binding to the Miro GTPases on the mitochondrial surface and to the kinesin motor proteins on microtubules. Similar to their function in mitochondria, TRAK proteins have recently been implicated in peroxisome motility. Studies have shown that TRAK1, in particular, can interact with the Miro proteins present on the peroxisomal membrane, forming a complex that allows peroxisomes to attach to kinesin motor proteins and move along microtubules (Nemani *et al.*, 2018). This indicates that peroxisomes and mitochondria share similar machinery for their movement within mammalian cells. The peroxisomal membrane protein Pex14 may contribute to this process by being as a docking factor to microtubules (Castro *et al.*, 2018). The mechanism appears to be similar to that in mitochondria, involving interaction with motor proteins and regulation of peroxisome motility in response to changes in the cellular environment (López-Doménech et al., 2018; Castro et al., 2018).

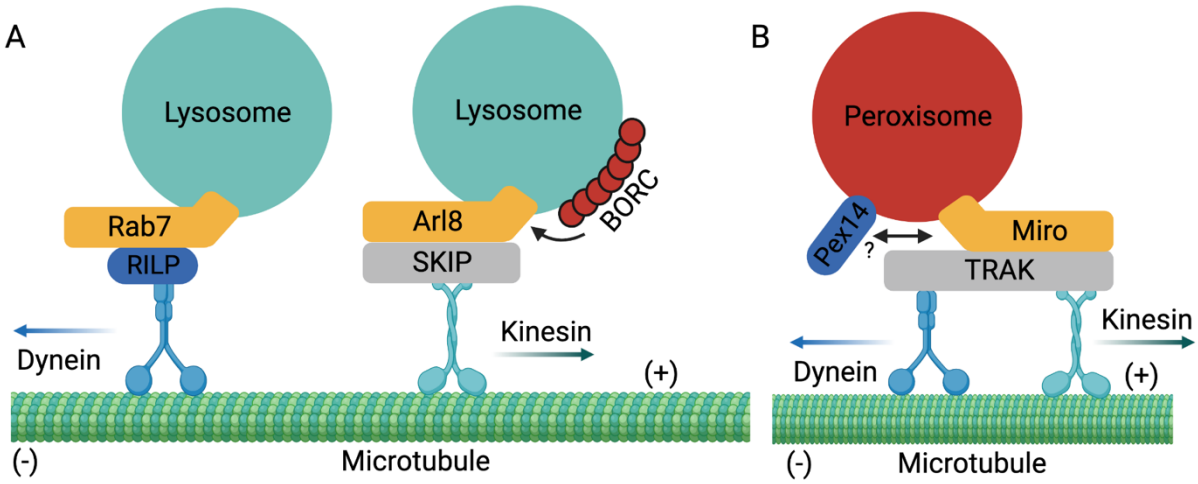

Figure 1.4 The current models showing the lysosome and peroxisome motility in mammals. A) Rab7 and RILP form a complex with dynein for lysosome minus-end directed movement. Arl8 and SKIP are required for the plus-end movement with kinesin. B) The tail-anchored Miro protein is targeted to

peroxisome by Pex19. TRAK and Miro form a complex with both kinesin for plus-end and dynein for minus-end movement.

1.5 Intracellular organelle inheritance, from the attachment of the cargo to the Myosin V motors to the detachment.

The movement of organelle is one of the essential responses to stimuli and that for maintaining the cellular homeostasis. Organelles must multiply and be transported to their appropriate locations to ensure inheritance. They change their morphology and locations based on the cell requirement, for instance during cell division (Jongsma, Berlin and Neefjes, 2015). Organelle transport is an accurate mechanism facilitated by molecular motors that require several highly regulated mechanisms. For instance, in the well-studied yeast *Saccharomyces cerevisiae* organelle transport start with i) The attachment of the organelle to the myosin motor through its receptor with actin filaments oriented to the correct orientation. ii) The motor protein movement along actin filaments toward the growing bud. iii) The termination process by which the organelle is unloaded from the myosin motor when positioned in the proper location in the bud. Same regulation of organelle transport is also applied in human cells, where the proper orientation of the cytoskeletal tracks, the movement of the motor on the cytoskeleton, and the attachment and detachment of organelles on the motor are regulated. In human cells, the long-range organelle transport is primarily on microtubules using dynein and kinesin motors. However, the short-range transport or tethering at the cell periphery are carried on actin networks where the cargoes can be transferred from kinesin to myosin V motors (Hancock, 2014). On the other hand, in *Saccharomyces cerevisiae,* the transport of some organelles is carried out on myosin V motors utilising actin filaments (Weisman, 2006).

Organelle inheritance is a process that required coordination with the cell cycle and regulated in a spatial and temporal manners (Peng and Weisman, 2008a; Legesse-Miller et al., 2006). In the following sections, current understanding of the dynamics of organelle inheritance primarily in *S. cerevisiae* will be outlined, with a particular in focus on vacuole and peroxisome inheritance during cell division.

1.6 Regulation of Myosin V Mediated Transport

Budding yeast possesses two myosin V proteins, namely Myo2 and Myo4, whereas human cells contain three isoforms of myosin V, namely Va, Vb, and Vc (Lu et al., 2014; Hammer and Wagner, 2013). Myosin V proteins primarily consist of three domains: motor, neck, and cargo binding domain (CBD) **Figure 1.5**. Each one of these domains has a specific function. The movement along actin cables requires the motor and the neck domains to ensure efficient transportation. The motor domain is responsible for binding to actin filaments and plays a crucial role in ATP hydrolysis, which provides the necessary energy for the motor domain to move along actin (Trybus, 2008). The neck domain regulates motor domain movement. It contains IQ motifs that are binding sites for Mlc1 (the myosin light chain) and calmodulin in yeast to provide stability (Stevens and Davis, 1998; Brockerhoff et al., 1994). Calmodulin is responsible for recruiting calcium which triggers a conformational change of the myosin V to activate the movement (Wang et al., 2004; Trybus et al., 2007). It has been demonstrated that in mammalian cells, calcium plays a regulatory role in controlling the activity of myosin Va. Specifically, it alleviates the inhibitory conformation of myosin Va, leading to its activation *in vitro*.

Auto-inhibition is a state in which the motor protein is inactively folded, with both the motor domain and the cargo binding domain bound to each other. This inactive state can be changed when the motor protein is binding to the cytoskeleton and/or cargo (Sckolnick et al., 2013; Li et al., 2005). Auto-inhibition is found in both actin and microtubule-based motors. Auto-inhibition of kinesin and dynein (the microtubules based motors) can be relieved on binding to adaptor proteins or cargo (Verhey and Hammond, 2009; Hammond *et al.*, 2010; Torisawa *et al.*, 2014; Kelliher *et al.*, 2018; Qiu, Zhang and Xiang, 2019; Siddiqui *et al.*, 2019). It has been shown in an *in vitro* study that myosin Va in mammalian cells exhibited both extended and auto-inhibition conformations, where the motor domain is docked to the cargo binding domain in the auto-inhibited structure (Heissler and Sellers, 2016; Li et al., 2004; Liu et al., 2006; Sato et al., 2007a; Krementsov et al., 2004; Wang et al., 2004; Thirumurugan et al., 2006;). Moreover, a yeast study has identified the potential docking sites for both motor and cargo binding domains and demonstrated, through genetic mutants, that auto-inhibition may play a role in cargo transport (Donovan and Bretscher, 2015).

The myosin V cargo binding domain (CBD) is the domain responsible for the attachment and detachment of the cargoes. This domain is required for the transport of organelles to their proper cellular locations. It can attach through organelle-specific adaptors (Lu, Li and Zhang, 2014; Cross and Dodding, 2019). It has been shown that the yeast myosin V, Myo2, and the mammalian MyoVa have cargo binding regions where adaptor proteins are likely to bind in competition with each other (Taylor Eves *et al.*, 2012; Wei *et al.*, 2013; Tang *et al.*, 2019). This results in high competition between adaptors to bind their regions in a specific time and location. Even though the organelle adaptors are not conserved between yeast and humans, they do exhibit certain similarities in structural characteristics and regulatory mechanisms

Figure 1.6

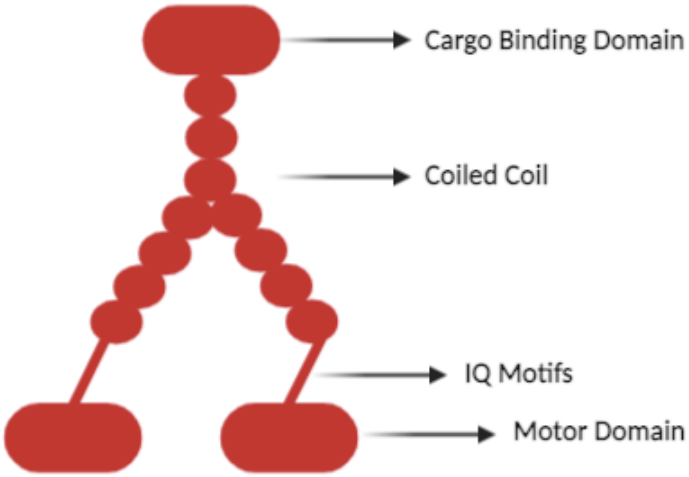

Figure 1.5 The distinct structural domains of myosin V. The IQ motif is responsible for binding to calmodulin and Mlc1 and the motor domain is required for ATP hydrolysis. The dimerization of myosin V occurs through the coiled coil domain.

There are several adaptors known to be required for binding to the cargo binding domain (CBD). In *Saccharomyces cerevisiae,* the myosin V, Myo2, and the vacuolar adaptor Vac17 are required for Vacuole transport (Hill et al., 1996; Catlett and Weisman, 1998). It was also shown that Myo2 binds to other adaptors such as Inp2 for peroxisome and Mmr1 for mitochondria (Simon et al., 1995; Fagarasanu et al., 2006a; Tang et al., 2019). The Rab GTPases such as Sec4 and Ypt11 have shown to be involved in secretary vesicles and Golgi late element inheritance due to their binding to Myo2 (Chernyakov et al., 2013; Jin et al., 2011; Lewandowska et al., 2013; Taylor Eves et al., 2012; Arai et al., 2008). In mammalian cells, the protein Rab11a interact to myosin Va and Vb to enhance membrane tethering

(Inoshita and Mima, 2017). Rab27a has been shown that it mediates melanosome inheritance by binding to melanophilin and myosin Va **Figure 1.6** (Barral and Seabra, 2004).

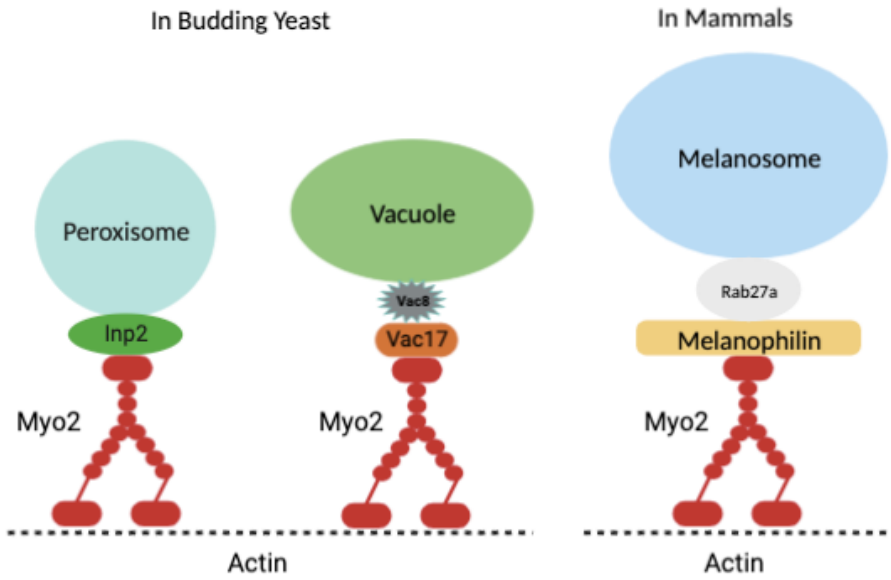

Figure 1.6 Different organisms with conserved mechanism of binding to cargo adaptors. Although adaptors proteins are not conserved across organisms, the mechanism attaching the motor to the organelle is likely similar. In yeast, vacuole can be attached to Myosin V via Vac17 and Vac8, and Inp2 for peroxisome, while in mammals the myosin Va attaches to melanophilin and Rab27a for melanosome transport.

The movement of an organelle is initiated after the binding between the Myosin V and its organelle-specific adaptor. This binding is causing conformational changes to the myosin V as shown in mammalian and yeast cells (Tang et al., 2019; Pylypenko et al., 2013). Also, this binding is considered to activate the motor and enhance the track selection and actin-binding (Oberhofer et al., 2017; Donovan and Bretscher, 2012; Knoblach and Rachubinski, 2016; Weisman, 2006; Westermann, 2014)

When the organelle reaches its required destination, it detaches from myosin V in which the organelle inheritance is terminated (Tang *et al.*, 2003). It has been shown that CK2 can phosphorylate myosin V to release the cargo during mitosis (Karcher *et al.*, 2001). In addition, during melanosome transport, melanophilin, the melanosome myosin adaptor has been shown to be phosphorylated and ubiquitylated to release the melanosome from myosin V (Rogers *et al.*, 1999). In *Saccharomyces cerevisiae,* it was shown that cargo release from

myosin V is regulated and coordinated with the cell cycle. The degradation of organelle adaptors is also highly regulated indicating that this mechanism requires proper release of the cargo in the proper location. Taken together, the mammalian melanosome adaptor melanophilin, and the yeast vacuolar adaptor Vac17, have been shown to be phosphorylated and ubiquitylated in the same manners then degraded by the proteasome (Yau *et al.*, 2014; Yau, Wong and Weisman, 2017; Park *et al.*, 2019). This indicates that the mechanism of cargo transport and release shared some similarities.

1.7 Myosin V-dependent organelle transport in Yeast

In the model organism *Saccharomyces cerevisiae,* during cell division, Myo2 and Myo4 are required for transporting cargoes from the mother cell to the bud (Bretscher, 2003; Weisman, 2006; Knoblach and Rachubinski, 2015a). Myo2 has been shown to be responsible for peroxisome, vacuole, mitochondria, secretory vesicles, lipid droplets, and late Golgi transport to the bud (Simon, Swayne and Pon, 1995; Hill, Catlett and Weisman, 1996; Catlett and Weisman, 1998; Pruyne, Schott and Bretscher, 1998; Hoepfner *et al.*, 2001; Arai *et al.*, 2008; Knoblach and Rachubinski, 2015b). It has been shown that Myo2 is involved in microtubule spindle positioning during mitosis (Yin et al., 2000; Hwang et al., 2003; Miller et al., 2000; Lee et al., 2000; Liakopoulos et al., 2003). It also has a role during mating where it can transport Fus2 protein to the bud tip for breaking down the cell wall. On the other hand, Myo4 has been shown to be required for transporting messenger ribonucleoprotein (mRNA) such as She3 for the transport of cortical ER and She2 for Ash1 mRNA transport (Long *et al.*, 2000; Estrada *et al.*, 2003; Dunn *et al.*, 2007; Sheltzer and Rose, 2009; Singer-Krüger and Jansen, 2014) **Figure 1.7**.

The binding between the motor proteins and the adapters can also be regulated by other regulatory mechanisms. For instance, Cdk1 phosphorylates Myo2, and Vac17 which is essential for vacuole transport. Interestingly, other adaptors such as Inp2 for peroxisome and Mmr1 for mitochondria contain putative Cdk1 sites, thereby suggesting that this may be a common regulatory step in transport complex assembly (Peng and Weisman, 2008a). The Rab GTPases such as Rab11a and Rab27a are also regulating the binding of myosin to their cargoes in mammalian cells (Inoshita and Mima, 2017). In addition, the regulation of organelle inheritance requires multiple events, including the specific regulation of the organelle

adaptors and a wider regulation that regulate the overall organelle inheritance. For example, the protein kinase Ptc1 has been shown to be involved in stabilizing the mitochondria, vacuole, and peroxisome adaptors during inheritance (Roeder *et al.*, 1998; Jin *et al.*, 2009). Another example is the Rab Ypt11 is required for binding to Myo2 binding to regulate mitochondria, ER, and late Golgi elements inheritance, respectively (Itoh *et al.*, 2002; Buvelot Frei *et al.*, 2006; Arai *et al.*, 2008; Chernyakov, Santiago-Tirado and Bretscher, 2013).

Many Myo2 adaptors contain PEST sequences. This sequence is responsible for rapid protein degradation and is frequently regulated. It is typically contain a high abundance of glutamic acid, serine, proline, and threonine amino acid residues (Rechsteiner and Rogers, 1996). It has been shown that Myo2 organelle adaptors, Vac17, Inp2, Mmr1 and the astral microtubule adaptor, Kar9, contain PEST sequences and are degraded in the bud during organelle transport termination (Tang *et al.*, 2003; Fagarasanu *et al.*, 2006; Kammerer, Stevermann and Liakopoulos, 2010; Obara *et al.*, 2022). Taken together, this indicates the conserved mechanisms occurred during cell division across different organelles.

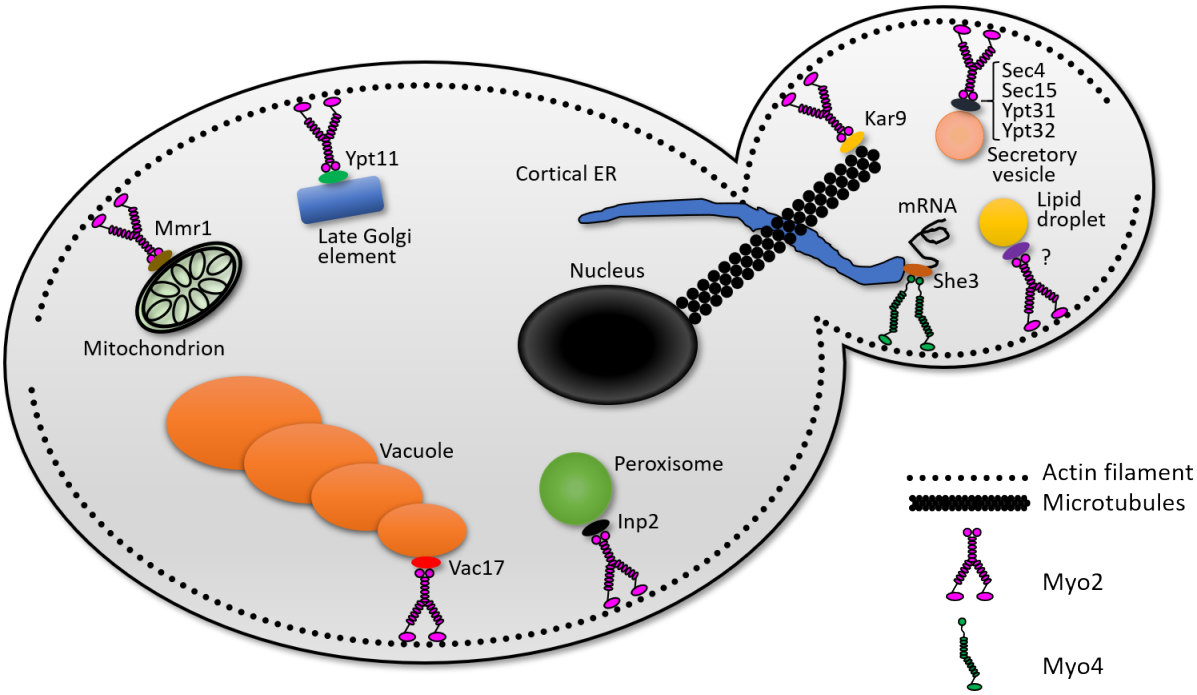

Figure 1.7 Organelle inheritance in *S. cerevisiae*. Myo2 and Myo4, are crucial for transporting organelles along actin towards the budding cell. Myo2 consists of two distinct regions that form the CBD. Depending on their interaction with these regions, Myo2 receptors are classified into two groups. Mmr1 and Vac17 compete for one site, while Inp2, Kar9, Sec4, and Rab GTPases utilise another site.

1.8 Vacuole inheritance

As described above **(Section 1.2)** vacuoles in yeast are similar to lysosomes in mammals. The mechanisms involved in the inheritance of vacuoles during cell division have been well-studied compared to other yeast organelles. It has been shown that vacuole inheritance requires the presence of actin filaments and the myosin V Myo2 protein (Hill, Catlett and Weisman, 1996). Specific amino acids on Myo2 cargo binding domain have been shown to be specifically required for vacuole inheritance (Ishikawa *et al.*, 2003). These are D1297, D1296, E1293, N1304, G1248. Vacuole inheritance is also regulated throughout the cell cycle (Gomes de Mesquita et al., 1991; Jin and Weisman, 2015; Weisman et al., 1987; Raymond et al., 1990; Weisman and Wickner, 1988). During the G1 phase, vacuoles can form tubular/vesicular structure known as (Segregation structures) that originate from the vacuole's side nearest to the emerging bud and move from the mother to the bud by the myosin V motor Myo2 (Weisman, 2006). This transport is firstly controlled in a temporal and spatial manner where the cyclin-dependent kinase, Cdk1, phosphorylates Myo2 and Vac17. The phosphorylation is critical for their interaction (Peng and Weisman, 2008a).

This interaction between Vac17 and Myo2 in the mother cell is regulated via another vacuolar membrane protein Vac8. Vac8 is an armadillo protein containing eleven continuous armadillo (ARM) repeats. These repeats are characterized by a series of alpha-helical segments that fold into a superhelical structure, usually required for protein-protein interaction suggesting that they are required for many Vac8 functions (Pan and Goldfarb, 1998; Wang, Catlett and Weisman, 1998). Vac8 is an essential protein for vacuole maintenance that can be associated with vacuole via myristylation and palmitoylation (Wang, Catlett and Weisman, 1998; Tang *et al.*, 2006). Once the Myo2-Vac17-Vac8 transport complex is formed, the transport of vacuoles is started. A recent study on Vac8 structural analysis revealed the Vac8/Vac17 complex and identified the regions on Vac8 required for the interaction with Vac17 and vacuole inheritance *in vivo* (Kim *et al.*, 2023). Even though the Vac17/Myo2 complex has not been resolved, a bioinformatic study followed by an *in vitro* analysis identified the possible Myo2/Vac17 interaction regions (Liu *et al.*, 2022), this interaction region is affected by Myo2 CBD mutations previously identified genetically to interfere with vacuole inheritance (Taylor Eves *et al.*, 2012).

The interaction between Vac17 and Myo2 can be released by degrading Vac17 once at the bud tip leading to release of the vacuole (Yau et al., 2014, 2017; Tang et al., 2003). This process is known as vacuole inheritance termination. It is known that Vac17 is regulated during the cell cycle by translation, phosphorylation, and degradation and its levels peak during the time of vacuole inheritance (Tang *et al.*, 2003; Peng and Weisman, 2008a). The E3 ubiquitin ligase Dma1 has been shown to ubiquitinate Vac17 for proteasome degradation (Yau *et al.*, 2014). This degradation of Vac17 is regulated by its PEST motif (Tang *et al.*, 2003). Even though it was shown the secretory vesicles are transported to the mother-bud neck with Myo2 (Schott et al., 1999; Govindan et al., 1995; Pruyne et al., 1998), vacuoles are not transported back to the mother-bud after they are deposited into the bud. However, in some mutant backgrounds, vacuoles remain attached to Myo2 and are incorrectly transported to the mother bud-neck later in the cell cycle (Yau *et al.*, 2014; Yau, Wong and Weisman, 2017; Wong *et al.*, 2020).

In these mutants, Vac17 breakdown is prevented, and vacuoles are mis-positioned. The key regulators of vacuole inheritance termination process are the PAK kinases Cla4 and Ste20. They are localised to the bud cortex and have been shown to be involved in many cellular processes such as septin ring assembly, cytokinesis, and actin cytoskeleton polarization besides their role in vacuole transport (Peter et al., 1996; Boyce and Andrianopoulos, 2011; Cvrčková et al., 1995; Bartholomew and Hardy, 2009; Kumar et al., 2009). These kinases can stimulate a cascade of reactions by activating Dma1. When the vacuole reaches the bud, Cla4 phosphorylates Vac17, which leads to Vac17 ubiquitination by Dma1, then to degradation by the proteasome **Figure 1.8** (Yau *et al.*, 2014; Yau, Wong and Weisman, 2017). In addition, the casein kinase Yck3 and the Vps41 proteins are required for vacuole inheritance termination independent of the Cla4 and Dma1 pathway. They play roles in phosphorylating Vac17 and Myo2 at several phosphosites to release Vac17 and vacuole from Myo2. In the yeast strain with Vac17 mutations that prevent Yck3 and Vps41 phosphorylation, vacuoles remain bound to Myo2 and are subsequently transported to the mother-bud neck site suggesting that vacuole inheritance termination process is regulated by two independent pathways **Figure 1.8** (Wong *et al.*, 2020). It remains unclear why two

distinct mechanisms are needed to release vacuole and Vac17 from Myo2, particularly when defects in vacuole trafficking do not cause cell death. One possibility is that the degradation of Vac17 prevents the reformation of Myo2-Vac8-Vac17 which could result in sequestration of Myo2 and Vac8 from performing their other roles. Alternatively, Vac17 degradation might facilitate the synthesis of new Vac17 during the subsequent cell cycle, promoting vacuole transport. Thus, investigating vacuole transport further could shed light on the physiological rationale behind these mechanisms.

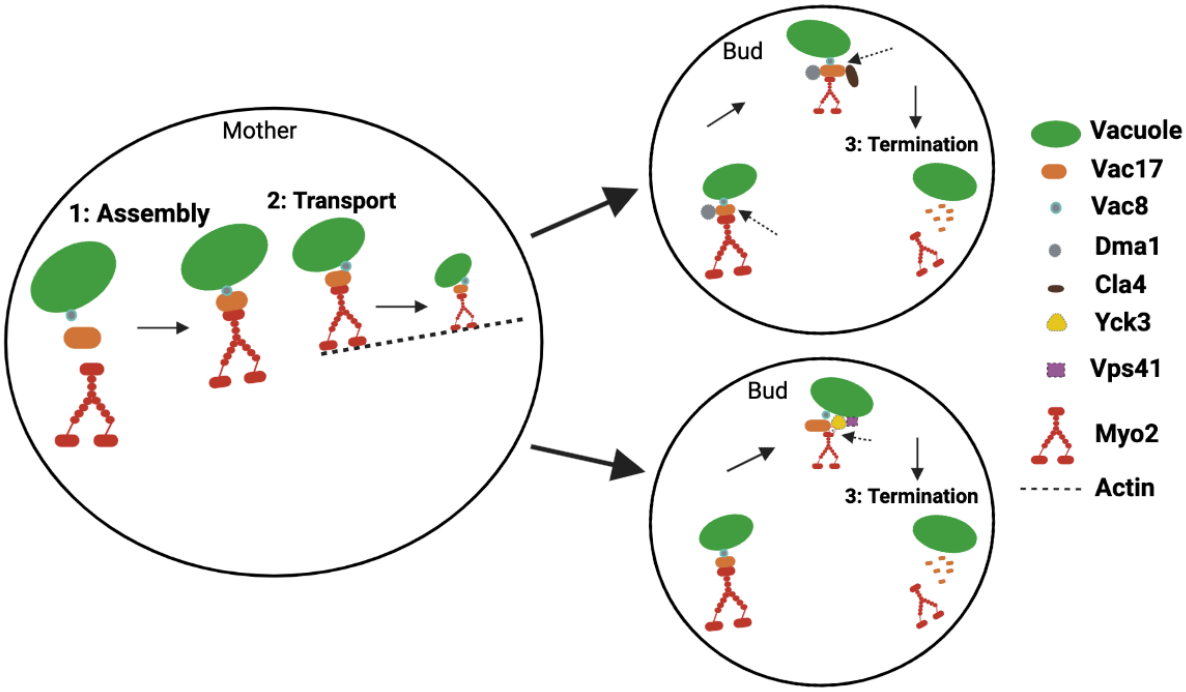

Figure 1.8 A schematic representation showing the current model of vacuole inheritance in *S. cerevisiae*. The model shows the three crucial steps in vacuole inheritance and the molecular factors involved in the process with the recent factors identified in vacuole inheritance termination where there are two independent pathways in regulating this process.

1.9 Peroxisome inheritance

In *S. cerevisiae,* peroxisomes are inherited by a process in which pre-existing peroxisomes grow and divide to generate new ones. It has been shown that peroxisome inheritance is dependent on the presence of actin filament and Myo2, the class V myosin motor protein (Hoepfner *et al.*, 2001). Peroxisome inheritance also requires polarization of the actin

cytoskeleton since it has been shown that they are closely associated and that the depolymerization of actin filaments results in peroxisome movement deficiency. It has been shown cells with a temperature sensitive mutant *myo2-66* peroxisome inheritance is abolished suggesting the movement of peroxisomes on actin filament is mediated by Myo2. This demonstrates that the migration of peroxisomes from the mother to the bud through the actin filament relies on Myo2 **Figure 1.9** (Hoepfner *et al.*, 2001).

Peroxisome inheritance in *S. cerevisiae,* is controlled by Inp1 and Inp2 proteins. Inp1 is a peripheral membrane protein that has been shown to be peroxisomal (Huh *et al.*, 2003). Inp1 is responsible for peroxisome retention in the mother cell and deleting the *INP1* gene frequently causes mother cells to lack peroxisomes compared to the bud. Additionally, overproducing *INP1* causes the retention of more peroxisomes in the mother cell (Fagarasanu *et al.*, 2005).

The peroxisomal membrane protein, Inp2, is recognised as a Myo2 adaptor for peroxisome. It mediates peroxisomal movement from the mother cell to the bud through its interaction with the Myo2 cargo binding domain (CBD) (Fagarasanu *et al.*, 2006). Another *in vitro* study has revealed the complex of Inp2 and Myo2 interaction suggesting that there is a specific Myo2 interaction site (MIS) on Inp2 specifically required for Inp2/Myo2 interaction and peroxisome inheritance (Tang *et al.*, 2019). Inp2 has been suggested to have a role in peroxisome division by coordinating between the peroxisome fission and transport and ensuring that there are an equal number of peroxisomes shared between the bud and the mother (Knoblach and Rachubinski, 2015).

Inp2 levels are tightly regulated throughout the cell cycle. It reaches a peak after cells being released from G1 phase. Higher levels of phosphorylation of Inp2 are detected at the beginning and the end of the cell cycle (Fagarasanu *et al.*, 2006). Mutating specific amino acids such as W1407, Y1415, Q1447, Y1483 and Y1484 in the Myo2 CBD causes a reduction in the interaction with Inp2, thereby affecting the transport of peroxisome to the bud. It has been shown in wild type conditions when peroxisome are delivered to their correct location, Inp2 is degraded, whereas in cells containing Myo2-Y1483A are not able to transport peroxisomes to the bud, and peroxisomes in mother cells have an elevated level of Inp2 (Fagarasanu *et al.*, 2009). Although Inp2 contains multiple PEST sequences required for its rapid breakdown, the

exact PEST sequence that regulates Inp2 breakdown during the termination of peroxisome inheritance has not yet been identified. In *S. cerevisiae,* Pex19 has been shown to contribute to peroxisome inheritance through its interaction with Myo2 (Otzen *et al.*, 2012), whereas in *H. polymorpha,* it is essential for Inp2 and Myo2 interaction (Saraya *et al.*, 2010).

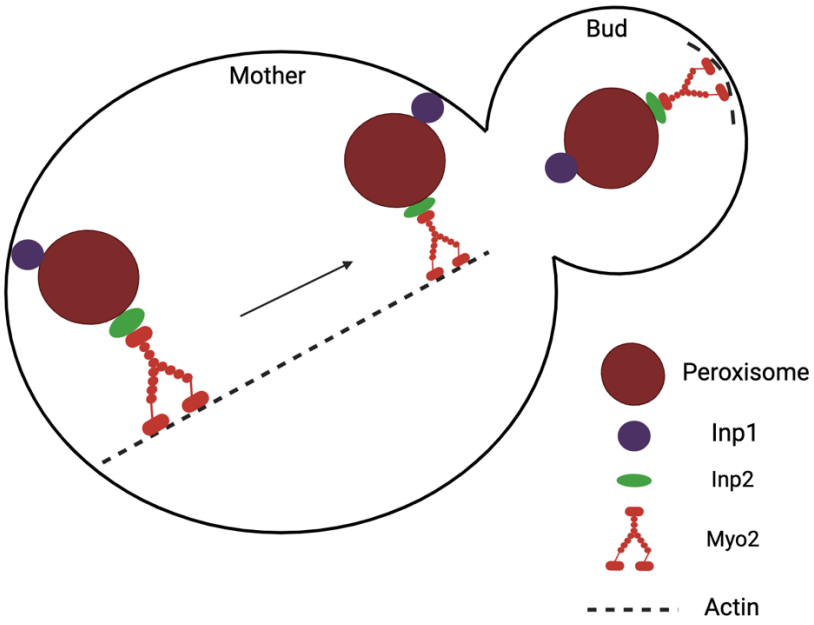

Figure 1.9 Model showing the functions of Inp1 and Inp2 in peroxisome inheritance. Peroxisomes normally locate at the cell cortex in the mother cell. Inp1 protein retains peroxisomes to the mother cell by a cortical anchor. When cell cycle is initiated Inp2 is synthesised and located at some peroxisomes. The increased level of Inp2 after binding to peroxisomes will allow the formation of Inp2-Myo2 transport complex. Myo2 takes bound peroxisomes to the presumptive bud site along polarised actin cables. In the bud, both Inp2 and Myo2 are responsible for the localization of peroxisomes. Inp2 then will be detached from Myo2 since its level decreases because of the cell cycle turnover. Some peroxisomes may return with Myo2 to mother-bud neck and by the time of cytokinesis they remain in the bud and get anchored to the cell cortex depending on Inp1 protein. Updated from (Fagarasanu et al., 2006).

1.10 Secretory vesicles transport

Another essential organelle to be transported during cell growth are secretory vesicles. They are important in facilitating the bud expansion and growth, and during the cytokinesis, they are required for sealing the mother-bud interface (Schott et al., 1999; Johnston et al., 1991). The *myo2-66* mutant was found to have an effect on secretory vesicles movement (Lillie and Brown, 1994; Johnston et al., 1991). The Rab GTPase Ypt31/32 has been shown to promote secretory vesicles growth and transport by binding to Myo2 (Lipatova *et al.*, 2008). When

secretory vesicles reach the bud, they get tethered to the bud tip prior to membrane fusion (Donovan and Bretscher, 2015). These steps require Myo2 to bind to the Rab family GTPases Sec15 and Sec4 (Jin *et al.*, 2011). Additionally, Smy1 (the kinesin-like myosin passenger protein) is required for promoting the interaction between Sec4 and Myo2 (Lwin, Li and Bretscher, 2016). Eventually, at the later stages, in the bud, secretory vesicles can be released by Sec4-GTP hydrolysis and the exocyst tethering complex (Donovan and Bretscher, 2012).

1.11 Mitochondrial inheritance.

Mitochondria are essential organelles that should be transported during cell division and cannot be formed *de novo* (McConnell *et al.*, 1990). There are various pathways which can control mitochondria inheritance depending on Myo2. This organelle is controlled during transport and approximately 50% of mitochondria is inherited (Simon et al., 1997; Boldogh et al., 2003). Mmr1 is the mitochondrial adaptor for Myo2, and it has been shown that it competes with other adaptors on binding Myo2 at a specific region (Taylor Eves *et al.*, 2012; Tang *et al.*, 2019) which suggests that there is a high coordination mechanism to transport organelles. Besides Mmr1, Rab GTPase Ypt11 is also invovled in Myo2-dependent inheritance, anchoring in the bud, and connecting mitochondria to the ER (Chernyakov et al., 2013; Arai et al., 2008; Lewandowska et al., 2013; McFaline-Figueroa et al., 2011; Itoh et al., 2002, 2004; Taylor Eves et al., 2012). In addition, the GTPase Gem1, the mitochondria rho (MIRO) has also been shown to support Myo2-dependent transport. However, each one of the proteins mentioned above might function via separate pathways (Frederick, Okamoto and Shaw, 2008). The involvement of MIRO on mitochondria dynamics is conserved in higher eukaryotes (Fransson, Ruusala and Aspenström, 2003, 2006).

Mitochondria retention to either the bud or the mother cell periphery is controlled by a complex known as MECA which consists of several proteins. Num1 and Mdm36 have been shown to anchor ER and mitochondria to the cell periphery (Lackner *et al.*, 2013). Another protein responsible for mitochondria retention is Mfb1 which functions independently of Num1 (Pernice, Vevea and Pon, 2016). For retaining mitochondria in the bud, Mmr1, besides its function as a Myo2 adaptor, might anchor mitochondria to the bud cortex (McFaline-Figueroa *et al.*, 2011). However, it is challenging to differentiate between the polarised transport to the bud and anchoring at the bud cortex. It seems that Mmr1 is functioning more

likely as an adapter than a tether (Taylor Eves *et al.*, 2012), because Num1 deletion leads to more mitochondria in the bud (Lackner et al., 2013; Klecker et al., 2013), whereas Mmr1 deletion leads to more mitochondria in the mother (Itoh, Toh-E and Matsui, 2004; McFaline-Figueroa *et al.*, 2011; Taylor Eves *et al.*, 2012).

Another contributor to mitochondrial inheritance is the cytoskeleton (Klecker and Westermann, 2020). Mitochondria binds to Arp2/3 proteins via the mitochore which gets facilitated by Puf3 (García-Rodríguez, Gay and Pon, 2007). Subsequently, actin polymerization might direct mitochondria towards the bud (Boldogh *et al.*, 2001). The ERMES complex including Mmm1, Mdm12, Mdm10, Mdm34 and Gem1 may be involved in recruiting Arp2/3 (Boldogh *et al.*, 1998, 2003; Kornmann *et al.*, 2009). However, the significance of this pathway in mitochondrial inheritance remains unclear. Mitochondrial morphology is also linked to mitochondrial inheritance through regulated fission and fusion. These processes are also required for the overall health of mitochondria (Böckler *et al.*, 2017). Multiple studies have suggested that only the healthy and functional mitochondria are transported to the bud (Vevea et al., 2013; McFaline-Figueroa et al., 2011; Higuchi et al., 2013).

There are several proposed mechanisms for selecting and retaining healthy mitochondria in the bud. One possibility is the anchoring of mitochondria at the bud tip, which may serve as a method for selecting and keeping healthy mitochondria in the bud (Knoblach and Rachubinski, 2015a). Another potential mechanism involves the movement of healthy mitochondria along actin cables, where they move in the opposite direction of retrograde actin flow (Higuchi *et al.*, 2013). Additionally, mitochondrial asymmetrical transport has also been implicated in this process (McFaline-Figueroa *et al.*, 2011; Hughes and Gottschling, 2012; Pernice, Vevea and Pon, 2016). However, the specific mechanisms underlying the selection and retention of transported mitochondria remain elusive.

1.12 Nuclear inheritance

In the process of nuclear inheritance, the duplicated nuclear chromosomes are evenly distributed between the mother cell and the daughter cell. Before nuclear inheritance occurs, the spindle pole bodies (SPB) which function as a microtubule organizing centres are also duplicated (Yamamoto et al., 1990; Adams and Kilmartin, 2000).

The SPBs facilitate the mitotic spindle alignment along the cell polarity axis. Kar9, which acts as a Myo2 adaptor and Dyn1, as a microtubule motor-based protein are essential for maintaining the alignment of the spindle that is followed by nuclear inheritance (Miller and Rose, 1998; Eshel et al., 1993; Hwang et al., 2003). In contrast to other organelles, inheritance of the nuclear material requires both the microtubule cytoskeleton and the actin. Kar9 functions by connecting the astral microtubules and actin filaments and guides the astral microtubules to the bud cortex along actin filaments **Figure 1.7**, while Dyn1 relies on binding with microtubules. The correct localization of Kar9 along microtubules is dependent on Bim1, a protein that binds to microtubules (Miller and Rose, 1998; Beach *et al.*, 2000; Miller, Cheng and Rose, 2000). In addition, there are two cell cycle checkpoints required to ensure correct chromosome segregation (**see Figure 1.10 A**) (Caydasi and Pereira, 2012). The first is the spindle assembly checkpoint (SAC), which gets activated during metaphase when the microtubules fail to bind to the kinetochore in a bipolar manner (Musacchio and Salmon, 2007). The second is the spindle position checkpoint (SPoC) which is activated during anaphase to prevent the cell from exiting mitoses if the alignment of the spindle is not maintained parallel to the cell polarity axis (Caydasi, Ibrahim and Pereira, 2010).

The kinase Kin4 is a key protein of the SPoC and negatively regulates mitotic exit upon spindle misalignment **Figure 1.10 B**. It is not involved in SAC (Pereira and Schiebel, 2005; D'Aquino et al., 2005). Kin4 phosphorylates Bfa1, another SPoC factor, which in complex with Bub2 can function as a GTPase-activating protein (GAP) for Tem1 GTPase, the activator of (MEN) the mitotic exit network (Maekawa et al., 2007; Bardin et al., 2000). Tem1-GTP initiates a kinase chain reaction resulting in mitotic exit through the activation of phosphatase Cdc14 (Lee *et al.*, 2001; Mohl *et al.*, 2009). Elm1 is an upstream regulator kinase of Kin4, which phosphorylates Kin4 at the Thr209 position in the kinase activation domain (Moore et al., 2010; Caydasi et al., 2010b). The localisation of Kin4 is also regulated during SPoC by Rts1 phosphatase (Chan and Amon, 2009). The overexpression of *KIN4* cause cell lethality by blocking the cell cycle since it has a role in inhibiting MEN activation, however, overexpression of T209A does not affect cell viability (Moore et al., 2010; Caydasi et al., 2010b). Throughout the cell cycle, Kin4 primarily localises to the cortex of the mother cell. However, during the G1 phase, it can also be found at the spindle pole bodies, and later during anaphase, it

localises to the bud neck (D'Aquino *et al.*, 2005). Lte1, is an inhibitor to Kin4, it can interact with Kin4 to inhibit Kin4 function in the bud. Since it is considered as Kin4 inhibitor, it can indirectly promote MEN activation (Bertazzi, Kurtulmus and Pereira, 2011; Falk, Chan and Amon, 2011). Another kinase required for MEN activation is the PAK kinase Cla4 which functions upstream to Lte1, while the paralog of Cla4, Ste20, activates MEN directly. This activation is likely to be through the GAP complex Bfa1/Bub2. Dma1/2 additionally contribute to SPOC by managing Elm1 positioning at the bud neck, which in turn affects Kin4 phosphorylation (Merlini *et al.*, 2012) **Figure 1.10.**

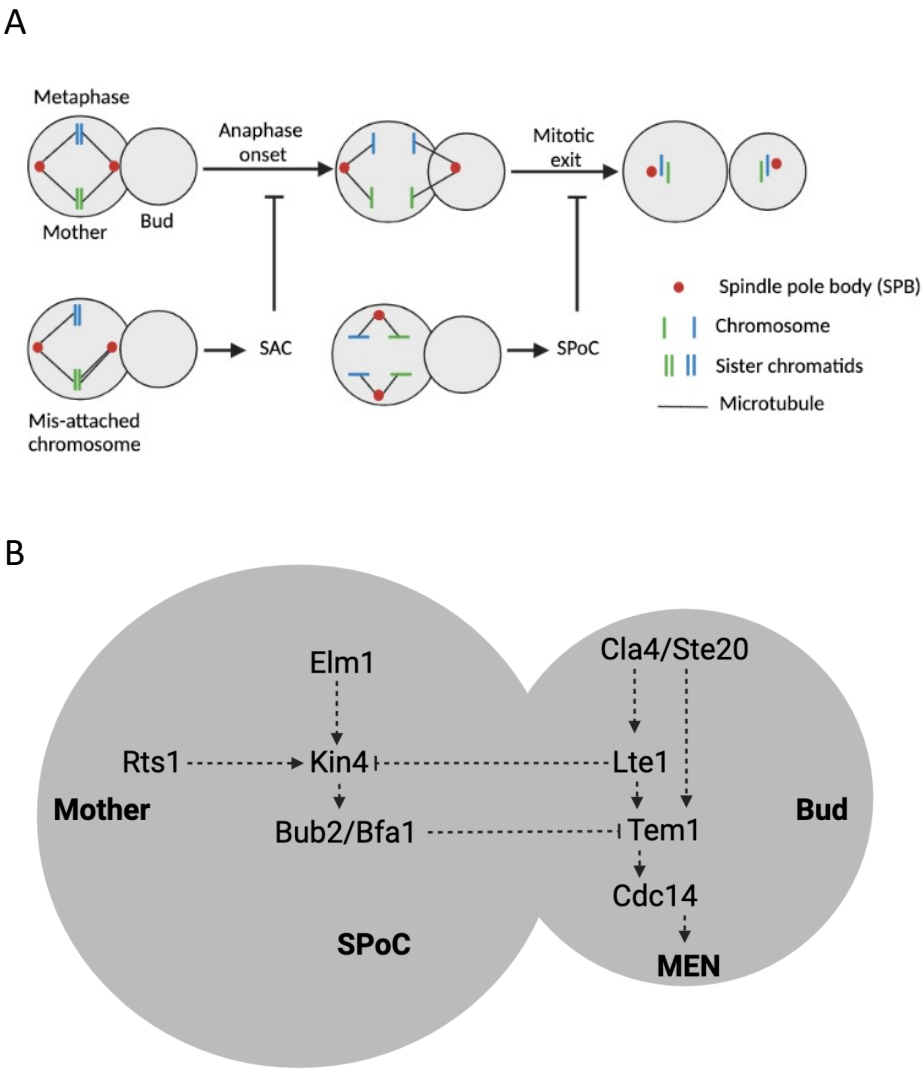

Figure 1.10 Schematic representation showing the regulation of the chromosome segregation and the checkpoints required. A) During the transition from metaphase to anaphase, the spindle assembly checkpoint (SAC) is activated when improper attachment occurs between microtubules and kinetochores, while the spindle position checkpoint (SPoC) can halt the cell cycle via inhibiting the

mitotic exit network (MEN) in late anaphase. B) The spatial distribution of molecular factors involved in SPoC and MEN.

1.13 Diseases related to Myosin V in mammalian cells.

In mammalian cells, there are three types of myosin V motors have been identified. These are Va, Vb and Vc (van der Velde et al., 2013; Heissler and Sellers, 2016). Myosin Va is predominantly found in the brain, while Vb and Vc are primarily present in non-neuronal tissues, including lung, stomach, colon, prostate, and pancreas (Rodriguez and Cheney, 2002). MyoVb is also expressed in both the polarised and non-polarised cells, predominantly localising to the plasma membrane (Lapierre *et al.*, 2001). The dysfunction of myosin V-dependent transport is particularly evident in polarised cell types, such as gut epithelial cells. In these cells, a complex consisting of Rab11, Slp4, Myosin Vb, and Munc18 facilitates the transport of vesicles to the apical surface, where it interacts with STX3 to facilitate membrane fusion(Vogel *et al.*, 2015). MyoVb mutations have been shown to cause cell polarity defect, which eventually leads to microvillus inclusion disease (MVID) in which the gut cannot absorb nutrients (van der Velde et al., 2013; Müller et al., 2008; Thoeni et al., 2014).

MyoVb conditional or constitutive knockout in mice serves as a model for MVID (Schneeberger et al., 2015; Cartón-García et al., 2015). The loss of function mutants in Rab8 and Rab11 result in MVID (Sato *et al.*, 2007; Sobajima *et al.*, 2015). Moreover, the progression of gastric cancer has been shown to be associated with the MyoVb downregulation (Dong *et al.*, 2012). The importance of myosin Va extends to neurons. MyoVa has been shown to be required for transporting endoplasmic reticulum (ER) into the dendritic spines of Purkinje neurons (Wagner, Brenowitz and Hammer, 2011). MyoVa functions as a tether in synapses for facilitating neurotransmitter release and has also been shown to be recruited to secretory granules carrying Rab27 and rabphillin-3A or granuphilin-a/b (Brozzi *et al.*, 2012; Maschi, Gramlich and Klyachko, 2018).

Mutations in MyoVa lead to Griscelli syndrome, which is a disorder marked by neurological deficits and pigmentation insufficiency. (Van Gele et al., 2009; Pastural et al., 1997; Çağdaş et al., 2012; Takagishi and Murata, 2006). Pigmentation abnormalities can be linked to the involvement of myosin Va in the functioning of melanocytes. Myosin Va is responsible for the

correct placement of melanosomes to ensure appropriate pigmentation (Wu *et al.*, 1998). Melanosomes are a type of specialised organelles that are closely related to lysosomes. They possess unique capabilities to produce and store melanin, a pigment responsible for absorbing light (Raposo and Marks, 2007). Melanin provides a protective shield against harmful UV radiation. The melanosomes movement from the centre to the periphery of the cell entails bidirectional transportation. This movement occurs along microtubule pathways with assistance from motor proteins such as kinesin and dynein (Vancoillie et al., 2000a, 2000b; Hara et al., 2000). Transportation to the cell periphery and placement at the cell cortex requires melanophilin, Rab27, and MyoVa. The correct delivery of the keratinocytes requires prior melanosomes (Strom et al., 2002; Fukuda et al., 2002).

Melanophilin is the Myosin-specific adaptor for melanosome transport **Figure 1.6** (Wu et al., 2002b; Provance et al., 2002). Rab27a is also essential for melanosome transport through likely an indirect interaction with MyoVa (X. Wu *et al.*, 2002). Rab36 is also involved in melanophilin interaction with MyoVa cargo binding domain (CBD) by likely facilitating the (Rab-interacting lysosomal protein–like 2) RILPL2 interaction with MyoVa (Cao *et al.*, 2019). Notably, melanophilin contains PEST sequences similar to the yeast vacuole myosin adaptors Vac17. Deleting any of the PEST sequences in melanophilin results in melanosome mislocalisation due to the stabilisation in melanophilin (Fukuda and Itoh, 2004). Melanophilin is also regulated by phosphorylation and ubiquitination and degradation by proteasome similar to Vac17 (Park *et al.*, 2019).

1.14 Aims and objectives.

The main aim of this research was to determine how myosin adaptors bind to the motor protein and how this binding is maintained during organelle inheritance and identifying novel proteins that might be involved in organelle transport. This was done by:

1) Investigations in Vac17 and Inp2 binding to Myo2 and identification of the specific functional sites required for both Vac17/Myo2 Inp2/Myo2 binding required for vacuole and peroxisome inheritance.
2) Studying the novel role of Kin4 and its paralog Frk1 in maintaining the interaction between Vac17/Inp2 with Myo2 by preventing the early disassembly of the transport complex during vacuole and peroxisome inheritance.

3) Performing a genetic screen to identify novel proteins that may be required in vacuoles or peroxisome inheritance and dynamics.

During this research Myo2 binding sites required for both vacuole and peroxisome transport have been identified in the adaptor proteins Vac17 and Inp2, respectively. In addition, a stable MIS models have been developed that can be further analysed and studied to understand the regulation of organelle adaptors in the mother cell (Chapter3). Utilising these models to validate the role of Kin4 and Frk1 (kinases recently discovered by our lab shown to be required for vacuole and peroxisome transport) in protecting the stability of Myo2 adaptors Vac17 and Inp2 in mother cell was further analysed (Chapter4). Lastly, analysing vacuole and peroxisome dynamics in the genetic screen identified the casein kinase Yck1 and Yck2 protein to be involved in peroxisome inheritance through regulating the Inp1 protein which is required for peroxisome retention in the mother cell (Chapter5).

(Part of the work presented in (Chapter 4) has been incorporated into a research article that has been published) https://www.mdpi.com/2218-273X/13/7/1098

In addition to the research described in this thesis the candidate has also contributed to the published research study in which pex27 was demonstrated to be required for Vps1 dependent fission in peroxisomes (Ekal, Alqahtani and Hettema, 2023). https://doi.org/10.1242/jcs.246348

Chapter2 Material and Methods

2.1 Chemicals and enzymes

Chemicals, oligonucleotides, and materials used for this study were supplied by Merck (previously Sigma-Aldrich). Restriction enzymes and buffers were purchased from New England Biolabs (NEB). dNTPs and PCR buffers and DNA polymerases were purchased from Bioline UK. Gel extraction and miniprep kits were supplied by Bioline and Qiagen, respectively. All the growth media supplements and components were purchased from ForMedium. D-Glucose was provided by Fisher Scientific UK. All equipment used for protein and DNA work were provided by Geneflow and BioRad, respectively.

2.2 Strains and plasmids

2.2.1 Yeast strains.

Table 2. 1 Yeast strains used.

Strain name	Genotype	Reference
BY4741	*MATA his3Δ1 leu2Δ0 met15Δ0 ura3Δ0*	Euroscarf
BY4742	*MATα his3Δ1 leu2Δ0 lys2Δ0 ura3Δ0*	Euroscarf
TEF2-mCherry (N' mCherry Matα)	*MATα his3Δ1 leu2Δ0 met15Δ0 URA3Δ0 lys+can1Δ::GAL1pr-SceI::STE2pr-SpHIS5 lyp1Δ::STE3pr-LEU2;NAT::TEF2pr mCherry-XXX.*	(Yofe et al., 2016)
VPH1-mNG	*MATa his3Δ1 leu2Δ0 met15Δ0 Vph1-mNG-URA3*	Lab stock
PEX11-mNG	*MATa his3Δ1 leu2Δ0 met15Δ0 Pex11-mNG-URA3*	Lab stock
dnm1Δ/vps1Δ	*BY4742 dnm1Δ::kanMX4 vps1Δ::loxp.*	Lab stock
dnm1Δvps1Δki4Δ	*BY4742 dnm1Δ::kanMX4 vps1Δ::loxp. kin4::hphMX4*	Lab stock
inp2Δ	*BY4742 inp2Δ::kanMX4.*	Euroscarf
kin4Δ	*BY4741 kin4Δ::kanMX4.*	Euroscarf

frk1Δ	*BY4741 frk1Δ::kanMX4.*	Euroscarf
frk1Δkin4Δ	*BY4742 frk1Δ::kanMX4. kin4::hphMX4*	Lab stock
elm1Δ	*BY4741 elm1Δ::kanMX4*	Euroscarf
frk1Δkin4Δinp2Δ	*BY4742 frk1Δ::kanMX4 kin4::hphMX4 inp2Δ::natMX6*	Lab stock
vac17Δ	*BY4742 vac17Δ::kanMX4*	Euroscarf
dnm1Δ/vps1Δ	*BY4742 dnm1Δ::kanMX4 vps1Δ::his3MX6.*	Lab stock
dnm1Δvps1Δinp2Δ	*BY4742 dnm1Δ::kanMX4 vps1Δ::loxp inp2Δ::hphMX4*	Lab stock
dnm1Δ/vps1Δ	*BY4742 dnm1Δ::kanMX4 vps1Δ::loxp.*	Lab stock
frk1Δkin4Δdma1Δ	*BY4741 frk1Δ::kanMX4 kin4Δ::hphMX6 dma1Δ::his3MX6*	Lab stock
frk1Δkin4Δvac17Δ	*BY4741 frk1Δ::kanMX4 kin4Δ::hphMX6 vac17Δ::natMX6.*	Lab stock
frk1Δkin4Δinp2Δ	*BY4741 frk1Δ::kanMX4. kin4Δ::hphMX6 Inp2Δ::natMX6*	Lab stock
Myo2-GFP frk1Δkin4Δinp2Δ	*BY4741 MYO2::MYO2-GFP-his3MX6 frk1Δ::kanMX4 kin4Δ::hphMX6 Inp2Δ::natMX6*	Lab stock
myo2-D1297N	*BY4742 myo2Δ::KanMX4, pRS413-myo2-D1297N (HIS3)*	Lab stock
Myo2-GFP-inp2Δ	*MYO2::MYO2-GFP-his3MX6 Inp2Δ::natMX6*	Lab stock
Myo2-GFP-vac17Δ	*MYO2::MYO2-GFP-his3MX6 vac17Δ::natMX6*	Lab stock
PJ69-4A	*MAT*a, *trp1-901, leu2-3, ura3-52, his3-Δ200, Δgal4, Δgal80, LYS2::GAL1-HIS3, GAL2-ADE2, met::GAL7-lacZ*	James *et al*., 1996
PJ69-4α	*MAT*α, *trp1-901, leu2-3, ura3-52, his3-Δ200, Δgal4, Δgal80, LYS2::GAL1-HIS3, GAL2-ADE2, met::GAL7-lacZ*	James *et al*., 1996
Myo1-GFP- inp2Δ	*BY4742 Myo1-GFP-hphMX6 inp2Δ::his3MX6*	This study

Myo1-GFP-vac17Δ	*BY4742 Myo1-GFP-hphMX6 vac17Δ::his3MX6*	This study
TEF2-mCherry-CLA4	*N' mCherry Matα CLA4::natMX6-TEF2-mCherry-CLA4*	(Yofe et al., 2016)
TEF2-mCherry-KIN4	*N' mCherry Matα CLA4::natMX6-TEF2-mCherry-KIN4*	(Yofe et al., 2016)
WT- (N'GAL1/10)-YCK1	*BY4742 GAL1/10-his3MX6-YCK1*	This study
WT- (N'GAL1/10)-YCK2	*BY4742 GAL1/10-his3MX6-YCK2*	This study
dnm1Δvps1Δ(N'GAL1/10) YACK1	*BY4742 dnm1Δ::kanMX4 vps1Δ::loxp GAL1/10-his3MX6-YCK1*	This study
dnm1Δvps1Δ(N'GAL1/10) YACK1	*BY4742 dnm1Δ::kanMX4 vps1Δ::loxp GAL1/10-his3MX6-YCK2*	This study

2.2.2 E. coli strains

Table 2. 2 E. coli strains used.

Strain	Genotype	Usage	Source
DH5α	*supE44 ΔlacU169 (ϕ80 lacZ ΔM15) hsdR17 recA1 endA1 gyrA96 thi-1 relA1*	Plasmid amplification and recovery of plasmid DNA from *S. cerevisiae* following *in vivo* homologous recombination.	Hanahan, (1983)

2.2.3 Plasmids

All plasmids utilised in this research are listed in **Table 2.3.** Some plasmids were generated by using a homologous recombination-based approach in *S. cerevisiae* **Section 2.3.6,** while others were constructed through restriction digestion and ligation followed by transformation in *E. coli* **Section 2.5**. For yeast plasmids, the original vectors Ycplac111 and Ycplac33 (Gietz and Sugino, 1998) were employed. The desired insert such as promoters: *GAL1/10, HIS3 and TPI1* or the endogenous promoter of the gene of interest were inserted between EcoRI and SacI sites. N-terminal tag fragments were inserted between SacI and BamHI sites and C-terminal tag fragments were inserted between PstI and HindIII sites. The

open reading frames ORFs were inserted into the remaining restriction sites in the multiple cloning sites.

Table 2. 3 Plasmids used for this study.

Plasmid name	Vector backbone	Promoter	Insert	Source
pAUL3	Ycplac33	*HIS3*	*mNG-PTS1*	Lab stock
pAUL28	Ycplac111	*HIS3*	*mRuby2-PTS1*	Lab stock
pLE120	Ycplac33	*INP2*	*INP2-mNG*	Lab stock
pLE107	Ycplac33	*INP2*	*INP2-TEV-2XProtA*	Lab stock
pAA2	Ycplac33	*VPH1*	*VPH1-GFP*	This study
pAA3	Ycplac33	*INP2*	*INP2mis-mNG*	This study
pAA4	Ycplac33	*INP2*	*INP2mis-TEV-2XProtA*	This study
pAA24	Ycplac33	*VAC17*	*VAC17Lmis-GFP*	This study
pAA37	Ycplac33	*VAC17*	*VAC17Smis-GFP*	This study
pAA38	Ycplac33	*VAC17*	*VAC17Smis- TEV-2XProtA*	This study
pAA40	Ycplac33	*VAC17*	*VAC17R135E/K138D- TEV-2XProtA*	This study
pAA41	Ycplac33	*VAC17*	*VAC17R135E- GFP*	This study
pAA43	Ycplac33	*VAC17*	*VAC17K138D- GFP*	This study
pAA57	Ycplac33	*VAC17*	*VAC17R142E- GFP*	This study
pAA39	Ycplac33	*VAC17*	*VAC17R135E/K138D- GFP*	This study
pAA59	Ycplac33	*VAC17*	*VAC17R142E/K138D- GFP*	This study
pAA58	Ycplac33	*VAC17*	*VAC17R135E/R142E- GFP*	This study
pAA45	Ycplac33	*INP2*	*INP2-S139A-TEV-2XProtA*	This study
pLE125	Ycplac33	*INP2*	*INP2-T323A-TEV-2XProtA*	Lab stock
pAA46	Ycplac33	*INP2*	*INP2-S283A-TEV-2XProtA*	This study
pAA47	Ycplac33	*INP2*	*INP2-S544A-TEV-2XProtA*	This study
pAA48	Ycplac33	*INP2*	*INP2-T511A-TEV-2XProtA*	This study
pAA49	Ycplac33	*INP2*	*INP2-T527A-TEV-2XProtA*	This study
pAA55	Ycplac33	*INP2*	*INP2-S283A/S544A-TEV-2XProtA*	This study
pAA54	Ycplac33	*INP2*	*INP2-T527A/T511A-TEV-2XProtA*	This study

pAA67	PGAD-C1	GAL4	*MYO2*	Lois Weisman
pAA68	PGAD-C1	GAL4	*MYO2-E1293K*	Lois Weisman
PAA69	PGAD-C1	GAL4	*MYO2-D1296N*	Lois Weisman
pAA70	PGAD-C1	GAL4	*MYO2-D1297N*	Lois Weisman
pAA71	PGAD-C1	GAL4	*MYO2-N1304D*	Lois Weisman
pAA72	PGBD-C1	GAL4	*VAC17*	Lois Weisman
pAA73	PGBD-C1	GAL4	*INP2*	Lois Weisman
pAA60	PGBD-C1	GAL4	*VAC17-R135E*	This study
pAA61	PGBD-C1	GAL4	*VAC17-K138D*	This study
pAA62	PGBD-C1	GAL4	*VAC17-R142E*	This study
pAA63	PGBD-C1	GAL4	*VAC17-R135E/K138D*	This study
pAA65	PGBD-C1	GAL4	*VAC17-R142E/K138D*	This study
pGH75	Ycplac33	*INP1*	*INP1-TEV-2XProtA*	Lab stock
pAA64	PGBD-C1	GAL4	*VAC17-R135E/R142E*	This study
pAA66	PGBD-C1	GAL4	*INP2mis*	This study

2.3 DNA procedures

2.3.1 Polymerase chain reaction (PCR)

All PCR reactions were used to amplify regions whether from the genomic DNA or plasmids. Promega/Biovision pfu polymerase was used for mutagenesis PCR. All the primers listed in **Table 2.5** were ordered from Merck (previously known as Sigma Aldrich) after being designed in Snapgene software.

Table 2. 4 PCR reaction mixture composition.

Component	MyTaq pol.	Velocity pol.	Pfu pol.
Template	1 µl gDNA or plasmid	1 µl gDNA or plasmid	1 µl 40-50 ng plasmid
Reaction buffer	10 µl 10x MyTaq buffer	2.5 µl 5x HiFi buffer	2.5 µl 10x pfu buffer
Forward primer	5 µl of 5µM	5 µl of 5 µM	1 µl of 5 µM
Reverse primer	5 µl of 5µM	5 µl of 5 µM	1 µl of 5 µM
dNTPs	-	2.5 µl of 2.5 mM	4 µl of 2.5 mM

DNA polymerase	0.5 µl of 5 U/µl	0.5 µl 5 U/µl	0.5 µl 5 U/µl
ddH2O	28.5 µl	33.5 µl	15 µl
Total volume	50 µl	50 µl	25 µl

Standard cycling conditions of each reaction:

step	MyTaq pol.	Velocity pol.	Pfu pol.
Initial denaturation	95 ℃ 2-3 min	98 ℃ 2-3 min	94 ℃ 2 min
Denaturation	95 ℃ 30 sec	98 ℃ 30 sec	94 ℃ 30 sec
Annealing	50-55 ℃ 30 sec	50-55 ℃ 30 sec	50-55 ℃ 1 min
Elongation	72℃ 30 sec/kb	72℃ 15 sec/kb	68℃ 2 min/kb
Final Elongation	72℃ 10 min	72℃ 10 min	68℃ 10 min
Termination	10℃	10℃	10℃

Annealing temperature was calculated depending upon the nucleotide composition of the primers. The following equation was used to determine the approximate annealing temperature: (TA°C) = (TM°C) - 5°C where (TM°C) = 4 x (#G + #C) + 2 x (#A + #T); where TM and TA are the melting temperature and annealing temperature, respectively. Mostly, after every PCR reaction, 5µl was loaded on an agarose gel to check if the product produced is in the correct size.

Table 2. 5 The primers used for this study: F and R stands for (Forward and Reverse)

Name code	Sequence (5' to 3')	Description
VIP4904 F	**CCAGAAGTAGTTTAGGGTCATTTATAATTGAGAGGCAACGTCTG**	**For Vac17-S-mis deletion**
VIP4905 R	**CAGACGTTGCCTCTCAATTATAAATGACCCTAAACTACTTCTGG**	**For Vac17-S-mis deletion**
VIP4650 F	**CAATCCACCAGAAGTAGTTTAGGGTCATTTACTCCATCGAAACCACCAAAAAAATCGG**	**For Vac17-L-mis deletion**
VIP4651R	**CCGATTTTTTTGGTGGTTTCGATGGAGTAAATGACCCTAAACTACTTCTGGTGGATTG**	**For Vac17-L-mis deletion**

VIP4917 F	**TTAGGGTCATTTCAACCTGAACCATTGAAAATAATTGAG**	**For Vac17-R135E**
VIP4918 R	**CTCAATTATTTTCAATGGTTCAGGTTGAAATGACCCTAA**	**For Vac17-R135E**
VIP 5041 F	**CCATTGAAAATAATTGAGGAGCAACGTCTGTGTATGG**	**For Vac17-R142E**
VIP 5042 R	**CCATACACAGACGTTGCTCCTCAATTATTTTCAATGG**	**For Vac17-R142E**
VIP 4919 F	**TTTCAACCTCGACCATTGGATATAATTGAGAGGCAACGT**	**For Vac17-K138D**
VIP 4920 R	**ACGTTGCCTCTCAATTATATCCAATGGTCGAGGTTGAAA**	**For Vac17-K138D**
VIP 4915F	**GTTTAGGGTCATTTCAACCTGAACCATTGGATATAATTGAGAGGCAACGTC**	**For Vac17-K138D/R135E**
VIP 4916 R	**GACGTTGCCTCTCAATTATATCCAATGGTTCAGGTTGAAATGACCCTAAAC**	**For Vac17-K138D/R135E**
VIP 5043 F	**CCATTGGATATAATTGAGGAGCAACGTCTGTGTATGG**	**For Vac17-R142E on K138D**
VIP 5044 R	**CCATACACAGACGTTGCTCCTCAATTATATCCAATGG**	**For Vac17-R142E on K138D**
VIP 4860 F	**AACCAATACAATCAACCATGGTAAAGGCAGAAAGTCACCCCGTTCTT**	**For Inp2-mis deletion**
VIP 4861 R	**AAGAACGGGGTGACTTTCTGCCTTTACCATGGTTGATTGTATTGGTT**	**For Inp2-mis deletion**
VIP 4836 F	**TACAAAAATTTCGCGCATTCGCTGGCCCTTTTCCTGCTCTCCTCTTCCCCGAATTCGAGCTCGTTTAAAC**	**To introduce GAL1 to Yck1**
VIP 4837 R	**TTGGTGAGGTTGTTAACTGCTAGAGTGGTACTTGCTATGGGCATGGACATCATTTTGAGATCCGGGTTTT**	**To introduce GAL1 to Yck1**
VIP 4785 F	**GTTGTTTCTACTGAACACAGCATATAAGCCAAGAAAATAGTTTTCCAAAAGAATTCGAGCTCGTTTAAAC**	**To introduce GAL1 to Yck2**
VIP 4786 R	**ACAGCTAAACCAGAGTTCGTTGCTGTCAAAGGACTTTGCACTTGAGACATCATTTTGAGATCCGGGTTTT**	**To introduce GAL1 to Yck2**
VIP 5021 F	**CCTTATTTCTGGGGTAATTAATCAGCG**	**Anneals at GAL1 promoter**

VIP 4645 R	**GCCATACCGAAGTCGATCAAATG**	**Check GAL1 insertion for Yck1**
VIP 4647R	**GTTGACCCGGTCTTCCGATC**	**Check GAL1 insertion for Yck2**
VIP 3617 F	**CTTCAAAAATAGACAAAGACTTGCGTTGACCTTCTTTGATGAAATGG**	**For Vac17-S222A**
VIP 3618 R	**CCATTTCATCAAAGAAGGTCAACGCAAGTCTTTGTCTATTTTTGAAG**	**For Vac17-S222A**
VIP 3619 F	**GATTTTGATTCTGATCAAGATGCTATCATTCTACCAAACATAAGTACC**	**For Vac17-T240A**
VIP 3620 R	**GGTACTTATGTTTGGTAGAATGATAGCATCTTGATCAGAATCAAAATC**	**For Vac17-T240A**
VIP 5011 F	**GATATGAATCATTACAGGTTAGCACTACATCTTGATCAATC**	**For Inp2-S139A**
VIP 5012 R	**GATTGATCAAGATGTAGTGCTAACCTGTAATGATTCATATC**	**For Inp2-S139A**
VIP 5013 F	**CATAGTTTTATATCAAGAGTGGCACTTATTTCAATTGCTGACG**	**For Inp2-S283A**
VIP 5014 R	**CGTCAGCAATTGAAATAAGTGCCACTCTTGATATAAAACTATG**	**For Inp2-S283A**
VIP 5017 F	**CTCATTACTTTCTGGAAAGCCTCGAAAATTTGTGGCA**	**For Inp2-T511A**
VIP 5018 R	**TGCCACAAATTTTCGAGGCTTTCCAGAAAGTAATGAG**	**For Inp2-T511A**
VIP 5019 F	**ATACAAAAGGTATCCCCAGCCAATACAATCAACCATG**	**For Inp2-T527A**
VIP 5020 R	**CATGGTTGATTGTATTGGCTGGGGATACCTTTTGTAT**	**For Inp2-T527A**
VIP 4945 F	**ATCCTCAAAGGCAGAAAGGCACCCCGTTCTTCGTCAG**	**For Inp2-S544A**
VIP 4546 R	**CTGACGAAGAACGGGGTGCCTTTCTGCCTTTGAGGAT**	**For Inp2-S544A**

2.3.2 Plasmid miniprep

Qiagen Qiaquick Miniprep kit was used for this technique. 5ml of 2TY-Ampicillin **Section 2.4** overnight culture was firstly centrifuged at 8,000 rpm for 3 min in a universal tube. Supernatant was poured off and the pellet was washed with 250 µl of the precooled buffer I and transferred into a 1.5 ml Eppendorf tube. 250 µl buffer II was added into the same tube

then inverted 4-6 times and kept for 1 min at room temperature. Next, 350 µl of N3 buffer was added followed by inverting the tubes 4-6 times again. The tube was then centrifuged at 13,000 rpm for 10 min. Subsequently, the supernatant was transferred to the spin column containing the filter and centrifuged at 13,000 for 1 min followed by discarding the flow-through. 750 µl of the washing buffer was added to the tube and centrifuged again for 1 min at 13,000 rpm, followed by additional centrifugation for 1 min at 13,000 rpm to remove any residual solution. Finally, 50 µl of elution buffer was added to the tube and incubated at room temperature for 3-4 minutes then centrifuged for 1 min at 13,000 rpm then DNA concentration was checked by Nanodrop.

2.3.3 Agarose gel electrophoresis.

Samples such as PCR products, plasmids, or digested plasmids/PCR were examined by agarose gel electrophoresis. In general, 1% agarose gel was prepared by melting 0.5 g of agarose in 50 ml of 1XTBE using the 10X TBE buffer. Ethidium bromide was then added to a final concentration of 0.5 µg/ml. DNA samples were mixed with DNA loading buffer at 1X final concentration from 6X DNA loading buffer before loaded to the agarose gel. Bioline Hyper ladder was used for alongside the DNA samples to estimate the DNA fragments size. 1X TBE buffer was used to run gels at constant voltage of 90-95 V. Finally, an ultraviolet transilluminator imaging system (GeneSys) was used to examine the DNA bands.

6X DNA loading buffer: 0.25% bromophenol blue (w/v), 30% glycerol (v/v), 0.25% xylene cyanol FF (w/v).

10X TBE buffer: 0.9M Tris-Borate, 10mM EDTA, pH 8.0

2.3.4 DNA digestion and gel extraction

Restriction digests were conducted in a 50 µl reaction volume, which included 5 µl of 10x NEB CutSmart™ Buffer, 1 µl of each required restriction enzyme, and 1 µg of plasmid DNA. The reaction volume was adjusted to 50 µl with dH2O. The tubes were then incubated at 37°C for a minimum of 4 hours or overnight. After visualising the gel using a long-wavelength UV transilluminator, the relevant DNA bands were excised from the gel. Gel extractions were performed using the QIAquick kit (Qiagen), following the manufacturer's instructions.

2.3.5 DNA ligation

Ligation reaction was carried out in a total volume of 20 µl with 3:1 insert:vector molar ratio used. 50 ng of the digested extracted vector was added to the relevant amount of digested extracted insert. The total volume of the reaction mixture was made up to 20 µl with dH2O after adding 2 µl 10X ligase buffer and 0.5 µl T4 DNA ligase (Promega). The mixture reaction was then incubated for 2 hours or preferably left overnight at 37°C for optimal ligation and transformed into chemically competent *E. coli* cells the next day.

2.3.6 Homologous recombination-based cloning

The homologous recombination based on DNA editing was performed for introducing tags, genes, or genes with desired mutation in a vector **Figure 2.1**. Simply, any vector of interest was linearised by restriction digestion and the insert (promoter, ORF and tag) can be amplified by PCR using primers designed to anneal to the start and the end of the region of interest with 20 nucleotides flank that is identical to each side of the desired insertion sites in the vector. The linearised vector was circularised with the insert by transforming them into yeast in which the homologous recombination is employed. The transformed cells were then plated on selective media to select for the recombinant plasmid.

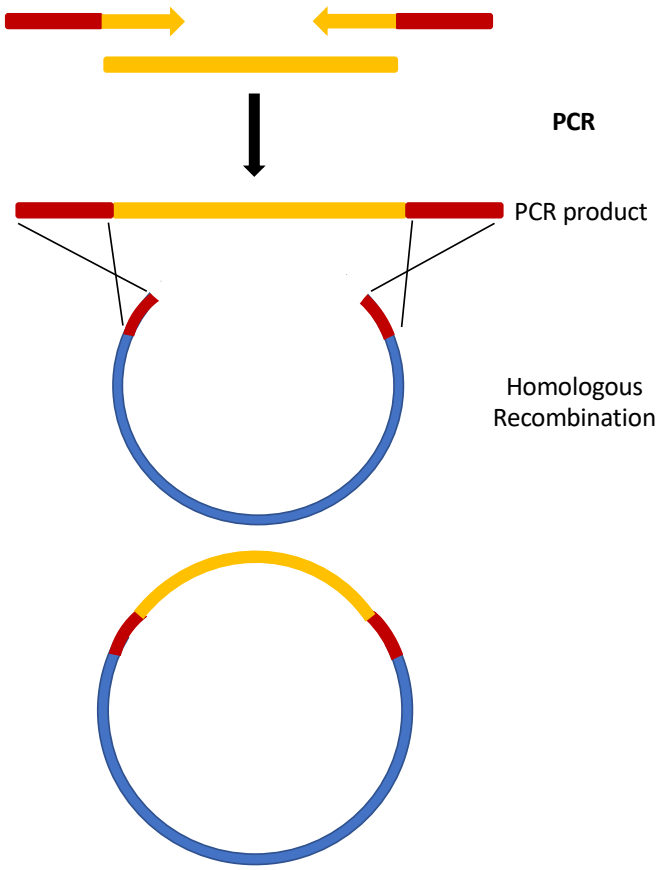

Figure 2.1 Homologous recombination method utilised in *S. cerevisiae* for plasmids constructions. Homologous recombination is carried out to produce a recombinant vector. Forward and reverse primers (indicated in red and yellow arrows) were designed to produce a PCR product carrying the desired DNA insert (yellow) flanked by approximately 20 nucleotides homologous to sequences in the vector (red) in which it was digested with the appropriate restriction enzymes and was transformed into *S. cerevisia*e along with the PCR product.

2.3.7 Site directed mutagenesis.

Pfu DNA polymerase (Promega/Biovision) was used to perform site directed mutagenesis. PCR products carrying the desired mutation were subjected to DpnI digestion at 37°C for 1 hour, to digest original template DNA. A 5 µl aliquot of the PCR product was subjected to agarose gel electrophoresis for analysis, while 1 µl of the reaction mixture was used for transformation into electrocompetent *E. coli* cells. Following transformation, several individual colonies were selected and grown in liquid culture to obtain plasmid DNA for miniprep. Subsequently, the plasmids were sent for sequencing to verify the presence of the intended mutations.

2.3.8 DNA sequencing

The plasmid clones were subjected to confirmation of their sequences through the Sanger sequencing method, which was performed by Source Bioscience. The obtained sequencing data was analysed using the SnapGene software and the ClustalW multiple sequence alignment online tool.

2.4 Growth media

All the components necessary for cell growth in the media were dissolved in Millipore water and sterilised by autoclaving at 121°C. Antibiotics were added, if needed, to their final concentration once the media had cooled down to 50°C after autoclaving. The media components used were supplied by Difco Laboratories and ForMedium, while D-Glucose was provided by Fisher Scientific UK. The yeast strains were incubated at 30°C, both on liquid and solid media. Amino acids were supplemented in plates for strains with auxotrophic markers as required. Antibiotics were employed to select for resistance associated with selection markers.

Table 2. 6 The culture media and components.

Media	Components with concentration
Yeast minimal media (YM1)	0.5% Ammonium Sulphate, 0.19% Yeast Nitrogen Base, 400 µl NaOH (for 1L media to make pH 6.5), 2% glucose
Yeast minimal media 2 (YM2)	0.5% Ammonium Sulphate, 0.19% Yeast Nitrogen Base, 1% Casamino acids, 2% Agar (for plates), 10m of 100X of stock amino acids and Uracil (2mg/ml) (for. 1L media)
YM2, URA-	0.5% Ammonium Sulphate, 0.19% Yeast Nitrogen Base, 1% Casamino acids, 2% Agar (for plates), 10m of 100X of stock amino acids (leu, 3mg/ml; trp 2 mg/ml) (for1L media)
YM2, URA-, Clonat	0.5% Ammonium Sulphate, 0.19% Yeast Nitrogen Base, 1% Casamino acids, 2% Agar (for plates), 1ml of 1000X Clonat stock (100mg/ml) (for 1L media)
YPD	2% Bacto Peptone (Difco), 1% Yeast Extract, 2% D-Glucose, 2% Agar (for plates) (for 1L media).
YPD, Clonat	2% Bacto Peptone (Difco), 1% Yeast Extract, 2% D-Glucose, 2% Agar (for plates), 1ml of 1000X clonat stock (100 mg/ml) (for 1L media)
2TY-Ampicillin	1.6% Tryptone (ForMedium), 1% Yeast Extract (ForMedium), 0.5% NaCl, 2% Agar (ForMedium) (for plates), 75 µg/ml Ampicillin

2.5 *E. coli* protocols and methods.

2.5.1 Preparation of chemical competent *E. coli* DH5α cells

Based on the rubidium chloride method (Hanahan, 1983), the *E. coli* DH5α competent cells were prepared. From 2TY plates, a single colony was grown overnight in liquid 2TY medium at 37°C. Secondary culture was started by inoculating the overnight culture in 200 ml of 2TY medium in 1L flask starting with 0.05 OD_{600} and grown at 30°C with shaking until mid-log phase (0.5-0.6 OD_{600}). Cells were incubated on ice for 15 min before centrifuged at 3000 rpm (Sigma 4-16K) at 4°C for 10 min. Subsequently, the supernatant was discarded and 75 ml of ice-cold solution I was used to resuspend the pellet and re-incubated on ice for 20 min. 3000 rpm centrifugation for 10 min was carried out to pellet the cells again. The pellet was resuspended with 16 ml of ice-cold Solution II. From the cell suspension 200 µl were taken as aliquots and transferred to 1.5 ml Eppendorf tubes. Finally, cells were snap freezed with liquid nitrogen and stored at -80°C.

Solution I: 100mM rubidium chloride, 50mM manganese chloride, 10mM calcium chloride, 30mM potassium acetate, 15% w/v glycerol, pH 5.8.

Solution II: 10mM MOPS, 10mM rubidium chloride, 75mM calcium chloride, 15% w/v glycerol, pH 6.8.

2.5.2 *E. coli* chemical transformation

Chemically competent DH5α cells were thawed on ice. 0.5 µl plasmid miniprep (approximately 100 ng) was added to 40 µl of cells and incubated on ice for 20 minutes (for ligation purposes). The tube was then heat-shocked in a 42°C water bath for 2 minutes and replaced back on ice water for 5 minutes. Subsequently, 900 µl of 2TY media were added to the tube which was then incubated at 37°C for 30-45 minutes. The tube was centrifuged for 1 minute at 8000 rpm, and 850 µl supernatant was pipetted off. The pellet was resuspended in the remaining liquid by gently mixing using a pipette. Finally, the contents were plated out onto a 2TY plate containing ampicillin (75 µg/ml), and was incubated overnight at 37°C.

2.5.3 Preparation of electrocompetent cells

1L of secondary culture was prepared from overnight grown *E. coli* DH5α cells in 2TY medium with 0.05 OD_{600} and grown for 4 to 5 hours at 30°C with shaking to ~0.5-0.6 OD_{600}. Cells were

then chilled on ice for 15 min before harvested by centrifugation at 3,000rpm for 15 min. Then supernatant was discarded before resuspending the pellet with 500ml of ice-cold 10% (v/v) glycerol. The same procedure was repeated as above but with 250ml of ice-cold 10% (v/v) glycerol. Cells were also harvested for one last time as above with less volume of 50 ml of ice-cold 10% (v/v) glycerol. Finally, after discarding the supernatant from the last spin, the pellet was resuspended in 750 µl of 10%(v/v) ice cold glycerol then cells were aliquoted (50 µl in each tube) in 1.5 ml Eppendorf tubes and snap-frozen into the liquid nitrogen and stored in the -80°C. Note: every centrifugation step was carried out at 4°C.

2.5.4 *E. coli* transformation through electroporation

To prepare the transformation, 40 µl of carefully mixed electro-competent DH5α cells were combined with 10 µl of yeast total DNA, diluted 1:10 in TE. The cell-DNA mixture was then transferred into an electroporation 2 mm cuvette (Geneflow), and subjected to electroporation using the 'EC2' mode (V=2.5kV) on a Micropulser electroporator (BIORAD). Following the electroporation, 600 µl of 2TY media was added, and the cells were incubated at 37°C for 30 minutes. After incubation, the tube was centrifuged at 5,000 rpm for 5 minutes using an Eppendorf 5424 centrifuge, and the resulting pellet was plated onto 2TY-ampicillin plates (75 µg/ml). Finally, the plates were incubated overnight at 37°C.

2.6 Yeast protocols

2.6.1 Yeast growth and maintenance

All liquid or solid media were used for the growth of yeast strains with incubation at 30°C. Amino acids were added according to the auxotrophic marker required. The usage of antibiotics was used to select for resistance selection cassettes. All strains required for storing in the -80 °C were mixed with the 50% (v/v) glycerol stock. In case of inducing gene expression, strains with *GAL1/10* promoter were grown in YM2 2% raffinose overnight and transferred to YM2 2% galactose for induction. For imaging analysis, cells were grown for overnight and diluted for secondary culture starting with 0.1 OD_{600} and grown for 4-5 hour until 0.5-0.6 OD_{600} then imaged.

2.6.2 One step transformation

200 µl of yeast overnight culture was centrifuged for 1 min at 12,000rpm in an Eppendorf tube then supernatant was discarded. 5 µl (50µg) single stranded DNA was added to the pellet with vortex, then 1µg of plasmid DNA (2-3 µl) was added before adding 50 µl of one step buffer and then tube was mixed with vortex to mix all components altogether. Incubation for 2-3 hours was applied with an occasional vortexing. The tube was heat shocked at 42°C for 30 min and cells were plated on selective plates and incubated for 2-3 days at 30°C.

One step buffer: 0.2M LiAc pH 5.0, 40% (w/v) PEG (Polyethylene glycol) 3350, 0.1M DTT.

2.6.3 High efficiency transformation

Yeast cells were cultured overnight in YPD medium. The following day, the cells were diluted in fresh YPD medium to an initial optical density at 600 nm (OD_{600}) of 0.1 and incubated in a shaking incubator at 30°C until reaching an OD_{600} of 0.5. Subsequently, the cells were harvested by centrifugation at 2500 rpm for 5 minutes. The resulting cell pellet was then resuspended in a 1 ml solution of 1X TE/LiAc (composed of 10 mM Tris-Cl pH 7.4, 1 mM EDTA, and 100 mM LiAc at pH 7.5) and centrifuged for 2 minutes at 5000 rpm. The supernatant was discarded, and this step was repeated. Finally, the cell pellet was resuspended in 50 µl of 1X TE/LiAc. Next, the DNA components were added, including the digested vector and 5 µl of the PCR product insert. The resulting mixture was combined with 300 µl of sterile 40% PEG3350 solution (in 1X TE/LiAc) and 5 µl of single-stranded salmon testes DNA (10 mg/ml, Sigma-Aldrich). The suspension was incubated at room temperature for 30 minutes, followed by further incubation at 30°C for an additional 30 minutes. Subsequently, the cells were heat-shocked in a 42°C water bath for 15 minutes, followed by centrifugation at 13,000 x g for 1 minute using an Eppendorf microfuge. The supernatant was carefully removed, and the resulting pellet was resuspended in 50 µl of 1X TE before being plated onto selective plates for auxotrophic markers. In the specific experiments described in the results section, YM2 ura- plates were used and incubated at 30°C for 3 days. If selectable markers conferring antibiotic resistance were employed, the cells were first recovered in YPD medium for 4 hours at 30°C after transformation before being plated out.

1X TE/LiAc: For 10ml-1ml of 10X TE, 1ml of 1M LiAc (Lithium acetate) pH7.5, 8ml of ddH2O.

PEG 40% w/v: For 5ml-500µl of 10X TE, 500µl of LiAc, 4ml of 50% PEG 3350.

10X TE: 100mM Tris pH8.0, 10mM EDTA pH8.0.

2.6.4 Yeast genomic DNA isolation

A 5 ml overnight culture of cells in YPD medium was collected in a 2 ml screw cap tube using sequential centrifugation for 1 minute at 12,000 rpm in an Eppendorf 5424 centrifuge. The resulting pellet was resuspended in 1 ml of sterile MilliQ-H2O and centrifuged at 12,000 rpm for 1 minute. After discarding the supernatant, the cells were resuspended in the remaining volume. To the cell suspension, 200 µl of TENTS solution (containing 20 mM Tris-Cl at pH 8, 1 mM EDTA, 100 mM NaCl, 2% Triton X-100, 1% SDS), 200 µl of 0.5 mm glass beads, and 200 µl of phenol/chloroform/isoamyl alcohol (25:24:1) were added. The tube was then subjected to high-speed shaking in a bead beater for 1 minute. Following bead beating, the tube was centrifuged for 30 seconds at 12,000 rpm. Then, 200 µl of TENTS solution was added, and the contents were vortexed for 5-10 seconds. The tube was centrifuged for 5 minutes at 12,000 rpm, and the resulting aqueous (top) phase was carefully transferred into a new 1.5 ml tube. To this tube, 200 µl of phenol/chloroform was added, and the mixture was vortexed for 10 seconds before centrifuging for 5 minutes at 12,000 rpm. Next, 300 µl of the supernatant was transferred to a fresh 1.5 ml tube, and DNA was precipitated by adding 30 µl of 3M NaAc (pH 5.2) and 700 µl of 100% ethanol (EtOH). The tube was vortexed, placed on ice for 15 minutes, and then centrifuged for 15 minutes at 12,000 rpm. The supernatant was discarded, and the resulting DNA pellet was washed with 500 µl of 70% EtOH. After centrifuging at maximum speed for 5 minutes, the supernatant was removed, and the pellet was air dried. Finally, the DNA pellet was resuspended in 100 µl of 1X TE buffer (10 mM Tris-Cl pH 7.4, 1 mM EDTA) containing 2 µl of RNase (10 mg/ml). The tube was incubated for 10 minutes at room temperature, followed by repeating the DNA precipitation steps as described above. The final DNA pellet was air dried and resuspended in 100 µl of 1X TE before storage at -20°C.

TENTS: 20mM Tris-HCl pH 8.0, 1mM EDTA, 100mM NaCl, 2%(v/v) Triton X-100, 1%(w/v) SDS.
1X TE: 10mM Tris-Cl pH8.0, 1mM EDTA.

2.6.5 Epitope tagging and gene deletion in genome

The gene modification or deletion were performed as described in (Longtine et al., 1998). All the gene tagging and knockout cassettes were amplified by PCR with selection markers. For tagging, 50 nucleotides (forward-primer red) **Figure 2.2 upper panel** was designed identical to the region upstream of the ORF stop codon. For gene deletion, the same 50 nucleotides forward primer (forward-primer grey) **Figure 2.2 lower panel** is designed identical to the region upstream of the ORF start codon. The reverse primer (light blue) contains 50 nucleotides downstream to the ORF stop codon. After amplifying the region of interest by PCR, the fragment was transformed to yeast by High-efficiency transformation and cells were grown on desired selective medium for 3-4 days. Subsequently, the correct clones were verified by PCR to confirm the modification.

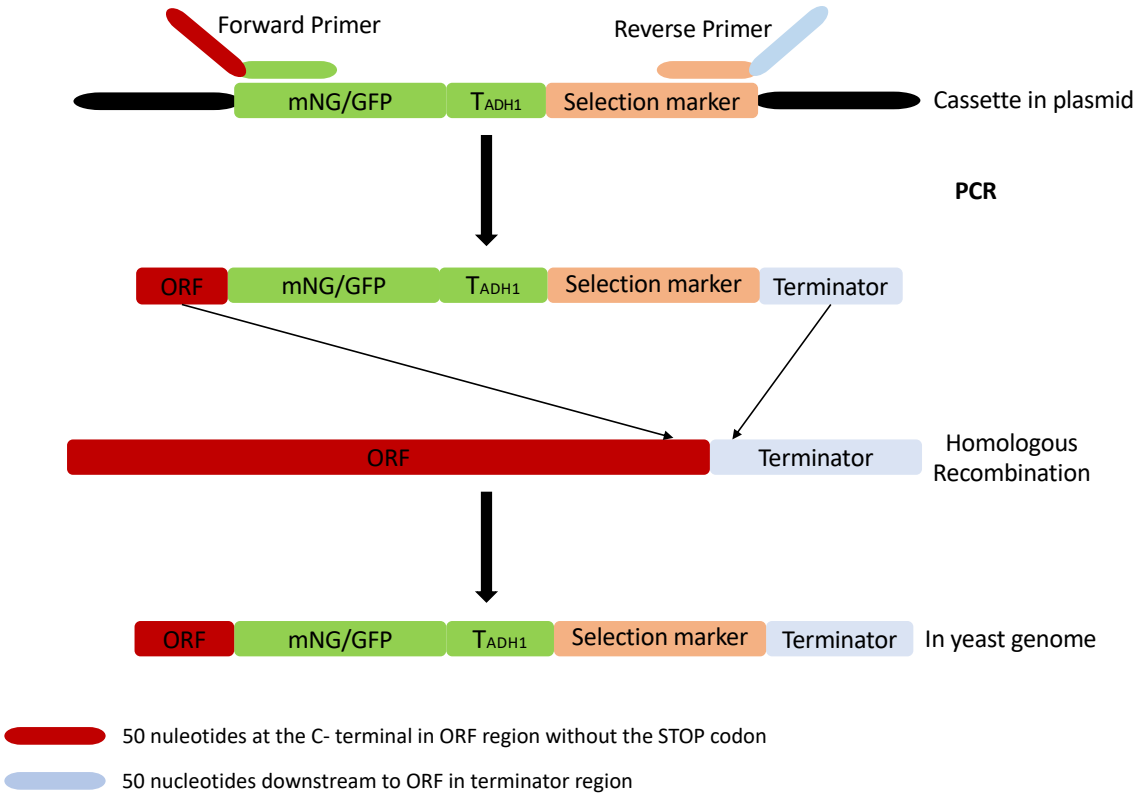

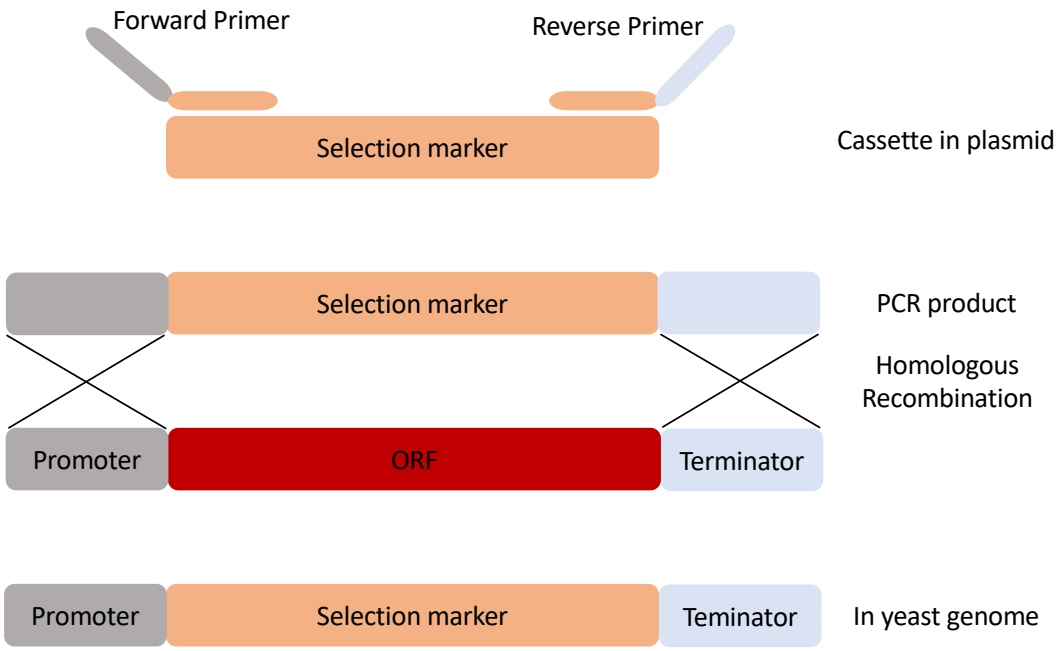

Figure 2.2 Schematic representation of the methods used to modify genes for the tagging at the C-terminus of ORF or gene deletion. Upper panel demonstrates the epitope tagging at the C-terminus of open reading frames (ORF). Lower panel demonstrates gene deletion. PCR products were transformed *S. cerevisiae* by high efficiency transformation to obtain the desired strains. TADH1 indicates *ADH1* terminator.

2.6.6 Pulse chase experiment

All proteins under the control of the *GAL1/10* inducible promoter were used for the Pulse-chase experiment. To induce the protein expression rapidly, cells were grown overnight at 30°C in a 2% raffinose selective media in which expression is switched off, but not glucose repressed. Next, cells were diluted 1:10 in galactose (2% w/v) containing appropriate selection and incubated for 2 hours upon which the protein is highly expressed. After that, cells were centrifuged and resuspended into a fresh medium with glucose to switch off the *GAL1/10* promoter expression. Subsequently, cells were imaged by epifluorescence microscopy.

2.6.7 FM4-64 Staining

The lipophilic dye FM4-64 (Invitrogen) was used to stain the vacuolar membrane (Vida and Emr, 1995). Cells from a 1-2 ml of logarithmically growing culture were harvested though centrifugation for 3 min at 3000 rpm and resuspended in 200µl YPD medium containing FM4-

64 (1µg/µl final concentration) and incubated at 30°C for an hour then centrifuged and supernatant was discarded. Next, cells were washed three times with the appropriate minimal medium then resuspended in 200µl of medium and added to 3 ml of fresh selective medium and incubated for 3 hours at 30°C and finally imaged using epifluorescence microscopy.

2.6.8 Yeast two-hybrid assay

The *S. cerevisiae* strain (PJ69-4A mat a) was transformed with plasmids carrying the activation domain (*LEU2*) with Myo2 wild type and other Myo2 mutants separately. (PJ69-4A mat α) transformed with plasmids carrying the binding domain (*TRP*) with Vac17/Inp2 wild type and or their mutants. The transformed cells were mated on a YPD plate for 1 day. Cells were grown for 2 days on SC Leu-Trp- media to select for diploids. Diploid cells were grown for 3-4 days on SC Leu-Trp-Ade-His- and SC Leu-Trp-Ade-His- + 3AT (3mM, 6mM, and 10mM 3-aminotriazole). Finally, plates were imaged using the same setting for all images.

2.7 Protein procedures

2.7.1 SDS-PAGE

8-12% gels of sodium dodecyl sulphate polyacrylamide gel electrophoresis SDS-PAGE were prepared as described (Sambrook and Russell, 2006) using the components as indicated in the following table.

Table 2. 7 The components and their concentrations of SDS-PAGE gels.

Components	Resolving gel (12%)	Stacking Gel (4%)
ddH2O	3.39ml	3.025ml
APS 10% (w/v) stock	100µl	50µl
Protogel (Acrylamide, Bis-acrylamide mix) 30% stock	4ml	0.67ml
Stacking buffer 4X stock	-	1.25ml
TEMED 1000X stock	10µl	5µl
Resolving buffer 4X stock	2.5ml	-
Total Volume	**10ml**	**5ml**

2.7.2 TCA extraction of yeast cells.

Yeast cells were grown overnight then diluted 1:10 starting with 0.1 OD_{600} and grown for 4-5 hours until 0.5 OD_{600} then 10 OD_{600} of cells were collected at 12000 rpm for 1 min. The supernatant was discarded, and the pellet was resuspended with 500µl of NaOH lysis buffer and left on ice for 10 min. After that, 71µl of 40% TCA in dH2O (Trichloro acetic acid) were added to the mixture followed by centrifugation at 13000 rpm for 5 min at 4°C. Subsequently, the supernatant was discarded, and pellet was neutralised by adding 10µl of 1M Tris Base, pH 9.4 then 90µl of 1X SDS loading dye. Samples were then boiled at 95°C
for 10 min and ran on SDS-PAGE gel at voltage (100-150V).

Lysis buffer: 0.2M NaOH and 0.2% β-ME.

2.7.3 Western blot analysis

After separating proteins using SDS-PAGE, proteins were transferred to a nitrocellulose membrane by a wet transfer apparatus (Bio-Rad) using constant current (200mA) for 120 min. Subsequently, 5% (w/v) skimmed milk in the TBST buffer was used for blocking for 1 hour at room temperature or overnight at 4°C. Next, the membrane was incubated with the primary antibody for 1 hour or overnight at 4°C. The membrane was washed 3 times with TBST. Secondary antibody was added and incubated with the membrane for 1 hour at room temperature. After the secondary antibody usage, the membrane was washed with TBST 3 times. Antibodies were used at the following dilutions: anti-Protein A antibody (1:2500) purchased from Merck, anti-GFP antibody (1:3000) purchased Roche, anti-Pgk1 antibody (1:7000) purchased from Invitrogen and anti-mouse antibody (1:10000) purchased Invitrogen. Finally, the blot was enhanced with ECL (Enhanced Chemi-Luminescence). For quantification of protein levels, western-blots containing unsaturated protein bands were analysed in Image Lab software (version 6.1, Bio-Rad). For plotting graphs and statistical analysis GraphPad Prism 10.0.0 (153) (accessed on 12 June 2023) software was used.

PRB (Protein Running Buffer) 10X: 30.28g Tris Base, 144.13g Glycine, 1% (w/v) SDS. Top up to 1L.

Transfer buffer: 15.13g Tris Base, 56.25g Glycine, 4L dH2O, 1L Methanol.

TBS 10X: 24.23g Tris HCl, 80.06 g NaCl. Mix in 800 ml ddH2O. Adjust pH to 7.6 with HCl. Top up to 1 L.

TBST: For 1 L; 100 ml of 10X-TBS + 900 ml ddH2O + 1 ml Tween20.

2.7.4 Cycloheximide

Cells were grown overnight. Next morning cells were diluted to 0.1 OD_{600} and grown until 0.5 /0.6 OD_{600}. Untreated samples were collected before the addition of cycloheximide at final concentration of 200 µg/ml then samples were taken every 20 minutes afterwards. Finally, samples were analysed by western blotting.

2.7.5 Co-immunoprecipitation and protein pull down.

For this experiment 60 OD_{600} units of yeast cells were collected and washed with 50mM HEPES-KOH pH7.6 then frozen at -80 °C. 600µl of lysis buffer were added after thawing the pellet. Next, 400µl of glass beads were added to the mixture and cells were beaten by the bead beater for 30 sec and kept on ice for 2 min. The same procedure was repeated for the second time before centrifuging the tubes for 5 min at 13,000 rpm at 4°C. 400-500µl of supernatant was transferred to another tube and replaced by a lysis buffer with the same amount. Samples were beaten again following the same procedure mentioned above. Subsequently, samples were centrifuged, and supernatant was pooled with the previous one then followed by another centrifugation for 5 min at 13,000 rpm at 4°C. 45µl of supernatant was taken as an input. Next, the supernatant was added to the pre-washed GFP-Trap beads with lysis buffer and incubated at 4°C for 2-3 hours. After incubation, another 45µl was taken as an unbound and beads were washed three times with a lysis buffer containing 10% glycerol with no protease inhibitor. 100µl of 1X protein loading dye was added then samples were boiled at 95°C for 10 min and analysed by western blot.

Lysis buffer: 50mM HEPES-KOH, pH 7.6, 150mM KCl, 100mM β-glycerol phosphate, 25mM NaF, 1mM EGTA, 1mM MgCl2, 0.15% Tween-20, 1mM PMSF (or Protease inhibitor cocktail).

Wash buffer: 50mM HEPES-KOH, pH 7.6, 150mM KCl, 100mM β-glycerol phosphate, 25mM NaF, 1mM EGTA, 1mM MgCl2, 0.15% Tween-20, 10% Glycerol.

2.8 Microscopy protocol

Yeast cells were grown overnight and diluted to grow to log phase (0.5-0.6 OD_{600}) and imaged by epifluorescence microscopy. Cells were grown in minimal medium and imaged at room temperature with the following setting: Axiovert 200M (Carl Zeiss MicroImaging, Inc.) microscope equipped with an Exfo X-cite 120 excitation light source, band pass filters (Carl Zeiss MicroImaging, Inc. and Chroma Technology Corp.), plan 63X/1.4 NA oil apochromat or

an α plan-Fluar 100X/1.45 NA oil objective lens (Carl Zeiss MicroImaging, Inc.), and a digital camera (Orca ER; Hamamatsu). Image acquisition was performed using either Volocity software (Improvision) or ZEN (by Zeiss) software.

2.8.1 Image analysis

Fluorescence images were acquired as z-stacks with a spacing of 0.5µm, and subsequent editing was performed using Adobe Photoshop. The individual image stacks for red and green fluorescence were merged, with the resulting composite images assigned to the red and green channels in Photoshop, respectively. In the case of the bright field images, only the most focused image was captured and added to the blue channel in Photoshop. The brightness and contrast were adjusted to highlight only the cell perimeters.

2.9 Bioinformatics analysis

All DNA and protein sequences were taken from the main source known as: *Saccharomyces* Genome Database (SGD). Protein BLAST (http://blast.ncbi.nlm.nih.gov/Blast.cgi) was used to look for proteins homologues. Multiple DNA sequence alignment was performed using (https://www.genome.jp/tools-bin/clustalw). Jalview software was used for the identification of conserved amino acid sequences. The protein structure and binding prediction was performed by ColabFold binding prediction. ColabFold essentially provides a user-friendly interface to utilize AlphaFold's capabilities within Google Colab. The sequences of proteins of interest were added in ChimeraX-1.4 software as an input then the binding prediction run was carried out on Colabfold using the Google Colab software via ChimeraX-1.4 software. Five prediction models were then produced and the one with the highest confidence of pLDDT value is utilised for further analysis. Finally, all protein structure and protein-protein interaction analysis were performed on PYMOL software.

2.10 Statical analysis.

All statistical analysis mentioned in the figure legends were performed by GraphPad (PRISM). ns means not significantly different. *p values< 0.005; ** <0.01; *** <0.001; two tailed Student t-test or 2way Anova test. Error bars represent the SEM (Standard Error Mean). N=3

Chapter3 Identification of specific Myosin V binding motifs on the cargo receptor proteins, Vac17 and Inp2 that are required for vacuole and peroxisome transport in *S. cerevisiae*.

3.1 Introduction.

Yeast organelles must multiply by growth and division and are transported to their appropriate locations during inheritance, and this requires three highly regulated mechanisms. First, is the attachment of the organelle to the motor through its adaptor. Second, is the movement on actin filaments toward the growing bud. Third, the organelle release from the myosin motor when delivered to the bud tip, which is a process known as the termination of organelle inheritance (**Figure 1.8**). All these steps require coordination with the cell cycle and regulation in spatial and temporal manners (Legesse-Miller *et al.*, 2006; Peng and Weisman, 2008b). Hence, understanding the dynamics of organelle inheritance in *S. cerevisiae* remains an essential question to unravel. The research described in this chapter focused on vacuole and peroxisome transport during cell division.

The mechanisms behind the inheritance of vacuoles during cell division have been well-studied compared to other yeast organelles (**Section 1.8**). During the G1 phase, vacuoles can form segregation structures which are pulled into the bud by Myo2 along actin filaments. However, this transport is firstly controlled in a temporal and spatial manner where the cyclin-dependent kinase, Cdk1, phosphorylates Myo2 protein and its vacuole receptor Vac17. This phosphorylation event is crucial for the Vac17 and Myo2 interaction (Peng and Weisman, 2008b). The interaction between Vac17 and Myo2 requires Vac8 (Wang et al., 1998; Pan and Goldfarb, 1998). Once the complex of Myo2-Vac17-Vac8 is formed transport along actin cables to the bud can take place. Once the vacuole reaches the bud tip, Vac17 is released from

Myo2 and targeted for breakdown which prevents vacuoles from remaining associated with Myo2 and actin filaments (Yau et al., 2014, 2017; Tang et al., 2003).

Analogous to vacuole inheritance, inheritance of peroxisome depends on the presence of actin filaments, Myo2 (class V myosin motor protein) and Inp2 the peroxisomal adaptor of peroxisome inheritance (Hoepfner *et al.*, 2001; Fagarasanu *et al.*, 2006). However, peroxisome transport is less well characterised but it is expected that transport spatiotemporally controlled and limited evidence exists that supports this hypothesis (Yau et al., 2014, 2017; Wong et al., 2020). In order to understand how the transport of vacuoles and peroxisomes is regulated, it is critical to understand how the early stages of organelle inheritance are initiated in which the interaction between Myo2 and its adaptors occurs. This chapter focuses on understanding how Vac17 and Inp2 bind to Myo2 and initiate vacuole and peroxisome inheritance.

3.2 Vac17 has a conserved binding motif with Myo2 required for vacuole inheritance.

Much data supports the idea that Vac17 is the specific vacuolar protein required for vacuole inheritance. It binds Myo2 to ensure vacuoles are transported to the bud during cell growth. Specific amino acids in Myo2 are required for vacuole inheritance (Ishikawa *et al.*, 2003). These are D1297, D1296, E1293, N1304, G1248. Furthermore, it has been demonstrated that residues from 110-170 (known as Myo2 interaction site-MIS) of Vac17 are involved in the specific binding to Myo2 and that these residues are required for vacuole inheritance **Figure 3. 1 A** (Ishikawa *et al.*, 2003). Since this mechanism is highly regulated from the binding step between Vac17 and Myo2 (in the early stage of the cell cycle) until the dissociation step (in the late stage of the cell cycle), it was of interest to investigate how this mechanism is regulated and maintained by studying how Vac17 binds Myo2 and what are the specific residues responsible for the binding. To start this study a bioinformatic analysis was carried out of the Vac17 sequence between several yeast species. This revealed a highly conserved motif between amino acids 119-142 which we considered might be required for vacuole inheritance **Figure 3. 1.** However, the sequence between amino acid 119-130 was shown to be required for Vac17 phosphorylation by the casein kinases I (Yck3) and the vacuolar membrane protein (Vps41), which regulate dissociation of Vac17 from Myo2 when the vacuole reaches the bud (Wong *et al.*, 2020). Hence, based on Vac17 sequence analysis and

to avoid the interference of phenotypes during our *in vivo* study on Vac17-MIS, we excluded the region from 119-130 from this study and only focused on the sequence between 131-144 and hypothesised that it is required for vacuole inheritance.

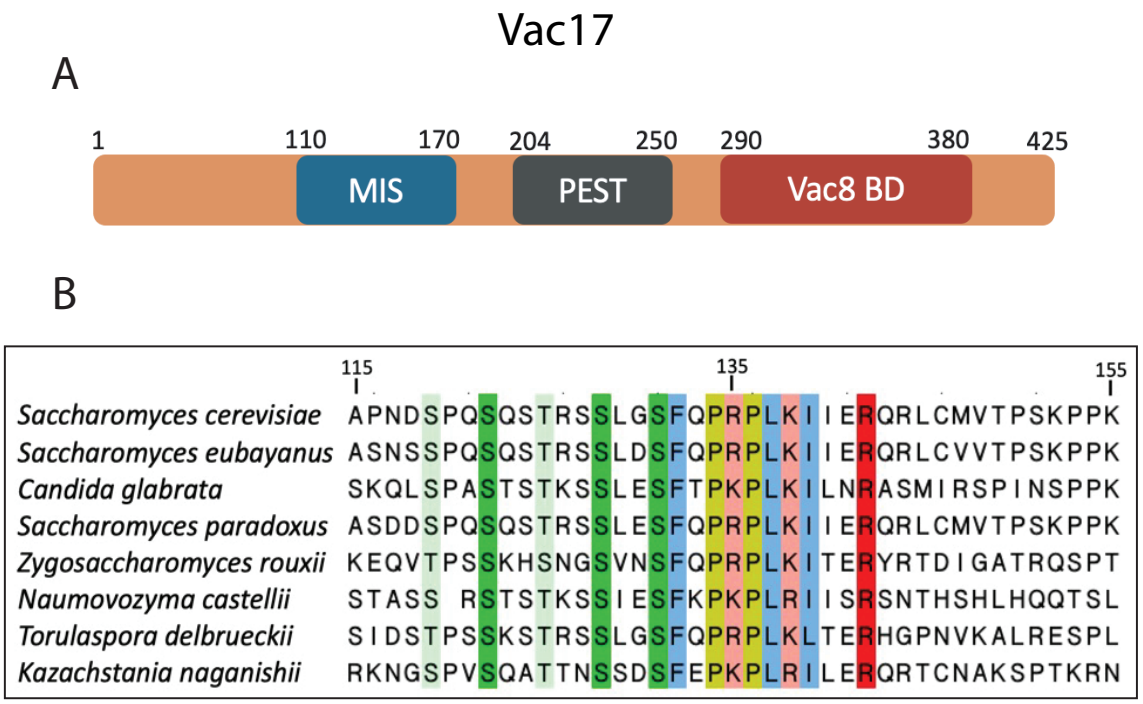

Figure 3. 1 Bioinformatic analysis of Vac17-MIS revealed a highly conserved site. A) A schematic diagram showing the different domains in Vac17. MIS refer to Myo2 interaction site, PEST refer to the sequence required for the Vac17 breakdown by the proteasome and BD refers to the Vac8 binding domain. B) ClustalW was utilised to create multiple alignment of the conserved site of Vac17 from different yeast species. All the highlighted residues are the most conserved residues compared to the unhighlighted residues.

3.3 Confirming that the hypothetical Vac17-MIS is required for vacuole inheritance.

Having identified a highly conserved motif on Vac17 in the region known to be required for the Myo2 interaction we sought to understand whether this shorter motif (131-143) (referred to as L-mis hereafter with L meaning Large) on Vac17 is required for vacuole inheritance and whether it identifies the specific region on Vac17 that binds to Myo2. Hence, this *vac17L-mis* mutant was constructed on a plasmid tagged with GFP under the Vac17 endogenous promoter carrying the 13 amino acids deletion from amino acid 131-143 (*vac17L-mis)* within the MIS and transformed it into *vac17Δ* cells. With the wild type cells transformed

with Vac17-GFP plasmid were used as controls in which we can see normal vacuole inheritance. In addition, *vac17Δ* cells were transformed with either empty plasmid or Vac17-GFP plasmid. Vacuole inheritance was then analysed and divided into 3 categories with i) cells showing normal vacuole inheritance where the vacuolar signal (FM4-64) is present in the mother and the bud ii) cells showing no vacuole signal present in the bud iii) cells showing weak vacuole signal in the bud. *vac17Δ* cells transformed with the empty plasmid showed no rescue in vacuole inheritance and full rescue in vacuole inheritance with the Vac17-GFP plasmid, in which in this case Vac17-GFP has already delivered vacuoles to the bud and gets broken down by the proteasome. However, the expression of the *vac17L-mis* mutant resulted in a very strong effect in vacuole inheritance with *vac17L-mis*-GFP being colocalised with vacuoles in the mother cell. This colocalization is similar to what has been shown with the Myo2-*D1297N* mutant was shown to effect vacuole inheritance (Yau *et al.*, 2014) **Figure 3. 2 A and B**. This result suggest that this region is specific for the binding of Vac17 to Myo2 and inheritance of vacuoles.

Within the L-MIS region identified above there are 6 highly conserved amino acids from 134-139 including of 2 positively charged residues (R135 and K138) as well as hydrophobic residues thought to be essential for the Vac17-Myo2 interaction. Hence, it was intriguing to minimise the deletion to 6 amino acids from amino acid 134-139 (*vac17S-mis)* (S refers to small deletion). A *vac17S-mis* mutant was constructed on a plasmid tagged with GFP and transformed to *vac17Δ* cells along with applying all the controls utilised with *vac17L-mis* result. As before transformation with wild type Vac17 led to a full rescue of vacuole inheritance and with the *vac17S-mis* mutant we found the same significant effect on vacuole inheritance, similar to the large MIS deletion **Figure 3. 2 A and B.** Both mutants resemble the *vac17Δ* phenotype. Hence, these results interestingly suggest deletion of only a few amino acids in this region is sufficient to affect inheritance and therefore probably binding with Myo2.

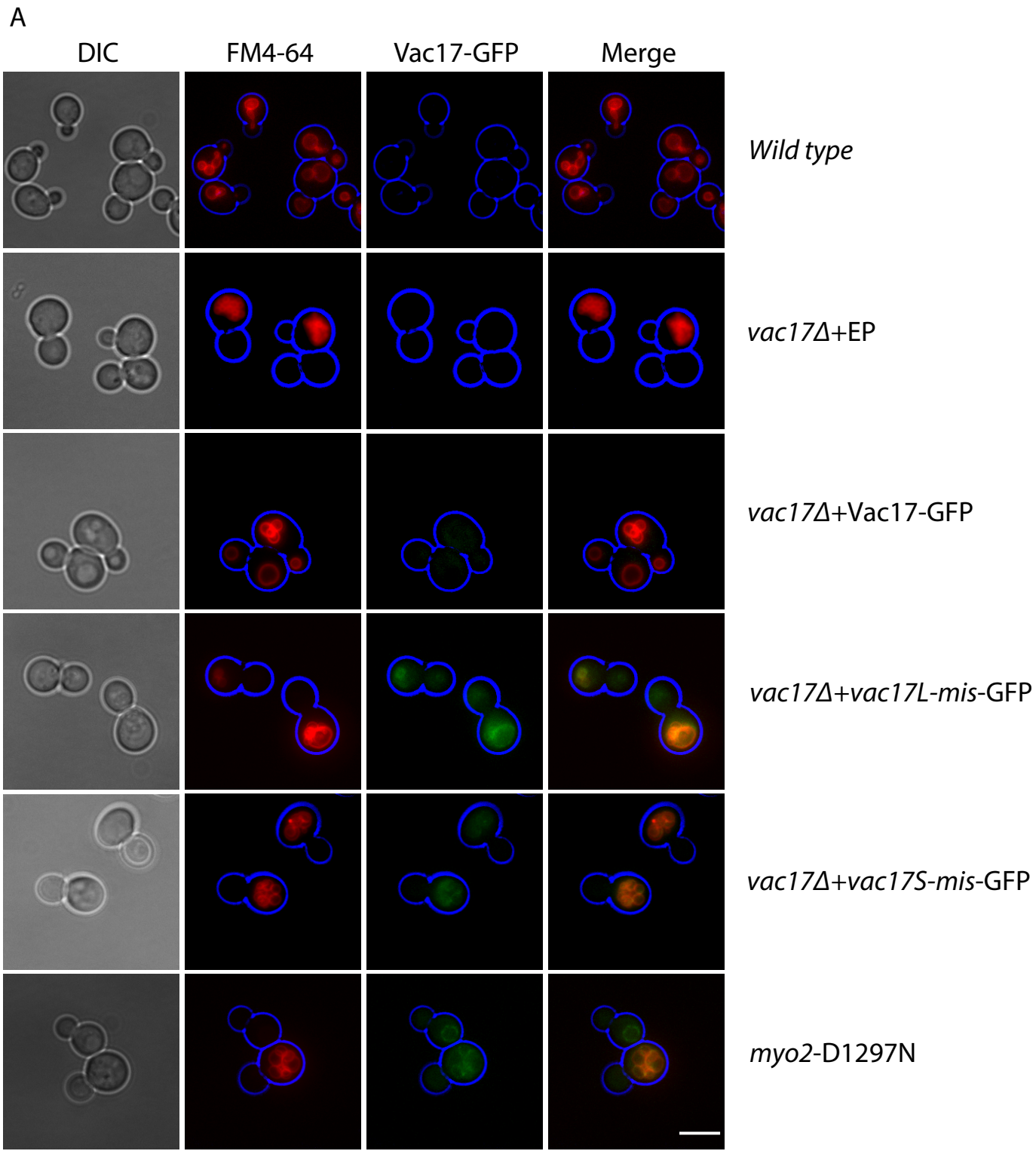
A
DIC
FM4-64
Vac17-GFP
Merge
Wild type
vac17Δ+EP
vac17Δ+Vac17-GFP
vac17Δ+vac17L-mis-GFP
vac17Δ+vac17S-mis-GFP
myo2-D1297N

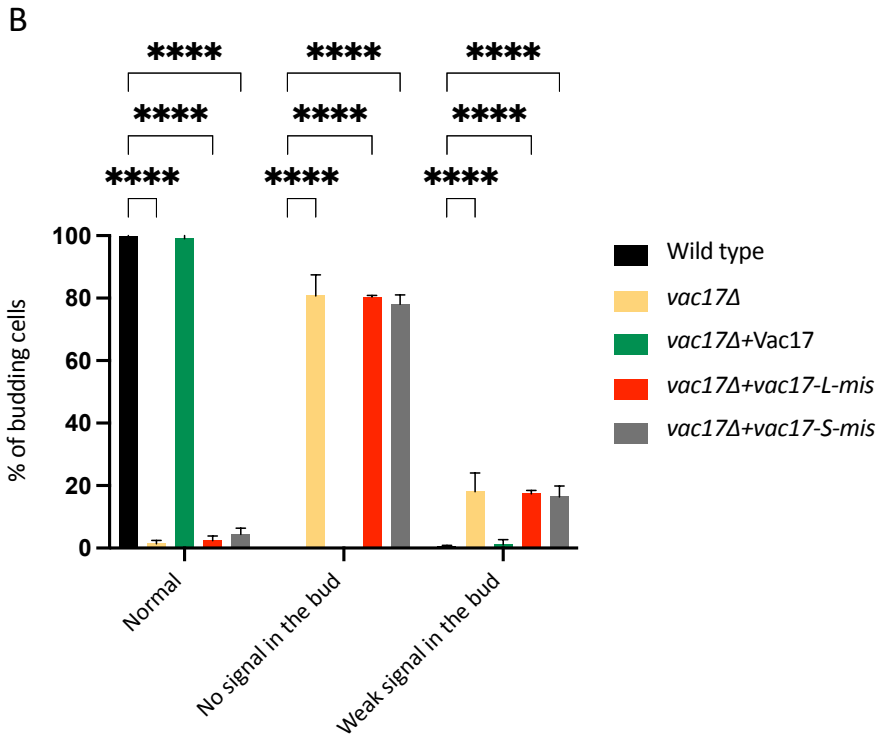

Figure 3. 2 The highly conserved MIS on Vac17 is required for vacuole transport. A) Vacuole transport is defective in *vac17Δ* cells containing *vac17L-mis* and *vac17-S-mis* resembling *vac17Δ* phenotype. Myo2-*D1297N* mutant was utilised as a control to show the localisation of Vac17-GFP when the interaction with Myo2 is prevented. The transformed cells were grown logarithmically then incubated with FM4-64 for an hour for staining vacuoles. Cells were then washed 3 times and incubated with fresh media for 3-4 hours then analysed by epifluorescence microscopy. Scale bar is 5µm. B) quantification analysis with a minimum of 100 cells counted in 3 independent experiments. Error bars indicate SEM (Standard Error Mean). N=3. * p-value < 0.01; **** p-value < 0.0001; 2way ANOVA test.

3.4 Structural prediction of Vac17-Myo2 interaction.

Vac17 is known to be the vacuolar adaptor for Myo2 in transporting vacuoles during cell division but the structural details of the Vac17 binding interaction Myo2 remain unknown. According to the bioinformatics analysis and the *in vivo* experiments shown in the above **Sections 3.2 and 3.3**, it is clearly suggested that the Vac17-MIS region, narrowed down to be between 6 to 13 residues, is likely to be the main region that forms a stable interaction complex with Myo2. Previous studies have attempted to resolve the Myo2 cargo binding domain (CBD) in complex with Vac17 MIS, but they were unsuccessful in yielding any crystals (Liu *et al.*, 2022), thus we decided not to proceed with crystallography but instead utilised a

bioinformatic method in which the structure of Myo2-CBD can be predicted in complex with Vac17-MIS. For this we utilised ColabFold software (**see section 2.9)**. ColabFold has been known as a powerful tool in predicting the protein structure with high accuracy (Baek *et al.*, 2021; Jumper *et al.*, 2021). Myo2-CBD from amino acid (1152-1574) and Vac17-MIS from amino acid (112-157) were submitted to the software as an input to run the prediction. The resulted prediction complex showed a C-terminal helix from (I139-R142) and N-terminal loop from (R135-K138) on Vac17-MIS that interact with a helix structure on Myo2-CBD. Moreover, 3 residues on Vac17 (R135, K138 and R142) **Figure 3. 3** showed specific interaction to the Myo2-CBD surface that consist of (E1293, D1296, D1297 and N1304) **Figure 3. 3**. Previous study have shown that mutations in residues E1293K, D1297N and N1304D of Myo2 effect the interaction between Vac17/Myo2 as well as vacuole inheritance (Taylor Eves *et al.*, 2012) which further supports the predicted structure.

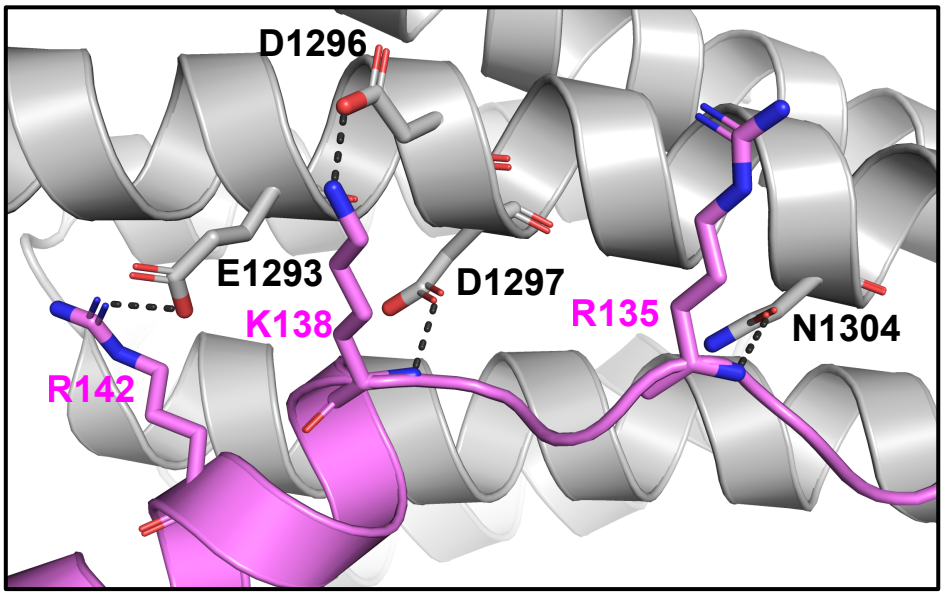

Figure 3. 3 A schematic diagram showing the prediction structure of Myo2-CBD in complex with Vac17-MIS. The Myo-CBD/Vac17-MIS interface in the predicted structure containing residues R135, K138 and R142 interacting with residues E1293, D1296, D1297 and N1304.

3.5 Specific site directed mutagenesis in Vac17 MIS was used to determine the key residues required for vacuoles inheritance.

Examining the predicted complex allowed the molecular basis of the Myo2-CBD/Vac17-MIS interaction to be explored further. Although the residues on Myo2 were already known, it was intriguing to discover the essential residues for the binding on Vac17. Mutation of Vac17 residues would allow vacuole specific interactions to be disrupted while mutations on Myo2 might affect several mechanisms in the cell (Catlett and Weisman, 1998; Jin *et al.*, 2011). Hence, an *in vivo* study with a small site directed mutagenesis screen was conducted by making Vac17 mutants carrying single or double amino acid mutations. Since we observed 3 positively charged residues on Vac17-MIS (R135, K138 and R142), the positive charges were converted to a negatively charged residues starting with single mutants (R135E, K138D and R142E) and double mutants (R135E/K138D) or (R135E/R142E) or (K138D/R142E). All these Vac17 mutants were constructed on a plasmid carrying Vac17 with the desired mutation tagged with GFP under its endogenous promoter and transformed into *vac17Δ* cells and analysed by imaging. Vac17 wild type plasmid transformed into *vac17Δ* was used as a control. As single mutants, the cells expressing the *vac17-R135E* mutation did not show any defects in their vacuole inheritance phenotype whereas those expressing the *K138D* and *R142E* mutations showed a significant level of effect on vacuole inheritance (40% of the cells showed a defect in the inheritance) compared to the control (where there is no inheritance defect) **Figure 3.4 A and C**. All double mutants showed very strong effects on vacuole inheritance as shown in **Figure 3.4 B and D**. This result suggests that the mutagenesis analysis is consistent with the predicted structure shown in **Section 3.4**.

A

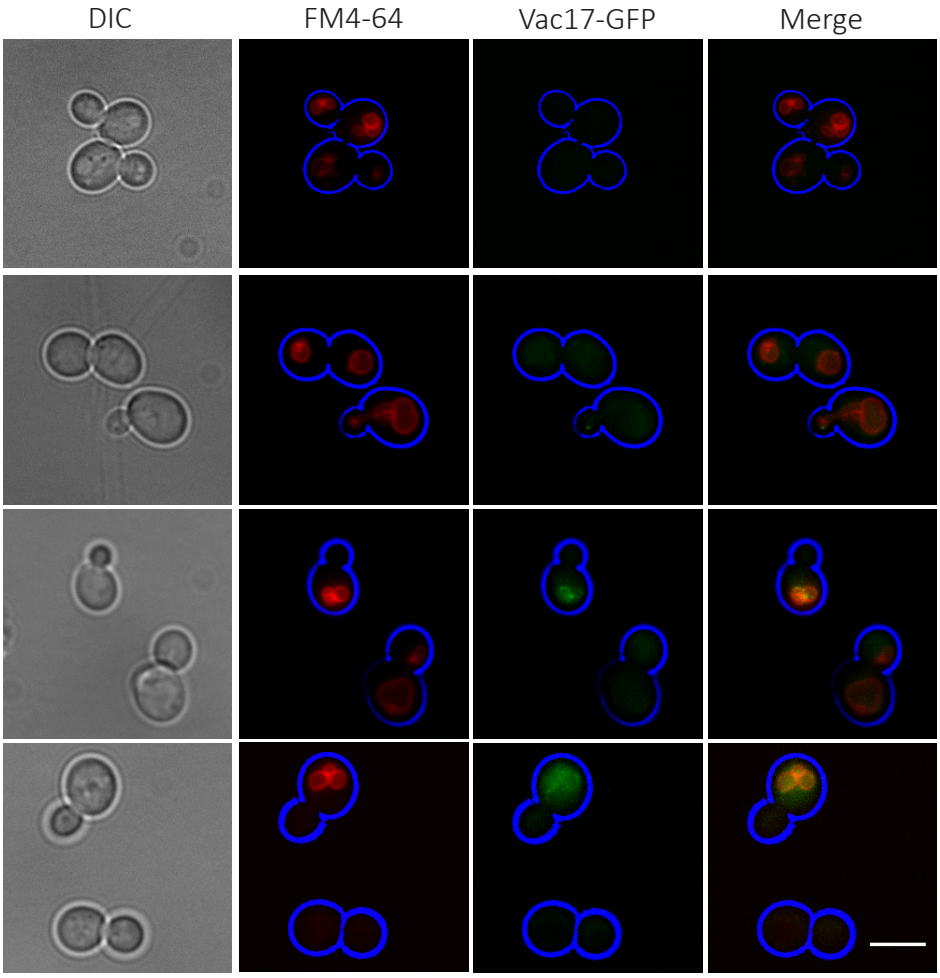
DIC
FM4-64
Vac17-GFP
Merge
vac17Δ+ Vac17-GFP
vac17Δ+vac17R135E-GFP
vac17Δ+vac17K138D-GFP
vac17Δ+vac17R142E-GFP

B

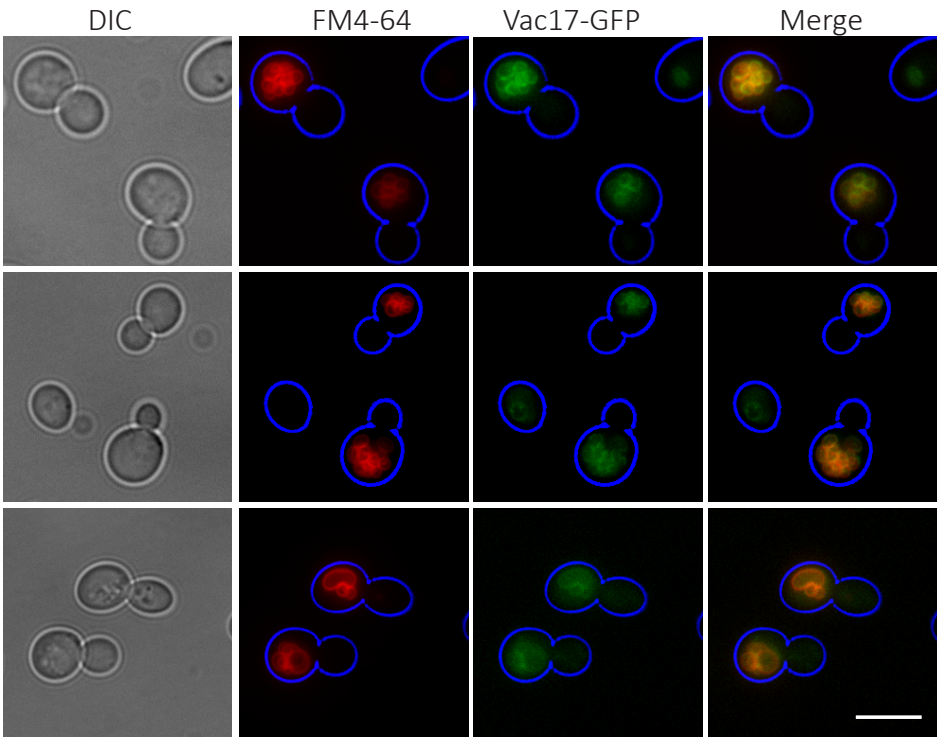
DIC
FM4-64
Vac17-GFP
Merge
vac17Δ+vac17 R135E/R142E-GFP
vac17Δ+vac17 R135E/K138D-GFP
vac17Δ+vac17 K138D/R142E-GFP

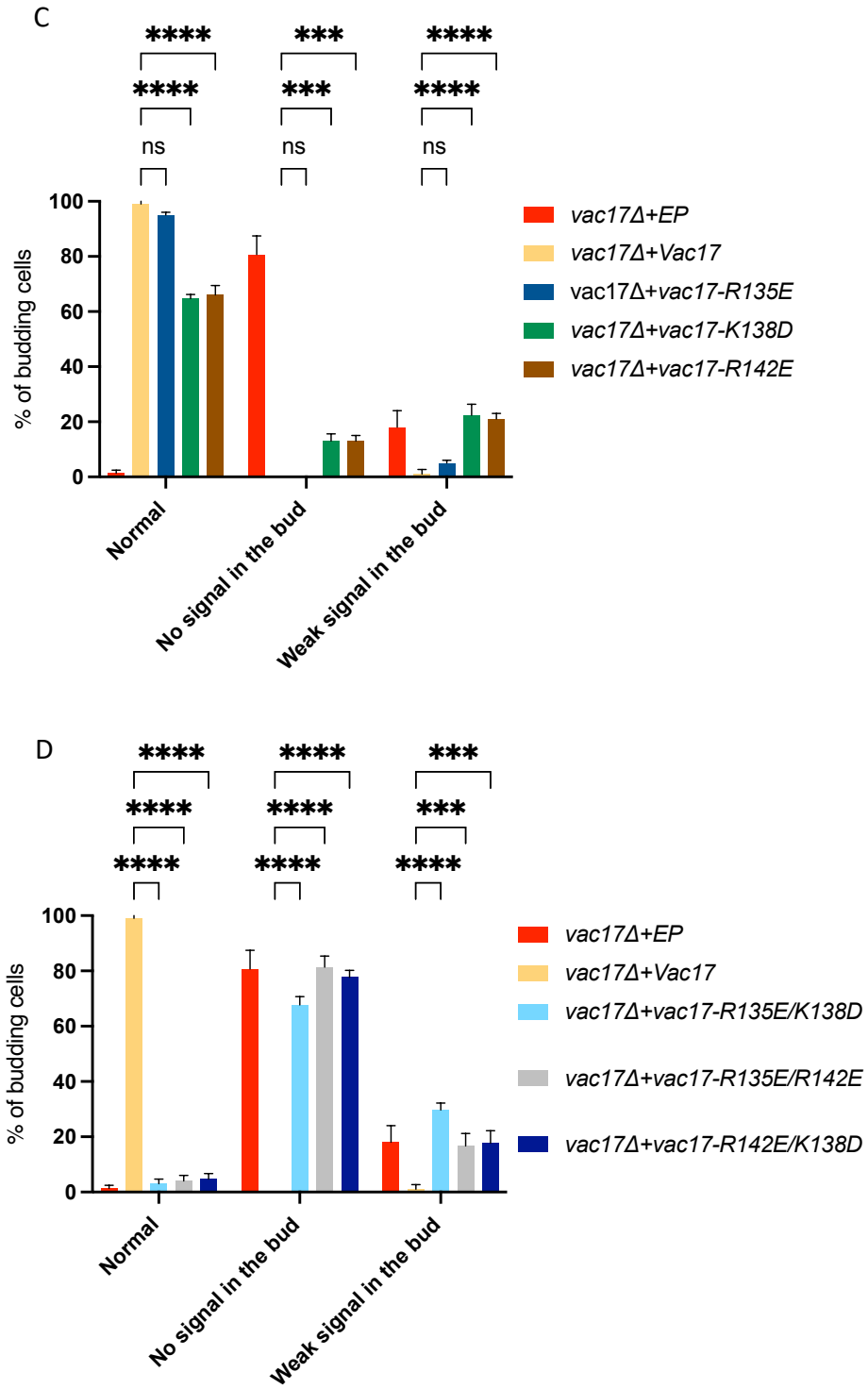

Figure 3. 4 Vacuole inheritance is affected with Vac17-MIS double mutants. Cells were grown logarithmically then incubated with FM4-64 for an hour for staining vacuoles. Cells were then washed 3 times and incubated with fresh media for 3-4 hours then analysed by imaging. (A) Vac17-MIS (K138D and R142E) single mutants showing mild effect on vacuole inheritance compared to (R135E) where there was no effect. (B) Vac17-MIS double mutants defective in vacuole inheritance resembling *vac17Δ* cells. Scale bar is 5µm. (C and D) quantification analysis with a minimum of 100 cells counted in 3 independent experiments. Error bars indicate SEM (Standard Error Mean). N=3. * p-value < 0.01; **** p-value < 0.0001; 2way ANOVA test.

3.6 Yeast two-hybrid assay confirms the sites of interaction between Myo2 and Vac17.

We next asked if we can further verify and analyse these potential MIS residues to determine if they are required for Myo2 interaction. To do this a yeast two-hybrid assay was used. Plasmids expressing Myo2 cargo binding domain CBD from amino acid (1113-1574) and several Myo2 mutants linked to the GAL4 activation domain were provided by Lois Wiesman lab as well as Vac17 fused to GAL4 binding domain provided by the same lab (Taylor Eves *et al.*, 2012). A control experiment showing Vac17/Myo2 interaction and several Myo2 mutants where there is no interaction between Vac17/Myo2 mutants was conducted to reproduce the results shown previously (Taylor Eves *et al.*, 2012). An Inp2 construct was also used as a positive control for Myo2 and *myo2* mutant interactions **Figure 3.5 A, B and C.** The single and double mutations in Vac17-MIS were constructed by site directed mutagenesis for this project. Mat *α* cells were transformed with (TRP) plasmids carrying Vac17 single or double mutation fused with the GAL4 binding domain and crossed with Mat a cells transformed with (LEU) plasmids carrying Myo2 and its mutants fused with the GAL4 activation domain. The mated cells were then selected on plates containing synthetic complete medium (LEU-TRP-) and the growing cells were re-selected on synthetic complete medium (LEU-TRP-ADE-HIS-) containing different concentration of 3-aminotriazole. The white growing cells on the plates indicate that there is an interaction, and the pink growing cells represents no interaction due to the consequence of not expressing the *ADE2* gene. This approach indicated that there was no interaction of *vac17-K138D* or *vac17-R142E* with Myo2 as single mutants and (*R135E/K138D*, *K138D/R142E*, *R135E/R142E*) as double mutants **Figure 3.6 A and B, Figure 3.7 A and B.** This result is in complete agreement with the previous experiment in **Section 3.5**. As in that experiment the *vac17-R135E* single mutant has similar phenotype to wild type Vac17 suggesting that altering this site has a minor contribution to the Vac17/Myo2 interaction and vacuole inheritance compared to the K138 and R142 residues. Interestingly, both *vac17-K138D* and *R142E* showed rescue in the interaction with *myo2-D1296N* and myo2-*E1293K* respectively with *vac17-R142E* showing stronger interaction in combination with *myo2-E1293K* shown in **Figure 3.6 A and B**. This observation provides strong genetic evidence that Vac17 R142 interacts with Myo2 E1293 and strongly validates the structural model.

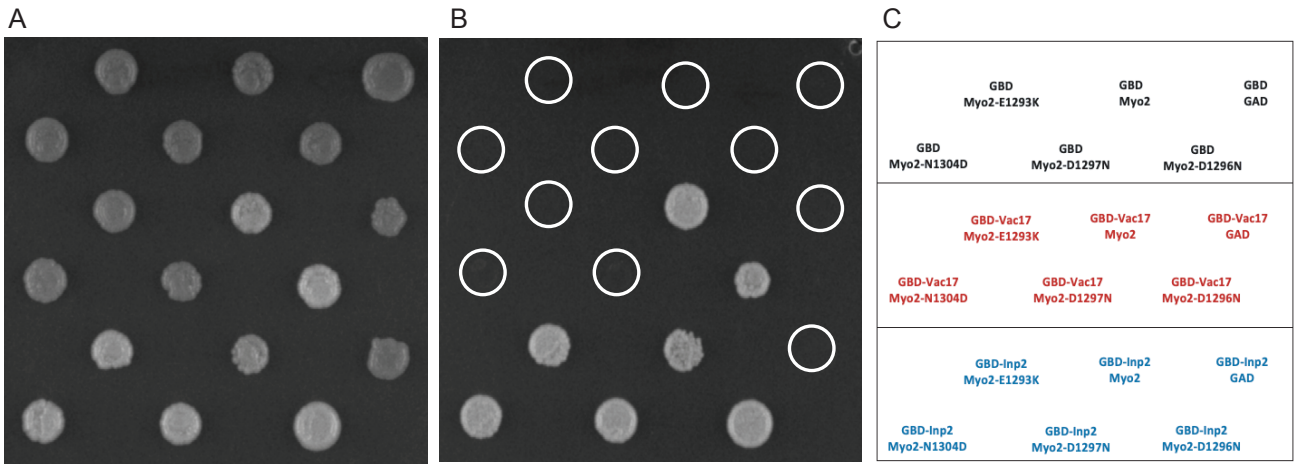

Figure 3. 5 Vac17 and Inp2 interact with Myo2-CBD in yeast two-hybrid test. (A) Mat a cells were transformed with plasmids carrying the activation domain and Mat α cells with plasmids carrying the binding domain. Transformed cells were mated and reselected as diploid on leu-trp- plates. (B) Cells were then grown on leu-trp-ade-his- and leu-trp-ade-his- containing different concentration of 3-aminotriazole (3mM, 6mM and 10mM) to select for the interactions. Inp2 was utilised as positive control and showing that all the residues affecting Vac17 interaction do not affect Inp2 interaction. (C) A schematic diagram showing how the cells were ordered on petri dish in which they represent the same locations in section A and B.

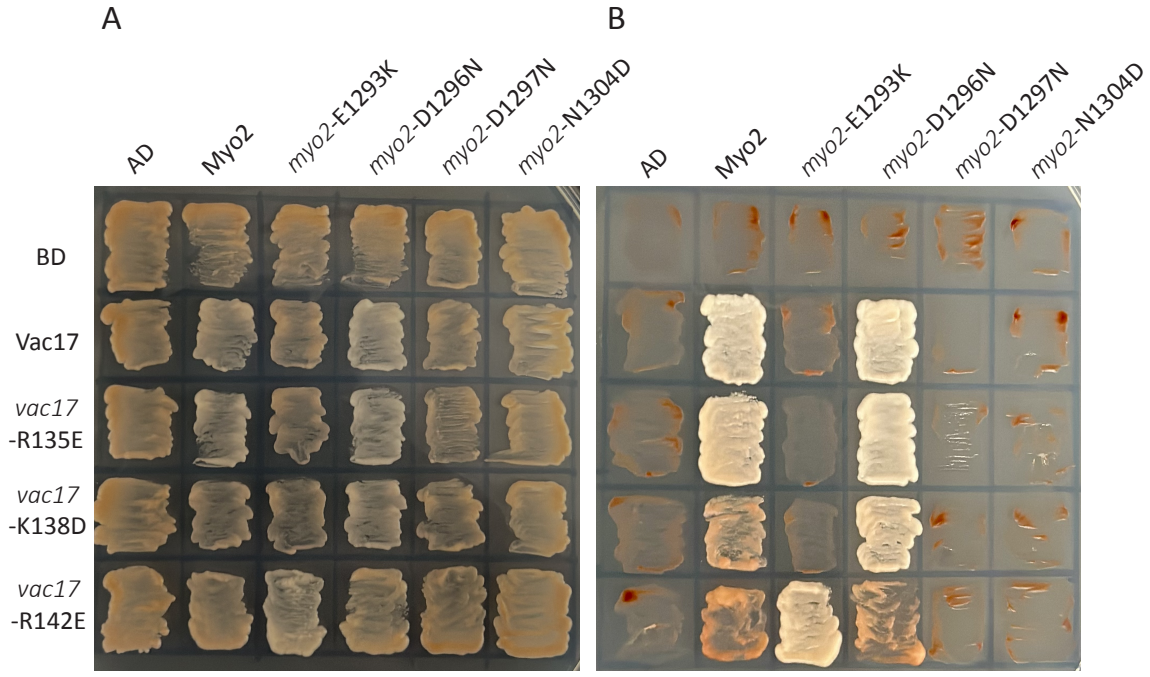

Figure 3. 6 Vac17 single MIS mutants affected Myo2 interaction. Vac17 does not interact to Myo2-CBD in yeast two-hybrid test in some Vac17 single MIS mutants such as *vac17-K138D*, *vac17-R142E* where *vac17-R135E* resembled wild type Vac17 interaction. (A) Mat a cells were transformed with plasmids carrying the activation domain and Mat α cells with plasmids carrying the binding domain. Transformed cells were mated and reselected as diploid on leu-trp- plates. (B) Cells were then grown on leu-trp-ade-his- and leu-trp-ade-his- containing different concentration of 3-aminotriazole (3mM, 6mM and 10mM) to select for the interactions.

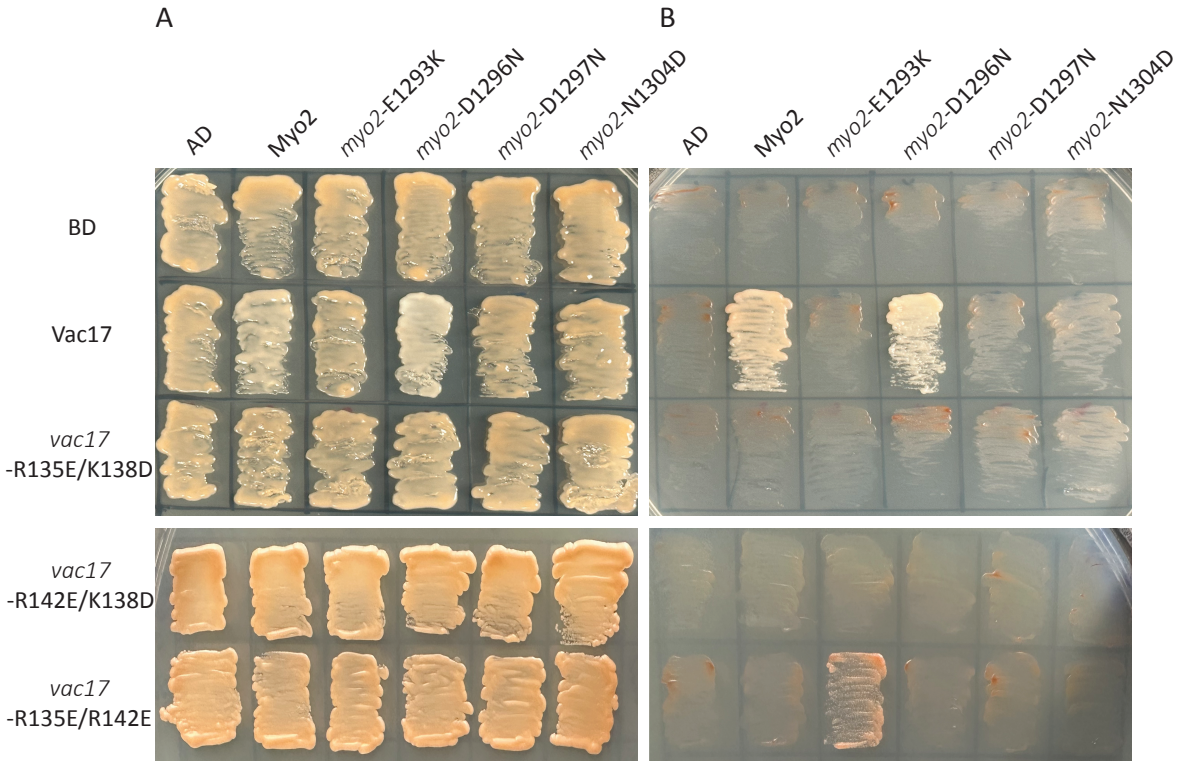

Figure 3. 7 Vac17 double MIS mutants affected Myo2 interaction. Vac17 does not interact to Myo2-CBD in yeast two-hybrid test in all Vac17 double MIS including *vac17-R135E/K138D*, *vac17-R142E/K138D* and *vac17-R135E/R142E* compared to wild type Vac17. (A) and (B) explaining the same procedure utilised in the previous **Figures 3.5 and 3.6**.

3.7 Elevated level of Vac17-MIS mutant do not rescue vacuole inheritance deficiency.

When vacuole reaches the bud tip Vac17 is targeted for breakdown to release the vacuole from Myo2 and Vac8 complex (Yau *et al.*, 2014; Yau, Wong and Weisman, 2017; Wong *et al.*, 2020). The breakdown process is regulated by phosphorylation and ubiquitylation events mediated by Cla4 and Dma1, respectively. Dma1 is recruited to Vac17 after it is being phosphorylated at amino acid residue T240 by an unknown factor (Yau et al., 2014). Once the vacuole reaches the bud tip, Cla4 phosphorylates Vac17 at amino acid residue S222, which allows Dma1 to ubiquitinate Vac17 resulting in Vac17 breakdown by the proteasome (Yau et al., 2017). However, introducing S222A and or T240A mutations into Vac17 prevents Vac17 breakdown resulting in elevated Vac17 levels and accumulating of Vac17 in the bud (Yau *et al.*, 2014; Yau, Wong and Weisman, 2017). Therefore, we asked whether elevating the *vac17-mis* mutant by adding S222A or T240A mutations would rescue the vacuole inheritance due to the higher level of *vac17-mis* available. This might clarify whether having more *vac17-mis*

would rescue the binding with Myo2 but with having normal levels of the *vac17-mis* is not enough to interact with Myo2. To test this, we utilised one of the Vac17 double mutants tagged with GFP (*vac17-R135E/K138D*) and introduced either S222A or T240A by site directed mutagenesis. A western blot analysis showed how that both S222A and T240A mutations led to an increase in the level of the *vac17-mis* mutant protein **Figure 3.8 A**. As shown below, imaging and statistical analysis revealed that introducing S222A or T240A mutations in *vac17-mis* did not rescue vacuole inheritance **Figure 3.8 B and C**. Hence, this result confirms that even with high levels of *vac17-mis* the interaction with Myo2 is not rescued as it is also suggested that the Vac17 MIS mutations strongly reducing the binding to Myo2.

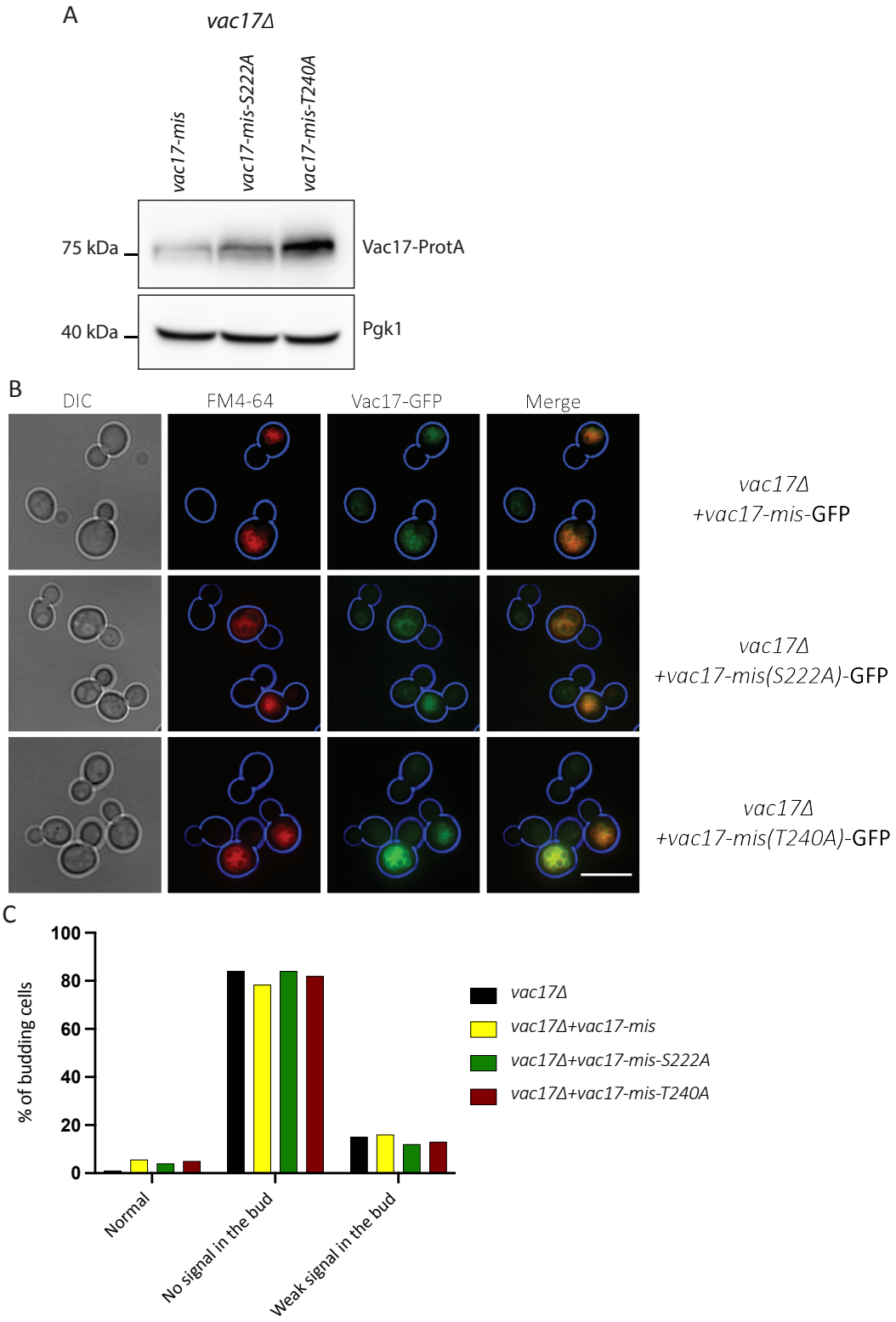

Figure 3. 8 Elevating Vac17-MIS mutant level does not rescue vacuole inheritance. (A) western blot analysis of *vac17-mis* with S222A and T240A mutations using anti protein A (B) cells were grown logarithmically then incubated with FM4-64 for an hour for staining vacuoles. Cells were then washed 3 times and incubated with fresh media for 3-4 hours then analysed by imaging. Vac17-MIS elevated level mutants showed no rescue in vacuole inheritance. Scale bar is 5µm. (C) quantification analysis with a minimum of 100 cells counted in each sample.

3.8 Cells failed to inherit vacuole with *vac17-mis* mutant can make them *de novo*.

Vacuoles can be formed *de novo* when cells are lacking vacuoles due to an inheritance defect (Jin and Weisman, 2015). Since we observed vacuole inheritance deficiency in cells containing the *vac17-mis* mutant, it was intriguing to test vacuole *de novo* formation in wild type cells and cells with *vac17-mi*s mutant. Therefore, *vac17Δ* cells were transformed with 2 plasmids, one with Vph1-GFP as a constitutive vacuolar marker and the other one either Vac17 or the *vac17-mis* mutant. FM4-64 dye was also used as a pulse label to visualise pre-existing vacuoles. The transformed cells expressing Vph1-GFP were subjected to incubation with FM4-64 at 30°C for an hour and then washed 3 times with fresh medium not containing FM4-64 and then incubated for 3-4 hours before imaging. FM4-64 stain can only label the pre-existing vacuoles and not the newly formed ones. After washing the cells, the vacuoles that did not form *de novo* are the only ones labelled with red. We observed that the vacuoles in cells expressing wild type Vac17 contained both the Vph1-GFP and FM4-64 labels whereas in a few cells expressing the *vac17-mis* mutant, the vacuoles in the bud were only labelled with Vph1-GFP compared to the mother cell where vacuoles were labelled with both Vph1-GFP and FM4-64 **Figure 3.9**. This demonstrates that vacuole inheritance is clearly affected in cells expressing the *vac17-mis* mutant and vacuoles are formed *de novo* in the bud. This result is consistent with previous observations (Jin and Weisman, 2015). Finally, our results suggests that *vac17-mis* mutant fails to inherit vacuoles and therefore form them *de novo* due to the inhibition in the interaction between *vac17-mis* mutant and Myo2.

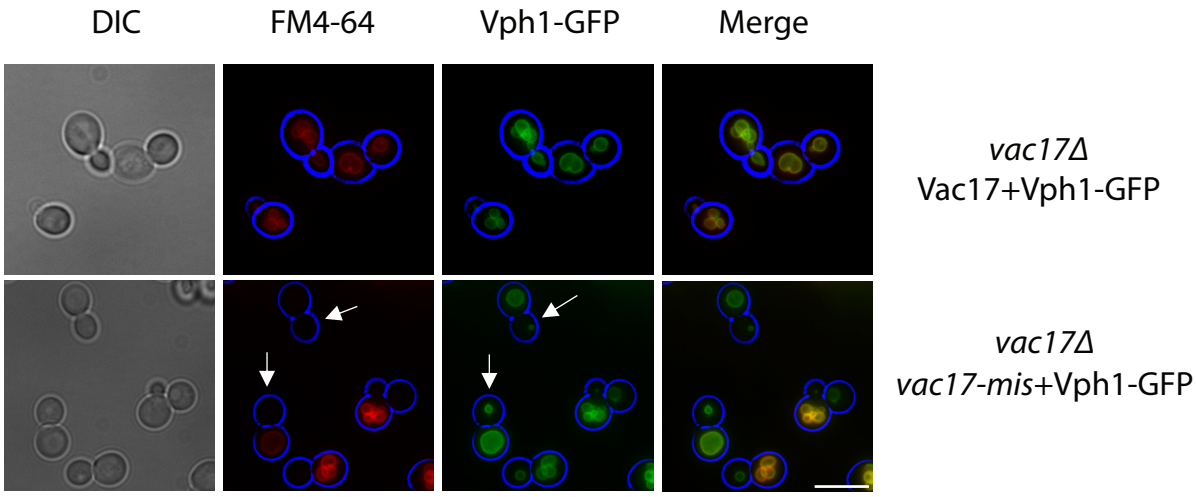

Figure 3. 9 Cells containing *vac17-mis* mutant with lacking vacuoles form them *de novo*. Cells transformed with Vph1-GFP as a constitutive vacuolar marker, were stained with FM4-64 (Red) for an hour and then washed 3 times with fresh medium then incubated for 3-4 hours at 30°C then imaged. Cells were labelled with both Vph1-GFP and FM4-64. Arrows indicate the *de novo* formed vacuole labelled with Vph1-GFP where they are not stained with FM4-64. Scale bar is 5µm.

3.9 Inp2 contains a functional MIS site required for peroxisome inheritance.

Inp2 is a peroxisomal membrane receptor required for myosin Myo2 binding and is needed for peroxisome inheritance. Inp2 interacts with Myo2 cargo binding domain (CBD) to mediate peroxisome transfer to the bud hence an *INP2* gene deletion results in peroxisome inheritance deficiency **Figure 3.11 A and 3.12 A** (Fagarasanu *et al.*, 2006). From the Myo2 CBD, it has been shown that certain amino acid residues including Y1415, W1407, Y1483 and Y1484 are important for Inp2 binding (Fagarasanu *et al.*, 2009). Mutations in these residues affect peroxisome transport to the bud, primarily by preventing the interaction with Inp2. A yeast two hybrid assay has been developed that detects the Inp2-Myo2 interaction (Fagarasanu *et al.*, 2006). Using this assay, the region between residue 504 to 618 of Inp2 was found to bind Myo2 independently of the whole Inp2 protein. However, this binding was not as strong as when the whole protein binds. In addition, in a recent *in vitro* study it was shown that Inp2 binds to Myo2 through a specific conserved motif containing 13 amino acids, from amino acid 530 to 543 can bind to Myo2-CBD with binding affinity of 30µM. (Tang *et al.*, 2019). Since it is intriguing to identify the specific residues essential for the binding, we performed a bioinformatic analysis for this region of Inp2 among several yeast species and we found that there are 6 amino acids from (F534-L539) with a consensus sequence (GF/LXLDI/VF/LK/R) which shown to be highly conserved residues in this region **Figure 3.10.**

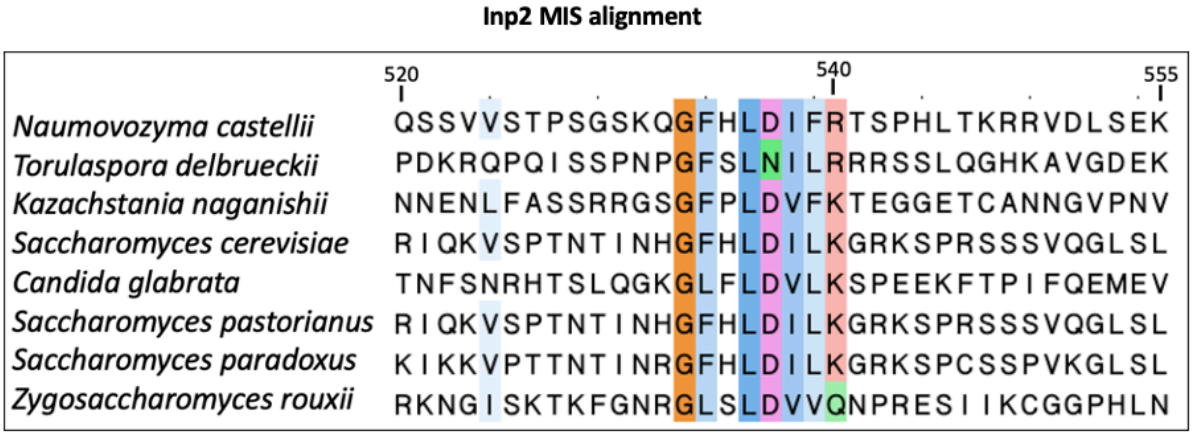

Figure 3. 10 Bioinformatic analysis of Inp2-MIS revealed a highly conserved site. ClustalW was utilised to create multiple alignment of the conserved site of Inp2 from different yeast species. All the highlighted residues are the most conserved residues compared to the unhighlighted residues.

3.9.1 Confirming that the Inp2 motif is required for peroxisomes inheritance.

We sought to do an *in vivo* study to gain more insight into the role of the 6 amino acids (F534-L539) motif in peroxisome inheritance. It has been reported that any mutations in Myo2 residues, which affect peroxisome inheritance, also affect the transportation of secretory vesicles since their Myo2 adaptors overlap in their binding region in Myo2 (Fagarasanu *et al.*, 2006; Tang *et al.*, 2019). Therefore, we hypothesised that making a mutation in Inp2 would not affect secretion and cell growth, in contrast to mutations in Myo2. To investigate the site identified further, wild type Inp2 and the *inp2-mis* mutant (with a deletion from residue 534-539) were tagged with mNeongreen (green fluorescent protein) were constructed on plasmids expressed under the Inp2 endogenous promoter. These plasmids were then co-transformed into *inp2Δ* cells with another plasmid carrying red fluorescent protein (mRuby2) fused with PTS1 (peroxisomal targeting signal) to visualise peroxisomes during imaging analyses. The *inp2Δ* cells transformed with empty plasmid were used as control where peroxisome inheritance was not rescued compared to those transformed with wild type Inp2-mNG. We found that Inp2-mNG was able to rescue peroxisome inheritance in *inp2Δ* cells and Inp2 was localised with peroxisomes in the bud. However, *inp2-mis*-mNG did not rescue peroxisome inheritance with peroxisomes and *inp2-mis* mutant was located in the mother cell suggesting that the 6 residues deleted are required for Inp2/Myo2 binding and peroxisome inheritance **Figure 3.11 A and B.** The inheritance defect was however not as strong as when the whole *INP2* gene is deleted, suggesting that additional parts of Inp2 also

contribute to peroxisome inheritance. Nonetheless it can be concluded that the 6 MIS residues on Inp2 are important for peroxisome inheritance.

In addition to the inheritance assay, a yeast two hybrid experiment was conducted to test the interaction between *inp2-mis* and Myo2. The result showed that the interaction between *inp2-mis* and Myo2 is severely affected, which adds further evidence to the hypothesis that this site is required for Inp2 interaction with Myo2 and thereby is required for peroxisome inheritance **Figure 3.11 C**.

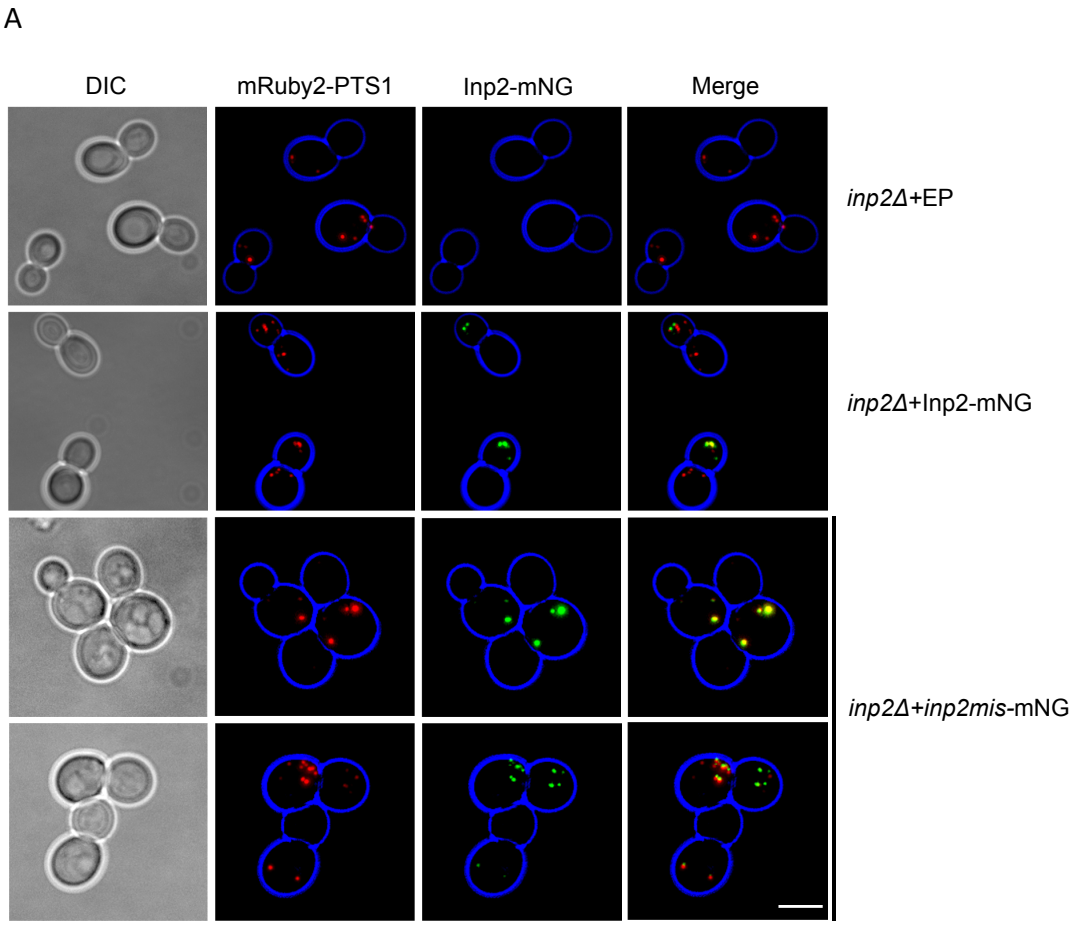

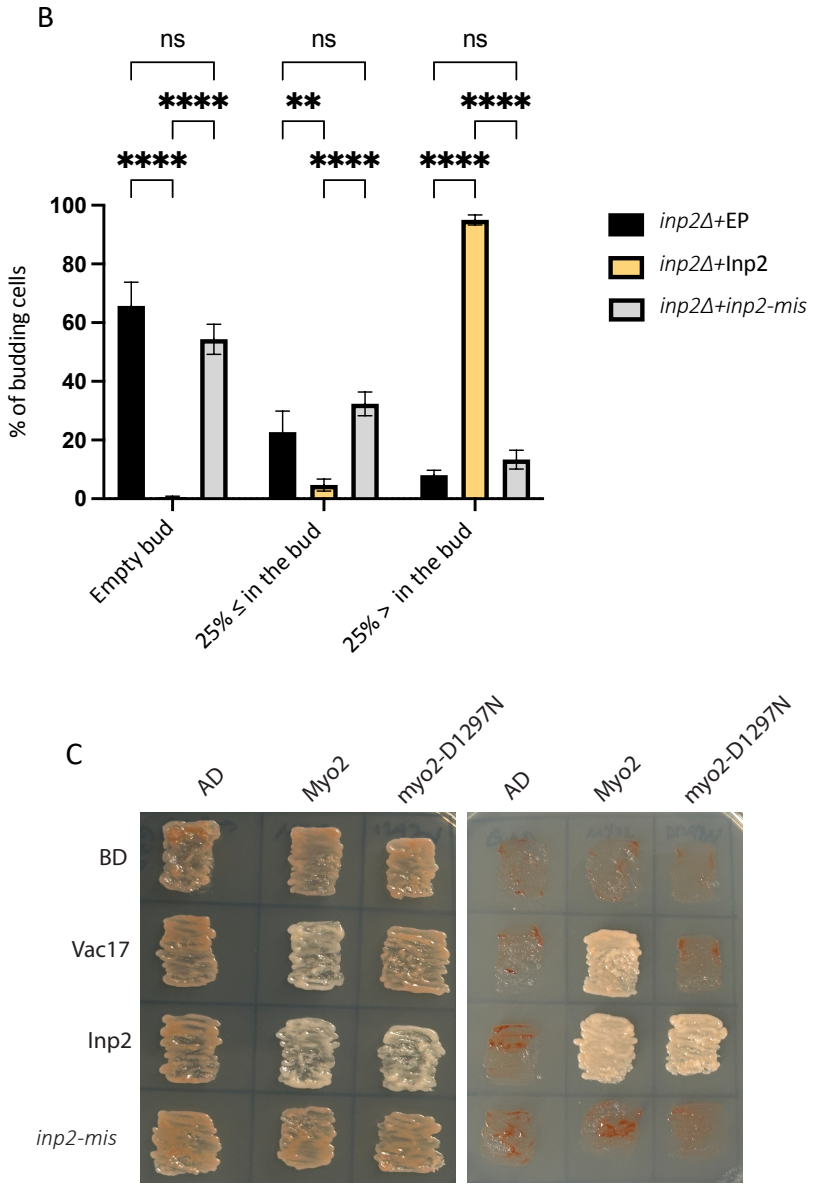

Figure 3. 11 Inp2 has a highly conserved MIS required for peroxisome transport. A) peroxisome transport is defective in *inp2Δ* cells containing *inp2-mis*-mNG where the Inp2-mNG plasmid rescued peroxisome inheritance. The mNeongreen tag was utilised to visualise the localisation of Inp2 along with peroxisomes in which they were labelled with red fluorescent protein fused with the peroxisomal targeting signal PTS1. The transformed cells were grown to log phase and imaged by epifluorescence microscopy. Scale bar is 5µm. B) quantification analysis with a minimum of 100 cells counted in 3 independent experiments. Error bars indicate SEM (Standard Error Mean). N=3. * p-value < 0.01; **** p-value < 0.0001; 2way ANOVA test. C) Mat a cells were transformed with plasmids carrying the activation domain and Mat α cells with plasmids carrying the binding domain. Transformed cells were mated and reselected as diploid on leu-trp- plates. Cells were then grown on leu-trp-ade-his- and leu-trp-ade-his- containing different concentration of 3 aminotriazole (3mM, 6mM and 10mM) to select for the interactions. Myo2-*D1297N* used as a control.

3.9.2 Inp2-MIS with the 6 amino acids deletion does not compete with Inp1 during peroxisome inheritance in *vps1Δ/dnm1Δ* cells.

S. cerevisiae is a yeast that divides in an asymmetrical fashion and organelles must be transported to the emerging bud. Complete peroxisome inheritance is accomplished by two opposing mechanisms i) retention by cortical anchoring in the mother cell and ii) transporting to the bud through the myosin motor. Inp1 and Inp2 are directly involved in these two mechanisms during cell growth. In a comprehensive localization study, Inp1, a peripheral membrane protein, was identified as being associated with peroxisomes. (Huh *et al.*, 2003). Inp1 has been implicated in the retention of peroxisomes, as its absence in *inp1Δ* cells often leads to a deficiency of retaining peroxisomes in the mother cells while the buds still possess them. This suggested that Inp1 plays a crucial role in retaining a majority of peroxisomes at the cortex of the mother cell (Fagarasanu *et al.*, 2005; Hulmes *et al.*, 2020). As described above in **Section 3.9.1** Inp2 is responsible for the mechanism opposing that of Inp1 which is the transport of peroxisomes to the emerging bud. Cells lacking Inp2 show peroxisomal inheritance defects resulting in buds that are devoid of peroxisomes **Figure 3.12 A** (Fagarasanu *et al.*, 2006).

During cell division, peroxisomes grow and divide by fission, and in *S. cerevisiae* Dnm1 and Vps1 have shown to be involved in this process **Figure 3.12 B**. In cells that are lacking Dnm1 and Vps1, peroxisome fission is abolished resulting in one elongated shaped peroxisome per cell that extends from the mother cell to the bud due to opposing mechanisms between Inp1 which is located at the mother cell tip and Inp2 that moves to the bud during the peroxisome transport (Knoblach *et al.*, 2013) **Figure 3.12 B and C**. Deletion of *INP2* or *INP1* in *dnm1Δ/vps1Δ* background will result in a single rounded shaped peroxisome localised in either the mother cell (on *INP2* gene deletion **Figure 3.12 C**) or the bud (on *INP1* gene deletion) compared to the elongated peroxisome shown in *dnm1Δ/vps1Δ* cells see also (Motley and Hettema, 2007).

To further characterise the role of the Inp2 MIS motif on a single peroxisome inheritance, we utilised *dnm1Δ/vps1Δ/inp2*Δ cells in which they have only one rounded peroxisome localised in the mother cell and transform them with the same plasmids constructed in the previous **Section 3.9.1** and analyse the single peroxisome dynamics. Imaging and quantification

analyses showed that the *dnm1Δ/vps1Δ/inp2*Δ cells transformed with Inp2-mNG showed a complete rescue to the *dnm1Δ/vps1Δ* phenotype (elongated peroxisome) with Inp2 decorating that elongated peroxisome in the bud and or in the bud neck. However, cells containing the *inp2-mis*-mNG were not able to rescue *dnm1Δ/vps1Δ* phenotype resulting in a (rounded peroxisome) co-localised with *inp2-mis*-mNG in the mother cell **Figure 3.13 A and B**. This result strongly supports that the Inp2 MIS motif binds to Myo2 and is crucial for peroxisome inheritance.

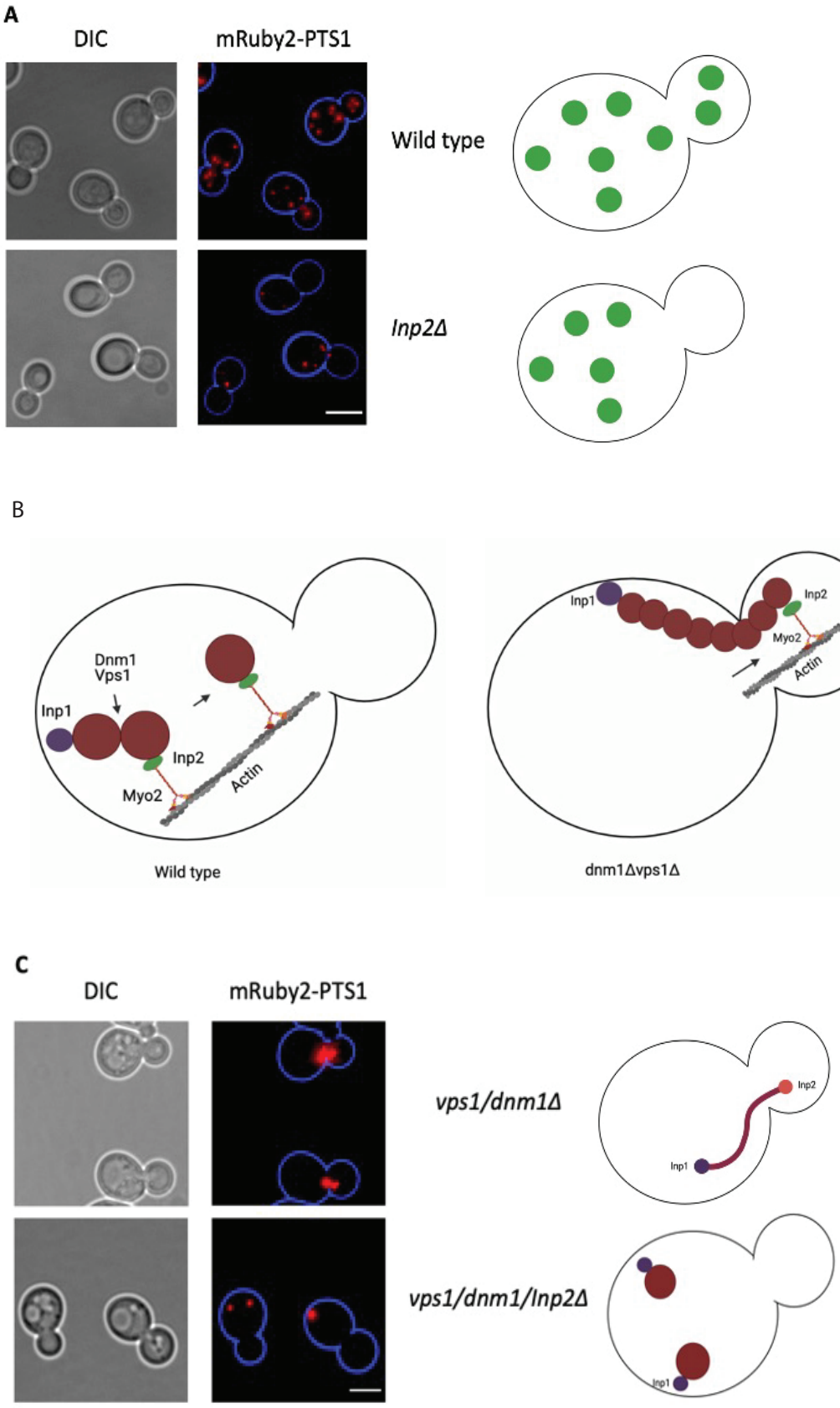

Figure 3. 12 Inp2 is required for peroxisome inheritance. A) peroxisomes visualised by mRuby2-PTS1 were imaged in wild type conditions and in *inp2Δ* cells along with a schematic diagram showing the

differences between the two backgrounds. B) A schematic diagram showing the current model for peroxisome division regulated by growth and fission. The process is regulated by Dnm1 and Vps1 since cells carrying *dnm1Δ/vps1Δ* resulting in a single elongated peroxisomes as shown in *dnm1Δ/vps1Δ* diagram. This elongation is due to the opposing mechanisms carried by Inp1 and Inp2. C) When additional deletion of Inp2 in *dnm1Δ/vps1Δ* cells is carried out the single elongated peroxisome is anchored by Inp1 in the mother cell in a rounded pattern due to the loss of Inp2 function.

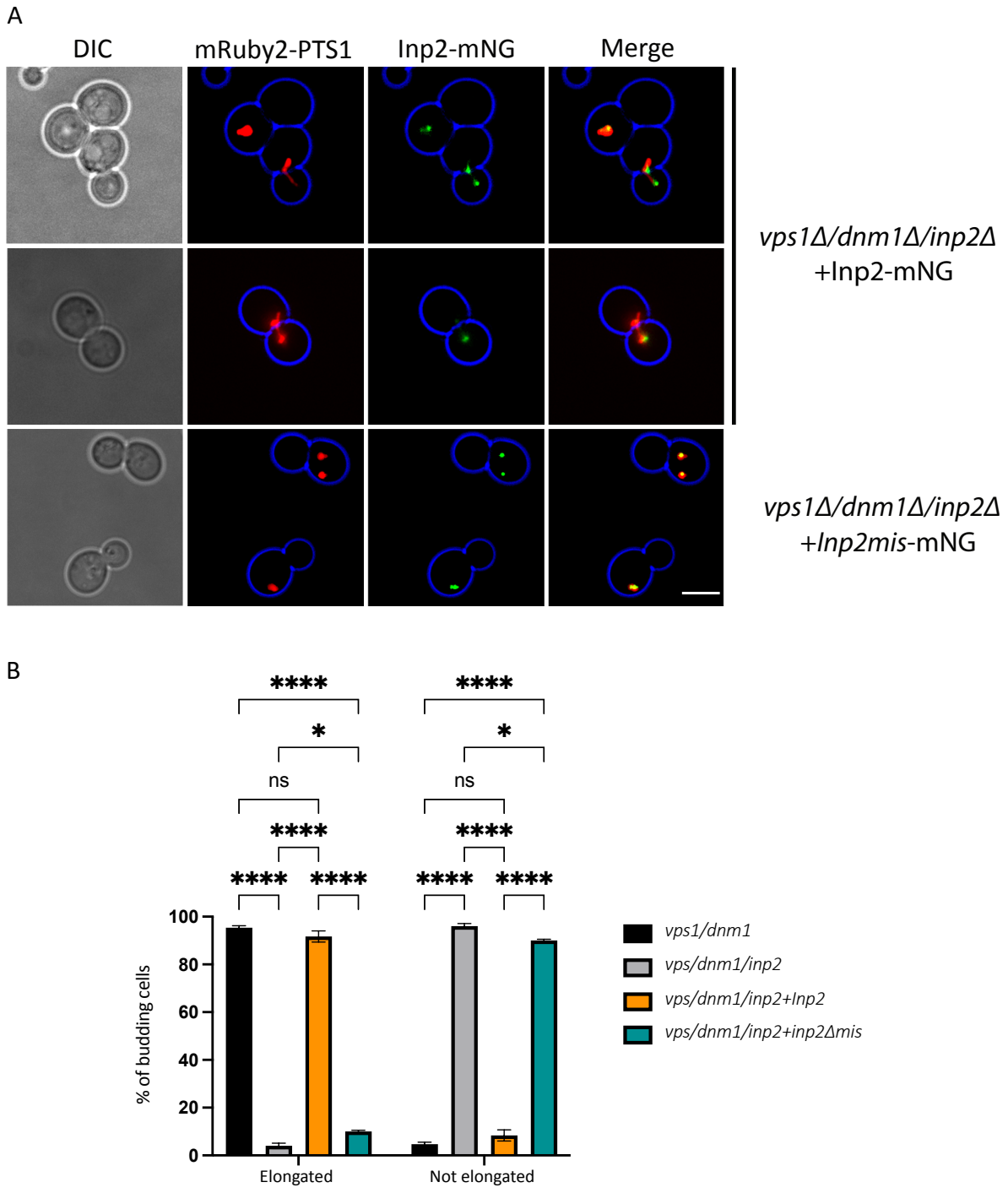

Figure 3. 13 Inp2 MIS motif is required for peroxisome transport in *vps1Δ/dnm1Δ* cells. A) The elongated single peroxisome transport is defective in *vps1Δ/dnm1Δ/inp2Δ* cells containing *inp2-mis*-mNG where the Inp2-mNG plasmid rescued the elongation phenotype. The mNeongreen tag was

utilised to visualise the localisation of Inp2 along with peroxisomes in which they were labelled with red fluorescent protein fused with the peroxisomal targeting signal PTS1. The transformed cells were grown to log phase and imaged by epifluorescence microscopy. Scale bar is 5µm. B) quantification analysis with a minimum of 100 cells counted in 3 independent experiments. Error bars indicate SEM (Standard Error Mean). N=3. * p-value < 0.01; **** p-value < 0.0001; 2way ANOVA test.

3.10 The interaction of Vac17 and Inp2 MIS mutants with Myo2 is severely affected in Co-immunoprecipitation experiment.

After identifying crucial residues in Vac17 and Inp2 that comprise their potential MIS's, it was important to test whether the MIS's affect interaction with Myo2 *in vivo* using co-immunoprecipitation. Hence, plasmids carrying wild type copy of either Vac17 or Inp2 or the 6 amino acids deletion of MIS in both Vac17 (*vac17S-mis)* from residue 134-139 and Inp2 (*inp2-mis)* from residue 534-539 were constructed. The wild type copies and *mis* mutant proteins were tagged with protein A tag and expressed under control of their endogenous promoters. Myo2-*GFP-vac17Δ* and Myo2-*GFP-inp2Δ* cells were transformed with the plasmids constructed. Myo2-GFP and Pex25-protein A strains were used as controls. Transformants were grown and lysed. The Myo2-GFP fusion protein was pulled down by GFP-Trap beads after adding the total lysate to the beads. Beads were washed 3 times and different western blot analyses were carried out to detect both Myo2-GFP and protein A tagged proteins. Whereas Inp2-ProtA and Vac17-ProtA readily co-precipitate with Myo2-GFP, their respective MIS mutants (red boxes) **Figure 3.14 A and B** co-precipitate much less efficiently. Taken together, we conclude that our results are consistent with the hypothesis that Vac17 and Inp2 MISs denote the primary interaction sites between Myo2 and Vac17 and Inp2 and validates the use of the ColabFold approach to predict binding interfaces.

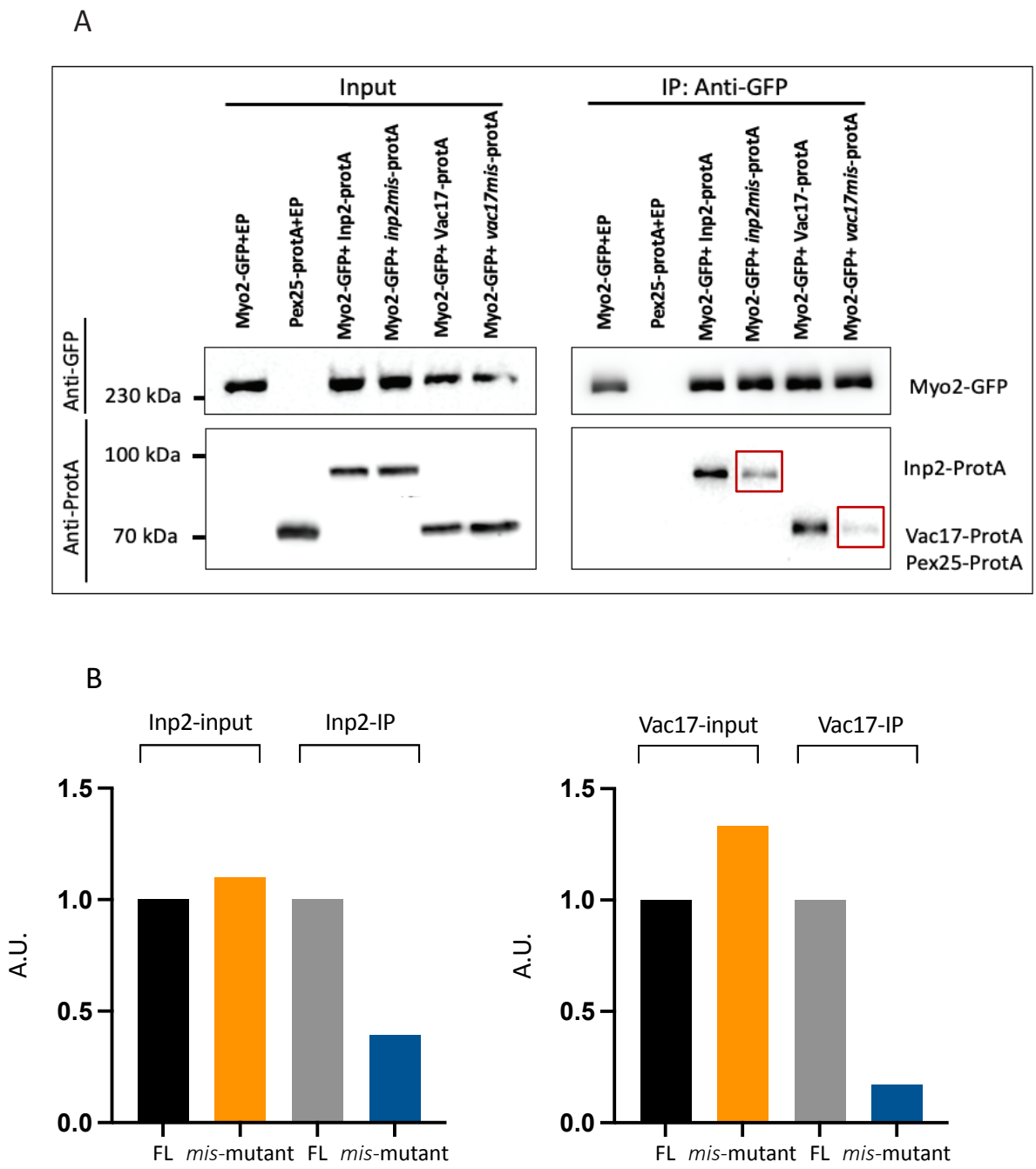

Figure 3. 14 Vac17 and Inp2 MIS mutants are strongly reduced in the interaction with Myo2. A) Vac17/Inp2 and *vac17S-mis* and *inp2-mis* and Myo2 interaction analysed by co-immunoprecipitation. The Input shows the total lysates before loading onto the GFP-Trap beads while IP after loading. Myo2 was tagged with GFP in the genome and Inp2/Vac17 and their MIS mutants tagged with Protein A were expressed from plasmids under control of their own promoter. Myo2-GFP was pulled down by incubating the total lysate with GFP-Trap beads. Beads were then washed 3 times and analysed by western blot. B) Quantification analysis showing reduction in MIS mutants in binding with Myo2 compared with Vac17 and Inp2.

3.11 The Vac17-MIS mutant level is stabilised when localised to the mother cell.

Organelle inheritance is a mechanism regulated by 3 sequential steps. i) The initiation of the binding between Myo2 and its adaptors. ii) The movement of organelles along actin cables to the daughter cell. iii) The release of organelles of Myo2 via the breakdown of the adaptor proteins. According to the literature, several proteins have shown to be involved in regulating the steps mentioned above and any disruption in the role of some of these proteins such as phosphorylation or ubiquitination events or interaction between proteins could cause organelle transport defect which could result in altering the adaptor proteins steady state levels such as Vac17 and Inp2 whether decreasing or increasing. For example, it has been shown that deleting *PTC1* gene affects vacuole and peroxisome inheritance due to the reduction in Vac17 and Inp2 steady state levels (Jin *et al.*, 2009). In addition, another study has shown that deleting *DMA1* and *DMA2* genes resulted in elevating Vac17 and Inp2 levels due to the prevention in their breakdown regulation (Yau *et al.*, 2014). These changes resulted in mispositioning (localised at either bud tip or mother-bud neck) of vacuoles and peroxisomes. It has also been reported that mutations in Myo2 that prevent Vac17 or Inp2 interactions result in elevation in these proteins levels (Fagarasanu *et al.*, 2009; Taylor Eves *et al.*, 2012). It was therefore intriguing to test how the MIS mutations developed in this study affect protein levels due to their prevention in binding with Myo2. To do this, *vac17Δ*/*inp2Δ* cells were transformed with Vac17-protein A /*vac17-mis*-protein A and Inp2-protein A/*inp2-mis*-protein A plasmids respectively and analysed by western blot. The analysis showed that both Vac17 and Inp2 MIS mutant protein levels were elevated due to the inheritance defect compared to wild type Vac17 and Inp2 **Figure 3.15 A and B**. This result is consistent with the observation that when the interaction is affected between Myo2 and Vac17 or Inp2 the protein level is elevated. In addition, we sought to check whether the stability of MIS mutants might be changed when the *de novo* synthesis of the protein is blocked by using cycloheximide as an inhibitor for protein synthesis (Schneider-Poetsch *et al.*, 2010). This would determine if MIS mutant breakdown is completely blocked after blocking its synthesis or it is only a delay in the breakdown compared to wild type. To test this hypothesis, a cycloheximide experiment was conducted in which we have used *vac17Δ* cells and transform it with either Vac17 or *vac17-mis* tagged with protein A. Cells were grown to log phase then treated with

cycloheximide. Untreated samples were collected before the addition of cycloheximide then samples were collected every 20 minutes for 4 times and analysed by western blot. The western blot analyses showed a delay in the *vac17-mis* mutant breakdown compared to wild type Vac17 **Figure 3.15 C**. Further evidence for the delay in the adaptor breakdown can be obtained from a different approach. Under normal conditions, Vac17 and Inp2 are broken down during the time of cytokinesis after the transport of vacuoles and peroxisomes is complete (Li *et al.*, 2021). Myo1 protein is considered to be one of the cytokinetic ring contraction markers (localised at the mother-bud neck), its expression increases during the cytokinesis process then decreases at the end (Bi and Park, 2012). We could use this system to investigate the delay in the breakdown of the MIS mutants by using Myo1 as marker to distinguish the breakdown between the adaptors in their wild type conditions and in inheritance deficiency conditions. Thus, we utilised Myo1-GFP*vac17Δ* or Myo1-GFP*inp2Δ* cells and transformed them with either the wild type copy of the adapter or the MIS copy and analyse them by imaging. The Myo1-GFP*vac17Δ* or Myo1-GFP*inp2Δ* were transformed with empty plasmid as control. Cells transformed with either the wild type Vac17 or Inp2 showed rescue in vacuole and peroxisome inheritance respectively. Cells transformed with the MIS mutants did not rescue the inheritance. Our analysis showed that both Vac17 and Inp2 MIS mutants still co-localised with their organelles and were visible in the mother cell during cytokinesis compared to the wild type copies **Figure 3.15 D**. This result indicates further that the breakdown of *vac17-mis* and *inp2-mis* is delayed.

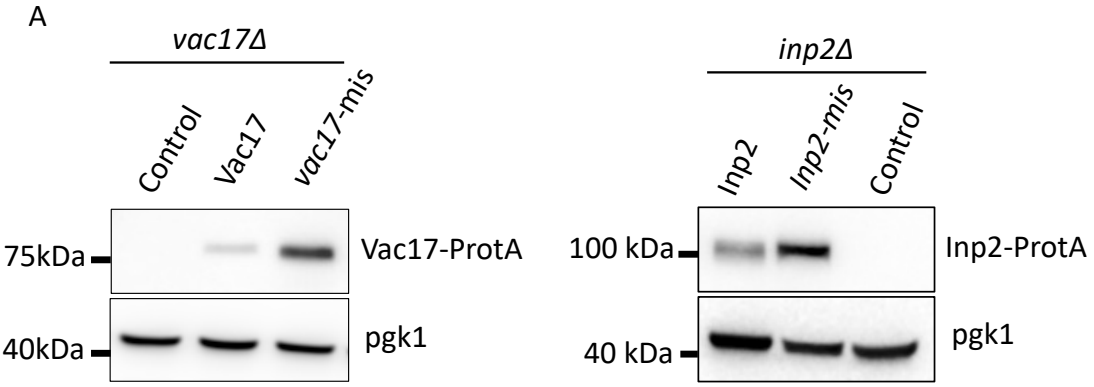

B

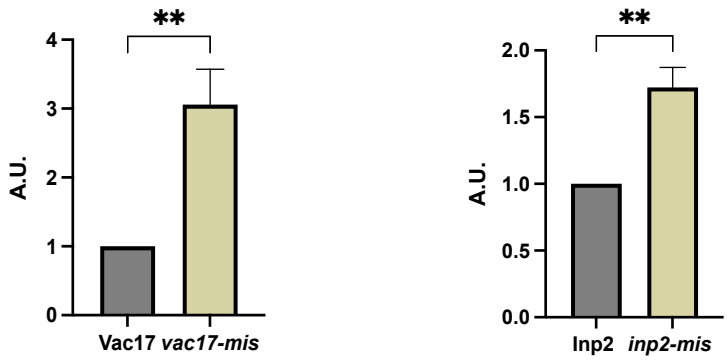
**
A.U.
4
3
2
1
0
Vac17 vac17-mis
**
A.U.
2.0
1.5
1.0
0.5
0.0
Inp2 inp2-mis

C

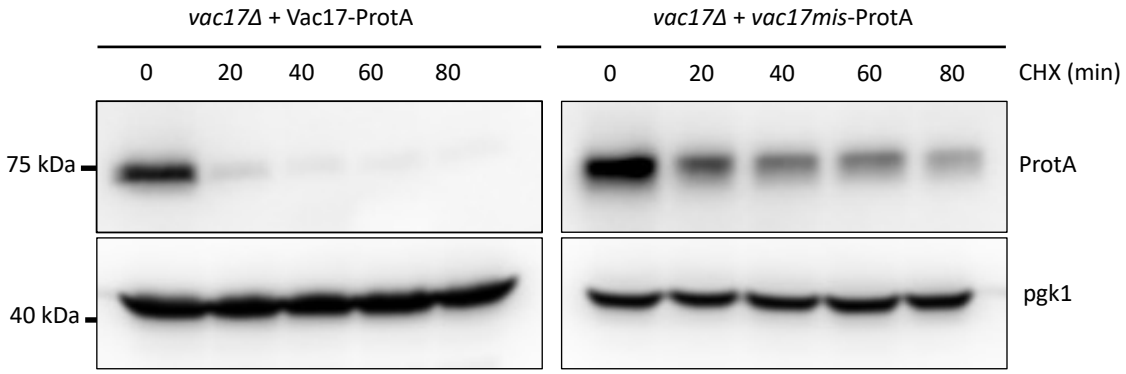
vac17Δ + Vac17-ProtA
vac17Δ + vac17mis-ProtA
0 20 40 60 80
0 20 40 60 80
CHX (min)
75 kDa
ProtA
40 kDa
pgk1

D

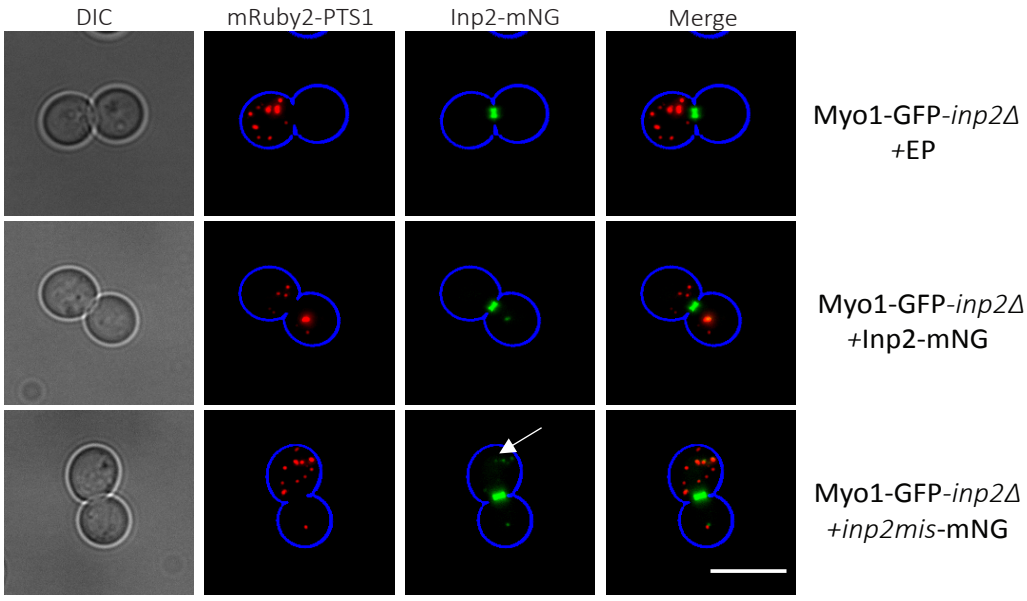
DIC
mRuby2-PTS1
Inp2-mNG
Merge
Myo1-GFP-inp2Δ +EP
Myo1-GFP-inp2Δ +Inp2-mNG
Myo1-GFP-inp2Δ +inp2mis-mNG

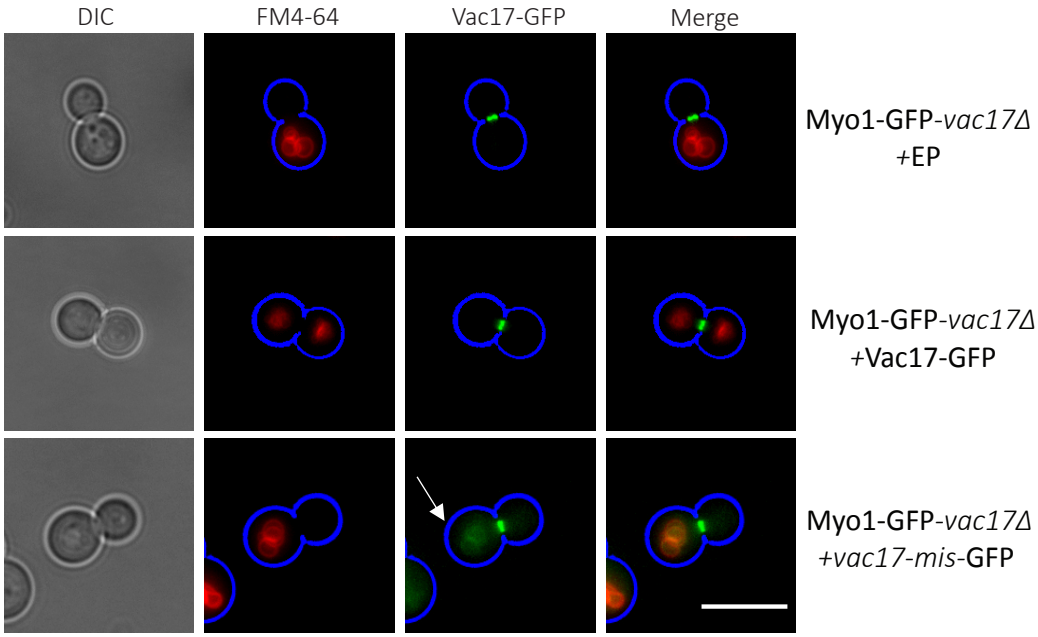

Figure 3. 15 MIS mutants are stabilised when the binding with Myo2 is affected. A) A western blot analysis showing the stability of the MIS mutant compared to the wild type copies of the adaptors with their quantification analysis in B. C) Western blot analysis showing the breakdown delay in the *vac17-mis* compared to the wild type Vac17 after treating the cells with Cycloheximide. D) Myo1-GFP was tagged in the genome (its signal was distinguished compared to other green fluorescent signals due to its fixed location in the cell, mother-bud neck) in *vac17Δ/inp2Δ* cells where the adaptors in their MIS mutants were expressed with (Vac17 with GFP) (Inp2 with mNG) arrows indicated. Vacuoles were labelled with FM4-64 applying the process mentioned in Chapter2 Section 2.5.6. Peroxisomes were labelled with mRuby2-PTS1. Scale bar is 5µm.

3.12 Vac17-MIS mutant can be targeted for normal breakdown when directed to the right location.

It is proposed that Vac17 breakdown occurs primarily in the bud since it is the final destination for vacuoles (Tang *et al.*, 2003; Yau *et al.*, 2014; Yau, Wong and Weisman, 2017). The key Vac17 residues known to be essential in Vac17 breakdown are S222 and T240. The T240 residue is regulated through phosphorylation by an unknown kinase. Upon its phosphorylation, Dma1 is then recruited to Vac17 and bind to T240. Once vacuoles reach the bud tip, Cla4 phosphorylates Vac17 at S222 residue which allow Dma1 to ubiquitinate Vac17. Mutating these residues to S222A or T240A blocks Vac17 breakdown in the bud (Yau et al., 2014, 2017). Since we observed a delay in *vac17-mis* mutant breakdown due to its effect on vacuole transport and the localisation and stability of the *vac17-mis* protein in the mother cell, the question raised was whether the *vac17-mis* mutant, when directed to the bud, would

undergo the usual process of targeted degradation or not. To test this idea, we transformed *vac17-mis* -GFP/*vac17-mis*-protein A plasmids into both wild type and *vac17Δ* cells. Cells transformed with GFP tagged proteins were analysed by imaging to visualise the localisation of the *vac17-mis* and FM4-64 was used as a vacuolar marker. On the other hand, cells transformed with protein A plasmids were analysed by western blot. The imaging and western blot analysis **Figure 3.16 A and B** showed that when the MIS mutant is directed to the bud in wild type cells (since they have wild type copy of *VAC17* gene and have normal vacuole inheritance) it is broken down in a way that resembles Vac17 breakdown in normal conditions **Figure 3.16 A and C**. However, by introducing the alanine mutations instead of the serine 222 and threonine 240 the residues required for Vac17 breakdown mentioned above along with the MIS mutant with both tags GFP and protein A and transform the plasmids into both wild type and *vac17Δ* cells, the breakdown of both (*vac17-mis-S222A/vac17-mis-T240A*) was prevented in wild type cells as shown in **Figure 3.16 B and C**. This result resembles *vac17-S222A* and *vac17-T240A* mutants when introduced to wild type cells (Yau *et al.*, 2014; Yau, Wong and Weisman, 2017). Taken together, these results suggest that the elevation in protein levels observed with Vac17-MIS mutant is due to the delay in the breakdown but not due to a defect in protein structure or folding as Vac17-MIS is still localised to vacuoles, which requires interaction with Vac8 and since breakdown is still sensitive to the spatiotemporal control observed for wild type Vac17.

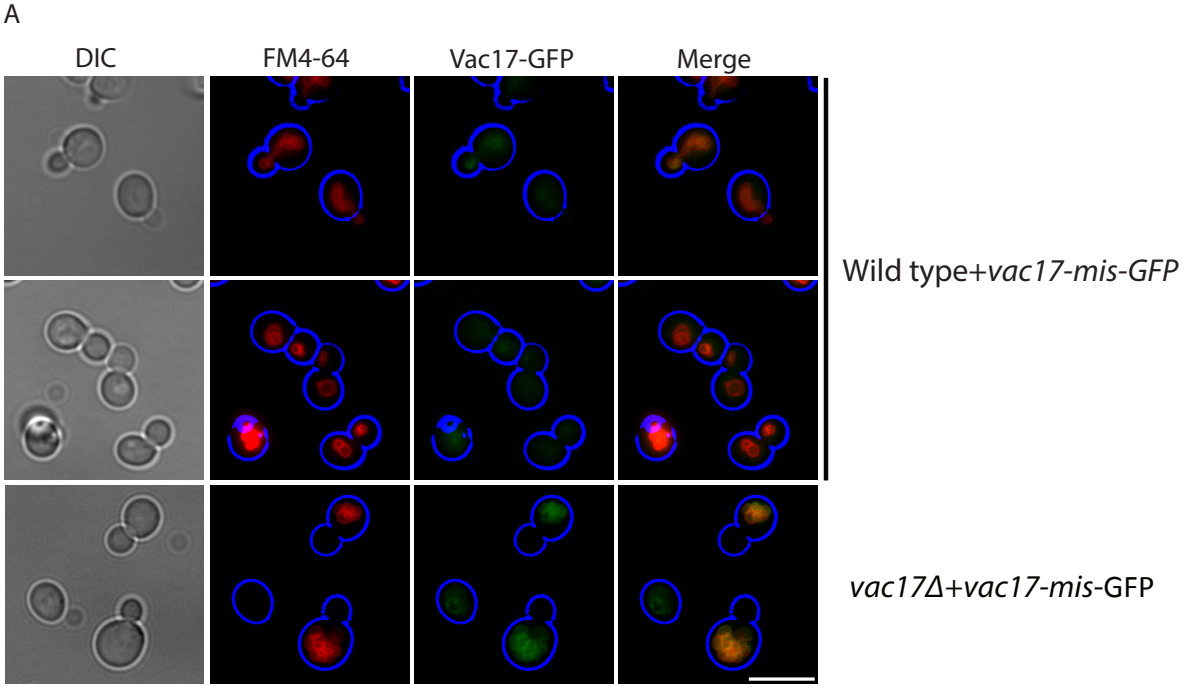

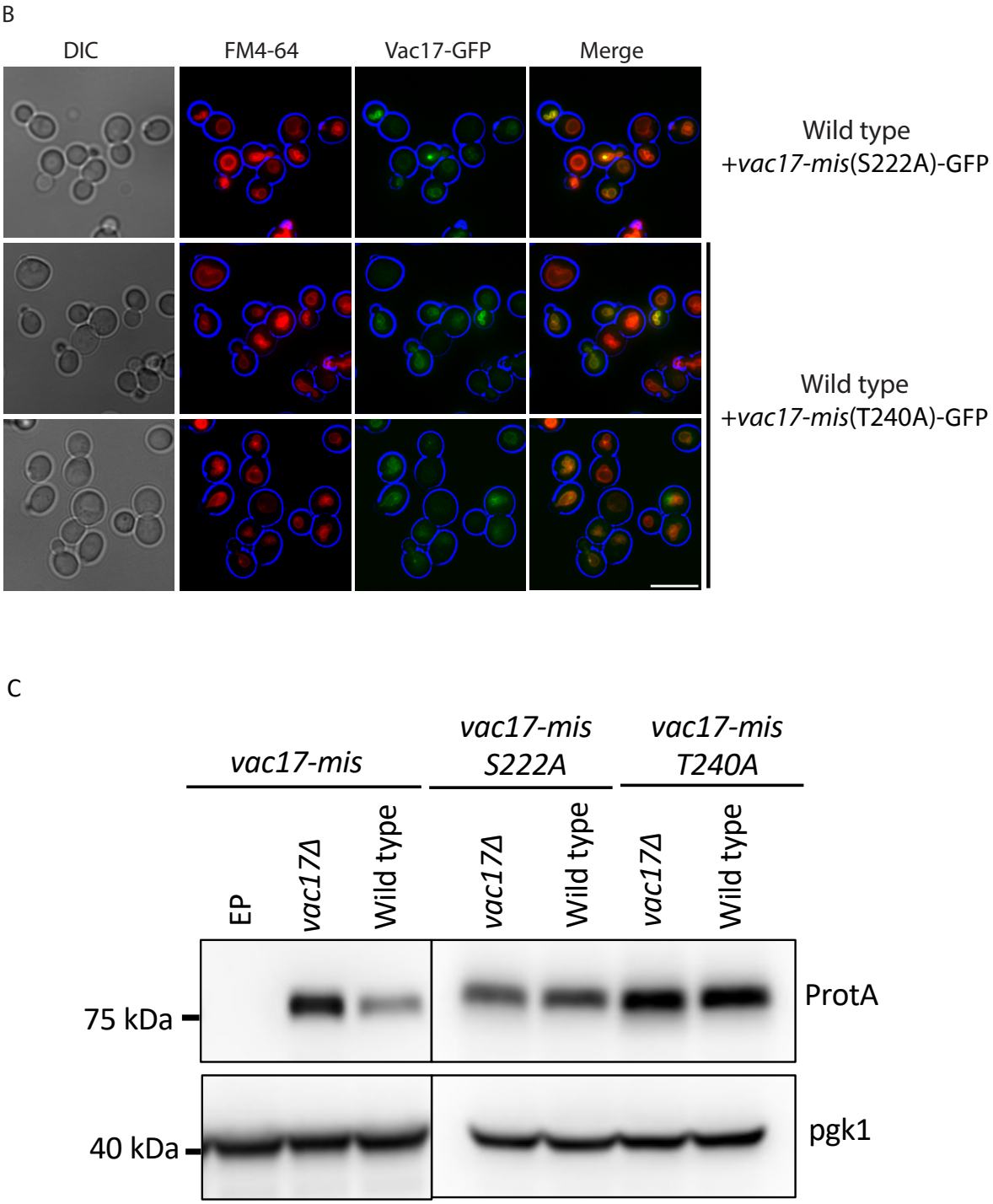

Figure 3. 16 The Vac17-MIS mutant is broken down when directed to the bud in wild type cells. A) *vac17-mis*-GFP expressed in both wild type and *vac17Δ* cells. B) *vac17-mis S222A* or *T240A* tagged with GFP expressed in both wild type and *vac17Δ* cells. C) The levels of Protein A tagged *vac17-mis*, *vac17-misS222A* and *vac17-misT240A* in either wild type or *vac17Δ* background. Scale bar is 5µm.

3.13 Discussion.

The Class V myosin, Myo2, transports organelles through interaction of its cargo binding domain with organelle-specific adaptors. This mechanism is highly regulated in temporal and spatial manners. The Myo2 vacuolar and peroxisomal adaptors Vac17 and Inp2 known to be required for Myo2 binding and thus required for vacuole and peroxisome inheritance. Initial validations suggested the potential Myo2 binding sites in Vac17 from amino acid 110 to 170 and Inp2 from amino acid 504 to 618 are the most regions likely to bind Myo2 (Ishikawa *et al.*, 2003; Fagarasanu *et al.*, 2006). In this chapter, we sought to determine how Vac17-MIS and Inp2-MIS specifically required for Myo2 interaction and show their effects on vacuole and peroxisome inheritance. Since it is critical to understand how the early stages of organelle inheritance are maintained in which the interaction between Myo2 and its adaptors occurs, we tried to narrow down the MIS regions and determine the critical residues of Vac17 and Inp2 involved in Myo2 binding and vacuole and peroxisome inheritance. This was through a combination of bioinformatics analysis followed by structural prediction analysis utilising ColabFold and *in vivo* study. It has been shown that Myo2 D1297, E1293, and N1304 residues were required for vacuole inheritance (Taylor Eves et al., 2012), in which these residues were revealed by the outcome of the ColabFold approach analysis in predicting binding interfaces with Vac17 MIS in this study and others (Liu et al., 2022). The experimental validations including the yeast two hybrid assay, co-immunoprecipitation conducted on the MIS regions in Vac17 and Inp2 demonstrated a profound effect on vacuole and peroxisome inheritance, suggesting that the identified regions are indeed specific for Vac17-Myo2 and Inp2-Myo2 binding and vacuole and peroxisome inheritance. In addition, in line with previous studies, we found that disruption of these interactions resulted in elevated levels of both Vac17 and Inp2 MIS mutants which confirms the similarity of the outcome (Ishikawa *et al.*, 2003; Fagarasanu *et al.*, 2009; Yau *et al.*, 2014). Our further analysis suggested that the elevation in the MIS protein levels is due to the delay in their breakdown by the proteasome. These observations provide valuable insights into the regulation of organelle inheritance and the role of Vac17-MIS and Inp2-MIS sites in mediating the interactions between Myo2 and its adaptor proteins. This study also highlights the potential of using these mutants as tools to further investigate the regulation of organelle transport and the mechanisms underlying the observed defects in organelle inheritance.

Chapter 4 Kin4 and Frk1 are required for vacuole and peroxisome inheritance essentially by protecting Vac17 and Inp2 adaptors in the mother cell.

4.1 Introduction

Organelle partitioning between mother and daughter cell is highly regulated spatially and temporally. The process starts in the mother cell by recruiting myosin motors to organelles followed by their transport along actin cables and ending by the release of the organelle at a proper location in the newly formed bud. Vacuole transport is initiated by the phosphorylation of Myo2 and Vac17 by Cdk1 to initiate their binding (Legesse-Miller et al., 2006; Peng and Weisman, 2008). When vacuoles reach the bud, they are released from the transport complex via specific phosphorylation and ubiquitination events on Vac17 carried out by several kinases and ubiquitin ligases proteins.

Vac17 contains a PEST motif that is required for its controlled degradation in which it is typically high in serine, proline, glutamic acid, and threonine amino acid residues (Rechsteiner and Rogers, 1996). According to several studies the Vac17 PESTΔ or Vac17 S222A or T240A (residues within the PEST motif) showed deficiency in Vac17 spatial breakdown regulation in the bud (Tang *et al.*, 2003; Yau *et al.*, 2014; Yau, Wong and Weisman, 2017). In these mutants the vacuoles are positioned incorrectly in the bud due to the continuous attachment Vac17 to Myo2 until late in the cell cycle. It has been proposed that the ubiquitin ligase Dma1 and the kinase Cla4 are recruited and active in the bud (Yau et al., 2014, 2017). After Vac17 phosohorylation at the threonine residue 240 Dma1 is recruited to Vac17 before Vac17 gets phosphorylated by Cla4 at the serine residue 222 upon which Dma1 ubiquitinate Vac17 to target it for proteasome breakdown. The Cla4 and Ste20 overexpression cause high degradation to Vac17, which results in a vacuole inheritance deficiency (Bartholomew and Hardy, 2009). This result indicates that when Cla4 and Ste20 are overexpressed, they can diffuse into the mother and cause an early breakdown to Vac17 in which it will result in vacuole inheritance deficiency. However, by expressing Vac17 PESTΔ, this defect by the Cla4 or Ste20 overexpression can be rescued (Bartholomew and Hardy, 2009). Moreover, it has

also been shown that the same mechanism is carried out in human cells in a very similar manner during melanosome inheritance in which Rab27a is required to bind to the adaptor melanophilin and MyoVa to mediate the transport followed by terminating the transport by phosphorylating and ubiquitylating the melanophilin adaptor (Barral and Seabra, 2004; Park *et al.*, 2019). However, much more is still required to be investigated. Hence, our lab has been interested to investigate more into the role of protein kinases in more details to unravel the molecular mechanisms regulating organelle transport through studying organelle inheritance in budding yeast.

A genome wide genetic screen conducted in the Hettema lab in collaboration with the Schuldiner lab (Rehovot, Israel) identified novel kinases required for vacuoles and peroxisomes inheritance (Ekal et al, manuscript in preparation). These factors are Kin4 and its paralog Frk1. Kin4 and Frk1 are threonine/serine kinases. Kin4 is mainly localised to the mother cell membrane whereas Frk1 to the cytosol according to SGD (*Saccharomyces* Genome Database) (D'Aquino *et al.*, 2005; Pereira and Schiebel, 2005). Initial findings following the screen demonstrated that they are required for maintaining the steady state levels of the Myo2 receptors Inp2 and Vac17 during the early stages of peroxisome and vacuole inheritance. Cells with *KIN4* and *FRK1* genes deletions end up with buds devoid of vacuoles and peroxisomes. After investigating further into the reason behind this, preliminary data conducted by Hettema lab found that Inp2 and Vac17 protein levels were much lower in *kin4Δ/frk1Δ* cells compared to wild type in which it suggests that Kin4 and Frk1 are required for maintaining the stability of Myo2 receptors during early stages of peroxisome and vacuole transport when in the mother cell. It has also been hypothesised that Kin4 and Frk1 antagonise Cla4 and Dma1 by preventing the early breakdown of Inp2 and Vac17 in the mother cell during peroxisome and vacuole transport. Therefore, this chapter will be focusing into the role of Kin4 and Frk1 in protecting Vac17 and Inp2 from the breakdown in early stages of peroxisome and vacuole inheritance. The MIS mutants generated for the work in chapter 3 were used as a tool to investigate the role of Kin4 and Frk1.

4.2 Kin4 and Frk1 contribute to vacuole and peroxisome transport during cell division.

The role of Kin4 in the inheritance was first discovered in the Hettema lab screen in a mutant background lacking a proper peroxisome fission machinery (in *dnm1Δ/vps1Δ* cells). Normally this mutant results in a single elongated peroxisome that extends from the mother cell to the bud as shown in **Figure 4.1**. By combining the *KIN4* gene deletion in *dnm1Δ/vps1Δ* cells the single peroxisome was no longer be elongated and ends up in the mother cell in a punctate pattern due to the inheritance defect resembling the same phenotype shown in *dnm1/vps1/inp2Δ* cells **Figure 4.1**.

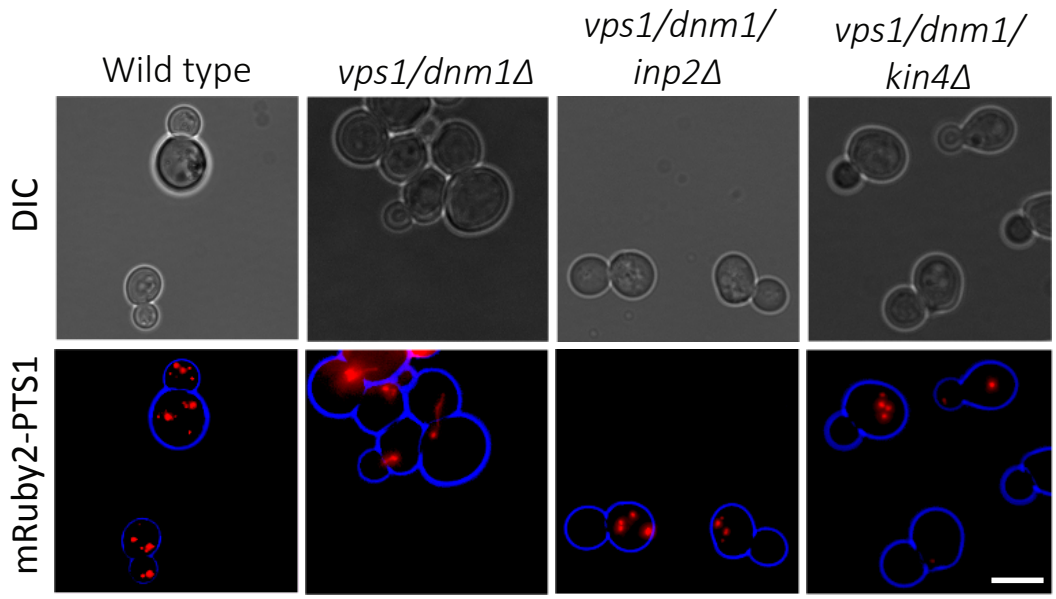

Figure 4. 1 Kin4 contributes to peroxisome transport. Peroxisomes partition efficiently in inheritance in wild type and *vps1Δ/dnm1Δ*, whereas additional *KIN4* deletion showed an inheritance defect similar to *vps1Δ/dnm1Δ/inp2Δ* cells. The red fluorescent protein fused with the peroxisomal targeting signal PTS1 was used to visualise peroxisomes. The transformed cells were grown to log phase and imaged by epifluorescence microscopy. Scale bar is 5µm.

The first stage of the study was to determine if the kinase deletion resulted in vacuole or peroxisome inheritance phenotype in otherwise wild type strain backgrounds. Preliminary data showed that peroxisome and vacuole inheritance in *kin4Δ* cells alone was not very strong but, by adding the *FRK1* gene deletion in *kin4Δ,* it exacerbated the inheritance deficiency for both peroxisomes and vacuoles. Hence, a proper imaging and quantification analysis in a mutant background for peroxisome and vacuole inheritance was required to confirm the reproducibility of the phenotype found from the preliminary data. For that we utilised *kin4Δ, frk1Δ, kin4Δ/frk1Δ, inp2Δ, vac17Δ* and wild type cells and transformed them with peroxisomal marker (mNG-PTS1) and used FM4-64 the vacuolar stain as a vacuolar marker. Cells were grown logarithmically and analysed by epifluorescence microscopy. Our statistical analysis demonstrates that the *kin4Δ/frk1Δ* mutant showed a strong peroxisome and vacuole inheritance deficiency resembling *inp2Δ* and *vac17Δ* mutants, respectively **Figure 4.2 A-D**. The single *kin4Δ* mutant showed a weak effect of organelle inheritance whereas organelle partitioning in the single *frk1Δ* mutant was indistinguishable from that to wild type cells. The synthetic enhancement between *KIN4* and *FRK1* gene deletions on organelle inheritance suggests that both Kin4 and Frk1 play a role in peroxisome and vacuole transport.

A

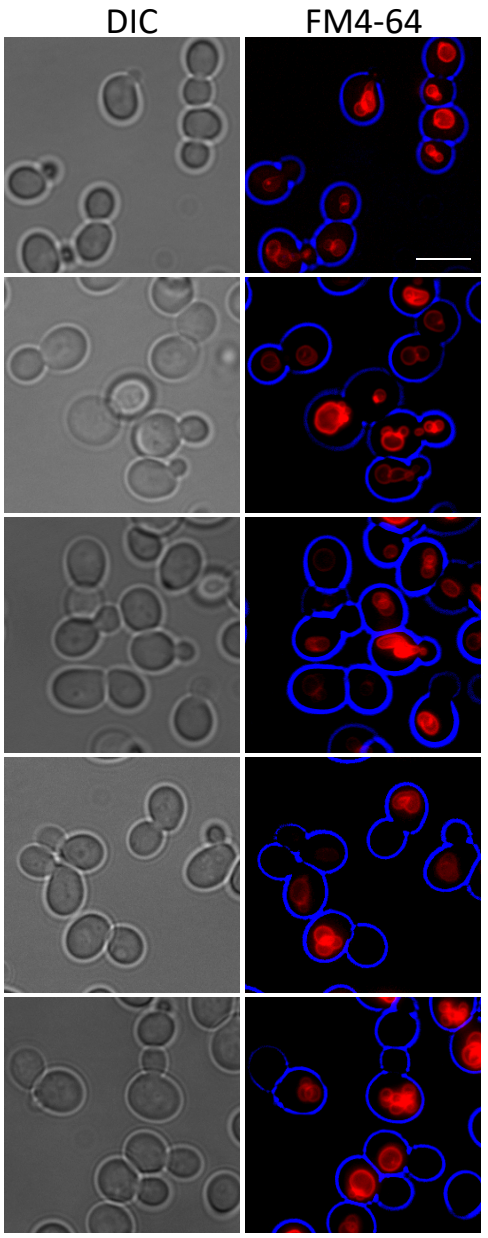
DIC
FM4-64
Wild type
frk1Δ
kin4Δ
frk1kin4Δ
vac17Δ

B

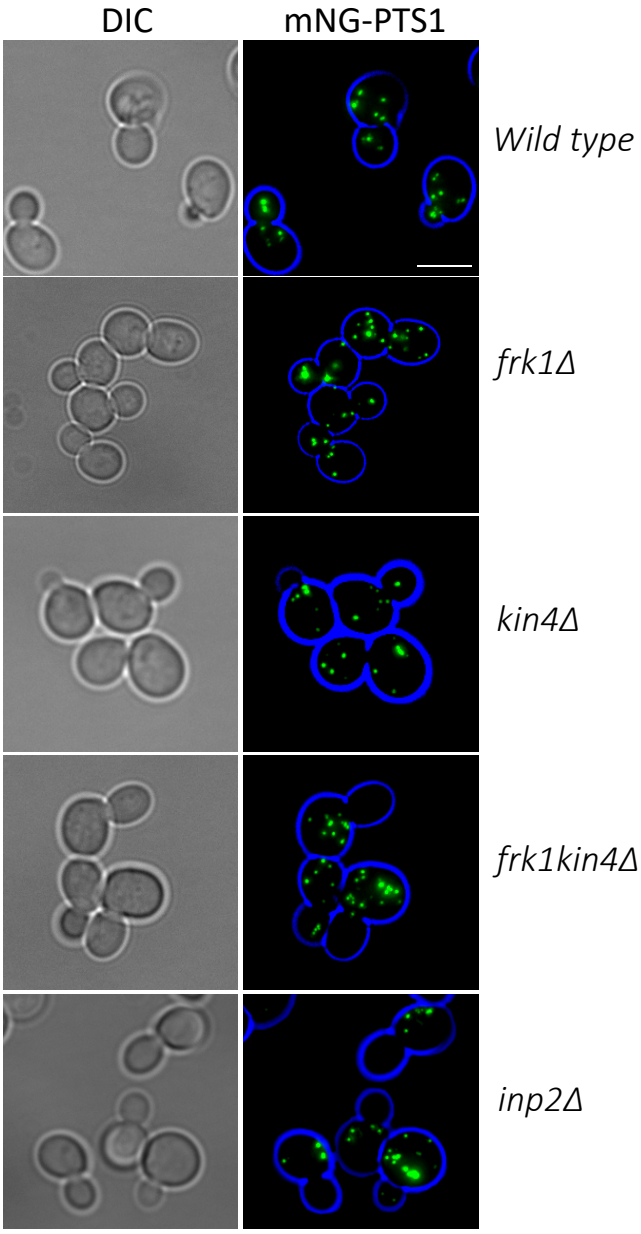
DIC
mNG-PTS1
Wild type
frk1Δ
kin4Δ
frk1kin4Δ
inp2Δ

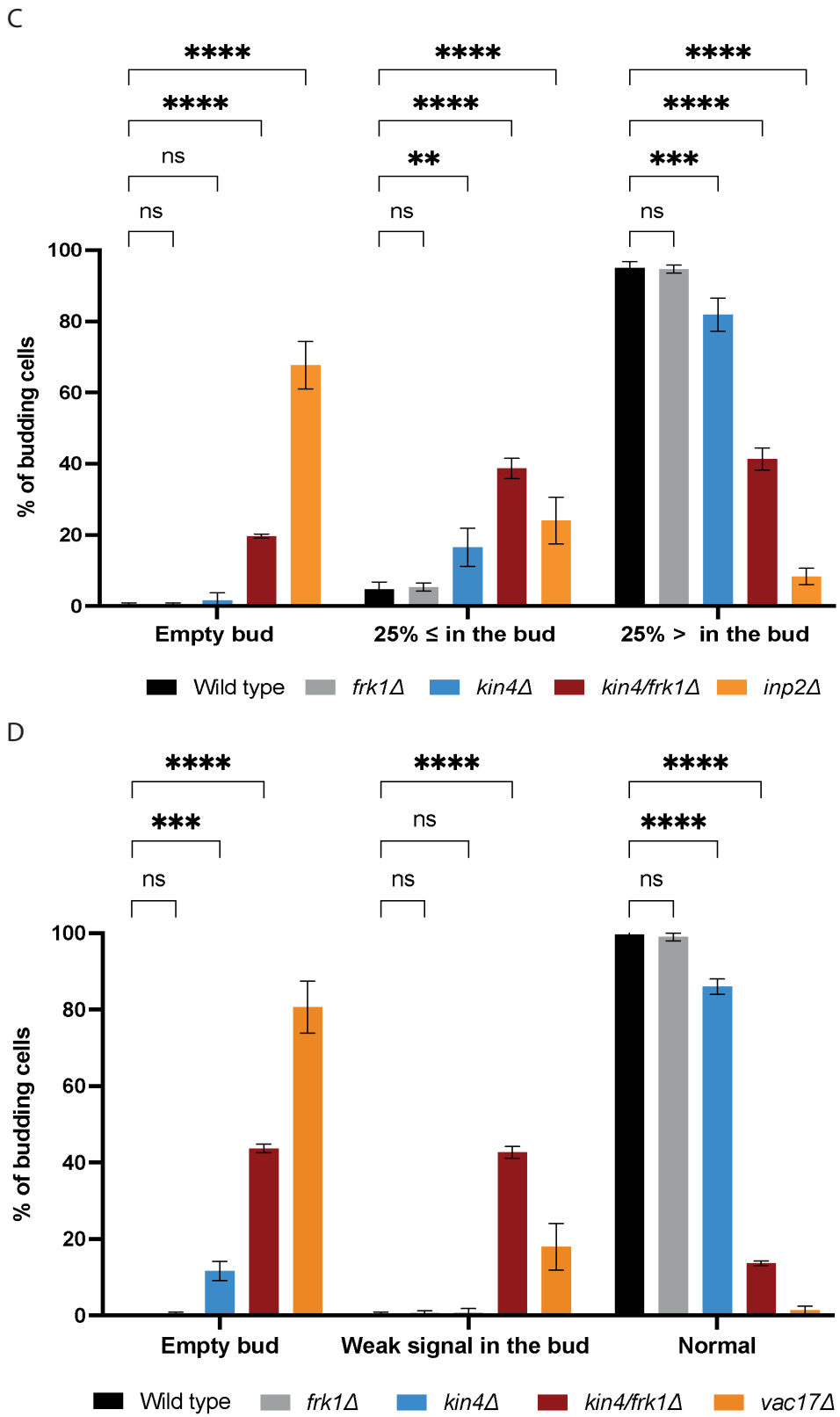

Figure 4. 2 Kin4 and Frk1 are required for peroxisome and vacuole inheritance. A+B) Peroxisomes and vacuoles inheritance were affected in *kin4Δ/frk1Δ* cells in which the phenotype resembled *inp2Δ* and *vac17Δ* phenotype compared to wild type cells. Vacuoles were labelled with FM4-64 and Peroxisomes were detected with green florescent protein known as mNeonGreen fused with the peroxisomal targeting signal PTS1. The transformed cells were grown to log phase and imaged by

epifluorescence microscopy. Scale bar is 5µm. C) Peroxisome and D) Vacuole quantification analysis with a minimum of 100 cells counted in 3 independent experiments. Error bars indicate SEM (Standard Error Mean). N=3. * p-value < 0.01; **** p-value < 0.0001; 2way ANOVA test.

4.3 Vac17 and Inp2 stability require Kin4 and Frk1 as protectors in the early stages of vacuole and peroxisome transport.

Since it was noticed that the inheritance defects of peroxisomes and vacuoles in *kin4Δ/frk1Δ* cells were similar to the effect seen in *INP2* and *VAC17* knockout mutants, respectively. Preliminary western blot data by Hettema lab suggested that the inheritance defects seen in *kin4Δ/frk1Δ* cells is due to breakdown of Inp2 and Vac17 protein levels. It showed that Inp2 and Vac17 steady state levels reduced in *kin4Δ/frk1Δ* cells compared to in wild type cells. However, it was also important to confirm the reproducibility of the effect shown. Hence, more western blots with quantification analysis were required. As a result, shown in **Figure 4.3**, we found that Inp2 and Vac17 protein levels were significantly and reproducibly decreased in *kin4Δ/frk1Δ* cells compared to in wild type cells. Our lab has found that Myo2 levels were not affected in *kin4Δ/frk1Δ* cells. This result confirms the primary analysis in which the inheritance defect seen is most likely a direct effect of decreased Inp2 and Vac17 protein levels.

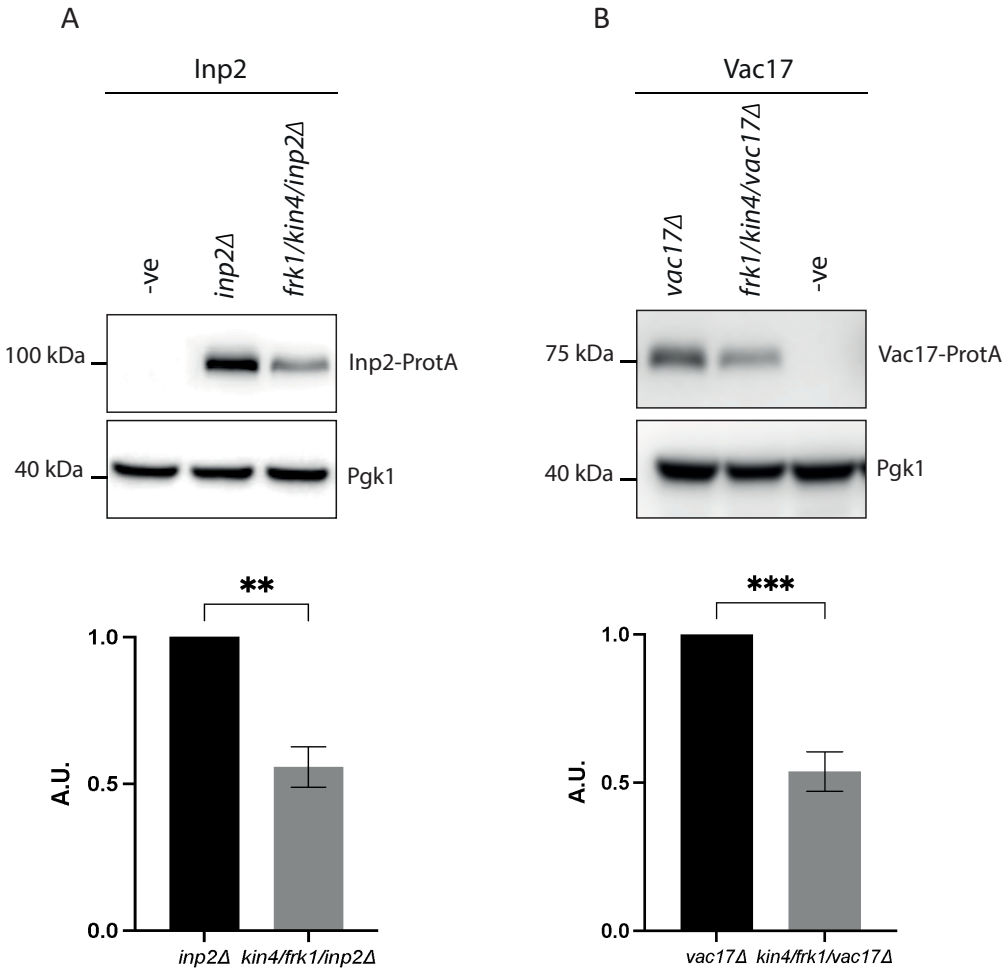

Figure 4. 3 Inp2 and Vac17 levels are affected in *kin4Δ/frk1Δ* cells. A+B) Inp2-protein A and Vac17 protein A were expressed in *inp2Δ*, *kin4Δ/frk1Δ/inp2Δ* and *vac17Δ*, *kin4Δ/frk1Δ/vac17Δ* cells, respectively. TCA extraction followed by western blot analysis was performed. The values of Inp2-protein A and Vac17-protein A were normalised against the Pgk1 bands. Normalised protein A signals were set to 1 A.U. where A.U. refers to arbitrary units. Error bars indicate SEM (Standard Error Mean). Number of repeats=3. ** p-value < 0.01; *** p-value < 0.001; **** p-value < 0.0001; two tailed Student's t-test.

4.4 Kin4 and Frk1 kinase activity is required for the regulation of peroxisome inheritance and Inp2 protein level.

Kin4 and Frk1 have a specific cAMP kinase domain required for their kinase activity and the protein required for this activation is Elm1. Elm1 phosphorylates Kin4 in the activation loop of the kinase domain at T209 residue. This phosphorylation is required for Kin4 activity in the spindle position checkpoint (SPoC) in early anaphase. However, in the case of Kin4, it has been shown that T209 phosphorylation is present throughout the cell cycle (Caydasi *et al.*, 2010; Moore *et al.*, 2010), suggesting that Kin4 activity is not restricted to anaphase and that its

activity might regulate other processes than SPoC. T209A kin4 defective allele has also been shown to have Kin4 with reduced activity (Aquino et al., 2005). It has been shown by the Hettema lab that Frk1 is also a target for Elm1 and is phosphorylated at the same residue T209 in the activation domain loop; that the T209A mutations do not affect Kin4 and Frk1 localisation or protein levels and that the kinase activity of Kin4 and Frk1 are required for vacuole inheritance. Hence, it was intriguing to check whether the kinase activity is also required for peroxisome inheritance and Inp2 level maintenance. For that, both Kin4 and Frk1 with their T209A mutants were constructed on plasmids tagged with GFP and expressed under their endogenous promoters. For imaging analysis Kin4-GFP and Kin4-*T209A*-GFP was transformed into two different mutant backgrounds *kin4Δ/frk1Δ* and *vps1Δ/dnm1Δ/kin4Δ* cells along with another plasmid carrying a peroxisomal marker to visualise peroxisome during imaging analysis. It was observed that in cells expressing Kin4-GFP peroxisome inheritance was restored whereas the cells expressing Kin4 T209A mutant, a clear peroxisome inheritance defect was observed **Figure 4.4**. The same plasmids were then utilised for a western blot analysis to determine Inp2-protein A levels. To do this *frk1Δ/kin4Δ/inp2Δ* cells were co-transformed with either the Kin4/Frk1-GFP or T209A mutants with Inp2-protein-A and analysed by western blot. As shown below, it was found that Inp2 levels were restored with Kin4 or Frk1-GFP but not with T209A mutants **Figure 4.5 A-B**.

Since it is known that Kin4 and Frk1 activation is dependent on Elm1 phosphorylation it was interesting to analyse peroxisome inheritance and Inp2 levels in *elm1Δ* cells. To do this, *elm1Δ* and wild type cells were transformed with either peroxisomal marker (mNG-PTS1) for imaging analysis or Inp2-Protein A for western blot analysis to check Inp2 protein levels. Interestingly, we found that many cells are defective in peroxisome inheritance in *elm1Δ* compared to wild type cells. In a western blot analysis Inp2 levels were lower in *elm1Δ* compared to wild type **Figure 4.5 C**. Taken together, these results suggest that Elm1 activation of Kin4 and Frk1 by phosphorylation in the kinase activity domain at T209 is required for normal peroxisome inheritance. This finding is analogous to that found by another member of the Hettema lab for vacuole inheritance and suggests that peroxisomes and vacuoles and their Myo2 receptors are regulated in a very similar way.

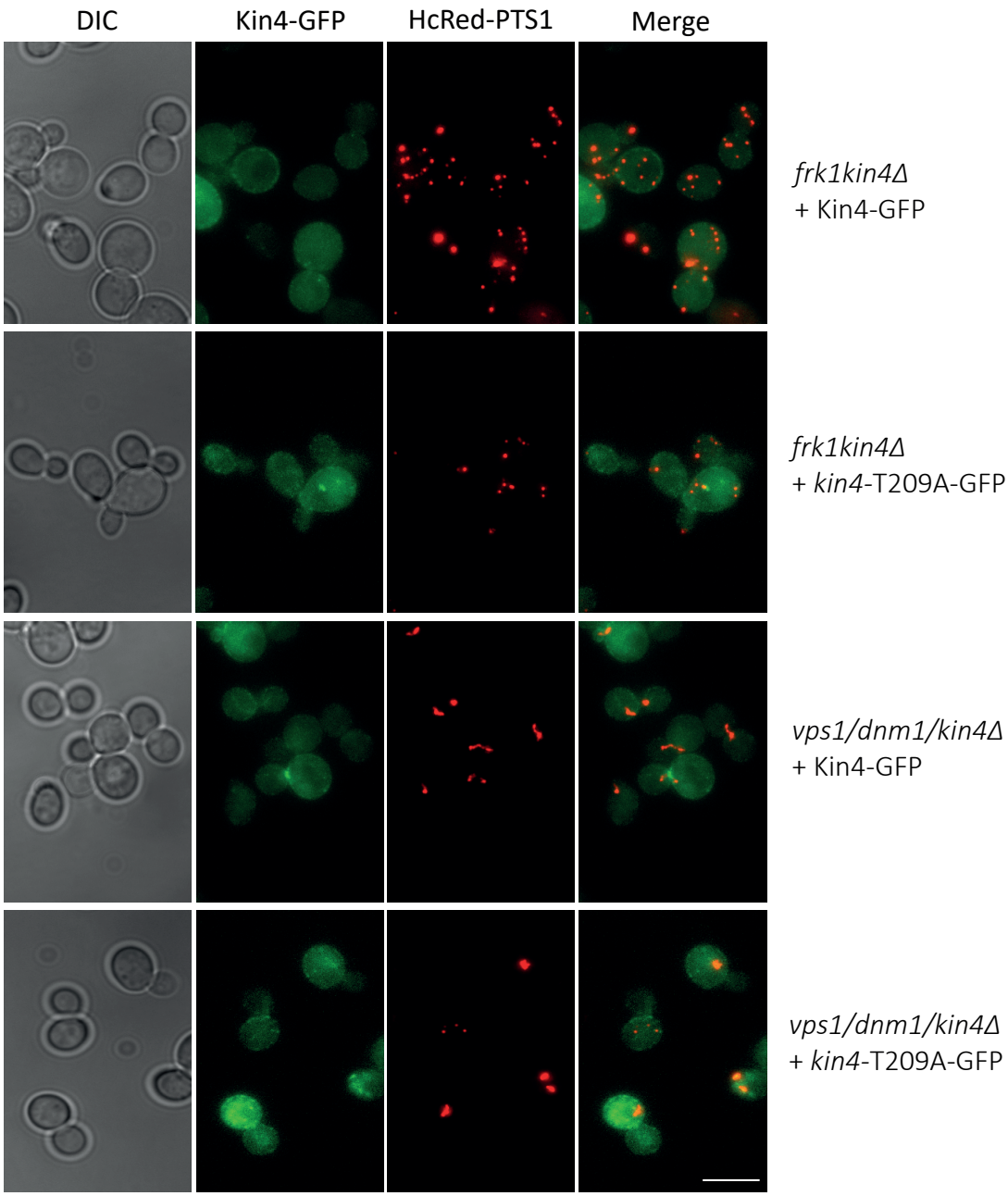

Figure 4. 4 Peroxisome inheritance is regulated by Kin4 kinase activity. Kin4-GFP in *frk1Δ/kin4Δ* and *vps1/dnm1/kin4Δ* show normal peroxisome inheritance where *Kin4-T209A* mutant did not restore the inheritance. Scale bar is 5µm.

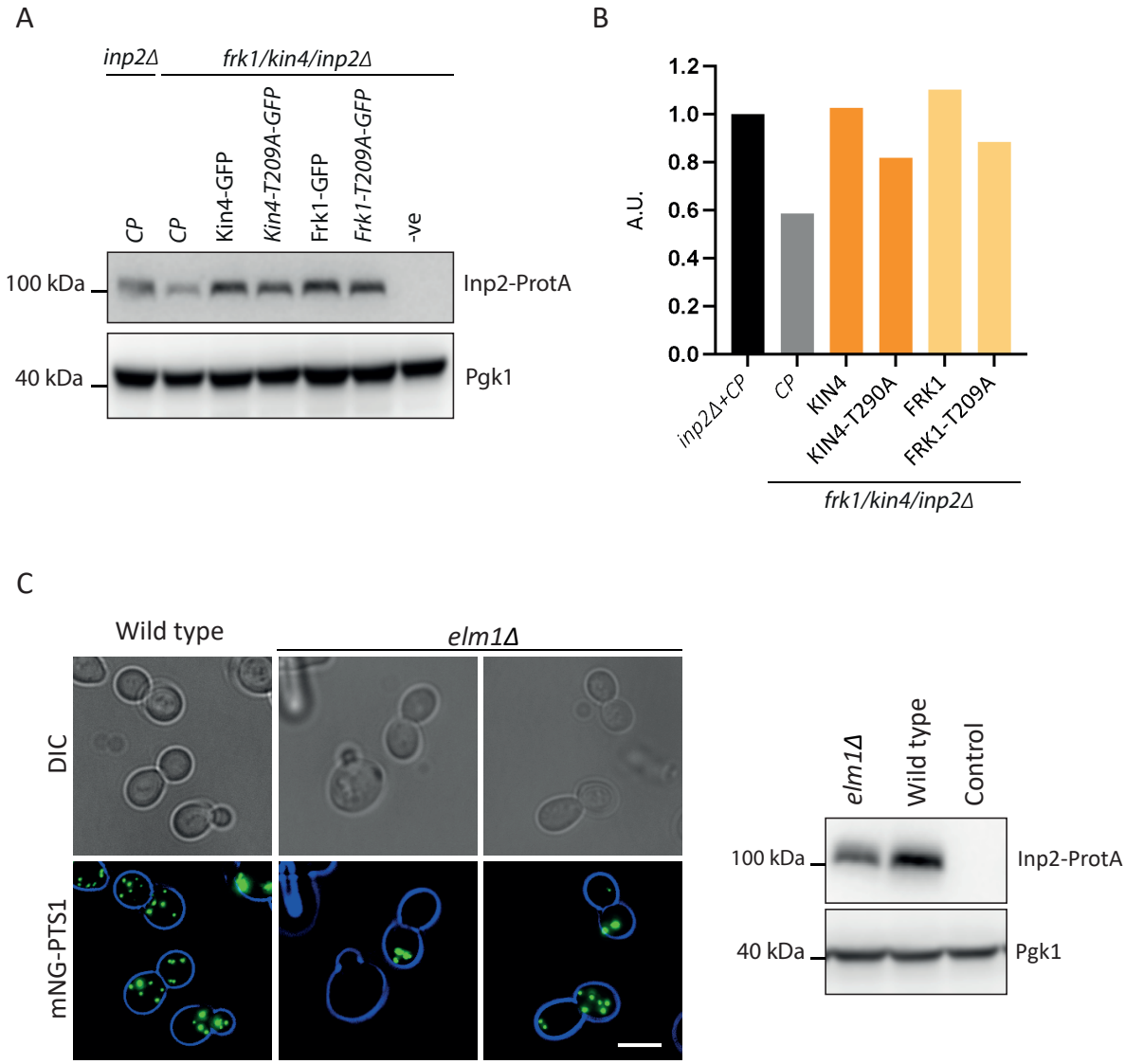

Figure 4. 5 The kinase activity of Kin4 and Frk1 is required for the regulation of Inp2 protein levels. A) Inp2 protein A level was analysed by western blot by Anti-protein A and anti-Pgk1. B) The values of Inp2-protein A were normalised against the Pgk1 bands. The control plasmid (CP)+*inp2Δ* was set to 1 A.U. and compared to other bands accordingly. A.U. refers to arbitrary units. C) Peroxisome inheritance and (D) Inp2 levels were analysed by fluorescence microscopy and western blot respectively. Scale bar is 5µm.

4.5 Inp2 interacts with Myo2 in *kin4Δ/frk1Δ* cells.

To gain more understanding into the effect on peroxisome inheritance observed in *kin4Δ/frk1Δ* cells, it was intriguing to distinguish whether the inheritance deficiency observed in these cells is due to the prevention in Myo2 and Inp2 interaction or due to the decreased levels of Inp2. To test this, a co-immunoprecipitation experiment was carried out in which

Myo2 was tagged with GFP in the genome in *inp2Δ* cells and *kin4Δ/frk1Δ/inp2Δ* cells. Cells were transformed with Inp2-protein A plasmid and Myo2-GFP was pulled down using GFP-Trap beads. Western blot analysis was conducted to detect for Myo2-GFP and Inp2-protein A. Our analysis has shown that Inp2 can still form a complex with Myo2 in *kin4Δ/frk1Δ* **Figure 4.6**. This suggests that the presence of the Kin4 and Frk1 are not required for the formation of the transport complex but for the maintenance of this complex during the subsequent steps. A similar experiment in the lab has similarly demonstrated that Vac17 can also still bind to Myo2 in *kin4Δ/frk1Δ* cells which strongly supports what we found with Inp2.

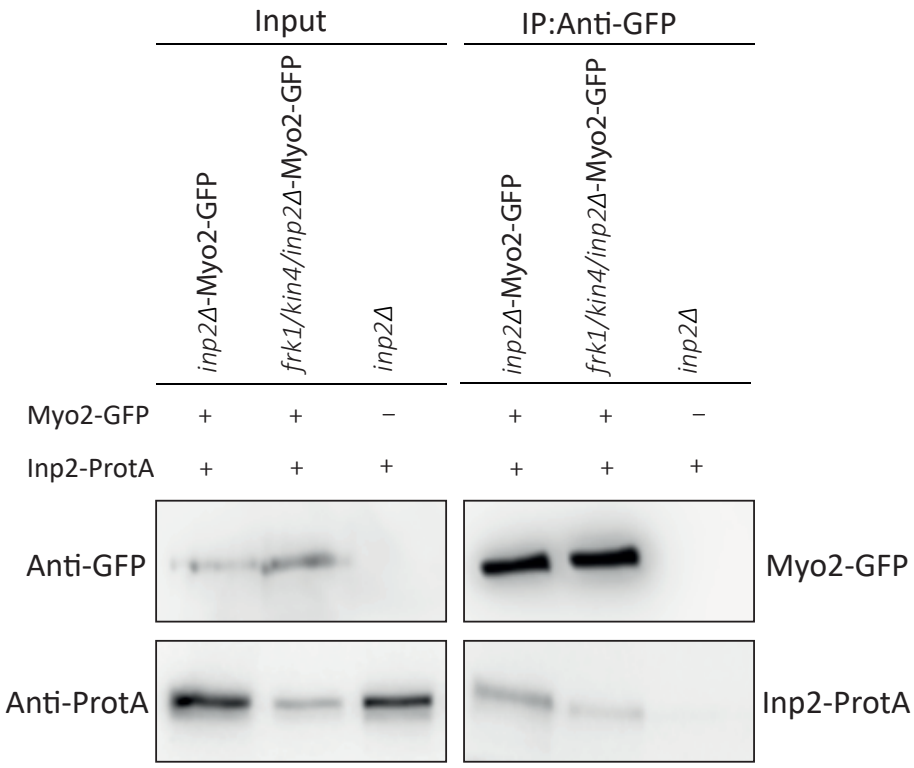

Figure 4. 6 The assembly of Inp2-Myo2 complex in *kin4Δ/frk1Δ* cells. The interaction between Myo2 and Inp2 was analysed by co-immunoprecipitation where Inp2-protein A was expressed on a plasmid under its own endogenous promoter and Myo2 was tagged with GFP in the genome.

4.6 The stability of Inp2 and Vac17 in the mother cell requires Kin4 and Frk1.

Kin4 is a kinase that is mainly localised to the mother cell periphery during the cell cycle, on the spindle pole bodies during G1 phase and at the bud neck during anaphase (Pereira and Schiebel, 2005; D'Aquino et al., 2005). According to previous reports, it has been shown that Kin4 is involved in activating the mitotic exit network (MEN) and thereby regulating activation of the mitotic exit network (MEN) when correct spindle orientation and positioning is achieved (D'Aquino *et al.*, 2005; Pereira and Schiebel, 2005; Caydasi *et al.*, 2010; Moore *et al.*, 2010). However, experiments conducted in the Hettema lab indicate that Kin4's role in MEN or SPoC is not linked to peroxisome and vacuole inheritance. This was through analysing the orientation of the mitotic spindle, which it showed similar spindle pole body alignment in both wild type and *kin4Δ/frk1Δ* whereas in the control *kar9Δ* cells it showed misalignment. Peroxisome inheritance was also similar to wild type cells when the spindle pole body is not aligned in *kar9Δ* cells. This indicates that Kin4 has another novel role in inheritance of organelles that has been investigated further in this project.

Due to the strong effect on Inp2 and Vac17 breakdown in *kin4Δ/frk1Δ* cells and the localisation of Kin4 to the mother cell cortex, we hypothesised that the stability of the receptors is dependent on Kin4 and Frk1 in the mother cell but not in the bud. To test this hypothesis, we used the MIS mutant model developed described in the previous chapter. Since these MIS mutants mainly localise to the mother cell and their steady state levels were much higher compared to wild type Inp2/Vac17 levels **Chapter 3, Section 3.11, Figure 3.15 A and B,** they were a useful tool to test our hypothesis that Kin4 and Frk1 act to protect the Myo2 adaptors in the mother cell. Hence, *inp2Δ*, *kin4Δ/frk1Δ/inp2Δ, vac17Δ,* and *kin4Δ/frk1Δ/vac17Δ* were transformed with either *inp2-mis*-protein A or *vac17-mis*-protein A plasmids, respectively and analysed by western blot. Our analysis showed that both *inp2-mis* and *vac17-mis* levels in *kin4Δ/frk1Δ/inp2Δ* and *kin4Δ/frk1Δ/vac17Δ* were much lower compared to their levels in the strains with the *inp2Δ* and *vac17Δ* deletions alone **Figure 4.7.** Therefore, this result suggests that Kin4 and Frk1 are required for the stability of Inp2 and Vac17 levels in the mother cell during peroxisome and vacuole inheritance. It also suggests that Inp2 and Vac17 are regulated in a very similar manner.

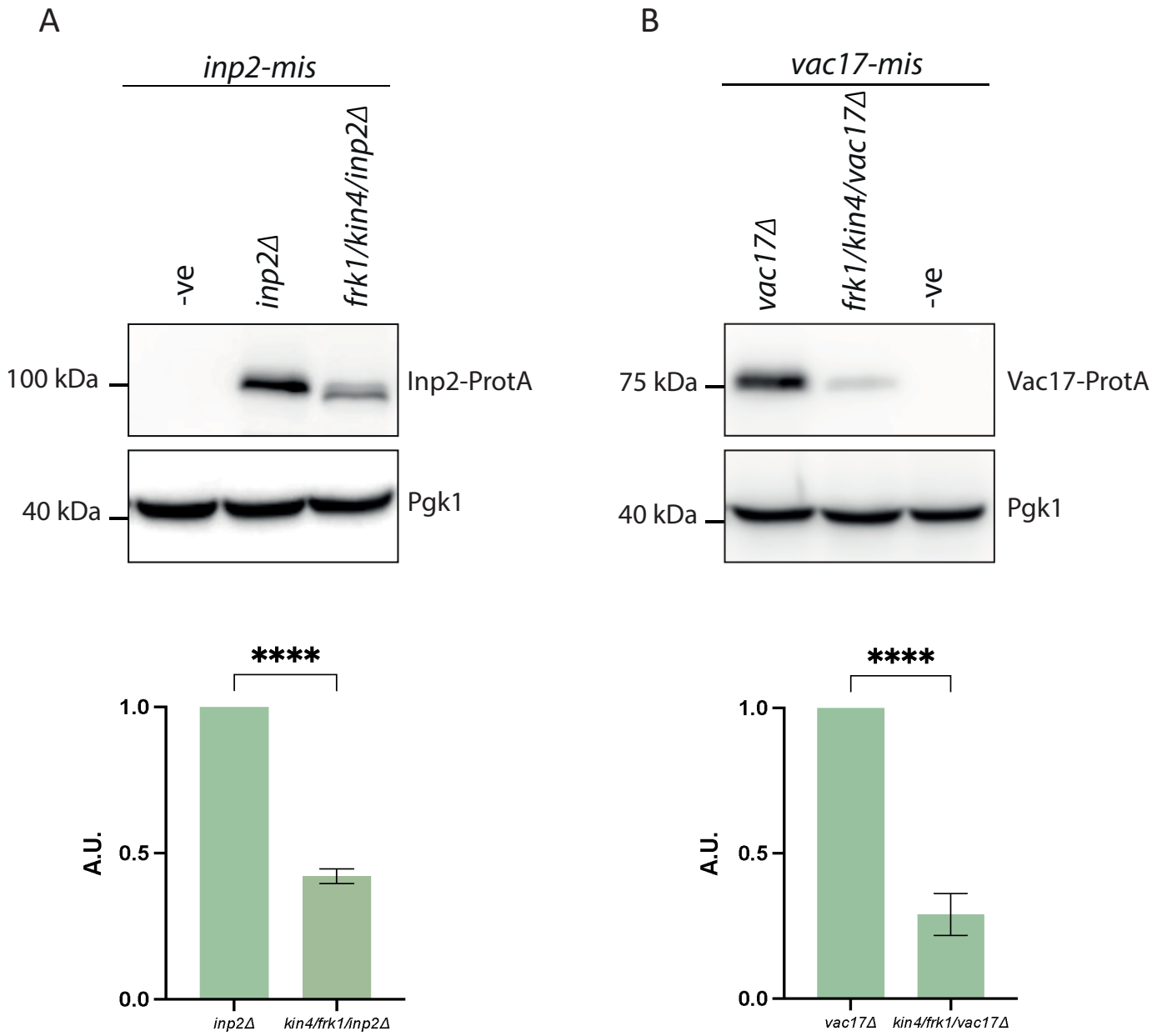

Figure 4. 7 Kin4 and Frk1 protect Vac17 and Inp2 in the mother cell. A+B) *inp2-mis*-protein A and *vac17-mis*-protein A were expressed in *inp2Δ* and *vac17Δ* as well as in *kin4/frk1/inp2Δ* or *kin4/frk1/vac17Δ* cells. TCA extraction followed by western blot analysis was performed. The values of *inp2-mis*-protein A and *vac17-mis*-protein A were normalised against the Pgk1 bands. Normalised protein A signals were set to 1 A.U. where A.U. refers to arbitrary units. Error bars indicate SEM (Standard Error Mean). N=3. ** p-value < 0.01; *** p-value < 0.001; **** p-value < 0.0001; two tailed Student's t-test.

4.7 Kin4 and Frk1 play a role in preventing premature breakdown of Inp2 and Vac17 in the mother cell.

During vacuole transport, the ubiquitin ligase Dma1 is recruited to Vac17 before it reaches the bud tip. It then gets activated by Cla4 to ubiquitylate and so initiate Vac17 breakdown in the bud. We hypothesised that Dma1 activation via Cla4 would occur earlier in the mother cell in *kin4Δ/frk1Δ* cells. This was as observed in the high level of degradation of Myo2 adaptor levels (Inp2 and Vac17) in both their wild type or MIS mutants in *kin4Δ/frk1Δ* cells **Figure 4.3 and Figure 4.7.**

To test this hypothesis, we used Inp2 and Vac17 MIS mutants that fail to transport peroxisomes and vacuoles but still get recruited to their organelles and localised to the mother cell. As shown in **Chapter 3 Figure 3.15 A and B**, the MIS mutants, which do not interact with Myo2, have upregulated levels when localised in the mother cell similar to when Dma1/Dma2-dependent breakdown is not activated via Cla4/Ste20 as shown in **Figure 4.8 C**. This resembles the *myo2-D1297N* and *myo2-Y1384A* mutants that affect Vac17 and Inp2 interactions in previous studies (Ishikawa *et al.*, 2003; Fagarasanu *et al.*, 2006; Taylor Eves *et al.*, 2012). Hence, based on our hypothesis we thought that if we delete *DMA1* gene in *kin4Δ/frk1Δ* cells, we would observe a rescue in the Vac17 and Vac17 MIS mutant protein levels. This was conducted by western blot analysis. Interestingly, after expressing the Vac17 and *vac17-mis* mutant in *kin4Δ/frk1Δ* and *kin4Δ/frk1Δ/dma1Δ*, we found that Vac17-protein A levels in both wild type and MIS mutant were rescued in *kin4Δ/frk1Δ/dma1Δ* compared to *kin4Δ/frk1Δ* resembling the expression of Vac17 and *vac17-mis* in wild type cells **Figure 4.8 A**. In addition, we expressed *vac17-mis-S222A* and *vac17-mis-T240A* tagged with protein A in *kin4Δ/frk1Δ/vac17Δ* cells, and we noticed that these mutants could restore Vac17 MIS levels, resembling the same result with *vac17-mis* levels in *kin4Δ/frk1Δ/dma1Δ* cells **Figure 4.8 B**. Interestingly, expression of *vac17-mis* mutant in *kin4Δ/frk1Δ/vac17Δ* did not result in an increased level compared to when the wild type Vac17 levels were expressed in *kin4Δ/frk1Δ/vac17Δ* cells **Figure 4.8 B**. Furthermore, *vac17-mis-S222A* was expressed in *kin4Δ/frk1Δ/vac17Δ,* and it was observed that it restored protein levels to normal levels with *vac17-mis* in *vac17Δ* cells **Figure 4.8 B**.

Since we hypothesised that Inp2 is regulated similarly to Vac17, we also expressed Inp2 and *inp2-mis* mutant in *kin4Δ/frk1Δ* and *kin4Δ/frk1Δ*/*dma1Δ* to determine whether Inp2 levels can be restored or not. Therefore, our western blot analysis showed that both Inp2 and *inp2-mis* levels are restored in *kin4Δ/frk1Δ*/*dma1Δ* compared to *kin4Δ/frk1Δ* **Figure 4.8 D and E**. Taken together, these results support the hypothesis that Kin4 and Frk1 antagonise Dma1 dependent activation by Cla4 during peroxisome and vacuole inheritance by preventing Dma1 early activation by Cla4 to target Vac17/Inp2 for breakdown.

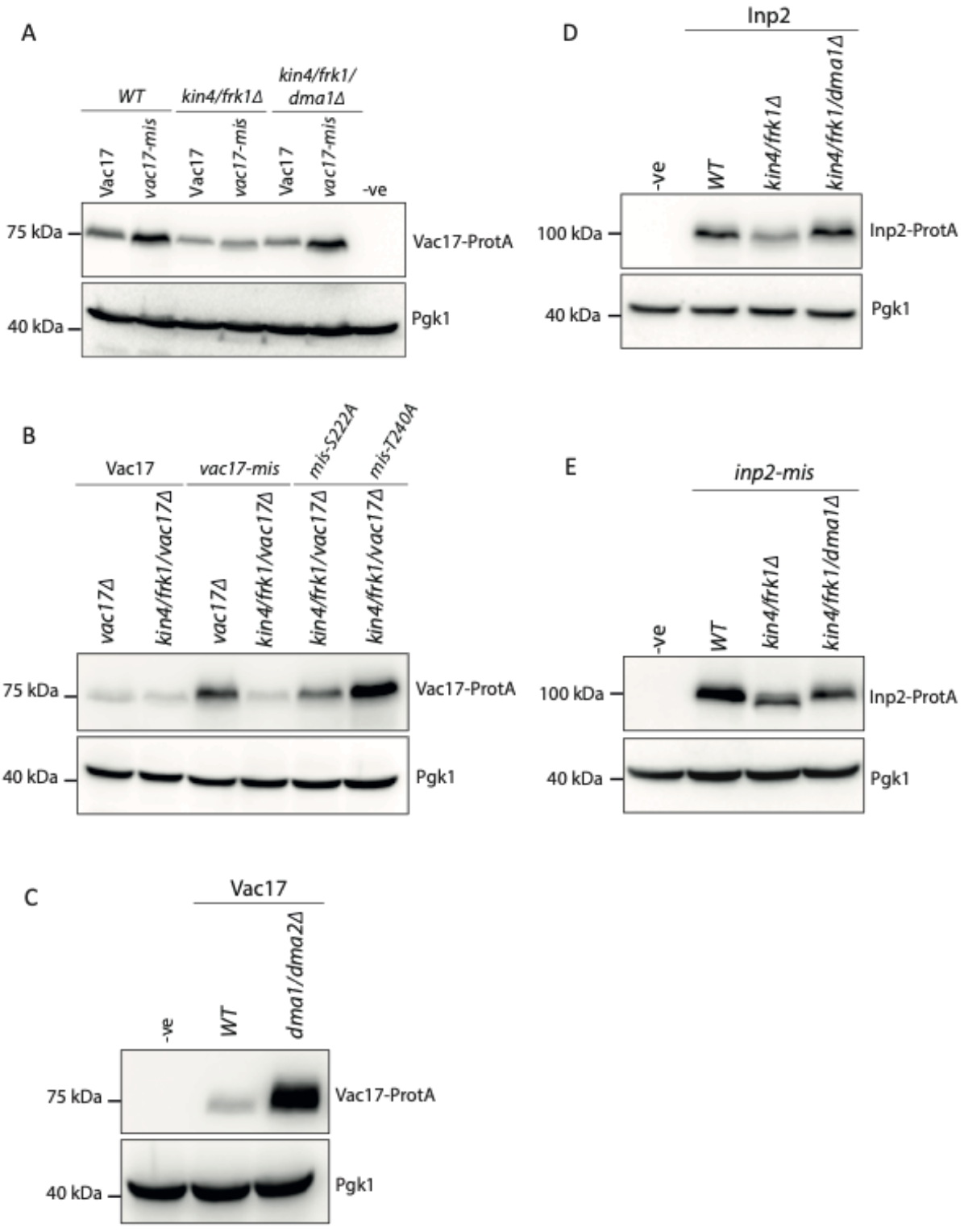

Figure 4. 8 Additional deletion of *DMA1* can restore Vac17 and Inp2 levels affected in *kin4Δ/frk1Δ* cells. A) Vac17 and Vac17-MIS protein levels were analysed by western blot in Wild type *kin4Δ/frk1Δ* and *kin4Δ/frk1Δ/dma1Δ*. B) Additional S222A or T240A mutations on Vac17-MIS were analysed in *kin4Δ/frk1Δ/vac17Δ* cells C) Vac17 protein levels in wild type and *dma1Δ/dma2Δ*. D/E) Inp2 and Inp2-MIS protein levels were analysed by western blot in Wild type, *kin4Δ/frk1Δ* and *kin4Δ/frk1Δ/dma1Δ*.

4.8 Inp2 is involved in the same pathway as Vac17, via Dma1 and Cla4 dependent breakdown.

Studies have shown how Cla4 and Dma1/Dma2 regulate the Myo2 receptor Mmr1 for mitochondria and Vac17 for vacuole (Yau *et al.*, 2014; Yau, Wong and Weisman, 2017; Obara *et al.*, 2022). Dma1 has been shown to recognise phosphorylated threonine residues in a consensus motif TXXI/L in Vac17. In this case, the T240 is the Dma1 recognition site (Yau *et al.*, 2014). However, even though Dma1/2 have shown to play role in both Mmr1 and Vac17 breakdown, the T240 in Vac17 is the only Dma1 site that has been identified to date. Cla4 has also been shown to phosphorylate serine residues in RXS consensus motif in Mmr1 S414 and Vac17 S222 (Yau, Wong and Weisman, 2017; Obara *et al.*, 2022). Due to the lack of information about the Dma1/2 or Cla4 sites on Inp2, it was an interesting candidate to be further analysed since previous data suggested that vacuole and peroxisomes are regulated in a similar way. Cla4 overexpression has been shown to affect peroxisome inheritance and to lead to a decrease in Inp2 protein levels (data generated from the Hettema lab). Hence, it was intriguing to identify whether there is a sequence required for Inp2 breakdown that is controlled by Dma1 and Cla4. This would provide more knowledge on whether Inp2 is controlled in the same manner as Mmr1 and Vac17 or whether it is regulated differently. Therefore, we analysed the Inp2 protein sequence for TXXI/L and RXS motifs. Possible sites for Dma1 binding were identified at positions T323, T511 and T527 and Cla4 phosphorylation sites at S139, S283 and S544. To test whether these residues are important for Inp2 function, we generated a small site directed mutagenesis screen in plasmids containing Inp2 with a single mutation in each residue mentioned above from serine or threonine to alanine. All Inp2 mutants were tagged with protein A and expressed under the Inp2 endogenous promoter. *inp2Δ* cells were transformed with different Inp2 mutants and analysed by western blot to determine if there were mutants that stabilise Inp2 levels. As a result, the S283A and T527A Inp2 levels were higher when compared to the control and other mutants. The S544A and T511A had slightly elevated Inp2 levels **Figure 4.9 A and B**. These results suggested that combining some mutations with each other could increase Inp2 level further. A combination between S283A/S544A (possible Cla4 sites) and T511A/T527A (possible Dma1 binding sites) were hypothesised to possibly give the strongest outcomes. Plasmids with each of these double mutants were constructed and transformed into both *inp2Δ* and *frk1Δ/kin4Δ/inp2Δ*

to determine whether the mutants would stabilise Inp2 levels more in *inp2Δ* cells and also rescue the Inp2 breakdown observed in *kin4Δ/frk1Δ/inp2Δ*. This would resemble the rescue seen in *kin4Δ/frk1Δ* after adding *DMA1* deletion as discussed in **Section 4.7 Figure 4.8 D**. This would indicate that the residues we mutated are possibly the Cla4 and Dma1 targets. Western blot analysis has shown that the combination of S283A/S544A mutations stabilises the Inp2 levels further in *inp2Δ* cells compared to single mutants. However, Inp2 levels were even higher with the T511A/T527A mutant compared to S283A/S544A combination and single mutants. We also observed that Inp2 T511A/T527A mutant combination were able to rescue Inp2 levels more compared to S283A/S544A combination in *kin4Δ/frk1Δ/inp2Δ* cells **Figure 4.9 C and D**. Taken together these results suggests that the sites we hypothesised to be Cla4 or Dma1 sites are strong candidate sites to be further analysed.

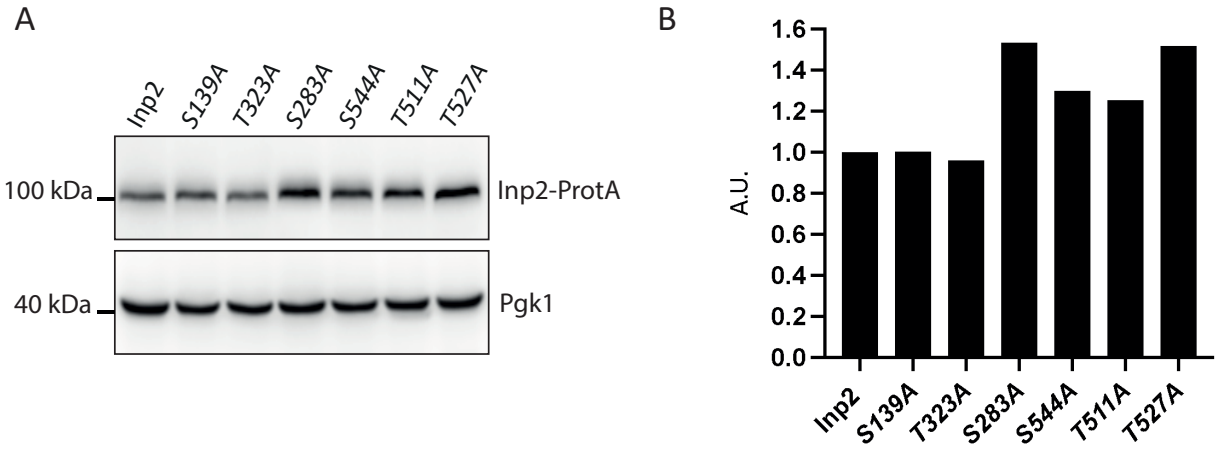

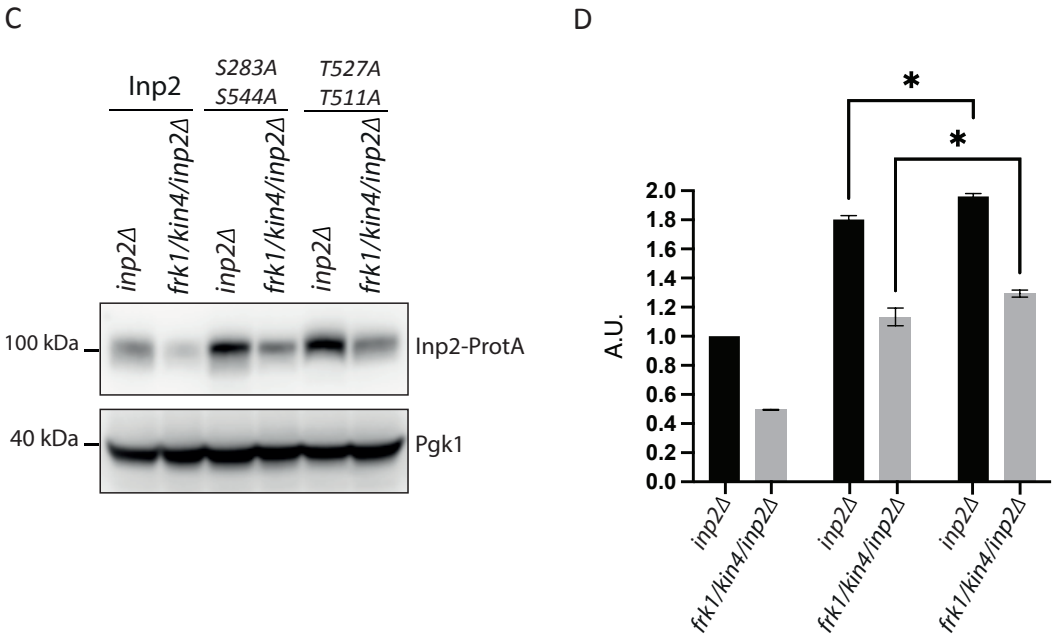

Figure 4. 9 Inp2 contains residues required for its breakdown. A) western blot analysis of Inp2 and various Inp2 mutants. B) The band value of Inp2 was normalised to 1 A.U. and compared to other bands accordingly. C) western blot analysis of Inp2 and Inp2 double mutants in *inp2Δ* and *frk1Δ/kin4Δ/inp2Δ* cells. D) From 3 independent experiments, the band value of Inp2 was normalised to 1 A.U. and compared to other bands accordingly where A.U. means arbitrary units.

4.9 Discussion.

Many factors are involved in peroxisome and vacuole inheritance. It is well known that organelle inheritance is partially regulated by phosphorylation and ubiquitination. Initial findings by the Hettema lab have suggested that protein kinase Kin4 and its paralog Frk1 are involved in the inheritance of vacuoles and peroxisomes because *kin4Δ/frk1Δ* cells do not inherit these organelles. It has also been suggested by Hettema lab that Kin4 kinase activity is necessary for the vacuole and stability of the Myo2 vacuolar receptors Vac17. In addition, it was also suggested that Kin4 and Frk1 play roles in preventing Dma1 early degradation in the mother cell. In this chapter, we firstly focused on reproducing the preliminary data found on the effect on vacuole and peroxisome inheritance and Vac17 and Inp2 levels. Confirming these results was done by several repeats and quantification analysis. Kin4 kinase activity was found to be required for peroxisome inheritance and overlaps with the same role found with vacuole inheritance. Utilising the generated MIS tools confirmed the hypothesis that Vac17 and Inp2 require Kin4 and Frk1 in the mother cell. Also, provides an additional insight about Dma1 early activation by Cla4 in the mother cell in *kin4Δ/frk1Δ* cells. Kin4 appears to inhibit

premature Dma1-dependent Vac17/Inp2 degradation in the mother cells according to the data provided by Hettema lab and in this study **Figure 4.10**. Additional deletion of *DMA1* in *kin4Δ/frk1Δ* cells rescued the MIS breakdown seen in *kin4Δ/frk1Δ*. This suggests that Dma1 activity is required for targeting Vac17 and Inp2 for proteasome breakdown. This could be through ubiquitinating specific amino acids. In *kin4Δ/frk1Δ* cells, we hypothesised that the breakdown of Vac17 and Inp2 could occur earlier. However, this was prevented in *kin4Δ/frk1Δ/dma1Δ* cells due to the absence of the main ubiquitination regulator in which it will result in not ubiquitinating the specific ubiquitination amino acids resulting in stabilising the levels of the MIS mutants. Cla4 overexpression is known to cause Vac17 degradation and recognise Vac17 via a specific motif, it is unclear whether the same pattern is similar to the peroxisomal protein Inp2. By analysing Inp2 protein sequence and looking for TXXI/L and RXS motifs, the study hypothesised potential Dma1 and Cla4 sites. The results we found with the combination of Inp2 S283A/S544A or T511A/T527A suggest that the hypothesised sites for Cla4 or Dma1 are intriguing candidates, since these results resemble the same result shown with *vac17*-S222A and *vac17*-T240A where it stabilises the protein levels compared to wild type Vac17, as well as rescuing the Vac17 protein degradation seen in *kin4Δ/frk1Δ* cells. Uncovering the specific residues targeted by Cla4 and Dma1 in Inp2 regulation will contribute to a better understanding of the mechanisms underlying organelle inheritance and potentially reveal conserved regulatory pathways across different organelles in yeast. Characterising the mechanism of transport of peroxisome and vacuole is crucial, and for this purpose, novel factors and further analysis needed to be carried out.

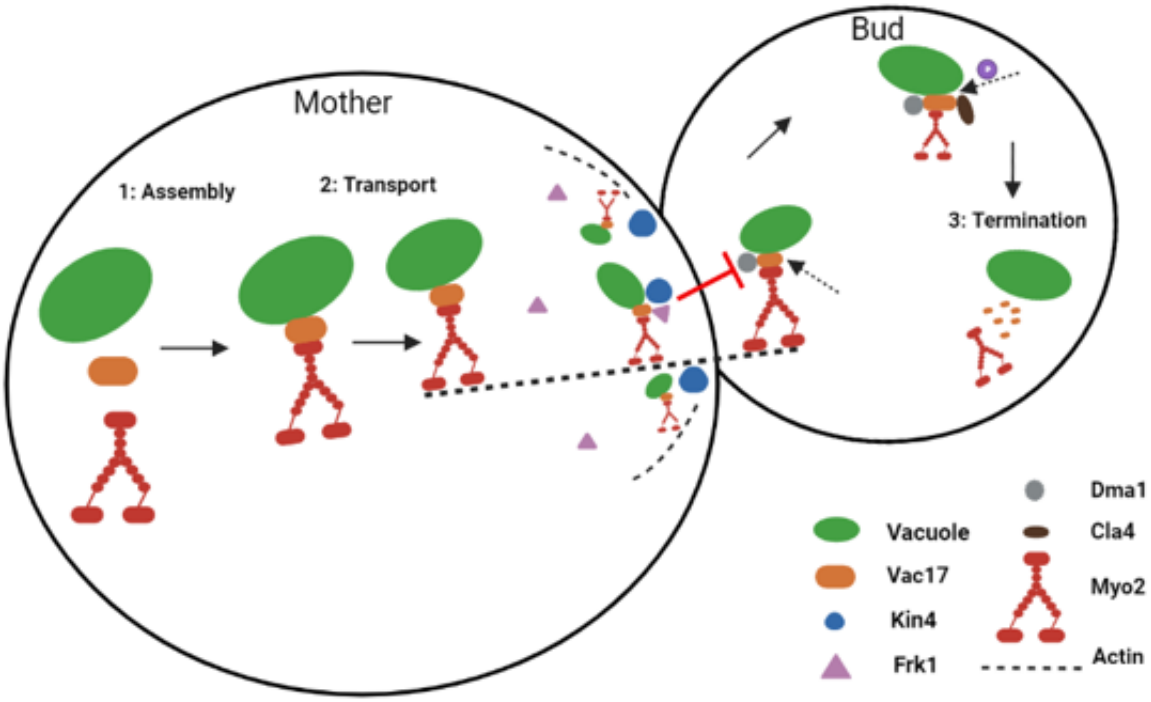

Figure 4. 10 Schematic representation showing the current model for the spatial and temporal regulation of vacuole inheritance in *S. cerevisiae*. Kin4 and Frk1 help maintain Vac17 levels on vacuoles, facilitating their transport to the bud. Dma1 is responsible for Vac17 degradation in the bud, ensuring proper vacuole inheritance. Without Kin4 and Frk1, premature Vac17 degradation by Dma1 inhibits vacuole movement to the bud.

Chapter 5 Identification of novel factors that regulate peroxisome and vacuole transport.

5.1 Introduction

Organelle inheritance is a vital process in cell biology, responsible for transmitting cellular compartments and their genetic information between generations. The budding yeast *Saccharomyces cerevisiae* grows asymmetrically and serves as an essential model organism for studying organelle inheritance, especially for peroxisomes and vacuoles, due to its well-established genetics, rapid growth, and ease of manipulation (Botstein and Fink, 2011). Investigating the mechanisms governing polarised organelle transport and subsequent inheritance in *S. cerevisiae* sheds light on the evolution, regulation, and function of these cellular compartments, as well as their implications for human health and disease.

During the division of yeast cells, peroxisomes undergo growth and division, followed by accurate segregation between the mother and daughter cells. The balance between polarised transport towards the bud and retention in the mother cell plays a critical role in ensuring equal segregation of peroxisomes (Hoepfner *et al.*, 2001). Inp1 is responsible for the retention of peroxisomes. It ensures that peroxisomes remain in the mother cell. On the other hand, Inp2 plays a crucial role in recruiting the class V myosin, Myo2, which facilitates the transport of peroxisomes along actin cables towards the bud. Together, these proteins coordinate the proper distribution of peroxisomes during cell division (Fagarasanu *et al.*, 2005, 2006). Vacuole inheritance involves the transport of a portion of vacuoles from the mother cell to the daughter cell, and Vac17 is known to mediate vacuole inheritance through its interaction with Myo2 (Ishikawa *et al.*, 2003).

Although numerous studies have identified various factors and processes involved in the proper inheritance of peroxisomes and vacuoles, the regulatory mechanisms overseeing these processes remain incompletely understood. Therefore, it is crucial to elucidate the mechanisms regulating peroxisome and vacuole transport during inheritance and to discover novel factors and proteins implicated in these processes. Genetic libraries have proven

invaluable for systematically addressing biological questions and identifying new factors essential for organelle inheritance. Several yeast libraries have been created for many screens in *S. cerevisiae*. Genetic libraries represent an efficient technique (Tong *et al.*, 2001; Cohen and Schuldiner, 2011) and have been developed not only for budding yeast but also for fission yeast *Schizosaccharomyces pombe* and bacteria such as *E. coli* (Tong *et al.*, 2001; Roguev *et al.*, 2007; Butland *et al.*, 2008; Typas *et al.*, 2008).

The work described in this chapter aimed to identify novel factors with significant roles in peroxisome and vacuole inheritance, emphasizing the roles of kinases, phosphatases, and ubiquitin ligases. By investigating these proteins' functions, researchers can obtain a more in-depth understanding of the regulatory mechanisms controlling organelle inheritance and reveal potential therapeutic targets for human diseases associated with peroxisome and vacuole dysfunctions.

5.2 Developing an overexpression library containing kinases, phosphatases, and ubiquitin ligases.

In order to establish our study on kinases, phosphatases and ubiquitin ligases, and due to the collaboration of the Hettema lab with the Maya Schuldiner's Laboratory at the Weizmann Institute, Israel our lab was provided with an overexpression library, which was developed using the SWAT technique (Yofe *et al.*, 2016). This collection comprises approximately 6,000 strains where the endogenous promoter of a specific gene has been substituted with *TEF2* promoter and labelled with an N-terminal mCherry tag (red tag) **Figure 5.1** (Weill *et al.*, 2018). These strains are systematically arranged in microtiter plates, and for each well, the gene regulated by the *TEF2* promoter is identified. In most cases, this leads to overexpression. Two specialised sub-libraries were then generated from the 6,000-gene collection. The first sub-library contains approximately 250 strains overexpressing kinases and phosphatases, while the second comprises approximately 250 strains overexpressing ubiquitin ligases.

Figure 5.1 Schematic representation of the overexpression sub-libraries created from SWAT library. NAT: nourseothricin antibiotic. *TEF2*: a yeast strong promoter.

5.2.1 Validating the functionality of the genetic screen.

Before undertaking a screen with each sub-library, some specific clones were selected to determine whether these were behaving as expected according to published literature. According to what has been studied previously, *CLA4* overexpression leads to excessive degradation to Vac17 (Bartholomew and Hardy, 2009). Additionally, recent work by our lab has shown that *KIN4* overexpression in *bfa1Δ* cells stabilises Vac17 and Inp2 levels resulting in peroxisomes or vacuoles mis-positioning to either bud tip or mother-bud neck (manuscript submitted). High Kin4 overexpression is toxic to cells due to the prevention to cells to exit from mitosis. Nonetheless library cells expressing *TEF2-mCherry-KIN4* were growing although somewhat slower. Probably the level of Kin4 expression was not so high as to block mitotic exit or the mCherry fusion somewhat affect Kin4 function. Therefore, it was very interesting that we check the functionality of our library by choosing these two kinases overexpression strains and analyse vacuole and peroxisome dynamics. Thus, *CLA4* and *KIN4* overexpressing strains were transformed with either a peroxisomal or vacuolar green fluorescent protein marker and logarithmically growing cells were analysed by microscopy. These strains were also transformed with a plasmid carrying either Inp2-protein A or Vac17-protein A expressed under control of their own promoters to analyse Inp2 and Vac17 protein levels by western blot. *CLA4* overexpression resulted in a defect of peroxisome and vacuole inheritance **Figure 5.2 A** and a reduction in the protein level of their Myo2 receptors, Inp2 and Vac17 proteins . On the other hand, Kin4 overexpression caused mis-localisation to peroxisomes and vacuoles and stabilised Inp2 and Vac17 levels compared to control **Figure 5.2 A and B.** Taken together,

this result suggests that this overexpression library is a beneficial tool to utilise for our analysis.

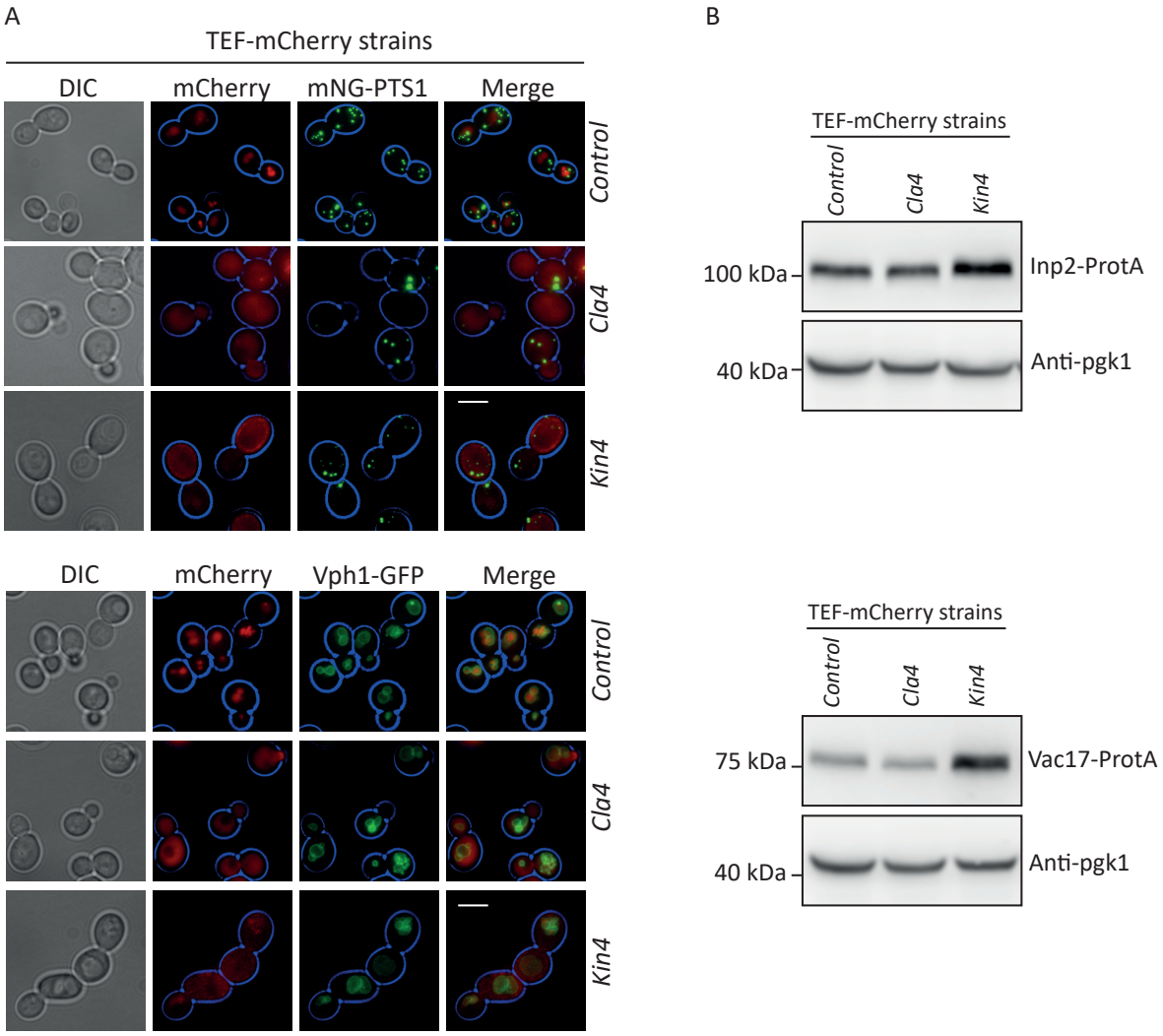

Figure 5.2 Cla4 and Kin4 overexpression affected peroxisome and vacuole transport. A) Overexpression strains of *CLA4* and *KIN4* expressed under *TEF2* promoter were transformed with peroxisomal and vacuolar markers as well as the control strain. B) Western blot analysis of Inp2 and Vac17 under Kin4 and Cla4 overexpression compared to the control. Scale bar is 5µm.

5.3 Screening of vacuoles and peroxisomes dynamics

Since the focus of this study was to analyse peroxisome and vacuole inheritance in the two sub-libraries, it was necessary to develop a way of to visualise peroxisomes and vacuoles to allow screening by microscopy. The library did not contain peroxisomal or vacuolar membrane genes tagged with any fluorescent proteins so in order to visualise the organelles, the overexpression library strains (Mat α) were crossed with a wild type (Mat **a**) strain that has either peroxisomal marker (Pex11) or vacuolar marker (Vph1) tagged with fluorescent

mNeongreen in the genome. Diploid cells were then selected that contain the overexpression gene and either the peroxisomal or vacuolar marker as shown in **Figure 5.3**. Both Pex11, a peroxisomal membrane protein, and Vph1, a vacuolar membrane protein, are abundant and clearly label the respective organelles. Importantly, this tagging does not interfere with peroxisome and vacuole distribution in dividing cells **Figure 5.4 A and B**. Consequently, these strains can be utilised for the subsequent phases of the study.

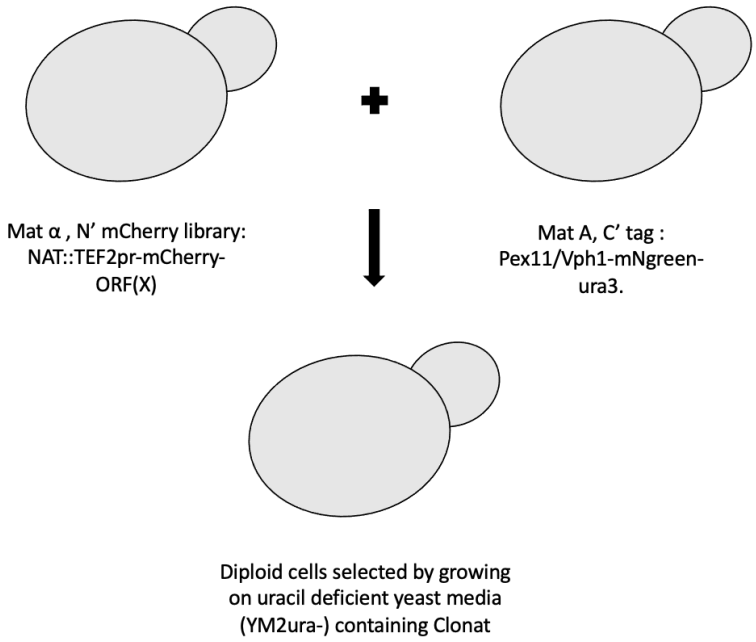

Figure 5.3 A diagram showing the mating between the overexpression library and the tagged strains. The overexpression library mat α was mated with the tagged strains mat a in YPD plate for two days. The grown diploid cells were then re-selected on medium that is uracil deficient and containing antibiotic cloNat. This allows for the proper selection of the diploid that contain both the overexpression gene and the tagged gene.

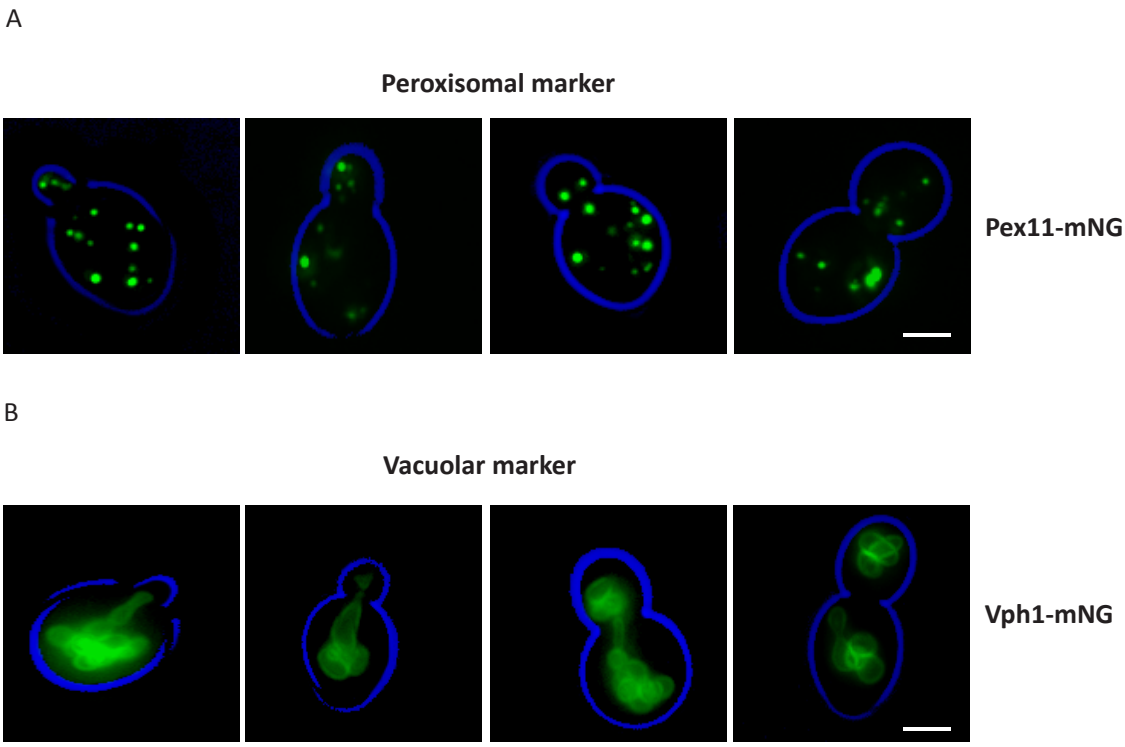

Figure 5.4 Fluorescent microscopy images of wild type cells. (A) The peroxisomal membrane protein Pex11 is tagged C-terminally with mNeongreen fluorescent protein (B) The vacuolar membrane protein Vph1 is tagged C-terminally with mNeongreen fluorescent protein. Both panels from the left to the right show cells with increasing bud size. Different stages of vacuole and peroxisome inheritance can be distinguished from small emerging bud till around the time of cytokinesis. Scale bar is 5µm.

5.4 The overexpression screening analysis.

Given that our primary objective was to thoroughly examine and systematically analyse peroxisome and vacuole inheritance in the developed fluorescently tagged libraries, optimizing their visualization for high-resolution microscopic analysis was of paramount importance. This was essential to generate reliable and accurate data, enabling us to better understand the molecular mechanisms underlying organelle inheritance and distribution.

The screening process potentially involved investigating a range of phenotypes. However, to streamline our research and maximise its relevance to only organelle transport and dynamics, our focus was strategically narrowed down to phenotypes specifically related to these processes. As depicted in **Figure 5.5 A and B**, we sought to characterise the subcellular localization, movement of peroxisomes and vacuoles. To achieve this, several factors were considered in the experimental design, such as the choice of appropriate markers and microscopy techniques. The selection of Pex11 and Vph1 as markers ensured the clear

visualization of peroxisomes and vacuoles, respectively, without interfering with their distribution in dividing cells. Furthermore, the use of epifluorescence microscopy, coupled with high-resolution objective lenses and optimised image acquisition software, allowed for precise capture of the desired phenotypes.

By concentrating on phenotypes associated with organelle transport and dynamics, the study aimed to uncover potential mechanisms, regulatory factors, and molecular pathways that govern peroxisome and vacuole inheritance in the tagged libraries. This targeted approach enabled more efficient screening and facilitated the identification of key players and processes involved in organelle transport, ultimately contributing to a better understanding of their roles in cellular function and division.

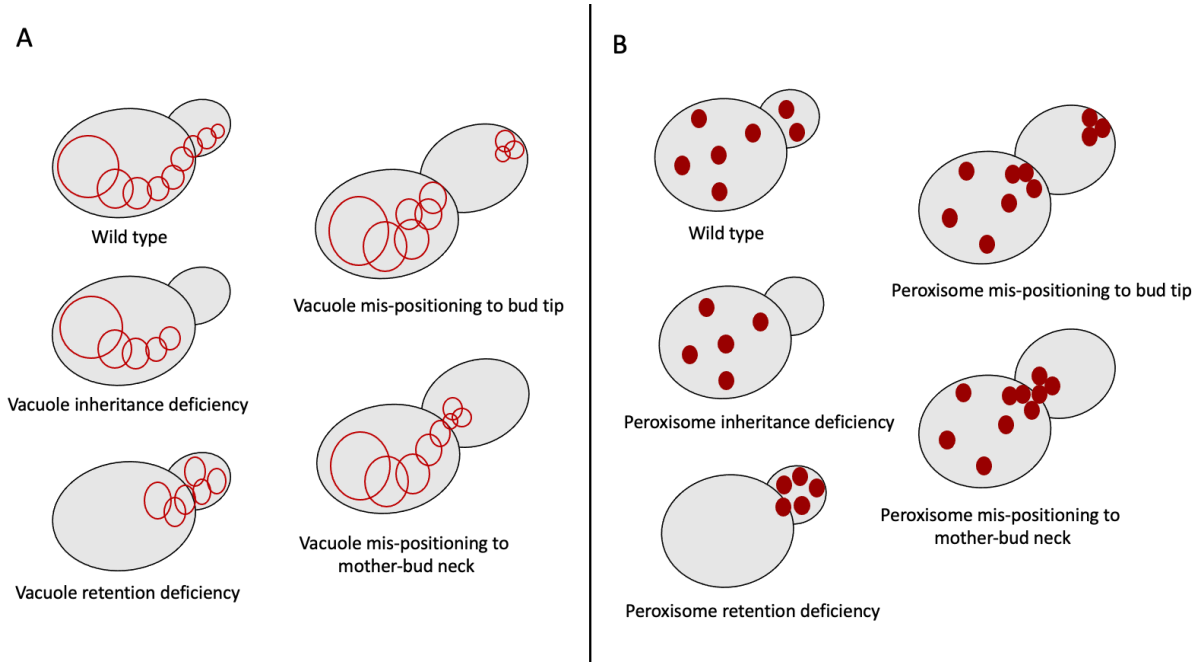

Figure 5.5 Schematic representation showing the potential phenotypes of peroxisome and vacuole inheritance and retention deficiencies due to the overexpression of kinases, phosphatases, and ubiquitin ligases. (A) represents the various vacuolar inheritance deficiencies expected from the screen (B) represents the various peroxisomal inheritance deficiencies expected from the screen.

5.5 The screening analysis outcome identified factors involved in peroxisome and vacuole inheritance.

The screening analysis conducted in the previous section, helped us with a valuable insight into finding some possible factors involved in peroxisome and vacuole inheritance. By focusing on the organelle dynamics, this study would aim to elucidate the molecular regulatory factors that may be involved in the inheritance of peroxisomes and vacuoles. Finding the essential proteins required for peroxisome vacuole inheritance has not only expanded our understanding of their roles in organelle inheritance but also encouraging the field for further research in this intriguing aspect.

The outcome of the screening analysis revealed several candidates that may play significant roles in peroxisome and vacuole inheritance **Figure 5.6**. Some of these factors are reported to be involved in membrane trafficking, cytoskeletal components, organelle biogenesis or in protein post translational modifications that orchestrate the correct organelle transport and positioning on specific time and space during cell division. In addition, many of the proteins found are primarily part of various complexes that are responsible for different mechanisms. As a result, among 500 strains screened for both organelles, 42 hits which represents 8.4% displayed different effects based on the different phenotypes related to peroxisome and vacuole inheritance mentioned in **Figure 5.5.** However, only 16.6% of the 42 hits exhibited a strong phenotype on either peroxisome or vacuole inheritance shown in **Figure 5.7 A and B**. The other 83.4 % of the hits were a moderate (42.9%) to mild (40.5%) effect. Interestingly, some of the hits found were similar to those reported in previous studies examining peroxisome, vacuole, and mitochondria inheritance under conditions of overexpression, deletion, or mutation such as *CLA4* **Figure 5.7 A and B**, *STE20*, *DMA1*, and *RSP5* (Fisk and Yaffe, 1999; Bartholomew and Hardy, 2009; Yau, Wong and Weisman, 2017). Additionally, the casein kinase Yck1 and its paralog Yck2 were identified as hits. Their overexpression results in a distinct phenotype compared to the other hits. Therefore, given the similarity between some of the identified hits and findings from previous and recent research, we hypothesised that expanding our search to include other hits whether high, medium and low could help refine our understanding of protein behaviour. Thus, we decided to further analyse all the hits found.

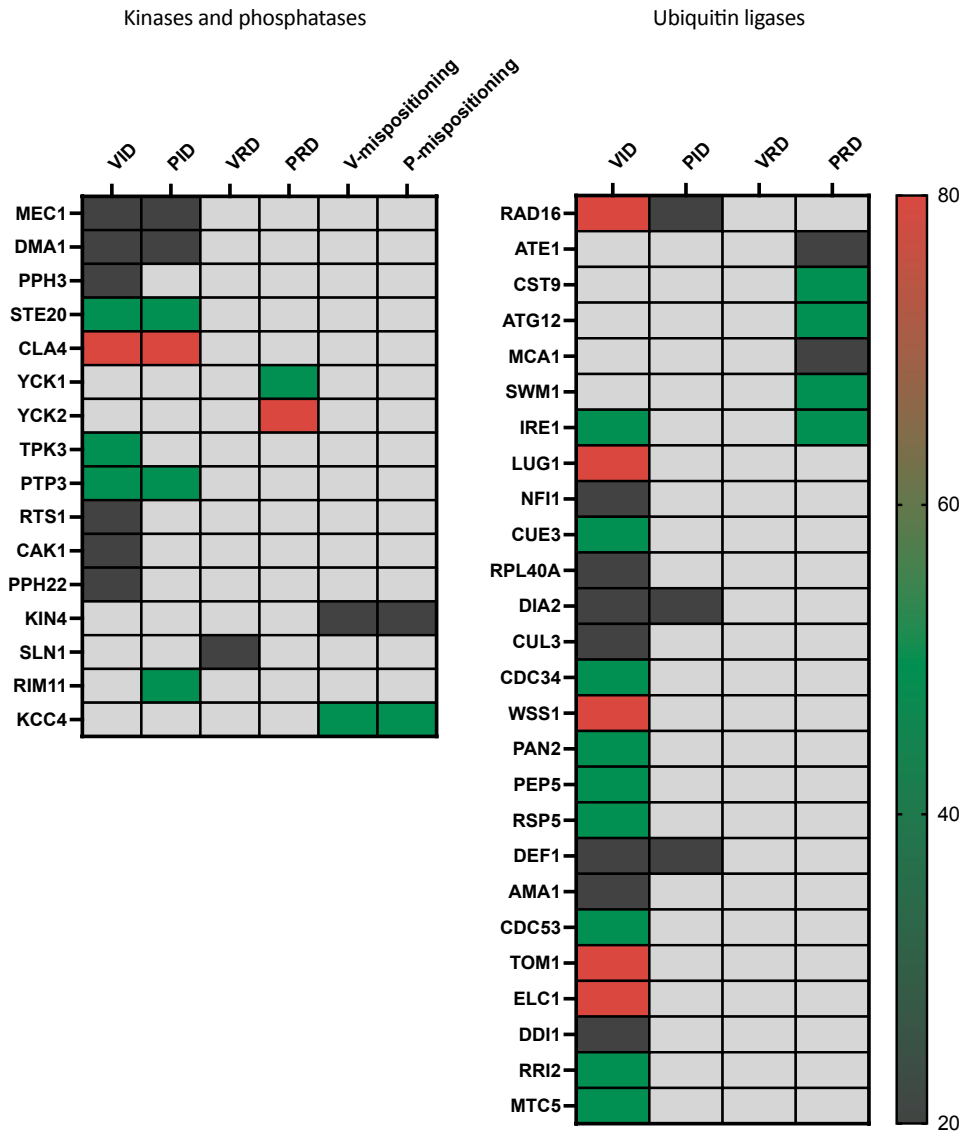

Figure 5.6 This heat map shows the total hits that have been found from the screening results. Hits were divided into 3 groups according to their level of effect starting with the strongest hits (Red), medium effect hits (Green), and the mild effect hits (Dark gray). In addition, hits were also divided into 6 groups according to their phenotypes starting with (VID) the vacuolar inheritance deficiency, peroxisomal inheritance deficiency (PID), vacuolar retention deficiency (VRD) and peroxisomal retention deficiency (PRD), vacuole mis-positioning and, peroxisome mis-positioning. The level of the effect was based on the number of the affected cells counted per sample. A minimum of 50 cells counted per sample.

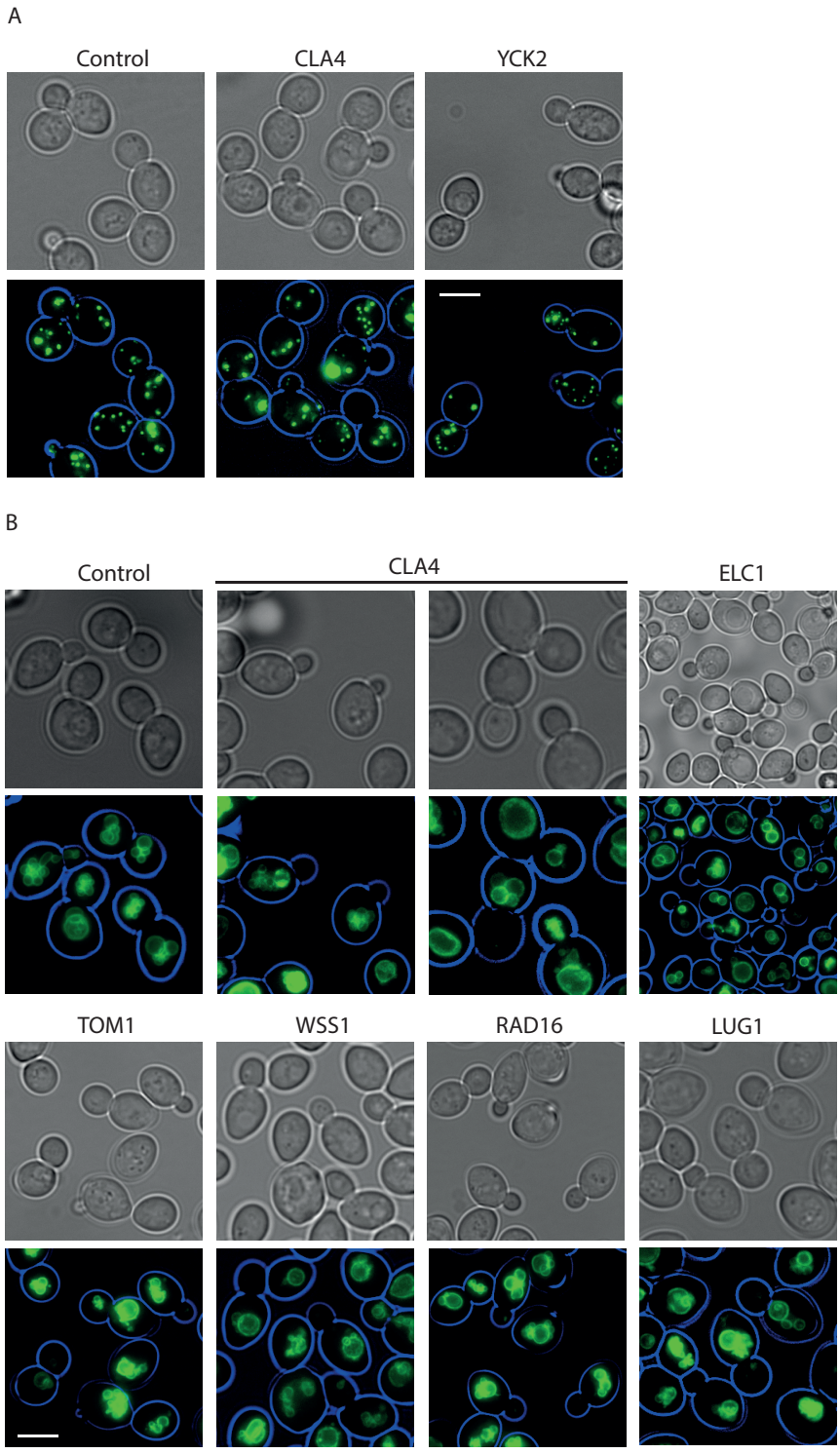

Figure 5.7 Peroxisome and vacuole inheritance affected in some overexpression strains. (A) Showing the peroxisome inheritance and retention deficiencies in the strains with strongest phenotypes hits compared to the control. (B) Showing the vacuolar inheritance deficiency in the strains with strongest phenotypes hits compared to the control. Scale bar is 5µm.

5.5.1 Analysis of the cellular localisation of the hits outlined from the screen.

It was very intriguing to analyse the localisation of the hits to get a better understanding of whether they are likely to be having a direct or indirect effect on vacuole and peroxisome inheritance. According to SGD (*Saccharomyces* Genome Database*)* out of the 42 hits found, 11 are mainly localised in the cytosol. Dma1 which has been found to regulate Vac17 is mainly localised in the cytosol. One of these 11 cytosolic localised hits showed a strong defect in vacuole inheritance shown in **Table 5.1**. 15 hits showed a localisation between the cytosol and nucleus resembling the same localization of Rsp5 which has been shown to affect mitochondria inheritance (Fisk and Yaffe, 1999). Among these 15 only 2 showed a strong effect to vacuole inheritance. Additionally, 6 hits were found to be mainly localised to the nucleus and only 2 of them were from the strong hits showing defect to vacuole inheritance. Cdk1, one of the proteins that mainly localised to nucleus is involved in vacuole inheritance by phosphorylating Vac17 (Peng and Weisman, 2008a). 4 Cell periphery localised hits, one showed a strong defect in peroxisome retention. The recently discovered Kin4 showed localisation to the cell periphery. 1 Hit beside CLA4 and STE20 showed localisation to the bud neck or bud tip, which they have shown their roles in the vacuole inheritance (Bartholomew and Hardy, 2009). 2 hits were localised to the vacuole membrane, resembling the same localisation of Yck3 and Vps41, the proteins required for vacuole inheritance termination in the bud (Wong *et al.*, 2020). Lastly, 1 hit was found to be localised to the endoplasmic reticulum (ER). Therefore, based on the similarity of the localisation between Kin4 and Yck1 and Yck2 and the importance of Kin4 role that recently discovered by Hettema lab, we decided to follow up with further analysing the role of Yck1 and Yck2. It has been recently reported that Inp1 N-terminal domain is required for plasma membrane binding to retain peroxisome to the mother cell during peroxisome inheritance (Hulmes *et al.*, 2020). Here, we found Yck1 and Yck2 as factors that might be involved in regulating Inp1 function or binding to the cell periphery thus regulating peroxisome retention.

Table 5.1 The localisation of the hits found from the screen. The highlighted genes are the ones that showed strong defect.

Localisation	Gene included
Cytosol	***MEC1, DMA1, PTP3, RTS1, CAK1, ATG12, LUG1, CUE3, PAN2, DEF1, AMA1.***
Nucleus	***RAD16, CST9, DIA2, NFI1, CDC34, WSS1.***
Cytosol and nucleus	***PPH22, RIM11, ATE1, MCA1, SWM1, RPL40A, CUL3, RSP5, CDC53, TOM1, ELC1, DDI1, RRI2, PPH3, TPK3***
Cell periphery	***KIN4, YCK1, YCK2, SLN1***
Bud neck – Bud tip	***CLA4, STE20, KCC4***
Vacuole membrane	***MTC5, PEP5***
Endoplasmic reticulum	***IRE1***

5.6 The casein kinases Yck1 and Yck2 overexpression affect peroxisome retention.

Based on the initial screening of peroxisome inheritance and dynamics we found that Yck1 and Yck2 were both identified in this screen. Yck1 and Yck2 are paralogs and their overexpression showed very similar phenotypes, affecting peroxisome retention in the mother cell. Interestingly, Yck1 and Yck2 were also identified as hits in another preliminary screen using the overexpressing sub-libraries which was investigating factors affecting Inp1 levels. Overexpression of *YCK1* and *YCK2* led to low levels of Inp1. Therefore, we decided to investigate the effects of *YCK1* and *YCK2* overexpression further. The first step was checking the reproducibility of the phenotypes found in these cells. To do this, new strains were generated that would lead to overexpression of either *YCK1* or *YCK2* under the *GAL1/10* conditional promoter. The *GAL1/10* promoter was inserted to replace their endogenous promoters in the genome. Control strains with the endogenous promoters intact were used as controls for comparison. The goal of these experiments was to validate the initial findings and gain further insight into the role of Yck1 and Yck2 in peroxisome dynamics. To assess the

reproducibility of the phenotypes observed in the initial screen, we cultured the newly constructed strains after transforming them with peroxisomal marker under both repressing (in glucose) and inducing (in galactose) conditions. The permissive conditions allowed for basal expression of Yck1 and Yck2, while the inducing conditions promoted their overexpression under the control of the *GAL1/10* promoter. The control strains were subjected to the same conditions to evaluate the effect of overexpression on the observed phenotypes. Following the growth of the strains under the different conditions, we assessed peroxisome dynamics, and distribution by using epifluorescence microscopy. Image analysis was employed to visualise the parameters in the various strains.

Our results demonstrated that when Yck1 and Yck2 were overexpressed under the *GAL1/10* promoter, peroxisome retention was significantly impacted compared to those in glucose conditions and those carrying strains expressing Yck1/Yck2 under their endogenous promoters **Figure 5.8 A**. To further investigate the influence of these two Ycks proteins on peroxisome retention, we introduced the same *GAL1/10* promoter to Yck1 and Yck2 in a different background strain. The *vps1Δ/dnm1Δ* strain was employed as cells contain a single elongated peroxisome which facilitates microscopic analysis. After constructing the strains, they were transformed with peroxisomal marker, and the same experiment performed. Our imaging analysis showed that Yck1 and Yck2 both affect peroxisome retention. However, in this *vps1Δ/dnm1Δ* strain background Yck2 overexpression led to a stronger phenotype than in cells with Yck1 overexpression. The single elongated peroxisome observed when cells were grown in the glucose containing medium was no longer observed in the galactose-containing medium. Instead of the single elongated peroxisome, the peroxisome was more globular in shape and was localised in the bud **Figure 5.8 B.** Taken together, these results confirmed the reproducibility of the phenotypes found in the initial screen. Overexpression of either Yck1 or Yck2 under the *GAL1/10* promoter resulted in significant alterations in peroxisome distribution compared to control strains. The phenotypes observed upon overexpression of Yck1 and Yck2 were similar, but Yck2 had a more prominent effect, suggesting that these kinases may play slightly different roles or one of them is more abundant or active than the other one in regulating peroxisome distribution.

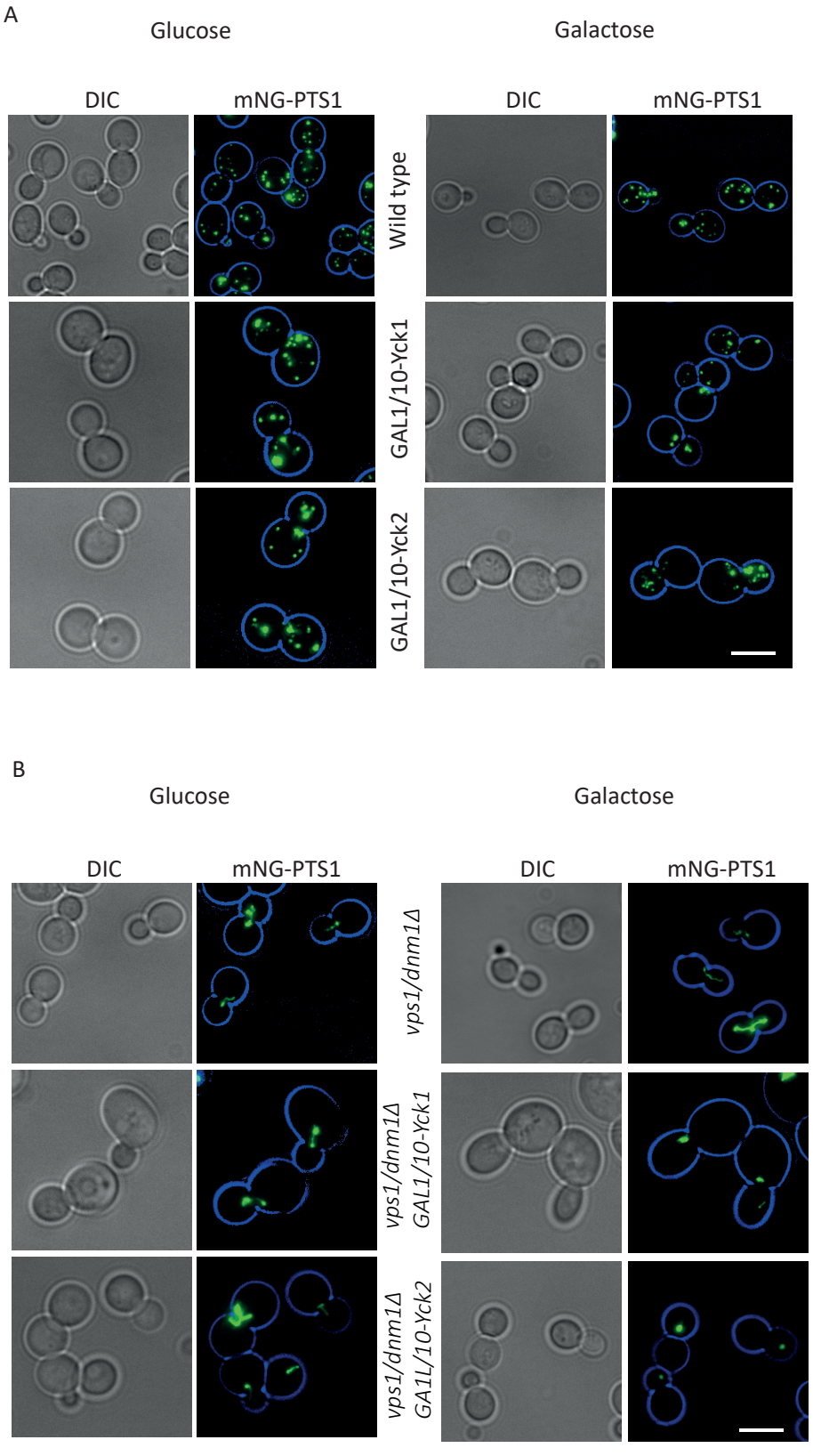

Figure 5.8 Yck1 and Yck2 regulate peroxisome retention. (A) Peroxisome retention is affected under galactose induction of Yck1 and Yck2 under the control of *GAL1/10* promoter compared to glucose and wild type cells containing Yck1 and Yck2 endogenous promoters grown in both glucose and galactose containing medium. (B) The same effect is shown in *vps1Δ/dnm1Δ*. All strains were transformed with a plasmid containing (mNG-PTS1) as a peroxisomal marker. Cells were grown

overnight on raffinose containing medium. Then were diluted and grown logarithmically in either glucose or galactose containing medium before imaging **Methods chapter section 2.6.7.** Scale bar is 5µm.

5.6.1 Yck1 and Yck2 when expressed under *GAL1/10* promoter regulate Inp1 function.

In order to investigate further into the molecular mechanisms that underpin the observed phenotypes seen in **Figure 5.8**, we carried out analysis to identify potential targets and pathways influenced by Yck1 and Yck2 kinases. To accomplish this, we conducted western blot analyses, which to determine the levels of Inp1, a protein responsible for peroxisome retention. This approach helped ascertain whether the observed effect was due to Inp1 protein or other cellular components impacted by the overexpression of Yck1 and Yck2 kinases.

To perform this analysis, we transformed *Gal1/10-Yck1* and *Gal1/10-Yck2* strains with Inp1-protein A, expressed from a single copy plasmid under its endogenous promoter. Western blot results revealed a reduction in Inp1 levels and a shift of the apparent molecular weight of the protein upon overexpression of Yck1 or Yck2 (compared galactose grown to glucose grown cells and wild type cells expressing Yck1 and Yck2 endogenous promoters) **Figure 5.9**. This result suggests that Yck1 and Yck2 may play roles in Inp1 phosphorylation. The information gathered from this experiment offers significant insights into the role of Yck1 and Yck2 in the regulation of peroxisome dynamics. Our findings suggest that these kinases could play a role in controlling peroxisome retention by modulating Inp1 protein levels and functionality.

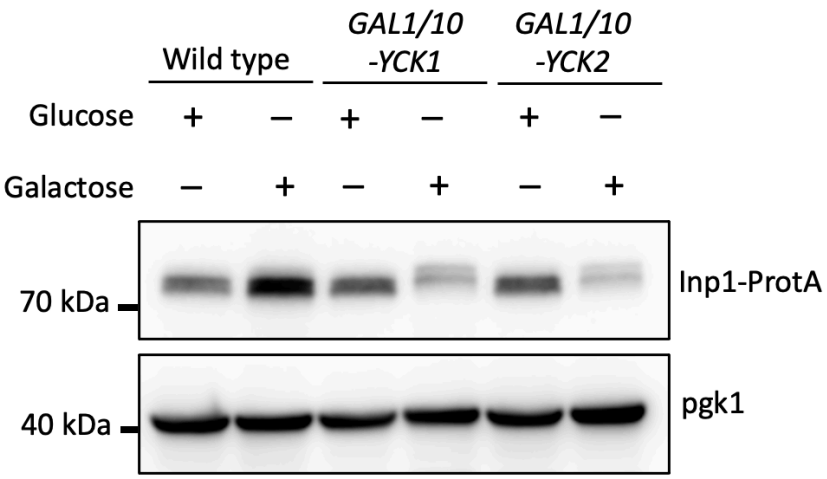

Figure 5.9 Inp1 function is affected by Yck1 and Yck2 overexpression. A western blot analysis showing the change in Inp1 pattern in galactose compared to glucose medium. Cells were transformed with a plasmid containing Inp1-Protein A expressed under its own promoter.

5.7 Discussion.

Overexpression screens provide more direct control over the levels and activity of the proteins of interest. However, there are some advantages and limitations. Overexpressing protein kinases, phosphatase or ubiquitin ligase allows for the direct manipulation of the levels and activity of the protein of interest. This can help elucidate the specific functions and signalling pathways associated with these proteins, providing more focused and targeted insights. On the other hand, overexpression of a protein can lead to non-physiological levels of the protein, disrupting normal regulatory mechanisms. This may result in aberrant signalling and cellular responses that do not accurately represent the natural function of the protein. Overexpression can lead to unintended off-target effects. Increased levels of a protein may interact with and phosphorylate non-specific substrates, leading to outcomes that do not reflect the true biological role of the protein.

In this chapter, our primary objective was to understand more about the regulation of peroxisome and vacuole inheritance and dynamics by undertaking screens to identify novel factors involved in the process. To achieve this, we used overexpression libraries comprising kinases, phosphatases, and ubiquitin ligases in *Saccharomyces cerevisiae*. Over the years, these proteins have been demonstrated to play a significant role in organelle inheritance regulation (Fisk and Yaffe, 1999; Peng and Weisman, 2008b; Bartholomew and Hardy, 2009;

Yau *et al.*, 2014; Yau, Wong and Weisman, 2017; Wong *et al.*, 2020), therefore making the screen was an effective and systematic approach to address our research question.

We firstly conducted the screen on wild-type cells, utilizing the potent *TEF2* promoter to drive high expression levels of genes instead of their native promoters. Subsequently, we performed microscopic imaging analysis using a method we developed. Pex11 and Vph1 tagging proved beneficial for enhancing the visualization of peroxisomes and vacuoles, as they are abundant proteins that effectively label organelle membrane structures. Moreover, although we mated the overexpression library with another wild-type strain for tagging purposes to visualise peroxisomes and vacuoles, the effects of gene overexpression in the library remained intact. For example, we observed that *CLA4* overexpression and its paralog *STE20* still produced strong to moderate phenotypes, similar to findings in the Cla4 study (Bartholomew and Hardy, 2009). This observation indicates that even with another wild-type copy of the gene expressed under its endogenous promoter, the overall effect of overexpression is still noticeable and not inhibited. Our analysis identified several novel genes in addition to known factors previously discovered to regulate peroxisome or vacuole inheritance. The comprehensive examination of this screen by utilizing strains overexpressing *YCK1* and *YCK2* under *GAL1/10* promoter revealed that these genes are potentially involved in organelle retention, particularly in peroxisomes. Taken together, based on the localisations of all these proteins and the importance of other proteins that share the same localisation that showed to be involved in organelle transport, it is suggested that these kinases might be interesting to be further analysed. Hence, this could be through another secondary knockout and overexpression screen in wild type background cells. Organelles such as vacuoles, peroxisomes and mitochondria can be analysed in these mutants. The steady state levels of the Myo2 adaptors Vac17, Inp2 and Mmr1 can also be checked to determine which candidates are involved in the stability or breakdown of these adaptors. This might identify novel factors involved in organelle inheritance to be used for further studies.

Chapter 6 General discussion and future research directions

6.1 Introduction.

Eukaryotic cells must maintain the proper distribution of their organelles for growth and survival under different metabolic stress conditions. In the budding yeast *Saccharomyces cerevisiae*, organelle transport to the bud requires the Class V myosins, Myo2 and Myo4. Many organelle adaptors and regulators have been identified as essential factors for organelle transport but the spatial and temporal regulations of organelle transport in yeast not fully understood. Therefore, our primary objective of this research study was to investigate the mechanisms required for vacuole and peroxisome transport, starting with investigating how Myo2 interaction sites (MIS) of Vac17 and Inp2 function in vacuole and peroxisome inheritance, respectively. The deeper analysis by (ColabFold) of the Vac17 MIS helped us to identify the potential amino acid residues that facilitate the contacts between Vac17 and the Myo2 cargo binding domain. These were then tested for their functionality by *in vivo* studies and found to indeed affect vacuole inheritance (Chapter 3). Our *in vivo* studies also validated the functionality of Inp2 MIS and found that it is required for peroxisome inheritance.

Kin4 and Frk1 were recently discovered by the Hettema lab to play a role in peroxisome and vacuole transport, but the mechanistic role of these kinases in organelle transport was not known. To study this, we utilised the MIS mutants developed in (Chapter 3) as a tool to further investigate Kin4 and Frk1 roles on Vac17 and Inp2 in the mother cell at the early stages of vacuole and peroxisome transport. Our data showed that the transport from the mother cell to the bud is coordinated spatially and temporally and concluded that the function of Kin4 antagonises the function of Cla4 in which each one of these can regulate vacuole and peroxisome transport from different spaces in the cell (Chapter 4).

Although many factors have been shown to regulate vacuole transport and Vac17, there might be other factors that are not yet revealed. Very little is known about how Inp1 and Inp2 are regulated during peroxisome inheritance. Therefore, we aimed to identify novel factors that are required for peroxisome and vacuole transport. This was done by utilising

overexpression libraries which was a useful method to approach biological questions. This approach led to the identification of the Yck1 and its paralog Yck2 as new potential factors involved in peroxisome retention and is described in (Chapter 5).

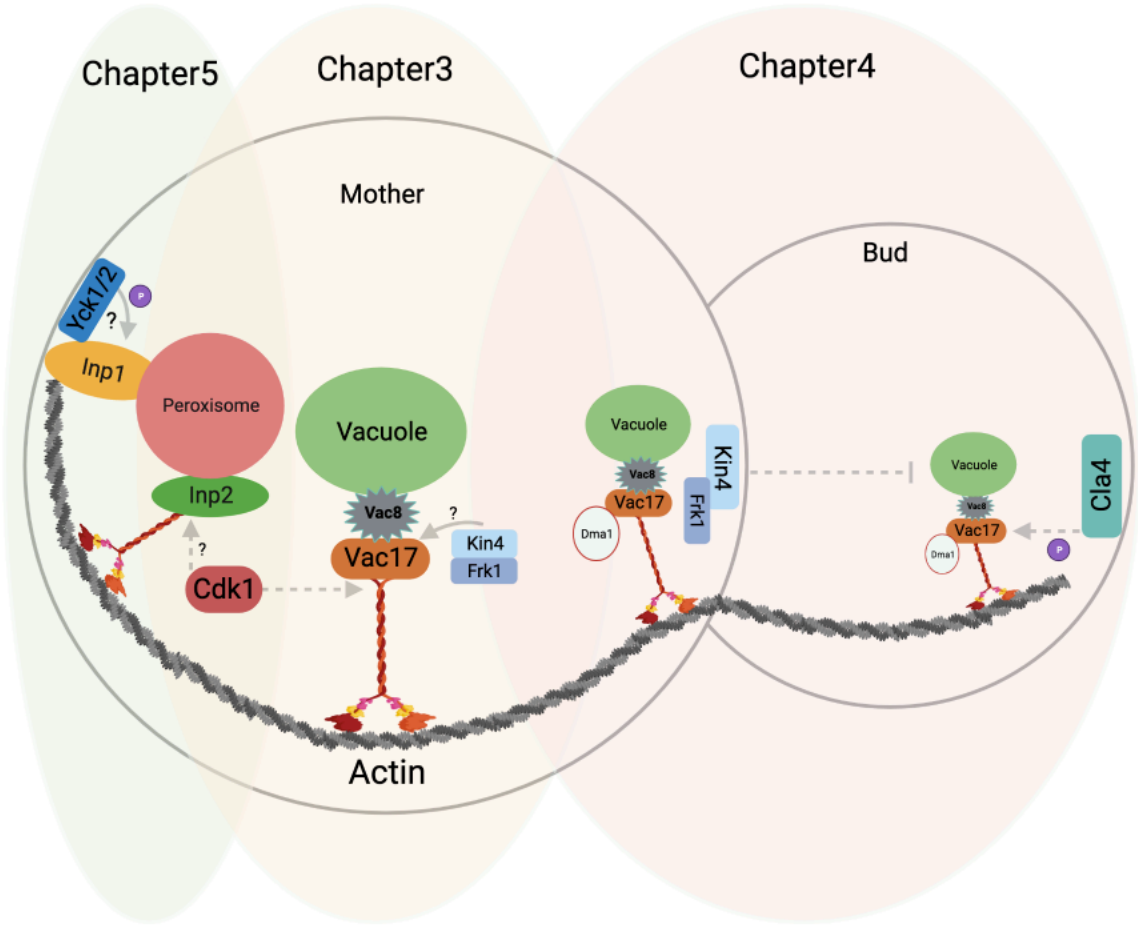

Figure 6. 1 A schematic representation showing the contribution of each chapter in this research study. Chapter 3 was focusing on determining the MIS in Vac17 and Inp2. Chapter4 was focusing on the role of Kin4 and Frk1 in protecting Vac17 and Inp2 from early degradation in the mother cell. Chapter5 was showing the novel factors that might be involved in the overall peroxisome movement and especially on retention in the mother cell.

6.2 Identification of the Myo2 interaction site (MIS) on the vacuolar and peroxisomal Myo2 receptors Vac17 and Inp2.

Initial studies have indicated the regions of Vac17 and Inp2 that bind Myo2 cargo binding domain (Ishikawa *et al.*, 2003; Fagarasanu *et al.*, 2006). In addition, recently published work was also investigating the Vac17 and Inp2 MIS's in complex with Myo2 using *in vitro* studies (Tang *et al.*, 2019; Liu *et al.*, 2022). The MIS regions that we identified through ColabFold were the same as those highlighted in these previous studies (Tang *et al.*, 2019; Liu *et al.*, 2022).

However, *in vivo* studies were lacking to investigate the functionality of these MIS residues revealed in the structural prediction.

It has been suggested that amino acid F534, L536, I538 and, L539 in Inp2 form hydrophobic interactions with Myo2-CBD (cargo binding domain)(Tang *et al.*, 2019). Our *in vivo* study on Inp2 MIS was undertaken through analysis of strains expressing a six amino acid deletion (from residue F534 to L539) of Inp2. These strains showed a defect in peroxisome inheritance, although the defect was not as strong as when the *INP2* gene is completely deleted. One possible explanation for this is that Pex19 is still present and able to contribute to the inheritance since it has shown to be a factor in peroxisome inheritance and binds both Inp2 and Myo2 (Ito *et al.*, 2001; Fagarasanu *et al.*, 2006). The other possibility is that there is another region in Inp2 that could still bind to Myo2 that has not yet been identified. A later study used *in vitro* approaches to show that reversing the charge of each as single amino acid mutation of the key interacting amino acids by using Vac17 MIS fragment (from residue 112 to 157) (R135E, K138E, R142E) perturbed the interaction with Myo2 CBD (Liu *et al.*, 2022). Our *in vivo* mutagenesis analysis conducted on the same three amino acids in Vac17 full length by making charge-reversing changes with single mutations showed an effect in vacuole inheritance only with Vac17 K138D and R142E. The Vac17 R135E mutation did not show any defect in vacuole inheritance and Vac17 could still bind to Myo2 in our yeast two hybrid analysis. This could be because the Vac17 R135 is contributing less to the Interaction compared to K138 and R142 residues. However, we found that mutating any two amino acids out of three exacerbated the defect in vacuole inheritance compared to the single mutants. We also found strong genetic evidence that when we reversed the charge in Vac17 R142 to glutamic acid (E) we were able to observe a strong rescue in the interaction with the Myo2-E1293K mutant. This finding implies that the interaction between Vac17 R142 and Myo2-E1293K is dependent on the electrostatic interactions between positively and negatively charged amino acids. The restoration of the interaction indicates that the original positive-negative interaction between these residues is critical for their binding.

6.3 Kin4 and Frk1 function in peroxisome and vacuole inheritance

This study has demonstrated that both Kin4 and Frk1 contribute to peroxisome and vacuole inheritance by maintaining Inp2 and Vac17 protein levels in the mother cell when the transport of peroxisome and vacuole is impaired in the Inp2 and Vac17 MIS mutants. In *kin4Δ/frk1Δ* cells protein levels of Inp2 and Vac17 MIS are reduced **Figure 4.7**. We found that the rescue in Vac17 and Inp2 MIS mutants breakdown in *kin4Δ/frk1Δ* can be through deleting *DMA1* gene. Expressing the *vac17-mis* (S222A and T240A) in *kin4Δ/frk1Δ* also resembled the same rescue as when *DMA1* gene is deleted in *kin4Δ/frk1Δ* cells. Analysing peroxisomes inheritance in *CLA4* overexpression cells showed defects in peroxisome inheritance as well as reduction in Inp2 protein levels **Figure5.2.** This suggests that Vac17 and Inp2 are regulated in the same manner. In this study, our mutational analysis on Inp2 provided in (**Chapter 4 Section 4.8**) suggests that Inp2 is targeted by Cla4 and Dma1. However, this would be strengthened by further studies including i) determining whether Inp2 ubiquitination is affected in S283A/S544A mutants because Vac17 S222A mutation has been shown to block Vac17 ubiquitination (Yau *et al.*, 2014). ii) Checking peroxisome localisation during inheritance in cells expressing Inp2 (S283A/S544A) and (T511A/T527A) mutants and determining whether there is peroxisome mis-positioning to bud tip and mother-bud neck. This might resemble the same effect seen on vacuole mis-positioning with *vac17-S222A* or *vac17-T240A* mutations (Yau *et al.*, 2014; Yau, Wong and Weisman, 2017). Another analysis would be to overexpress *CLA4* in cells expressing Inp2 with the (S283A/S544A) or (T511A/T527A) mutations and measure Inp2 levels. This would determine whether Inp2 mutants would rescue the degradation seen in *CLA4* overexposing cells with wild type Inp2. According to SGD Inp2 S544 residue has shown to be phosphorylated in phosphoproteome study (Lanz *et al.*, 2021). This might support our hypothesis that S544 is required for Cla4 phosphorylation. An alternative experiment to validate more about the effect shown on Inp2-MIS in *kin4Δ/frk1Δ* **Figure 4.7**, in showing the double bands would be through western blot experiment using cell lysate treated with phosphatase. This would allow for equal migration of the MIS mutant in both *inp2Δ* and *kin4Δ/frk1Δ* cells and would suggest that Inp2 is phosphorylated in the *kin4Δ/frk1Δ* cells.

It was shown by the Hettema lab and in this study that the Kin4 and Frk1 kinase activity is required for vacuole and peroxisome inheritance and for maintaining Vac17 and Inp2 protein

levels. This suggests that Kin4 and Frk1 might phosphorylate Vac17 and Inp2 *in vivo.* Therefore, would be important to identify the phosphosites in Vac17 and Inp2. An initial step would be to consider phosphosites in Vac17 and Inp2 that are shown to be phosphorylated according to previous studies and as listed in SGD (Swaney *et al.*, 2013; Lanz *et al.*, 2021; Zhou *et al.*, 2021). Strong consensus sites that Kin4 and Frk1 recognise and phosphorylate have not been reported however, there is some suggestion from a study of kinase site in *S. cerevisiae* that Kin4 shows a preference of serine with upstream basic residues (Mok *et al.*, 2010). According to other literature, Kin4 phosphorylates Bfa1 at specific serine residues (Maekawa *et al.*, 2007).There are 7 phosphorylated serine residues on Vac17 that have not been shown to be linked to any studies on Vac17 so far. There are also 12 serine residues on Inp2 after excluding the serine residues we utilised in this study and other studies (Swaney *et al.*, 2013; Lanz *et al.*, 2021; Zhou *et al.*, 2021). Mutagenesis analysis on these potential residues might identify the serine or threonine residues required for Kin4 and Frk1 phosphorylation. However, there might be other phosphosites that have not been identified yet. In this case it could be that more analysis is required. For example, mass spectrometry analysis on immunoprecipitated Vac17 and Inp2 from *kin4Δ/frk1Δ* cell might identify the potential phosphosites with a decreased phosphorylation. Currently, we lean towards the hypothesis that Kin4 antagonises Cla4 by preventing the early Cla4 phosphorylation of the adaptors which leads to the Dma1 activation in targeting the adaptors for early breakdown; however, since initial attempts by the Hettema lab, have so far been unsuccessful in identifying Kin4 specific phosphosites on Vac17 and Inp2, alternative explanations cannot be dismissed at this time. For example, kin4 might phosphorylate Cla4 if it enters the mother cell and that switches off its activity in the mother cell region.

6.4 Kin4 and Cla4 antagonistic functions as a general mechanism regulating organelle inheritance.

The idea that Kin4 and Cla4 act in antagonistic ways has been well developed in studies of the completion of nuclear inheritance. This process requires activation of the mitotic exit network (MEN) during late anaphase. After the spindle pole body (SPB) is segregated into the bud, the MEN is activated through Tem1-GTPase. Bfa1, the GTPase-activating protein (GAP) for Tem1, negatively regulates MEN activation. Kin4 phosphorylates Bfa1, which is necessary for its GAP activity, leading to downregulation of MEN activation (**Figure 1.10**). In wild type cells, Kin4 is

not active in the bud due to the role of its negative regulator Lte1, which is recruited to the bud cortex and requires Cla4 for its activity (Falk et al., 2011; Jensen et al., 2002; Höfken and Schiebel, 2002; Bertazzi et al., 2011).

In this study, we demonstrated that Kin4 and Cla4 also act in opposition in vacuole and peroxisome transport. This was due to the opposite effect seen when *KIN4* or *CLA4* is either overexpressed or deleted. For instance, in *kin4Δ/frk1Δ* cells Vac17 and Inp2 protein levels are reduced, and vacuole and peroxisome transport affected. This resembles the effect when Cla4 is overexpressed. On the other hand, when Kin4 is overexpressed Vac17 and Inp2 proteins levels are upregulated, and vacuole and peroxisome are mis-positioned in the bud (data generated by Hettema lab) also shown in **Figure 5.2**. This also resembles the effect when Cla4 and Ste20 are not functional (Yau et al., 2017). This raises the question of whether this antagonistic relationship is a general mechanism for spatially regulating transport processes. It could be proposed that Kin4 and Cla4 contribute to organelle inheritance by creating distinct regulatory environments within the cell, with Kin4 primarily localised in the mother cell and Cla4 in the bud, analogous to the model proposed for the regulation of mitotic exit (Falk et al., 2011; Jensen et al., 2002; Höfken and Schiebel, 2002; Bertazzi et al., 2011). As a result, they might regulate multiple processes spatially and temporally. If this intracellular localisation is disrupted due to gene overexpression or deletion of *KIN4* or *CLA4*, the precise regulation of organelle maintenance or inheritance would be directly affected **Figure 6.2** . Consequently, understanding how Kin4 and Cla4 intracellular localisations are established and maintained during the early stages of the cell cycle would be an interesting question to investigate in the future.

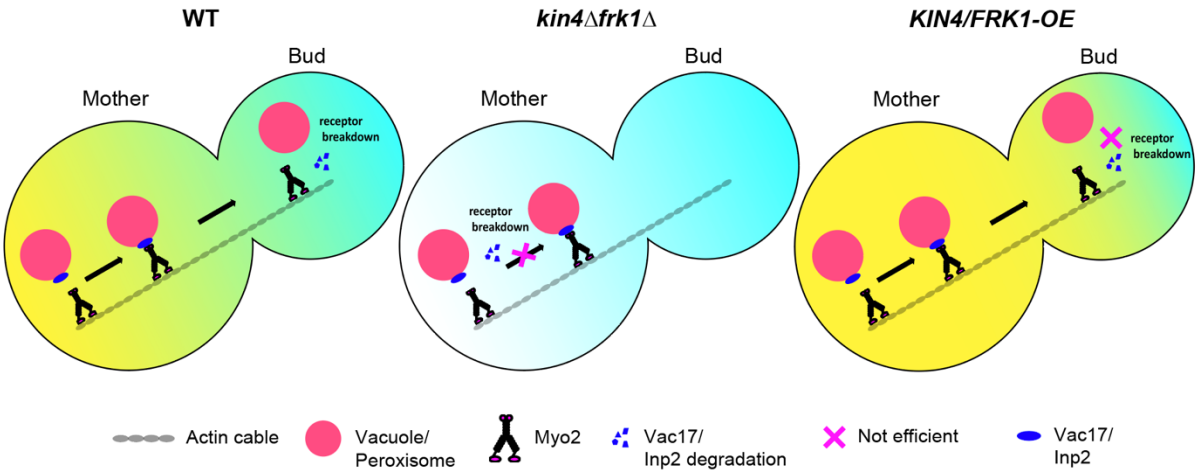

Figure 6. 2 A schematic model depicting the opposing functions of Kin4 and Cal4 in the spatial and temporal control of organelle transport. Kin4 and Frk1 are crucial for organelle transport, preserving Myo2 receptor levels like Vac17 and Inp2. Kin4 prevents premature receptor degradation in the mother cell, facilitating stable complex formation. Cla4 later triggers degradation in the bud, ensuring proper positioning; disruptions in Kin4 and Cla4 gradients result in organelle inheritance defects.

6.5 Yck1 and Yck2 are novel factors regulate peroxisome retention.

Yck1 and Yck2 are plasma membrane-bound casein kinases that share some functional redundancy in morphogenesis, septin assembly, and endocytic trafficking (Robinson *et al.*, 1993; Feng and Davis, 2000; Marchal, Haguenauer-Tsapis and Urban-Grimal, 2000; Babu *et al.*, 2002). They have been shown to be essential for protein phosphorylation and regulation and to modulate PEST motif phosphorylation of certain proteins (Marchal, Haguenauer-Tsapis and Urban-Grimal, 2000). The data shown in **Chapter 5** suggest that Yck1 and Yck2 are involved in peroxisome retention, a process thus far only known to involve the peroxisomal membrane protein Inp1 in *S. cerevisiae*. The N-terminal region ofInp1 has been shown to contribute to peroxisome retention through a direct interaction with lipids in the plasma membrane (Hulmes *et al.*, 2020). In the yeast *Hansenula polymorpha* Inp1 was also shown to bind the plasma membrane to facilitate peroxisome retention in the mother cell (Krikken *et al.*, 2020). In addition, it was shown that disruption of actin in this yeast by using Latrunculin A, caused Inp1 to become cytosolic suggesting that the localisation of Inp1 is dependent on the existence of an intact actin cytoskeleton. The Hettema lab has generated preliminary data indicating that Inp1 in *S. cerevisiae* also binds directly to actin, suggesting that this interaction may be necessary for peroxisome retention (data not published). Intriguingly, a previous

study (Robinson *et al.*, 1999) proposed that Yck activity might be required for regulating the association of proteins at the plasma membrane with the actin cytoskeleton, either directly or indirectly. Based on the results presented in **Chapter 5**, we hypothesised that Yck1 and/or Yck2 could be involved in peroxisome retention by regulating Inp1 function. Inp1 is a phosphoprotein with levels that fluctuate throughout the cell cycle (Fagarasanu et al., 2005 and SGD). Inp1 protein contains a strong PEST motif located from amino acid 280 to 361. Inp1 also contains five potential casein kinase recognition sites SxxS and one of them has shown to be phosphorylated in a phosphoproteome study (Lanz *et al.*, 2021) (shown in SGD). These could be the sites that are targeted by these two kinases to regulate Inp1 and its function. This could be investigated through a mutagenesis analysis of the residues that have been shown to be phosphorylated in Inp1 and analyse peroxisome retention in cells containing these Inp1 mutants. Another analysis would be to overexpress Yck1 and Yck2 in cells expressing Inp1 mutants and analyse Inp1 levels by western blot. This would determine if the change we noticed in Inp1 shown in **Figure 5.9** would likely be similar or behave differently. Additionally, it is also interesting to look at Inp1 association with actin under Yck1 and Yck2 overexpression conditions. Beside the hypothesis that Yck1 and Yck2 regulate Inp1, and Inp1 association with actin, it could also be that the actin cables are affected during the overexpression of Yck1 or Yck2 resulting in peroxisome to move toward the bud. Thus, more experiments and analysis are required.

6.6 Conclusion

It is important to understand the mechanism by which organelle receptors interact with myosin and move organelles. Discovering the adaptor structures is essential in developing an organelle specific MIS mutant model that does not affect the transport of other organelles but a single specific organelle. Our *in vivo* study of the MIS in Vac17 and Inp2 has led to the generation of cells in which specific organelle movement is inhibited and this has then been used to investigate the roles of Kin4 and Frk1 in the mother cell discussed in (Chapter 4). These MIS mutants might also contribute to enhancing understanding about the regulation in the mother cell from early stages. Cdk1 is one of the kinases involved in initiating the binding between Vac17 and Myo2 by phosphorylating in the mother cell at specific Cdk1 consensus sites (Peng and Weisman, 2008a) **Figure 6.1**. It has been also hypothesised that it might also regulate Inp2 since it contains Cdk1 consensus sites (Peng and Weisman, 2008a).

In addition, Kin4, Frk1, Cla4 and Ste20 contain Cdk1 sites that have been shown to be important for Cdk1 phosphorylation (Holt *et al.*, 2009). Therefore, many questions remain as to how the initiation of the transport complex is regulated and maintained until reaching the bud. For example, does the phosphorylation of Cdk1 affect the conformation of the adaptor protein in order to allow the MIS to bind Myo2? since some of these Cdk1 recognition sites are flanking the MIS regions in Vac17 and Inp2 **Figure 6.3**. Does Kin4 or Frk1 bind and phosphorylate Vac17 and Inp2 directly **Figure 6.1?** Does Kin4 or Frk1 require Cdk1 phosphorylation of the adaptors in order to be recruited to the transport complex and protect the adaptors? Is Kin4, Frk1, Cla4 and Ste20 phosphorylation by Cdk1 required for vacuole and peroxisome transport? Does Kin4 and Frk1 protect the adaptors by interacting with the breakdown machinery factors (Dma1 / Cla4) and prevent them from accessing the adaptors? Alternatively, do they protect the PEST sequence of the adaptors via binding the adaptors and phosphorylating them?

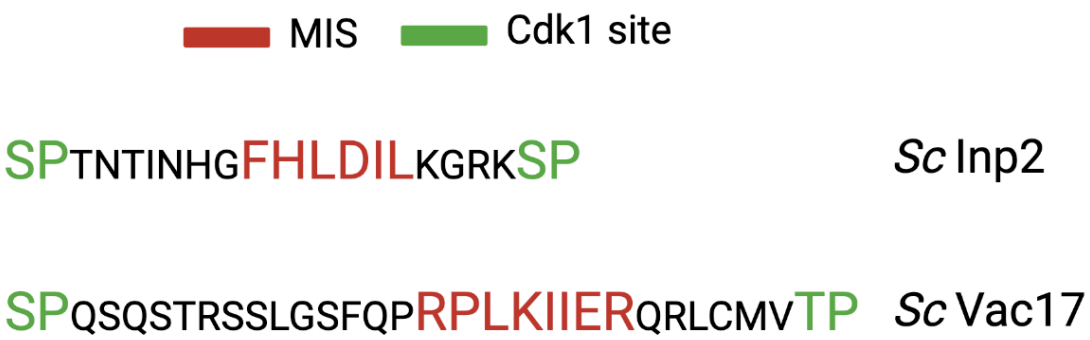

Figure 6. 3 Vac17 and Inp2 have Cdk1 recognition sites flanking their MIS regions. The residues marked in red colour correspond to the MIS region, while the residues marked in green colour correspond the Cdk1 sites in both Inp2 and Vac17 in *S. cerevisiae.*

Studying organelle inheritance mechanism in yeast might be extended to a broader relevance. In humans, melanosomes are essential in synthesizing and storing the melanin pigment which is important for skin and hair colour. Melanophilin is an essential protein for melanosome transport though binding to the myosin motor MyoVa (Marks and Seabra, 2001). Melanophilin has a PEST motif required for its rapid degradation. A Melanophilin PESTΔ mutant has shown a defect in its degradation resulting in perinuclear melanosome aggregation (Fukuda and Itoh, 2004). The similarities between lysosome and melanosome biogenesis and the functional similarities between yeast vacuoles and mammalian lysosomes

reveals that at least some of the regulatory mechanisms of organelle dynamics appear to be conserved across different organisms, from yeast to higher eukaryotes (Marks and Seabra, 2001).

The identification of potential target proteins and pathways paves the way for future studies aimed at understanding the precise molecular mechanisms by which Yck1 and Yck2 modulate peroxisome dynamics (Chapter5) **Figure 6.1**. This study not only enhances our understanding of the complex interplay between cellular components and organelle transport but also highlights the importance of targeted screening approaches for uncovering new molecular players in essential biological processes. Future studies building on these findings will undoubtedly provide a more comprehensive understanding of the molecular mechanisms governing organelle inheritance and their implications in health and disease. Understanding the role of these mechanisms in peroxisome and vacuole inheritance in *S. cerevisiae* will motivate research on mammalian cells and contribute to the identification of genetic deficiencies that cause either peroxisomal- or lysosomes-related diseases.

References

Adams, I. R. and Kilmartin, J. V. (2000) 'Spindle pole body duplication: A model for centrosome duplication?', *Trends in Cell Biology*, pp. 329–335. doi: 10.1016/S0962-8924(00)01798-0.

Al-Saryi, N. A. *et al.* (2017) 'Two NAD-linked redox shuttles maintain the peroxisomal redox balance in Saccharomyces cerevisiae', *Scientific Reports*, 7(1), p. 11868. doi: 10.1038/s41598-017-11942-2.

Arai, S. *et al.* (2008) 'Ypt11 Functions in Bud-Directed Transport of the Golgi by Linking Myo2 to the Coatomer Subunit Ret2', *Current Biology*, 18(13), pp. 987–991. doi: 10.1016/j.cub.2008.06.028.

Babour, A. *et al.* (2010) 'A Surveillance Pathway Monitors the Fitness of the Endoplasmic Reticulum to Control Its Inheritance', *Cell*, 142(2), pp. 256–269. doi: 10.1016/j.cell.2010.06.006.

Babst, M. *et al.* (2002) 'ESCRT-III: An endosome-associated heterooligomeric protein complex required for MVB sorting', *Developmental Cell*, 3(2), pp. 271–282. doi: 10.1016/S1534-5807(02)00220-4.

Babu, P. *et al.* (2002) 'Plasma membrane localization of the Yck2p yeast casein kinase 1 isoform requires the C-terminal extension and secretory pathway function', *Journal of Cell Science*, 115(24), pp. 4957–4968. doi: 10.1242/jcs.00203.

Baek, M. *et al.* (2021) 'Accurate prediction of protein structures and interactions using a three-track neural network', *Science*, 373(6557), pp. 871–876. doi: 10.1126/science.abj8754.

Balderhaar, H. J. klein. and Ungermann, C. (2013) 'CORVET and HOPS tethering complexes - coordinators of endosome and lysosome fusion', *Journal of Cell Science*, pp. 1307–1316. doi: 10.1242/jcs.107805.

Banta, L. M. *et al.* (1988) 'Organelle assembly in yeast: characterization of yeast mutants defective in vacuolar biogenesis and protein sorting.', *The Journal of cell biology*, 107(4), pp. 1369–1383. doi: 10.1083/jcb.107.4.1369.

Bardin, A. J., Visintin, R. and Amon, A. (2000) 'A mechanism for coupling exit from mitosis to partitioning of the nucleus', *Cell*, 102(1), pp. 21–31. doi: 10.1016/S0092-8674(00)00007-6.

Barral, D. C. and Seabra, M. C. (2004) 'The Melanosome as a Model to Study Organelle Motility in Mammals', *Pigment Cell Research*, pp. 111–118. doi: 10.1111/j.1600-0749.2004.00138.x.

Bartholomew, C. R. and Hardy, C. F. J. (2009) 'p21-activated kinases Cla4 and Ste20 regulate vacuole inheritance in Saccharomyces cerevisiae', *Eukaryotic Cell*, 8(4), pp. 560–572. doi: 10.1128/EC.00111-08.

Beach, D. L. *et al.* (2000) 'The role of the proteins Kar9 and Myo2 in orienting the mitotic spindle of budding yeast', *Current Biology*, 10(23), pp. 1497–1506. doi: 10.1016/S0960-9822(00)00837-X.

Bertazzi, D. T., Kurtulmus, B. and Pereira, G. (2011) 'The cortical protein Lte1 promotes mitotic exit by inhibiting the spindle position checkpoint kinase Kin4', *Journal of Cell Biology*, 193(6), pp. 1033–1048. doi: 10.1083/jcb.201101056.

Bi, E. and Park, H. O. (2012) 'Cell polarization and cytokinesis in budding yeast', *Genetics*, 191(2), pp. 347–387. doi: 10.1534/genetics.111.132886.

Böckler, S. *et al.* (2017) 'Fusion, fission, and transport control asymmetric inheritance of mitochondria and protein aggregates', *Journal of Cell Biology*, 216(8), pp. 2481–2498. doi: 10.1083/jcb.201611197.

Boldogh, I. *et al.* (1998) 'Interaction between mitochondria and the actin cytoskeleton in budding yeast requires two integral mitochondrial outer membrane proteins, Mmm1p and Mdm10p', *Journal of Cell Biology*, 141(6), pp. 1371–1381. doi: 10.1083/jcb.141.6.1371.

Boldogh, I. R. *et al.* (2001) 'Arp2/3 complex and actin dynamics are required for actin-based mitochondrial motility in yeast', *Proceedings of the National Academy of Sciences of the United States of America*, 98(6), pp. 3162–3167. doi: 10.1073/pnas.051494698.

Boldogh, I. R. *et al.* (2003) 'A Protein Complex Containing Mdm10p, Mdm12p, and Mmm1p Links Mitochondrial Membranes and DNA to the Cytoskeleton-based Segregation Machinery', *Molecular Biology of the Cell*, 14(11), pp. 4618–4627. doi: 10.1091/mbc.E03-04-0225.

Bonangelino, C. J., Catlett, N. L. and Weisman, L. S. (1997) 'Vac7p, a Novel Vacuolar Protein, Is Required for Normal Vacuole Inheritance and Morphology', *Molecular and Cellular Biology*, 17(12), pp. 6847–6858. doi: 10.1128/mcb.17.12.6847.

Bonangelino, C. J., Chavez, E. M. and Bonifacino, J. S. (2002) 'Genomic screen for vacuolar protein sorting genes in Saccharomyces cerevisiae', *Molecular Biology of the Cell*, 13(7), pp. 2486–2501. doi: 10.1091/mbc.02-01-0005.

Botstein, D. and Fink, G. R. (2011) 'Yeast: An experimental organism for 21st century biology', *Genetics*, 189(3), pp. 695–704. doi: 10.1534/genetics.111.130765.

Boyce, K. J. and Andrianopoulos, A. (2011) 'Ste20-related kinases: Effectors of signaling and morphogenesis in fungi', *Trends in Microbiology*, pp. 400–410. doi: 10.1016/j.tim.2011.04.006.

Bretscher, A. (2003) 'Polarized growth and organelle segregation in yeast: The tracks, motors, and receptors', *Journal of Cell Biology*, pp. 811–816. doi: 10.1083/jcb.200301035.

Brockerhoff, S. E., Stevens, R. C. and Davis, T. N. (1994) 'The unconventional myosin, Myo2p, is a calmodulin target at sites of cell growth in Saccharomyces cerevisiae', *Journal of Cell Biology*, 124(3), pp. 315–323. doi: 10.1083/jcb.124.3.315.

Brown, L. A. and Baker, A. (2003) 'Peroxisome biogenesis and the role of protein import', *Journal of Cellular and Molecular Medicine*, 7(4), pp. 388–400. doi: 10.1111/j.1582-4934.2003.tb00241.x.

Brozzi, F. *et al.* (2012) 'Molecular mechanism of Myosin Va recruitment to dense core secretory granules', *Traffic*, 13(1), pp. 54–69. doi: 10.1111/j.1600-0854.2011.01301.x.

Butland, G. *et al.* (2008) 'eSGA: E. coli synthetic genetic array analysis', *Nature Methods*, 5(9), pp. 789–795. doi: 10.1038/nmeth.1239.

Buvelot Frei, S. *et al.* (2006) 'Bioinformatic and Comparative Localization of Rab Proteins Reveals Functional Insights into the Uncharacterized GTPases Ypt10p and Ypt11p', *Molecular and Cellular Biology*, 26(19), pp. 7299–7317. doi: 10.1128/mcb.02405-05.

Çağdaş, D. *et al.* (2012) 'Griscelli syndrome types 1 and 3: Analysis of four new cases and long-term evaluation of previously diagnosed patients', *European Journal of Pediatrics*, 171(10), pp. 1527–1531. doi: 10.1007/s00431-012-1765-x.

Cantalupo, G. *et al.* (2001) 'Rab-interacting lysosomal protein (RILP): The Rab7 effector required for transport to lysosomes', *EMBO Journal*, 20(4), pp. 683–693. doi: 10.1093/emboj/20.4.683.

Cao, Q. J. *et al.* (2019) 'The cargo adaptor proteins RILPL2 and melanophilin co-regulate myosin-5a motor activity', *Journal of Biological Chemistry*, 294(29), pp. 11333–11341. doi: 10.1074/jbc.RA119.007384.

Carton-Garcia, F. *et al.* (2015) 'Myo5b knockout mice as a model of microvillus inclusion disease', *Scientific Reports*. England, 5, p. 12312. doi: 10.1038/srep12312.

Castro, I. G. *et al.* (2018) 'A role for Mitochondrial Rho GTPase 1 (MIRO1) in motility and membrane dynamics of peroxisomes', *Traffic*, 19(3), pp. 229–242. doi: 10.1111/tra.12549.

Catlett, N. L. and Weisman, L. S. (1998) 'The terminal tail region of a yeast myosin-V mediates its attachment to vacuole membranes and sites of polarized growth', *Proceedings of the National Academy of Sciences of the United States of America*, 95(25), pp. 14799–14804. doi: 10.1073/pnas.95.25.14799.

Caydasi, A. K. *et al.* (2010) 'Elm1 kinase activates the spindle position checkpoint kinase Kin4', *Journal of Cell Biology*. United States, 190(6), pp. 975–989. doi: 10.1083/jcb.201006151.

Caydasi, A. K., Ibrahim, B. and Pereira, G. (2010) 'Monitoring spindle orientation: Spindle position checkpoint in charge', *Cell Division*. doi: 10.1186/1747-1028-5-28.

Caydasi, A. K. and Pereira, G. (2012) 'SPOC alert-When chromosomes get the wrong direction', *Experimental Cell Research*, pp. 1421–1427. doi: 10.1016/j.yexcr.2012.03.031.

Chan, L. Y. and Amon, A. (2009) 'The protein phosphatase 2A functions in the spindle position checkpoint by regulating the checkpoint kinase Kin4', *Genes and Development*,

23(14), pp. 1639–1649. doi: 10.1101/gad.1804609.

Chernyakov, I., Santiago-Tirado, F. and Bretscher, A. (2013) 'Active segregation of yeast mitochondria by Myo2 is essential and mediated by Mmr1 and Ypt11', *Current Biology*, 23(18), pp. 1818–1824. doi: 10.1016/j.cub.2013.07.053.

Cohen, Y. and Schuldiner, M. (2011) 'Advanced Methods for High-Throughput Microscopy Screening of Genetically Modified Yeast Libraries', in *Methods in Molecular Biology*, pp. 127–159. doi: 10.1007/978-1-61779-276-2_8.

Cowles, C. R. *et al.* (1997) 'Novel Golgi to vacuole delivery pathway in yeast: Identification of a sorting determinant and required transport component', *EMBO Journal*, 16(10), pp. 2769–2782. doi: 10.1093/emboj/16.10.2769.

Cox, T. (2010) 'Gaucher disease: clinical profile and therapeutic developments', *Biologics: Targets & Therapy*, p. 299. doi: 10.2147/btt.s7582.

Cross, J. A. and Dodding, M. P. (2019) 'Motor–cargo adaptors at the organelle–cytoskeleton interface', *Current Opinion in Cell Biology*, pp. 16–23. doi: 10.1016/j.ceb.2019.02.010.

Cvrčková, F. *et al.* (1995) 'Ste20-like protein kinases are required for normal localization of cell growth and for cytokinesis in budding yeast', *Genes and Development*, 9(15), pp. 1817–1830. doi: 10.1101/gad.9.15.1817.

D'Aquino, K. E. *et al.* (2005) 'The protein kinase Kin4 inhibits exit from mitosis in response to spindle position defects', *Molecular Cell*, 19(2), pp. 223–234. doi: 10.1016/j.molcel.2005.06.005.

Delorme-Axford, E. *et al.* (2015) 'The yeast Saccharomyces cerevisiae: An overview of methods to study autophagy progression', *Methods*, 75, pp. 3–12. doi: 10.1016/j.ymeth.2014.12.008.

Dong, W. *et al.* (2012) 'Inactivation of MYO5B promotes invasion and motility in gastric cancer cells', *Digestive Diseases and Sciences*, 57(5), pp. 1247–1252. doi: 10.1007/s10620-011-1989-z.

Donovan, K. W. and Bretscher, A. (2012) 'Myosin-V Is Activated by Binding Secretory Cargo and Released in Coordination with Rab/Exocyst Function', *Developmental Cell*, 23(4), pp. 769–781. doi: 10.1016/j.devcel.2012.09.001.

Donovan, K. W. and Bretscher, A. (2015) 'Head-to-tail regulation is critical for the in vivo function of myosin V', *Journal of Cell Biology*, 209(3), pp. 359–365. doi: 10.1083/jcb.201411010.

Dunn, B. D. *et al.* (2007) 'Myo4p is a monomeric myosin with motility uniquely adapted to transport mRNA', *Journal of Cell Biology*, 178(7), pp. 1193–1206. doi: 10.1083/jcb.200707080.

Ebberink, M. S. *et al.* (2012) 'A novel defect of peroxisome division due to a homozygous

non-sense mutation in the PEX11β gene', *Journal of Medical Genetics*, 49(5), pp. 307–313. doi: 10.1136/jmedgenet-2012-100778.

Ekal, L., Alqahtani, A. M. S. and Hettema, E. H. (2023) 'The dynamin-related protein Vps1 and the peroxisomal membrane protein Pex27 function together during peroxisome fission', *Journal of Cell Science*, 136(6). doi: 10.1242/JCS.246348.

Eshel, D. *et al.* (1993) 'Cytoplasmic dynein is required for normal nuclear segregation in yeast', *Proceedings of the National Academy of Sciences of the United States of America*, 90(23), pp. 11172–11176. doi: 10.1073/pnas.90.23.11172.

Estrada, P. *et al.* (2003) 'Myo4p and She3p are required for cortical ER inheritance in Saccharomyces cerevisiae', *Journal of Cell Biology*, 163(6), pp. 1255–1266. doi: 10.1083/jcb.200304030.

Fagarasanu, A. *et al.* (2006) 'The Peroxisomal Membrane Protein Inp2p Is the Peroxisome-Specific Receptor for the Myosin V Motor Myo2p of Saccharomyces cerevisiae', *Developmental Cell*, 10(5), pp. 587–600. doi: 10.1016/j.devcel.2006.04.012.

Fagarasanu, A. *et al.* (2009) 'Myosin-driven peroxisome partitioning in S. cerevisiae', *Journal of Cell Biology*, 186(4), pp. 541–554. doi: 10.1083/jcb.200904050.

Fagarasanu, M. *et al.* (2005) 'Inp1p is a peroxisomal membrane protein required for peroxisome inheritance in Saccharomyces cerevisiae', *Journal of Cell Biology*, 169(5), pp. 765–775. doi: 10.1083/jcb.200503083.

Fagarasanu, M., Fagarasanu, A. and Rachubinski, R. A. (2006) 'Sharing the wealth: Peroxisome inheritance in budding yeast', *Biochimica et Biophysica Acta - Molecular Cell Research*, 1763(12), pp. 1669–1677. doi: 10.1016/j.bbamcr.2006.08.015.

Falk, J. E., Chan, L. Y. and Amon, A. (2011) 'Lte1 promotes mitotic exit by controlling the localization of the spindle position checkpoint kinase Kin4', *Proceedings of the National Academy of Sciences of the United States of America*, 108(31), pp. 12584–12590. doi: 10.1073/pnas.1107784108.

Feng, Y. and Davis, N. G. (2000) 'Akr1p and the Type I Casein Kinases Act prior to the Ubiquitination Step of Yeast Endocytosis: Akr1p Is Required for Kinase Localization to the Plasma Membrane', *Molecular and Cellular Biology*, 20(14), pp. 5350–5359. doi: 10.1128/mcb.20.14.5350-5359.2000.

Fidaleo, M. (2010) 'Peroxisomes and peroxisomal disorders: The main facts', *Experimental and Toxicologic Pathology*. Elsevier, 62(6), pp. 615–625. doi: 10.1016/j.etp.2009.08.008.

Fisk, H. A. and Yaffe, M. P. (1999) 'A role for ubiquitination in mitochondrial inheritance in Saccharomyces cerevisiae', *Journal of Cell Biology*, 145(6), pp. 1199–1208. doi: 10.1083/jcb.145.6.1199.

Fransson, Å., Ruusala, A. and Aspenström, P. (2003) 'Atypical Rho GTPases have roles in mitochondrial homeostasis and apoptosis', *Journal of Biological Chemistry*. United States,

278(8), pp. 6495–6502. doi: 10.1074/jbc.M208609200.

Fransson, Å., Ruusala, A. and Aspenström, P. (2006) 'The atypical Rho GTPases Miro-1 and Miro-2 have essential roles in mitochondrial trafficking', *Biochemical and Biophysical Research Communications*, 344(2), pp. 500–510. doi: 10.1016/j.bbrc.2006.03.163.

Frederick, R. L., Okamoto, K. and Shaw, J. M. (2008) 'Multiple pathways influence mitochondrial inheritance in budding yeast', *Genetics*, 178(2), pp. 825–837. doi: 10.1534/genetics.107.083055.

Fukuda, M. and Itoh, T. (2004) 'Slac2-a/Melanophilin Contains Multiple PEST-like Sequences That Are Highly Sensitive to Proteolysis', *Journal of Biological Chemistry*, 279(21), pp. 22314–22321. doi: 10.1074/jbc.401791200.

Fukuda, M., Kuroda, T. S. and Mikoshiba, K. (2002) 'Slac2-a/melanophilin, the missing link between Rab27 and myosin Va: Implications of a tripartite protein complex for melanosome transport', *Journal of Biological Chemistry*, 277(14), pp. 12432–12436. doi: 10.1074/jbc.C200005200.

Gandre-Babbe, S. and Van Der Bliek, A. M. (2008) 'The novel tail-anchored membrane protein Mff controls mitochondrial and peroxisomal fission in mammalian cells', *Molecular Biology of the Cell*, 19(6), pp. 2402–2412. doi: 10.1091/mbc.E07-12-1287.

García-Rodríguez, L. J., Gay, A. C. and Pon, L. A. (2007) 'Puf3p, a Pumilio family RNA binding protein, localizes to mitochondria and regulates mitochondrial biogenesis and motility in budding yeast', *Journal of Cell Biology*, 176(2), pp. 197–207. doi: 10.1083/jcb.200606054.

Van Gele, M., Dynoodt, P. and Lambert, J. (2009) 'Griscelli syndrome: A model system to study vesicular trafficking', *Pigment Cell and Melanoma Research*, pp. 268–282. doi: 10.1111/j.1755-148X.2009.00558.x.

Gerber, S. *et al.* (2017) 'Mutations in DNM1L, as in OPA1, result indominant optic atrophy despite opposite effectson mitochondrial fusion and fission', *Brain*, 140(10), pp. 2586–2596. doi: 10.1093/brain/awx219.

Gomes De Mesquita, D. S., Ten Hoopen, R. and Woldringh, C. L. (1991) 'Vacuolar segregation to the bud of Saccharomyces cerevisiae: An analysis of morphology and timing in the cell cycle', *Journal of General Microbiology*. England, 137(10), pp. 2447–2454. doi: 10.1099/00221287-137-10-2447.

Govindan, B., Bowser, R. and Novick, P. (1995) 'The role of Myo2, a yeast class V myosin, in vesicular transport', *Journal of Cell Biology*, 128(6), pp. 1055–1068. doi: 10.1083/jcb.128.6.1055.

Grabowski, G. A. (2008) 'Phenotype, diagnosis, and treatment of Gaucher's disease', *The Lancet*, pp. 1263–1271. doi: 10.1016/S0140-6736(08)61522-6.

Hammer, J. A. and Wagner, W. (2013) 'Functions of class v myosins in neurons', *Journal of Biological Chemistry*, pp. 28428–28434. doi: 10.1074/jbc.R113.514497.

Hammond, J. W. *et al.* (2010) 'Autoinhibition of the kinesin-2 motor KIF17 via dual intramolecular mechanisms', *Journal of Cell Biology*, 189(6), pp. 1013–1025. doi: 10.1083/jcb.201001057.

Hancock, W. O. (2014) 'Bidirectional cargo transport: Moving beyond tug of war', *Nature Reviews Molecular Cell Biology*, pp. 615–628. doi: 10.1038/nrm3853.

Hara, M. *et al.* (2000) 'Kinesin participates in melanosomal movement along melanocyte dendrites', *Journal of Investigative Dermatology*, 114(3), pp. 438–443. doi: 10.1046/j.1523-1747.2000.00894.x.

Heissler, S. M. and Sellers, J. R. (2016) 'Various Themes of Myosin Regulation', *Journal of Molecular Biology*, pp. 1927–1946. doi: 10.1016/j.jmb.2016.01.022.

Hettema, E. H. *et al.* (2000) 'Saccharomyces cerevisiae Pex3p and Pex19p are required for proper localization and stability of peroxisomal membrane proteins', *EMBO Journal*, 19(2), pp. 223–233. doi: 10.1093/emboj/19.2.223.

Hettema, E. H. *et al.* (2014) 'Evolving models for peroxisome biogenesis', *Current Opinion in Cell Biology*. Elsevier Ltd, 29(1), pp. 25–30. doi: 10.1016/j.ceb.2014.02.002.

Higuchi, R. *et al.* (2013) 'Actin dynamics affect mitochondrial quality control and aging in budding yeast', *Current Biology*, 23(23), pp. 2417–2422. doi: 10.1016/j.cub.2013.10.022.

Hill, K. L., Catlett, N. L. and Weisman, L. S. (1996) 'Actin and myosin function in directed vacuole movement during cell division in Saccharomyces cerevisiae', *Journal of Cell Biology*, 135(6), pp. 1535–1549. doi: 10.1083/jcb.135.6.1535.

Hill, S. M. *et al.* (2014) 'Life-span extension by a metacaspase in the yeast Saccharomyces cerevisiae', *Science*, 344(6190), pp. 1389–1392. doi: 10.1126/science.1252634.

Hoepfner, D. *et al.* (2001) 'A role for Vps1p, actin, and the Myo2p motor in peroxisome abundance and inheritance in Saccharomyces cerevisiae', *Journal of Cell Biology*, 155(6), pp. 979–990. doi: 10.1083/jcb.200107028.

Hoepfner, D. *et al.* (2005) 'Contribution of the endoplasmic reticulum to peroxisome formation', *Cell*, 122(1), pp. 85–95. doi: 10.1016/j.cell.2005.04.025.

Höfken, T. and Schiebel, E. (2002) 'A role for cell polarity proteins in mitotic exit', *EMBO Journal*, 21(18), pp. 4851–4862. doi: 10.1093/emboj/cdf481.

Hohfeld, J., Veenhuis, M. and Kunau, W. H. (1991) 'PAS3, a Saccharomyces cerevisiae gene encoding a peroxisomal integral membrane protein essential for peroxisome biogenesis', *Journal of Cell Biology*, 114(6), pp. 1167–1178. doi: 10.1083/jcb.114.6.1167.

Holt, L. J. *et al.* (2009) 'Global analysis of cdk1 substrate phosphorylation sites provides insiqhts into evolution', *Science*, 325(5948), pp. 1682–1686. doi: 10.1126/science.1172867.

Huber, A. *et al.* (2012) 'A subtle interplay between three Pex11 proteins shapes de novo formation and fission of peroxisomes', *Traffic*, 13(1), pp. 157–167. doi: 10.1111/j.1600-

0854.2011.01290.x.

Hughes, A. L. and Gottschling, D. E. (2012) 'An early age increase in vacuolar pH limits mitochondrial function and lifespan in yeast', *Nature*, 492(7428), pp. 261–265. doi: 10.1038/nature11654.

Huh *et al.* (2003) 'Global analysis of protein localization in budding yeast.', *Nature*, 425(6959), pp. 686–691. Available at: http://yeastgfp.ucsf.edu.

Hulmes, G. E. *et al.* (2020) 'The Pex3-Inp1 complex tethers yeast peroxisomes to the plasma membrane', *Journal of Cell Biology*, 219(10). doi: 10.1083/JCB.201906021.

Hurley, J. H. and Emr, S. D. (2006) 'The ESCRT complexes: Structure and mechanism of a membrane-trafficking network', *Annual Review of Biophysics and Biomolecular Structure*, pp. 277–298. doi: 10.1146/annurev.biophys.35.040405.102126.

Hutchins, M. U., Veenhuis, M. and Klionsky, D. J. (1999) 'Peroxisome degradation in Saccharomyces cerevisiae is dependent on machinery of macroautophagy and the Cvt pathway', *Journal of Cell Science*, 112(22), pp. 4079–4087. doi: 10.1242/jcs.112.22.4079.

Hwang, E. *et al.* (2003) 'Spindle orientation in Saccharomyces cerevisiae depends on the transport of microtubule ends along polarized actin cables', *Journal of Cell Biology*, 161(3), pp. 483–488. doi: 10.1083/jcb.200302030.

Inoshita, M. and Mima, J. (2017) 'Human Rab small GTPase– and class V myosin–mediated membrane tethering in a chemically defined reconstitution system', *Journal of Biological Chemistry*, 292(45), pp. 18500–18517. doi: 10.1074/jbc.M117.811356.

Ishikawa, K. *et al.* (2003) 'Identification of an organelle-specific myosin V receptor', *Journal of Cell Biology*, 160(6), pp. 887–897. doi: 10.1083/jcb.200210139.

Ito, T. *et al.* (2001) 'A comprehensive two-hybrid analysis to explore the yeast protein interactome', *Proceedings of the National Academy of Sciences of the United States of America*, 98(8), pp. 4569–4574. doi: 10.1073/pnas.061034498.

Itoh, T. *et al.* (2002) ' Complex Formation with Ypt11p, a rab-Type Small GTPase, Is Essential To Facilitate the Function of Myo2p, a Class V Myosin, in Mitochondrial Distribution in Saccharomyces cerevisiae ', *Molecular and Cellular Biology*, 22(22), pp. 7744–7757. doi: 10.1128/mcb.22.22.7744-7757.2002.

Itoh, T., Toh-E, A. and Matsui, Y. (2004) 'Mmr1p is a mitochondrial factor for Myo2p-dependent inheritance of mitochondria in the budding yeast', *EMBO Journal*, 23(13), pp. 2520–2530. doi: 10.1038/sj.emboj.7600271.

Jensen, S. *et al.* (2002) 'Spatial regulation of the guanine nucleotide exchange factor Lte1 in Saccharomyces cerevisiae', *Journal of Cell Science*, 115(24), pp. 4977–4991. doi: 10.1242/jcs.00189.

Jin, Y. *et al.* (2009) 'PTC1 is required for vacuole inheritance and promotes the association of

the myosin-V vacuole-specific receptor complex', *Molecular Biology of the Cell*, 20(5), pp. 1312–1323. doi: 10.1091/mbc.E08-09-0954.

Jin, Y. *et al.* (2011) 'Myosin V transports secretory vesicles via a Rab GTPase cascade and interaction with the exocyst complex', *Developmental Cell*, 21(6), pp. 1156–1170. doi: 10.1016/j.devcel.2011.10.009.

Jin, Y. and Weisman, L. S. (2015) 'The vacuole/lysosome is required for cell-cycle progression', *eLife*, 4(AUGUST2015), pp. 1–19. doi: 10.7554/eLife.08160.

Johnson, L. M., Bankaitis, V. A. and Emr, S. D. (1987) 'GENETIC APPROACH TO STUDY PROTEIN SORTING AND ORGANELLE ASSEMBLY IN YEAST.', in.

Johnston, G. C., Prendergast, J. A. and Singer, R. A. (1991) 'The Saccharomyces cerevisiae MYO2 gene encodes an essential myosin for vectorial transport of vesicles', *Journal of Cell Biology*, 113(3), pp. 539–551. doi: 10.1083/jcb.113.3.539.

Jones, J. M., Morrell, J. C. and Gould, S. J. (2004) 'PEX19 is a predominantly cytosolic chaperone and import receptor for class 1 peroxisomal membrane proteins', *Journal of Cell Biology*, 164(1), pp. 57–67. doi: 10.1083/jcb.200304111.

Jongsma, M. L. M., Berlin, I. and Neefjes, J. (2015) 'On the move: Organelle dynamics during mitosis', *Trends in Cell Biology*, pp. 112–124. doi: 10.1016/j.tcb.2014.10.005.

Jordens, I. *et al.* (2001) 'The Rab7 effector protein RILP controls lysosomal transport by inducing the recruitment of dynein-dynactin motors', *Current Biology*, 11(21), pp. 1680–1685. doi: 10.1016/S0960-9822(01)00531-0.

Jumper, J. *et al.* (2021) 'Highly accurate protein structure prediction with AlphaFold', *Nature*, 596(7873), pp. 583–589. doi: 10.1038/s41586-021-03819-2.

Kammerer, D., Stevermann, L. and Liakopoulos, D. (2010) 'Ubiquitylation regulates interactions of astral microtubules with the cleavage apparatus', *Current Biology*, 20(14), pp. 1233–1243. doi: 10.1016/j.cub.2010.05.064.

Kane, P. M. (2006) ' The Where, When, and How of Organelle Acidification by the Yeast Vacuolar H + -ATPase ', *Microbiology and Molecular Biology Reviews*, 70(1), pp. 177–191. doi: 10.1128/mmbr.70.1.177-191.2006.

Karcher, R. L. *et al.* (2001) 'Cell cycle regulation of myosin-V by calcium/calmodulin - Dependent protein kinase II', *Science*, 293(5533), pp. 1317–1320. doi: 10.1126/science.1061086.

Kaur, N. and Hu, J. (2009) 'Dynamics of peroxisome abundance: a tale of division and proliferation', *Current Opinion in Plant Biology*, 12(6), pp. 781–788. doi: 10.1016/j.pbi.2009.08.001.

Kelliher, M. T. *et al.* (2018) 'Autoinhibition of kinesin-1 is essential to the dendrite-specific localization of Golgi outposts', *Journal of Cell Biology*, 217(7), pp. 2531–2547. doi:

10.1083/jcb.201708096.

Kiel, J. A. K. W., Veenhuis, M. and van der Klei, I. J. (2006) 'PEX genes in fungal genomes: Common, rare or redundant', *Traffic*, 7(10), pp. 1291–1303. doi: 10.1111/j.1600-0854.2006.00479.x.

Kim, Hyejin *et al.* (2023) 'Structures of Vac8-containing protein complexes reveal the underlying mechanism by which Vac8 regulates multiple cellular processes', *Proceedings of the National Academy of Sciences of the United States of America*. United States, 120(118), p. e2211501120. doi: 10.1073/pnas.2211501120.

Kim, P. K. *et al.* (2006) 'The origin and maintenance of mammalian peroxisomes involves a de novo PEX16-dependent pathway from the ER', *Journal of Cell Biology*, 173(4), pp. 521–532. doi: 10.1083/jcb.200601036.

Klecker, T. *et al.* (2013) 'The yeast cell cortical protein Numl integrates mitochondrial dynamics into cellular architecture', *Journal of Cell Science*, 126(13), pp. 2924–2930. doi: 10.1242/jcs.126045.

Klecker, T. and Westermann, B. (2020) 'Asymmetric inheritance of mitochondria in yeast', *Biological Chemistry*, pp. 779–791. doi: 10.1515/hsz-2019-0439.

Klionsky, D. J. (1997) 'Protein transport from the cytoplasm into the vacuole', *Journal of Membrane Biology*, 157(2), pp. 105–115. doi: 10.1007/s002329900220.

Klionsky, D. J., Cueva, R. and Yaver, D. S. (1992) 'Aminopeptidase I of Saccharomyces cerevisiae is localized to the vacuole independent of the secretory pathway', *Journal of Cell Biology*, 119(2), pp. 287–300. doi: 10.1083/jcb.119.2.287.

Klionsky, D. J., Herman, P. K. and Emr, S. D. (1990) 'The fungal vacuole: Composition, function, and biogenesis', *Microbiological Reviews*, pp. 266–292. doi: 10.1128/mmbr.54.3.266-292.1990.

Klouwer, F. C. C. *et al.* (2015) 'Zellweger spectrum disorders: Clinical overview and management approach Inherited metabolic diseases', *Orphanet Journal of Rare Diseases*. Orphanet Journal of Rare Diseases, 10(1), pp. 1–11. doi: 10.1186/s13023-015-0368-9.

Knoblach, B. *et al.* (2013) 'An ER-peroxisome tether exerts peroxisome population control in yeast', *EMBO Journal*. Nature Publishing Group, 32(18), pp. 2439–2453. doi: 10.1038/emboj.2013.170.

Knoblach, B. and Rachubinski, R. A. (2015a) 'Sharing the cell's bounty - organelle inheritance in yeast', *Journal of Cell Science*, 128(4), pp. 621–630. doi: 10.1242/jcs.151423.

Knoblach, B. and Rachubinski, R. A. (2015b) 'Transport and retention mechanisms govern lipid droplet inheritance in saccharomyces cerevisiae', *Traffic*, 16(3), pp. 298–309. doi: 10.1111/tra.12247.

Knoblach, B. and Rachubinski, R. A. (2016) 'How peroxisomes partition between cells. A

story of yeast, mammals and filamentous fungi', *Current Opinion in Cell Biology*, pp. 73–80. doi: 10.1016/j.ceb.2016.04.004.

Knoops, K. *et al.* (2014) 'Preperoxisomal vesicles can form in the absence of Pex3', *Journal of Cell Biology*, 204(5), pp. 659–668. doi: 10.1083/jcb.201310148.

Knoops, K. *et al.* (2015) 'Yeast pex1 cells contain peroxisomal ghosts that import matrix proteins upon reintroduction of Pex1', *Journal of Cell Biology*, 211(5), pp. 955–962. doi: 10.1083/jcb.201506059.

Kobayashi, S., Tanaka, A. and Fujiki, Y. (2007) 'Fis1, DLP1, and Pex11p coordinately regulate peroxisome morphogenesis', *Experimental Cell Research*, 313(8), pp. 1675–1686. doi: 10.1016/j.yexcr.2007.02.028.

Koch, J. *et al.* (2016) 'Disturbed mitochondrial and peroxisomal dynamics due to loss of MFF causes Leigh-like encephalopathy, optic atrophy and peripheral neuropathy', *Journal of Medical Genetics*, 53(4), pp. 270–278. doi: 10.1136/jmedgenet-2015-103500.

Kornmann, B. *et al.* (2009) 'An ER-mitochondria tethering complex revealed by a synthetic biology screen', *Science*, 325(5939), pp. 477–481. doi: 10.1126/science.1175088.

Krementsov, D. N., Krementsova, E. B. and Trybus, K. M. (2004) 'Myosin V: Regulation by calcium, calmodulin, and the tail domain', *Journal of Cell Biology*, 164(6), pp. 877–886. doi: 10.1083/jcb.200310065.

Krikken, A. M. *et al.* (2020) 'Peroxisome retention involves Inp1-dependent peroxisome-plasma membrane contact sites in yeast', *Journal of Cell Biology*, 219(10). doi: 10.1083/JCB.201906023.

Kumar, A. *et al.* (2009) 'PAK thread from amoeba to mammals', *Journal of Cellular Biochemistry*, pp. 579–585. doi: 10.1002/jcb.22159.

Lackner, L. L. *et al.* (2013) 'Endoplasmic reticulum-associated mitochondria-cortex tether functions in the distribution and inheritance of mitochondria', *Proceedings of the National Academy of Sciences of the United States of America*, 110(6). doi: 10.1073/pnas.1215232110.

Lanz, M. C. *et al.* (2021) 'In-depth and 3-dimensional exploration of the budding yeast phosphoproteome', *EMBO reports*, 22(2). doi: 10.15252/embr.202051121.

Lapierre, L. A. *et al.* (2001) *Myosin Vb Is Associated with Plasma Membrane Recycling Systems*, *Molecular Biology of the Cell*.

Lazarow, P. B. and Fujiki, Y. (1985) 'Biogenesis of peroxisomes.', *Annual review of cell biology*, 1, pp. 489–530. doi: 10.1146/annurev.cb.01.110185.002421.

Lee, L. *et al.* (2000) 'Positioning of the mitotic spindle by a cortical-microtubule capture mechanism', *Science*, 287(5461), pp. 2260–2262. doi: 10.1126/science.287.5461.2260.

Lee, S. E. *et al.* (2001) 'Order of function of the budding-yeast mitotic exit-network proteins

Tem1, Cdc15, Mob1, Dbf2, and Cdc5', *Current Biology*, 11(10), pp. 784–788. doi: 10.1016/S0960-9822(01)00228-7.

Legesse-Miller, A. *et al.* (2006) 'Regulated phosphorylation of budding yeast's essential myosin V heavy chain, Myo2p', *Molecular Biology of the Cell*, 17(4), pp. 1812–1821. doi: 10.1091/mbc.E05-09-0872.

Lewandowska, A., MacFarlane, J. and Shaw, J. M. (2013) 'Mitochondrial association, protein phosphorylation, and degradation regulate the availability of the active Rab GTPase Ypt11 for mitochondrial inheritance', *Molecular Biology of the Cell*, 24(8), pp. 1185–1195. doi: 10.1091/mbc.E12-12-0848.

Li, K. W. *et al.* (2021) 'A preferred sequence for organelle inheritance during polarized cell growth', *Journal of Cell Science*, 134(21). doi: 10.1242/jcs.258856.

Li, S. C. and Kane, P. M. (2009) 'The yeast lysosome-like vacuole: Endpoint and crossroads', *Biochimica et Biophysica Acta - Molecular Cell Research*. Elsevier B.V., 1793(4), pp. 650–663. doi: 10.1016/j.bbamcr.2008.08.003.

Li, X. D. *et al.* (2004) 'Ca2+-induced activation of ATPase activity of myosin Va is accompanied with a large conformational change', *Biochemical and Biophysical Research Communications*, 315(3), pp. 538–545. doi: 10.1016/j.bbrc.2004.01.084.

Li, X. D., Ikebe, R. and Ikebei, M. (2005) 'Activation of myosin Va function by melanophilin, a specific docking partner of myosin Va', *Journal of Biological Chemistry*, 280(18), pp. 17815–17822. doi: 10.1074/jbc.M413295200.

Li, X. and Gould, S. J. (2003) 'The dynamin-like GTPase DLP1 is essential for peroxisome division and is recruited to peroxisomes in part by PEX11', *Journal of Biological Chemistry*, 278(19), pp. 17012–17020. doi: 10.1074/jbc.M212031200.

Liakopoulos, D. *et al.* (2003) 'Asymmetric loading of Kar9 onto spindle poles and microtubules ensures proper spindle alignment', *Cell*, 112(4), pp. 561–574. doi: 10.1016/S0092-8674(03)00119-3.

Lillie, S. H. and Brown, S. S. (1994) 'Immunofluorescence localization of the unconventional myosin, Myo2p, and the putative kinesin-related protein, Smy1p, to the same regions of polarized growth in Saccharomyces cerevisiae', *Journal of Cell Biology*, 125(4), pp. 825–842. doi: 10.1083/jcb.125.4.825.

Lipatova, Z. *et al.* (2008) 'Direct interaction between a myosin v motor and the Rab GTPases Ypt31/32 is required for polarized secretion', *Molecular Biology of the Cell*, 19(10), pp. 4177–4187. doi: 10.1091/mbc.E08-02-0220.

Liu, J. *et al.* (2006) 'Three-dimensional structure of the myosin V inhibited state by cryoelectron tomography', *Nature*, 442(7099), pp. 208–211. doi: 10.1038/nature04719.

Liu, Y. *et al.* (2022) 'Cargo Recognition Mechanisms of Yeast Myo2 Revealed by AlphaFold2-Powered Protein Complex Prediction', *Biomolecules*, 12(8), pp. 1–16. doi:

10.3390/biom12081032.

Long, R. M. *et al.* (2000) 'She2p is a novel RNA-binding protein that recruits the Myo4p-She3p complex to ASH1 mRNA', *EMBO Journal*, 19(23), pp. 6592–6601. doi: 10.1093/emboj/19.23.6592.

López-Doménech, G. *et al.* (2018) 'Miro proteins coordinate microtubule- and actin-dependent mitochondrial transport and distribution', *The EMBO Journal*, 37(3), pp. 321–336. doi: 10.15252/embj.201696380.

Lu, Q., Li, J. and Zhang, M. (2014) 'Cargo recognition and cargo-mediated regulation of unconventional myosins', *Accounts of Chemical Research*, 47(10), pp. 3061–3070. doi: 10.1021/ar500216z.

Lwin, K. M., Li, D. and Bretscher, A. (2016) 'Kinesin-related Smy1 enhances the Rab-dependent association of myosin-V with secretory cargo', *Molecular Biology of the Cell*, 27(15), pp. 2450–2462. doi: 10.1091/mbc.E16-03-0185.

M., F. and A., M. (2011) 'Lysosomal storage disorders: molecular basis and laboratory testing', *Human genomics*, 5(3), pp. 156–169. Available at: http://ovidsp.ovid.com/ovidweb.cgi?T=JS&PAGE=reference&D=emed10&NEWS=N&AN=21504867.

Ma, C. and Subramani, S. (2009) 'Peroxisome matrix and membrane protein biogenesis', *IUBMB Life*, 61(7), pp. 713–722. doi: 10.1002/iub.196.

Maekawa, H. *et al.* (2007) 'The yeast centrosome translates the positional information of the anaphase spindle into a cell cycle signal', *Journal of Cell Biology*, 179(3), pp. 423–436. doi: 10.1083/jcb.200705197.

Marchal, C., Haguenauer-Tsapis, R. and Urban-Grimal, D. (2000) 'Casein kinase 1-dependent phosphorylation within a PEST sequence and ubiquitination nearby lysines signal endocytosis of yeast uracil permease', *Journal of Biological Chemistry*. Â© 2000 ASBMB. Currently published by Elsevier Inc; originally published by American Society for Biochemistry and Molecular Biology., 275(31), pp. 23608–23614. doi: 10.1074/jbc.M001735200.

Marcusson, E. G. *et al.* (1994) 'The sorting receptor for yeast vacuolar carboxypeptidase Y is encoded by the VPS10 gene', *Cell*, 77(4), pp. 579–586. doi: 10.1016/0092-8674(94)90219-4.

Marks, M. S. and Seabra, M. C. (2001) 'The melanosome: Membrane dynamics in black and white', *Nature Reviews Molecular Cell Biology*, 2(10), pp. 738–748. doi: 10.1038/35096009.

Maschi, D., Gramlich, M. W. and Klyachko, V. A. (2018) 'Myosin V functions as a vesicle tether at the plasma membrane to control neurotransmitter release in central synapses', *eLife*, 7. doi: 10.7554/eLife.39440.

Mayer, A. and Wickner, W. (1997) 'Docking of yeast vacuoles is catalyzed by the ras-like GTPase Ypt7p after symmetric priming by Sec18p (NSF)', *Journal of Cell Biology*, 136(2), pp.

307–317. doi: 10.1083/jcb.136.2.307.

McConnell, S. J. *et al.* (1990) 'Temperature-sensitive yeast mutants defective in mitochondrial inheritance', *Journal of Cell Biology*, 111(3), pp. 967–976. doi: 10.1083/jcb.111.3.967.

McFaline-Figueroa, J. R. *et al.* (2011) 'Mitochondrial quality control during inheritance is associated with lifespan and mother-daughter age asymmetry in budding yeast', *Aging Cell*, 10(5), pp. 885–895. doi: 10.1111/j.1474-9726.2011.00731.x.

Mehta, A. *et al.* (2010) 'Fabry disease: A review of current management strategies', *Qjm*, pp. 641–659. doi: 10.1093/qjmed/hcq117.

Menendez-Benito, V. *et al.* (2013) 'Spatiotemporal analysis of organelle and macromolecular complex inheritance', *Proceedings of the National Academy of Sciences of the United States of America*, 110(1), pp. 175–180. doi: 10.1073/pnas.1207424110.

Merlini, L. *et al.* (2012) 'Budding yeast Dma proteins control septin dynamics and the spindle position checkpoint by promoting the recruitment of the Elm1 kinase to the bud neck', *PLoS Genetics*, 8(4). doi: 10.1371/journal.pgen.1002670.

Miller, R. K., Cheng, S. C. and Rose, M. D. (2000) 'Bim1p/Yeb1p mediates the Kar9p-dependent cortical attachment of cytoplasmic microtubules', *Molecular Biology of the Cell*, 11(9), pp. 2949–2959. doi: 10.1091/mbc.11.9.2949.

Miller, R. K. and Rose, M. D. (1998) 'Kar9p is a novel cortical protein required for cytoplasmic microtubule orientation in yeast', *Journal of Cell Biology*, 140(2), pp. 377–390. doi: 10.1083/jcb.140.2.377.

Mohl, D. A. *et al.* (2009) 'Dbf2-Mob1 drives relocalization of protein phosphatase Cdc14 to the cytoplasm during exit from mitosis', *Journal of Cell Biology*, 184(4), pp. 527–539. doi: 10.1083/jcb.200812022.

Mok, J. *et al.* (2010) 'Deciphering protein kinase specificity through large-scale analysis of yeast phosphorylation site motifs', *Science Signaling*, 3(109). doi: 10.1126/scisignal.2000482.

Moore, J. K. *et al.* (2010) 'The spindle position checkpoint is coordinated by the Elm1 kinase', *Journal of Cell Biology*, 191(3), pp. 493–503. doi: 10.1083/jcb.201006092.

Motley, A. M. *et al.* (2015) 'Reevaluation of the role of Pex1 and dynamin-related proteins in peroxisome membrane biogenesis', *Journal of Cell Biology*, 211(5), pp. 1041–1056. doi: 10.1083/jcb.201412066.

Motley, A. M. and Hettema, E. H. (2007) 'Yeast peroxisomes multiply by growth and division', *Journal of Cell Biology*, 178(3), pp. 399–410. doi: 10.1083/jcb.200702167.

Motley, A. M., Nuttall, J. M. and Hettema, E. H. (2012a) 'Pex3-anchored Atg36 tags peroxisomes for degradation in Saccharomyces cerevisiae', *EMBO Journal*, 31(13), pp. 2852–

2868. doi: 10.1038/emboj.2012.151.

Motley, A. M., Nuttall, J. M. and Hettema, E. H. (2012b) 'Pex3-anchored Atg36 tags peroxisomes for degradation in Saccharomyces cerevisiae', *EMBO Journal*. Nature Publishing Group, 31(13), pp. 2852–2868. doi: 10.1038/emboj.2012.151.

Motley, A. M., Ward, G. P. and Hettema, E. H. (2008) 'Dnm1p-dependent peroxisome fission requires Caf4p, Mdv1p and Fis1p', *Journal of Cell Science*, 121(10), pp. 1633–1640. doi: 10.1242/jcs.026344.

Müller, T. *et al.* (2008) 'MYO5B mutations cause microvillus inclusion disease and disrupt epithelial cell polarity', *Nature Genetics*, 40(10), pp. 1163–1165. doi: 10.1038/ng.225.

Musacchio, A. and Salmon, E. D. (2007) 'The spindle-assembly checkpoint in space and time', *Nature Reviews Molecular Cell Biology*, pp. 379–393. doi: 10.1038/nrm2163.

Nagotu, S. *et al.* (2008) 'Peroxisome proliferation in Hansenula polymorpha requires Dnm1p which mediates fission but not de novo formation', *Biochimica et Biophysica Acta - Molecular Cell Research*, 1783(5), pp. 760–769. doi: 10.1016/j.bbamcr.2007.10.018.

Nagral, A. (2014) 'Gaucher disease', *Journal of Clinical and Experimental Hepatology*. Elsevier Ltd, 4(1), pp. 37–50. doi: 10.1016/j.jceh.2014.02.005.

Nakatogawa, H. *et al.* (2009) 'Dynamics and diversity in autophagy mechanisms: Lessons from yeast', *Nature Reviews Molecular Cell Biology*. Nature Publishing Group, 10(7), pp. 458–467. doi: 10.1038/nrm2708.

Nemani, N. *et al.* (2018) 'MIRO-1 Determines Mitochondrial Shape Transition upon GPCR Activation and Ca2+ Stress', *Cell Reports*, 23(4), pp. 1005–1019. doi: 10.1016/j.celrep.2018.03.098.

Nichols, B. J. *et al.* (1997) 'Homotypic vacuolar fusion mediated by t- and v-SNAREs', *Nature*, 387(6629), pp. 199–202. doi: 10.1038/387199a0.

Nunnari, J. and Walter, P. (1996) 'Regulation of organelle biogenesis', *Cell*, 84(3), pp. 389–394. doi: 10.1016/S0092-8674(00)81283-0.

Obara, K. *et al.* (2022) 'Proteolysis of adaptor protein Mmr1 during budding is necessary for mitochondrial homeostasis in Saccharomyces cerevisiae', *Nature Communications*, 13(1). doi: 10.1038/s41467-022-29704-8.

Oberhofer, A. *et al.* (2017) 'Myosin Va's adaptor protein melanophilin enforces track selection on the microtubule and actin networks in vitro', *Proceedings of the National Academy of Sciences of the United States of America*, 114(24), pp. E4714–E4723. doi: 10.1073/pnas.1619473114.

Ogawa, N., DeRisi, J. and Brown, P. O. (2000) 'New components of a system for phosphate accumulation and polyphosphate metabolism in Saccharomyces cerevisiae revealed by genomic expression analysis', *Molecular Biology of the Cell*, 11(12), pp. 4309–4321. doi:

10.1091/mbc.11.12.4309.

Ohsumi, Y. (2001) 'Molecular dissection of autophagy: Two ubiquitin-like systems', *Nature Reviews Molecular Cell Biology*, pp. 211–216. doi: 10.1038/35056522.

Opaliński, Ł. *et al.* (2011) 'Membrane curvature during peroxisome fission requires Pex11', *EMBO Journal*, 30(1), pp. 5–16. doi: 10.1038/emboj.2010.299.

Otera, H. *et al.* (2010) 'Mff is an essential factor for mitochondrial recruitment of Drp1 during mitochondrial fission in mammalian cells', *Journal of Cell Biology*, 191(6), pp. 1141–1158. doi: 10.1083/jcb.201007152.

Otzen, M. *et al.* (2012) 'Pex19p Contributes to Peroxisome Inheritance in the Association of Peroxisomes to Myo2p', *Traffic*, 13(7), pp. 947–959. doi: 10.1111/j.1600-0854.2012.01364.x.

De Pace, R. *et al.* (2018) 'Altered distribution of ATG9A and accumulation of axonal aggregates in neurons from a mouse model of AP-4 deficiency syndrome', *PLoS Genetics*, 14(4). doi: 10.1371/journal.pgen.1007363.

Pan, D., Nakatsu, T. and Kato, H. (2013) 'Crystal structure of peroxisomal targeting signal-2 bound to its receptor complex Pex7p-Pex21p', *Nature Structural and Molecular Biology*, 20(8), pp. 987–993. doi: 10.1038/nsmb.2618.

Pan, X. and Goldfarb, D. S. (1998) 'YEB3/VAC8 encodes a myristylated armadillo protein of the Saccharomyces cerevisiae vacuolar membrane that functions in vacuole fusion and inheritance', *Journal of Cell Science*, 111(15), pp. 2137–2147. doi: 10.1242/jcs.111.15.2137.

Park, J. il *et al.* (2019) 'The absence of Rab27a accelerates the degradation of Melanophilin', *Experimental Dermatology*, 28(1), pp. 90–93. doi: 10.1111/exd.13840.

Pastural, E. *et al.* (1997) 'Griscelli disease maps to chromosome 15q21 and is associated with mutations in the myosin-Va gene', *Nature Genetics*, 16(3), pp. 289–292. doi: 10.1038/ng0797-289.

Pedersen, J. I. (1993) 'Peroxisomal oxidation of the steroid side chain in bile acid formation', *Biochimie*, 75(3–4), pp. 159–165. doi: 10.1016/0300-9084(93)90073-2.

Peng, Y. and Weisman, L. S. (2008a) 'The Cyclin-Dependent Kinase Cdk1 Directly Regulates Vacuole Inheritance', *Developmental Cell*, 15(3), pp. 478–485. doi: 10.1016/j.devcel.2008.07.007.

Peng, Y. and Weisman, L. S. (2008b) 'The Cyclin-Dependent Kinase Cdk1 Directly Regulates Vacuole Inheritance', *Developmental Cell*, 15(3), pp. 478–485. doi: 10.1016/j.devcel.2008.07.007.

Pereira, G. and Schiebel, E. (2005) 'Kin4 kinase delays mitotic exit in response to spindle alignment defects', *Molecular Cell*, 19(2), pp. 209–221. doi: 10.1016/j.molcel.2005.05.030.

Pernice, W. M., Vevea, J. D. and Pon, L. A. (2016) 'A role for Mfb1p in region-specific anchorage of high-functioning mitochondria and lifespan in Saccharomyces cerevisiae',

Nature Communications, 7. doi: 10.1038/ncomms10595.

Peter, M. *et al.* (1996) 'Functional analysis of the interaction between the small GTP binding protein Cdc42 and the Ste20 protein kinase in yeast', *EMBO Journal*, 15(24), pp. 7046–7059. doi: 10.1002/j.1460-2075.1996.tb01096.x.

Peters, C. *et al.* (2004) 'Mutual control of membrane fission and fusion proteins', *Cell*, 119(5), pp. 667–678. doi: 10.1016/j.cell.2004.11.023.

Platt, F. M. *et al.* (2018) 'Lysosomal storage diseases', *Nature Reviews Disease Primers*. doi: 10.1038/s41572-018-0025-4.

Platta, H. W., Girzalsky, W. and Erdmann, R. (2004) 'Ubiquitination of the peroxisomal import receptor Pex5p', *Biochemical Journal*, 384(1), pp. 37–45. doi: 10.1042/BJ20040572.

Price, A. *et al.* (2000) 'The docking stage of yeast vacuole fusion requires the transfer of proteins from a cis-SNARE complex to a Rab/Ypt protein', *Journal of Cell Biology*, 148(6), pp. 1231–1238. doi: 10.1083/jcb.148.6.1231.

Provance, D. W., James, T. L. and Mercer, J. A. (2002) 'Melanophilin, the product of the leaden locus, is required for targeting of myosin-Va to melanosomes', *Traffic*, 3(2), pp. 124–132. doi: 10.1034/j.1600-0854.2002.030205.x.

Pruyne, D. W., Schott, D. H. and Bretscher, A. (1998) 'Tropomyosin-containing actin cables direct the Myo2p-dependent polarized delivery of secretory vesicles in budding yeast', *Journal of Cell Biology*, 143(7), pp. 1931–1945. doi: 10.1083/jcb.143.7.1931.

Pu, J. *et al.* (2015) 'BORC, a Multisubunit Complex that Regulates Lysosome Positioning', *Developmental Cell*, 33(2), pp. 176–188. doi: 10.1016/j.devcel.2015.02.011.

Pu, J. *et al.* (2016) 'Mechanisms and functions of lysosome positioning', *Journal of Cell Science*, pp. 4329–4339. doi: 10.1242/jcs.196287.

Pylypenko, O. *et al.* (2013) 'Structural basis of myosin v Rab GTPase-dependent cargo recognition', *Proceedings of the National Academy of Sciences of the United States of America*, 110(51), pp. 20443–20448. doi: 10.1073/pnas.1314329110.

Qiu, R., Zhang, J. and Xiang, X. (2019) 'LIS1 regulates cargo-adapter-mediated activation of dynein by overcoming its autoinhibition in vivo', *Journal of Cell Biology*, 218(11), pp. 3630–3646. doi: 10.1083/JCB.201905178.

Raposo, G. and Marks, M. S. (2007) 'Melanosomes - Dark organelles enlighten endosomal membrane transport', *Nature Reviews Molecular Cell Biology*, pp. 786–797. doi: 10.1038/nrm2258.

Raymond, C. K. *et al.* (1990) 'Molecular analysis of the yeast VPS3 gene and the role of its product in vacuolar protein sorting and vacuolar segregation during the cell cycle', *Journal of Cell Biology*, 111(3), pp. 877–892. doi: 10.1083/jcb.111.3.877.

Raymond, C. K. *et al.* (1992) 'Morphological classification of the yeast vacuolar protein

sorting mutants: Evidence for a prevacuolar compartment in class E vps mutants', *Molecular Biology of the Cell*, 3(12), pp. 1389–1402. doi: 10.1091/mbc.3.12.1389.

Rechsteiner, M. and Rogers, S. W. (1996) 'PEST sequences and regulation by proteolysis', *Trends in Biochemical Sciences*, pp. 267–271. doi: 10.1016/S0968-0004(96)10031-1.

Rieder, S. E. and Emr, S. D. (1997) 'A novel RING finger protein complex essential for a late step in protein transport to the yeast vacuole', *Molecular Biology of the Cell*, 8(11), pp. 2307–2327. doi: 10.1091/mbc.8.11.2307.

Robinson, L. C. *et al.* (1993) ' Casein Kinase I-Like Protein Kinases Encoded by YCK1 and YCK2 are Required for Yeast Morphogenesis ', *Molecular and Cellular Biology*, 13(5), pp. 2870–2881. doi: 10.1128/mcb.13.5.2870-2881.1993.

Robinson, L. C. *et al.* (1999) 'The Yck2 yeast casein kinase 1 isoform shows cell cycle-specific localization to sites of polarized growth and is required for proper septin organization', *Molecular Biology of the Cell*, 10(4), pp. 1077–1092. doi: 10.1091/mbc.10.4.1077.

Rodriguez, O. C. and Cheney, R. E. (2002) 'Human myosin-Vc is a novel class V myosin expressed in epithelial cells', *Journal of Cell Science*, 115(5), pp. 991–1004. doi: 10.1242/jcs.115.5.991.

Roeder, A. D. *et al.* (1998) 'Mitochondrial inheritance is delayed in Saccharomyces cerevisiae cells lacking the serine/threonine phosphatase PTC1', *Molecular Biology of the Cell*, 9(4), pp. 917–930. doi: 10.1091/mbc.9.4.917.

Rogers, S. L. *et al.* (1999) 'Regulation of melanosome movement in the cell cycle by reversible association with myosin V', *Journal of Cell Biology*, 146(6), pp. 1265–1275. doi: 10.1083/jcb.146.6.1265.

Roguev, A. *et al.* (2007) 'High-throughput genetic interaction mapping in the fission yeast Schizosaccharomyces pombe', *Nature Methods*, 4(10), pp. 861–866. doi: 10.1038/nmeth1098.

Rosa-Ferreira, C. and Munro, S. (2011) 'Arl8 and SKIP Act Together to Link Lysosomes to Kinesin-1', *Developmental Cell*, 21(6), pp. 1171–1178. doi: 10.1016/j.devcel.2011.10.007.

Rothman, J. H. and Stevens, T. H. (1986) 'Protein sorting in yeast: Mutants defective in vacuole biogenesis mislocalize vacuolar proteins into the late secretory pathway', *Cell*, 47(6), pp. 1041–1051. doi: 10.1016/0092-8674(86)90819-6.

Saraya, R. *et al.* (2010) 'A conserved function for Inp2 in peroxisome inheritance', *Biochimica et Biophysica Acta - Molecular Cell Research*, 1803(5), pp. 617–622. doi: 10.1016/j.bbamcr.2010.02.001.

Sato, O., Li, X. D. and Ikebe, M. (2007) 'Myosin Va becomes a low duty ratio motor in the inhibited form', *Journal of Biological Chemistry*, 282(18), pp. 13228–13239. doi: 10.1074/jbc.M610766200.

Sato, T. *et al.* (2007) 'The Rab8 GTPase regulates apical protein localization in intestinal cells', *Nature*, 448(7151), pp. 366–369. doi: 10.1038/nature05929.

Schneeberger, K. *et al.* (2015) 'An inducible mouse model for microvillus inclusion disease reveals a role for myosin Vb in apical and basolateral trafficking', *Proceedings of the National Academy of Sciences of the United States of America*, 112(40), pp. 12408–12413. doi: 10.1073/pnas.1516672112.

Schneider-Poetsch, T. *et al.* (2010) 'Inhibition of eukaryotic translation elongation by cycloheximide and lactimidomycin', *Nature Chemical Biology*, 6(3), pp. 209–217. doi: 10.1038/nchembio.304.

Schott, D. *et al.* (1999) 'The COOH-terminal domain of Myo2p, a yeast myosin V, has a direct role in secretory vesicle targeting', *Journal of Cell Biology*, 147(4), pp. 791–807. doi: 10.1083/jcb.147.4.791.

Schrader, M. *et al.* (2000) 'Real time imaging reveals a peroxisomal reticulum in living cells', *Journal of Cell Science*, 113(20), pp. 3663–3671. doi: 10.1242/jcs.113.20.3663.

Schrader, M. and Fahimi, H. D. (2006) 'Peroxisomes and oxidative stress', *Biochimica et Biophysica Acta - Molecular Cell Research*, pp. 1755–1766. doi: 10.1016/j.bbamcr.2006.09.006.

Schrader, T. A. *et al.* (2022) 'PEX11β and FIS1 cooperate in peroxisome division independent of Mitochondrial Fission Factor', *Journal of Cell Science*, 135(13). doi: 10.1242/jcs.259924.

Sckolnick, M. *et al.* (2013) 'More than just a cargo adapter, melanophilin prolongs and slows processive runs of myosin Va', *Journal of Biological Chemistry*, 288(41), pp. 29313–29322. doi: 10.1074/jbc.M113.476929.

Seaman, M. N. J. (2004) 'Cargo-selective endosomal sorting for retrieval to the Golgi requires retromer', *Journal of Cell Biology*, 165(1), pp. 111–122. doi: 10.1083/jcb.200312034.

Sheltzer, J. M. and Rose, M. D. (2009) 'The class V myosin Myo2p is required for Fus2p transport and actin polarization during the yeast mating response', *Molecular Biology of the Cell*, 20(12), pp. 2909–2919. doi: 10.1091/mbc.E08-09-0923.

Sibirny, A. A. (2016) 'Yeast peroxisomes: Structure, functions and biotechnological opportunities', *FEMS Yeast Research*, 16(4), pp. 1–14. doi: 10.1093/femsyr/fow038.

Siddiqui, N. *et al.* (2019) 'PTPN21 and Hook3 relieve KIF1C autoinhibition and activate intracellular transport', *Nature Communications*, 10(1). doi: 10.1038/s41467-019-10644-9.

Simon, V. R., Karmon, S. L. and Pon, L. A. (1997) 'Mitochondrial inheritance: Cell cycle and actin cable dependence of polarized mitochondrial movements in saccharomyces cerevisiae', *Cell Motility and the Cytoskeleton*, 37(3), pp. 199–210. doi: 10.1002/(SICI)1097-0169(1997)37:3<199::AID-CM2>3.0.CO;2-2.

Simon, V. R., Swayne, T. C. and Pon, L. A. (1995) 'Actin-dependent mitochondrial motility in mitotic yeast and cell-free systems: Identification of a motor activity on the mitochondrial surface', *Journal of Cell Biology*, 130(2), pp. 345–354. doi: 10.1083/jcb.130.2.345.

Singer-Krüger, B. and Jansen, R. P. (2014) 'Here, there, everywhere: mRNA localization in budding yeast', *RNA Biology*, pp. 1031–1039. doi: 10.4161/rna.29945.

Smith, J. J. and Aitchison, J. D. (2009) 'Regulation of peroxisome dynamics', *Current Opinion in Cell Biology*, 21(1), pp. 119–126. doi: 10.1016/j.ceb.2009.01.009.

Smith, M. J. *et al.* (2006) 'Mapping the GRIF-1 binding domain of the kinesin, KIF5C, substantiates a role for GRIF-1 as an adaptor protein in the anterograde trafficking of cargoes', *Journal of Biological Chemistry*. United States, 281(37), pp. 27216–27228. doi: 10.1074/jbc.M600522200.

Sobajima, T. *et al.* (2015) 'Rab11a is required for apical protein localisation in the intestine', *Biology Open*, 4(1), pp. 86–94. doi: 10.1242/bio.20148532.

Stanley, W. A. *et al.* (2006) 'Recognition of a Functional Peroxisome Type 1 Target by the Dynamic Import Receptor Pex5p', *Molecular Cell*, 24(5), pp. 653–663. doi: 10.1016/j.molcel.2006.10.024.

Steinberg, S. J. *et al.* (2020) 'Zellweger Spectrum Disorder Summary GeneReview Scope Suggestive Findings', *Gene Reviews*. Available at: https://www.ncbi.nlm.nih.gov/books/NBK1448/.

Stevens, R. C. and Davis, T. N. (1998) 'Mlc1p is a light chain for the unconventional myosin Myo2p in saccharomyces cerevisiae', *Journal of Cell Biology*, 142(3), pp. 711–722. doi: 10.1083/jcb.142.3.711.

Strom, M. *et al.* (2002) 'A family of Rab27-binding proteins: Melanophilin links Rab27a and myosin Va function in melanosome transport', *Journal of Biological Chemistry*, 277(28), pp. 25423–25430. doi: 10.1074/jbc.M202574200.

Subramani, S. (1993) 'Protein import into peroxisomes and biogenesis of the organelle', *Annual Review of Cell Biology*, 9, pp. 445–478. doi: 10.1146/annurev.cb.09.110193.002305.

Sugiura, A. *et al.* (2017) 'Newly born peroxisomes are a hybrid of mitochondrial and ER-derived pre-peroxisomes', *Nature*, 542(7640), pp. 251–254. doi: 10.1038/nature21375.

Swaney, D. L. *et al.* (2013) 'Global analysis of phosphorylation and ubiquitylation cross-talk in protein degradation', *Nature Methods*, 10(7), pp. 676–682. doi: 10.1038/nmeth.2519.

Takagishi, Y. and Murata, Y. (2006) 'Myosin Va mutation in rats is an animal model for the human hereditary neurological disease, griscelli syndrome type 1', in *Annals of the New York Academy of Sciences*, pp. 66–80. doi: 10.1196/annals.1377.006.

Tanaka, C. *et al.* (2014) 'Hrr25 triggers selective autophagy-related pathways by phosphorylating receptor proteins', *Journal of Cell Biology*, 207(1), pp. 91–105. doi:

10.1083/jcb.201402128.

Tang, F. *et al.* (2003) 'Regulated degradation of a class V myosin receptor directs movement of the yeast vacuole', *Nature*, 422(6927), pp. 87–92. doi: 10.1038/nature01453.

Tang, F. *et al.* (2006) 'Vac8p, an armadillo repeat protein, coordinates vacuole inheritance with multiple vacuolar processes', *Traffic*, 7(10), pp. 1368–1377. doi: 10.1111/j.1600-0854.2006.00458.x.

Tang, K. *et al.* (2019) 'Structural mechanism for versatile cargo recognition by the yeast class V myosin Myo2', *Journal of Biological Chemistry*, 294(15), pp. 5896–5906. doi: 10.1074/jbc.RA119.007550.

Taylor Eves, P. *et al.* (2012) 'Overlap of cargo binding sites on myosin V coordinates the inheritance of diverse cargoes', *Journal of Cell Biology*, 198(1), pp. 69–85. doi: 10.1083/jcb.201201024.

Taylor, R. L. *et al.* (2017) 'Novel PEX11B mutations extend the peroxisome biogenesis disorder 14B phenotypic spectrum and underscore congenital cataract as an early feature', *Investigative Ophthalmology and Visual Science*, 58(1), pp. 594–603. doi: 10.1167/iovs.16-21026.

Thirumurugan, K. *et al.* (2006) 'The cargo-binding domain regulates structure and activity of myosin 5', *Nature*, 442(7099), pp. 212–215. doi: 10.1038/nature04865.

Thoeni, C. E. *et al.* (2014) 'Microvillus Inclusion Disease: Loss of Myosin Vb Disrupts Intracellular Traffic and Cell Polarity', *Traffic*, 15(1), pp. 22–42. doi: 10.1111/tra.12131.

Titorenko, V. I. and Rachubinski, R. A. (2001) 'The life cycle of the peroxisome', *Nature Reviews Molecular Cell Biology*, 2(5), pp. 357–368. doi: 10.1038/35073063.

Tong, A. H. Y. *et al.* (2001) 'Systematic genetic analysis with ordered arrays of yeast deletion mutants', *Science*, 294(5550), pp. 2364–2368. doi: 10.1126/science.1065810.

Torisawa, T. *et al.* (2014) 'Autoinhibition and cooperative activation mechanisms of cytoplasmic dynein', *Nature Cell Biology*, 16(11), pp. 1118–1124. doi: 10.1038/ncb3048.

Tower, R. J. *et al.* (2011) 'The peroxin Pex34p functions with the Pex11 family of peroxisomal divisional proteins to regulate the peroxisome population in yeast', *Molecular Biology of the Cell*, 22(10), pp. 1727–1738. doi: 10.1091/mbc.E11-01-0084.

Trybus, K. M. *et al.* (2007) 'Effect of calcium on calmodulin bound to the IQ motifs of myosin V', *Journal of Biological Chemistry*, 282(32), pp. 23316–23325. doi: 10.1074/jbc.M701636200.

Trybus, K. M. (2008) 'Myosin V from head to tail', *Cellular and Molecular Life Sciences*, pp. 1378–1389. doi: 10.1007/s00018-008-7507-6.

Typas, A. *et al.* (2008) 'High-throughput, quantitative analyses of genetic interactions in E. coli', *Nature Methods*, 5(9), pp. 781–787. doi: 10.1038/nmeth.1240.

Vancoillie, G. *et al.* (2000) 'Cytoplasmic dynein colocalizes with melanosomes in normal human melanocytes', *British Journal of Dermatology*, 143(2), pp. 298–306. doi: 10.1046/j.1365-2133.2000.03654.x.

Vancoillie, Garnet *et al.* (2000) 'Kinesin and kinectin can associate with the melanosomal surface and form a link with microtubules in normal human melanocytes', *Journal of Investigative Dermatology*, 114(3), pp. 421–429. doi: 10.1046/j.1523-1747.2000.00897.x.

Vanier, M. T. (2010) 'Niemann-Pick disease type C', *Orphanet Journal of Rare Diseases*. doi: 10.1186/1750-1172-5-16.

Vanier, M. T. (2015) 'Complex lipid trafficking in Niemann-Pick disease type C', *Journal of Inherited Metabolic Disease*, 38(1), pp. 187–199. doi: 10.1007/s10545-014-9794-4.

van der Velde, K. J. *et al.* (2013) 'An Overview and Online Registry of Microvillus Inclusion Disease Patients and their MYO5B Mutations', *Human Mutation*, 34(12), pp. 1597–1605. doi: 10.1002/humu.22440.

Verhey, K. J. and Hammond, J. W. (2009) 'Traffic control: Regulation of kinesin motors', *Nature Reviews Molecular Cell Biology*, pp. 765–777. doi: 10.1038/nrm2782.

Vevea, J. D. *et al.* (2013) 'Ratiometric biosensors that measure mitochondrial redox state and ATP in living yeast cells', *Journal of visualized experiments : JoVE*, (77). doi: 10.3791/50633.

Vitiello, S. P., Wolfe, D. M. and Pearce, D. A. (2007) 'Absence of Btn1p in the yeast model for juvenile Batten disease may cause arginine to become toxic to yeast cells', *Human Molecular Genetics*, 16(9), pp. 1007–1016. doi: 10.1093/hmg/ddm046.

Vogel, G. F. *et al.* (2015) 'Cargo-selective apical exocytosis in epithelial cells is conducted by Myo5B, Slp4a, Vamp7, and Syntaxin 3', *Journal of Cell Biology*, 211(3), pp. 587–604. doi: 10.1083/jcb.201506112.

Wada, Y. and Anraku, Y. (1992) 'Genes for directing vacuolar morphogenesis in Saccharomyces cerevisiae. II. VAM7, a gene for regulating morphogenic assembly of the vacuoles', *Journal of Biological Chemistry*, 267(26), pp. 18671–18675. doi: 10.1016/s0021-9258(19)37013-9.

Wagner, W., Brenowitz, S. D. and Hammer, J. A. (2011) 'Myosin-Va transports the endoplasmic reticulum into the dendritic spines of Purkinje neurons', *Nature Cell Biology*, 13(1), pp. 40–47. doi: 10.1038/ncb2132.

Wanders, R. J. A. (2018) 'Peroxisomal disorders: Improved laboratory diagnosis, new defects and the complicated route to treatment', *Molecular and Cellular Probes*. Elsevier, 40(September 2017), pp. 60–69. doi: 10.1016/j.mcp.2018.02.001.

Wang, F. *et al.* (2004) 'Regulated Conformation of Myosin V', *Journal of Biological Chemistry*, 279(4), pp. 2333–2336. doi: 10.1074/jbc.C300488200.

Wang, Y. X., Catlett, N. L. and Weisman, L. S. (1998) 'Vac8p, a vacuolar protein with armadillo repeats, functions in both vacuole inheritance and protein targeting from the cytoplasm to vacuole', *Journal of Cell Biology*, 140(5), pp. 1063–1074. doi: 10.1083/jcb.140.5.1063.

Warren, G. and Wickner, W. (1996) 'Organelle inheritance', *Cell*, 84(3), pp. 395–400. doi: 10.1016/S0092-8674(00)81284-2.

Wei, Z. *et al.* (2013) 'Structural basis of cargo recognitions for class V myosins', *Proceedings of the National Academy of Sciences of the United States of America*, 110(28), pp. 11314–11319. doi: 10.1073/pnas.1306768110.

Weill, U. *et al.* (2018) 'Genome-wide SWAp-Tag yeast libraries for proteome exploration', *Nature Methods*, 15(8), pp. 617–622. doi: 10.1038/s41592-018-0044-9.

Weisman, L. S. (2006) 'Organelles on the move: Insights from yeast vacuole inheritance', *Nature Reviews Molecular Cell Biology*, pp. 243–252. doi: 10.1038/nrm1892.

Weisman, L. S., Bacallao, R. and Wickner, W. (1987) 'Multiple methods of visualizing the yeast vacuole permit evaluation of its morphology and inheritance during the cell cycle.', *The Journal of cell biology*, 105(4), pp. 1539–1547. doi: 10.1083/jcb.105.4.1539.

Weisman, L. S. and Wickner, W. (1988) 'Intervacuole exchange in the yeast zygote: A new pathway in organelle communication', *Science*, 241(4865), pp. 589–591. doi: 10.1126/science.3041591.

Westermann, B. (2014) 'Mitochondrial inheritance in yeast', *Biochimica et Biophysica Acta - Bioenergetics*, pp. 1039–1046. doi: 10.1016/j.bbabio.2013.10.005.

Wickner, W. (2010) 'Membrane fusion: Five lipids, four SNAREs, three chaperones, two nucleotides, and a rab, all dancing in a ring on yeast vacuoles', *Annual Review of Cell and Developmental Biology*, pp. 115–136. doi: 10.1146/annurev-cellbio-100109-104131.

Wiemer, E. A. C. *et al.* (1997) 'Visualization of the peroxisomal compartment in living mammalian cells: Dynamic behavior and association with microtubules', *Journal of Cell Biology*, 136(1), pp. 71–80. doi: 10.1083/jcb.136.1.71.

Wijdeven, R. H. *et al.* (2016) 'Cholesterol and ORP1L-mediated ER contact sites control autophagosome transport and fusion with the endocytic pathway', *Nature Communications*. England, 7, p. 11808. doi: 10.1038/ncomms11808.

Wong, S. *et al.* (2020) 'Cargo Release from Myosin V Requires the Convergence of Parallel Pathways that Phosphorylate and Ubiquitylate the Cargo Adaptor', *Current Biology*, 30(22), pp. 4399-4412.e7. doi: 10.1016/j.cub.2020.08.062.

Wróblewska, J. P. *et al.* (2017) 'Saccharomyces cerevisiae cells lacking Pex3 contain membrane vesicles that harbor a subset of peroxisomal membrane proteins', *Biochimica et Biophysica Acta - Molecular Cell Research*. Elsevier, 1864(10), pp. 1656–1667. doi: 10.1016/j.bbamcr.2017.05.021.

Wu, X. *et al.* (1998) 'Visualization of melanosome dynamics within wild-type and dilute melanocytes suggests a paradigm for myosin v function in vivo', *Journal of Cell Biology*, 143(7), pp. 1899–1918. doi: 10.1083/jcb.143.7.1899.

Wu, X. *et al.* (2002) 'Rab27a is an essential component of melanosome receptor for myosin Va', *Molecular Biology of the Cell*, 13(5), pp. 1735–1749. doi: 10.1091/mbc.01-12-0595.

Wu, X. S. *et al.* (2002) 'Identification of an organelle receptor for myosin-Va', *Nature Cell Biology*, 4(4), pp. 271–278. doi: 10.1038/ncb760.

Wurmser, A. E., Sato, T. K. and Emr, S. D. (2000) 'New component of the vacuolar class C-Vps complex couples nucleotide exchange on the Ypt7 GTPase to SNARE-dependent docking and fusion', *Journal of Cell Biology*, 151(3), pp. 551–562. doi: 10.1083/jcb.151.3.551.

Yamamoto, A. *et al.* (1990) 'Solubilization of Aster-Forming Proteins from Yeast: Possible Constituents of Spindle Pole Body and Reconstitution of Asters In Vitro', *Cell Structure and Function*, 15(4), pp. 221–228. doi: 10.1247/csf.15.221.

Yau, R. G. *et al.* (2014) 'Release from Myosin V via Regulated Recruitment of an E3 Ubiquitin Ligase Controls Organelle Localization', *Developmental Cell*, 28(5), pp. 520–533. doi: 10.1016/j.devcel.2014.02.001.

Yau, R. G., Wong, S. and Weisman, L. S. (2017) 'Spatial regulation of organelle release from myosin V transport by p21-activated kinases', *Journal of Cell Biology*, 216(6), pp. 1557–1566. doi: 10.1083/jcb.201607020.

Yin, H. *et al.* (2000) 'Myosin V orientates the mitotic spindle in yeast', *Nature*, 406(6799), pp. 1013–1015. doi: 10.1038/35023024.

Yofe, I. *et al.* (2016) 'One library to make them all: Streamlining the creation of yeast libraries via a SWAp-Tag strategy', *Nature Methods*, 13(4), pp. 371–378. doi: 10.1038/nmeth.3795.

Yorimitsu, T. and Klionsky, D. J. (2005) 'Autophagy: Molecular machinery for self-eating', *Cell Death and Differentiation*, pp. 1542–1552. doi: 10.1038/sj.cdd.4401765.

Van Der Zand, A. *et al.* (2012) 'Biochemically distinct vesicles from the endoplasmic reticulum fuse to form peroxisomes', *Cell*, 149(2), pp. 397–409. doi: 10.1016/j.cell.2012.01.054.

Zhou, X. *et al.* (2021) 'Cross-compartment signal propagation in the mitotic exit network', *eLife*, 10, pp. 1–30. doi: 10.7554/eLife.63645.